On the World Ocean Circulation: Volume I

Some Global Features / North Atlantic Circulation

by

William J. Schmitz, Jr.

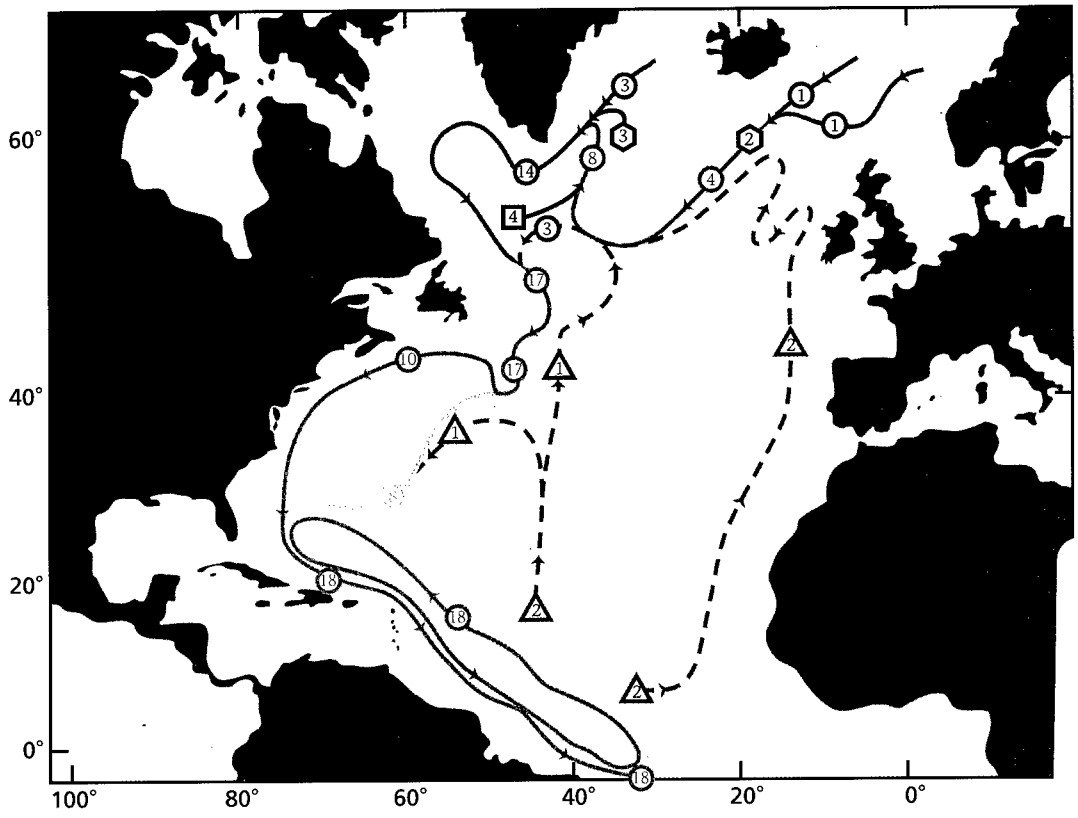

June 1996

Woods Hole Oceanographic Institution

Technical Report

WHOI-96-03

Funding was provided by the Office of Naval Research, Grant Nos. N00014-89-J-1039 and N00014-95-1-0356, and the Clark Foundation.

DISCLAIMER NOTICE

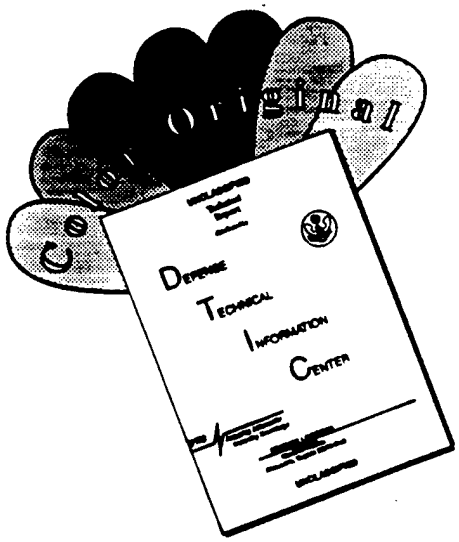

THIS DOCUMENT IS BEST QUALITY AVAILABLE. THE COPY FURNISHED TO DTIC CONTAINED A SIGNIFICANT NUMBER OF COLOR PAGES WHICH DO NOT REPRODUCE LEGIBLY ON BLACK AND WHITE MICROFICHE.

WHOI-96-03

On the World Ocean Circulation: Volume I

Some Global Features / North Atlantic Circulation

by

William J. Schmitz, Jr.

Woods Hole Oceanographic Institution
Woods Hole, Massachusetts 02543

June 1996

Technical Report

Funding was provided by the Office of Naval Research, Grant Nos. N00014-89-J-1039 and N00014-95-1-0356, and the Clark Foundation.

Approved for Distribution:

Philip L. Richardson, Chair
Department of Physical Oceanography

Front Cover Figure Caption: Circulation schematic for generic North Atlantic Deep Water (NADW), with green lines for transports (in Sverdrups in circles), a total of 18 Sv crossing the equator. Dark blue lines and symbols denote bottom water, red lines upper layer replacement flows. Squares represent sinking, hexagons entrainment, and triangles with dashed lines indicate slow water mass modification of Antarctic Bottom Water (AABW). Light blue lines indicate a separate mid-latitude path for Lower NADW (LNADW), 8 Sv, composed of 2 Sv modified AABW, 3 Sv Denmark Straits Overflow, and 3 Sv of entrained upper or intermediate layer replacement flow. There are 6 Sv of Middle NADW (MNADW), composed of 2 Sv modified AABW, 2 Sv Iceland-Scotland Overflow and 2 Sv entrained upper or intermediate layer replacement flow. Upper NADW (UNADW) is taken to be a result of 4 Sv convection in the Labrador Sea, with some mixing with modified Mediterranean Outflow Water.

Contents

Abstract

This is the first volume of a "final report" that summarizes, often in a speculative vein, what I have learned over the past 35 years or so about large-scale, low-frequency ocean currents, primarily with support from the Office of Naval Research (ONR). I was also fortunate to have been partially supported by the National Science Foundation, and during the preparation of this report, by the Clark Foundation.

This report is meant to be an informal, occasionally anecdotal, state-of-the-art summary account of the World Ocean Circulation (WOC). Seemingly simple questions about how ocean currents behave, such as where various brands of sea water are coming from and going to, have been exciting and difficult research topics for many years. This report is not remotely about "all" of the WOC, it is simply a set of comments about what I have looked into. I believe that the results in this report, although presented in a personal way, are consistent with community wisdom. The report is intended to be readable by non-specialists who have a basic scientific/technical background, especially in other oceanographic areas or meteorology or physics or the geophysical disciplines, not just by specialists in physical oceanography. Anyone wishing to get spun up on the observational basis for the WOC could use this report and associated reference lists as a starting point.

Volume I concentrates on the North Atlantic Ocean although there is preliminary discussion of global features. Highlights of this global summary are a new type of composite schematic picture of the World Ocean Circulation in its "upper layers" (Figure I-1) and new summaries (Figures I-12, 21, 91) of the global "thermohaline" circulation.

1. Introduction

This is the first volume of a "final report" that summarizes, often in a speculative vein, what I have learned over the last 35 years or so about large-scale, low-frequency ocean currents, primarily with support from the Office of Naval Research (ONR). I was also fortunate to have been partially supported by the National Science Foundation on a variety of earlier projects and, during the preparation of this report, by the Clark Foundation. A one-page summary of my activities over the years is contained in the Appendix. Many of my publications are contained in the references.

This description of the World Ocean Circulation (WOC) will address the general ocean circulation and mesoscale eddies, and also include occasional brief notes about other scales of variability. There may also be a few remarks about future research directions and problems as well as past accomplishments. The terms "general circulation" or "mean flow" or "average current(s)" will typically be used for large horizontal-scale (hundred kilometers and larger, often basin scale), quasi-stationary flow patterns. Mesoscale eddies typically have dimensions of 100–500 km, periods from days to, say, a few hundreds of days or so, and are usually the strongest where the general circulation (the primary mesoscale eddy energy source) is most intense. A Gulf Stream Ring will typically be about 250 km wide and propagating at a few centimeters per second, so in passing through a fixed site would register a period of 60 days or so. However, the term "mesoscale" can refer to one spatial dimension only, or be used without regard to time scale. As an example, in the general circulation there are "permanent" currents with a width that is order 100 km (mesoscale currents), but whose downstream dimension is roughly ocean-basin scale.

Perhaps the most common usage is simply to refer to mesoscale variability as encompassing a period range of, say, 10 to 200 days, but without specific regard to spatial scale. Secular scale would then be used for periods longer than mesoscale but shorter than a climate scale or the temporal mean, and not seasonal. The nomenclature climatic-scale will normally imply 1000 km or larger horizontal dimension and time scales of a few years or longer. With respect to vertical scale, I will normally discuss transports (in Sverdrups, $\equiv 10^6$ m^3 s^{-1}) in layers, typically four of them: upper, intermediate, deep, and near bottom. Property ranges for these layers will be discussed later. This report will not seriously address semi-annual or seasonal or bi-annual time

scales, or tides of any period, or, in general, fluctuations with period shorter than mesoscale. Mixed-layer or near-surface processes will not be discussed. The physical oceanography of the coastal ocean or enclosed basins is similarly outside the scope of this report.

The approach taken is primarily to synthesize diverse data-based results, obviously because I am an observationalist. There is, however, some discussion of how numerical model results relate to data, a research area I have pioneered (Schmitz and Holland, 1982, and following articles, see References). The association between eddies and the general ocean circulation at mid-latitudes has been a topic of strong interest in physical oceanography for several decades. We now have a comprehensive picture of the problem, and are at least close to a first order description and explanation. Since currents are themselves the primary source of eddies via instability mechanisms, the eddy field is as geographical and regional as are oceanic mean flows. Data and some specific numerical model runs can tend toward a similar geography. Eddy effects are typically not a major component of the dynamics of the interior of subtropical gyres but do contribute strongly to the dynamics of recirculations. This picture is a 100% turnaround (Schmitz *et al.*, 1983) from the view originally developed on the basis of the *Aries* Expedition that led to the formulation of the earliest cooperative, comparatively large group programs of the International Decade of Ocean Exploration: *i.e.* MODE[1] and POLYMODE.[2]

This report is meant to be an informal, occasionally anecdotal, state-of-the-art summary account of the WOC. Seemingly simple questions about how ocean currents behave, such as where various brands of sea water are coming from and going to, have been exciting and difficult research topics for many years. This report is not remotely about "all" of the WOC, it is simply a set of comments about what I have looked into. I believe that the results in this report, although presented in a personal way, are consistent with community wisdom. The report is intended to be readable by non-specialists who have a basic scientific/technical background, especially in other oceanographic areas or meteorology or physics or the geophysical disciplines, not just by specialists in physical oceanography. Anyone wishing to get spun up on the observational basis for the WOC could use this report and associated reference lists as a starting point. This

[1]Mid-Ocean Dynamics Experiment

[2]Joint U.S.–U.S.S.R. Mid-Ocean Dynamics Experiment (a combination of syllables of two earlier experiments, a U.S.S.R. POLYGON experiment and a U.S. Mid-Ocean Dynamics Experiment, MODE).

account is state of the art, so if a reader has basically no experience with the ocean circulation, standard textbooks might be referred to as one reads along. Very little will be said about methodology, for various reasons, the most obvious of which are limitations of space and time. Also, this topic has been the subject of a recent review (Leaman, 1990). But in any event, methods are only the means to the end, the latter being to learn what the ocean circulation is like, and to try to identify underlying mechanism(s).

Volume I concentrates on the North Atlantic Ocean although there is a preliminary discussion of global features. Highlights of this preliminary global summary are a new type of composite schematic picture of the WOC in its "upper layers" (Figure I-1) and new summaries (Figures I-12 and I-91) of "thermohaline" interbasin circulations. There are then discussions of subtropical and low-latitude and subpolar flow patterns in the North Atlantic (new or updated summaries are presented in Figures I-21, I-22, and I-89), followed by a description of the large scale NADW (North Atlantic Deep Water, see Table I-1 for water mass abbreviations) thermohaline cell, and also intermediate water, and finally the eddy field. I have done but little personal research on either very high or very low latitude flows, and this report will be accordingly deficient. Volume II will cover the Pacific and Indian Oceans, and Volume III will consider the Antarctic Circumpolar Current System and the South Atlantic Ocean in the context of a composite Southern Ocean and include an updated global summary. Lately, I have worked intensely on global exchanges (Schmitz, 1995) and this will be a dominant theme of Volume III, even to the extent of using interbasin and intergyre flow patterns when intercomparing the properties of the eddy field in the World's Oceans (Schmitz, 1996). That is, since the general circulation is the primary mesoscale eddy energy source in strong currents via a mixed barotropic/baroclinic instability mechanism, then the global characteristics of eddies can be related to the global similarities and differences in strong current systems. Since the directly wind-forced circulations are similar, the interbasin (thermohaline-related) circulations are where the global differences are found. This may lead to a somewhat different (global) picture of the coupling between thermohaline and wind-driven flows and eddies. I may also use Volume III to pick up loose ends from Volumes I and II.

2. A Few Global Circulation Characteristics

A schematic global summary map (Figure I-1) of many but obviously not all major current patterns in the upper ocean [encompassing the upper few hundred or a thousand meters, say, including the region of sharpest vertical density (temperature) contrast, the thermocline] will be used as the starting point for introducing what will turn out to be a lot of nomenclature and definitions. However, instead of dwelling on this topic all at once, it will be handled piecemeal throughout the report. The color coding scheme in Figure I-1 is such that red lines denote flows associated with subtropical circulations (15–40°, say), blue lines are used for subpolar and some polar circulations (latitudes higher than 40°, say), and purple lines identify equatorial and tropical current systems (latitudes less than 15°). A unique characteristic of Figure I-1, which is itself a totally new presentation, is the green flow lines indicating intergyre and interbasin exchanges. The major features of the world ocean circulation outlined in this section will be discussed in more detail throughout my report. The base map used in Figure I-1 is presented and discussed below.

An attempt was made in Figure I-1 to reproduce as faithfully as possible the horizontal dimensions of the current system components drawn. It should be understood that many ocean currents are not adequately mapped on a 5 x 5 or even a 2 x 2 degree grid because horizontal scales are shorter than this. In my opinion it is in the ocean interior areas (except near the subtropical front) where 2 x 2° or 5 x 5° thinking might apply. Boundary currents, or boundary current systems, along with special areas (equatorial, high latitude, frontal) are usually foci for critical and energetic ocean circulation phenomena, and may typically have ~ 100 km width scales. Current systems right at the equator have a lot of vertical diversification even in the upper ocean, and what is represented in Figure 1 includes the equatorial undercurrent-related flows but not currents (including those at the sea surface, shown below) in other upper ocean depth ranges in that area, or in general wherever vertical overlap is difficult to depict. Flow patterns for the North and Tropical Indian Ocean are not present in Figure I-1 because they are special cases. With respect to the most general global features, there is a quasi-stationary circulation pattern called a subtropical gyre occupying roughly the entire width of all "other" ocean basins at mid latitudes (in Figure I-1), with approximate latitudinal extent 15–40°. Other general features are sub-basin-scale recirculation gyres associated with western boundary current systems, subpolar and tropical

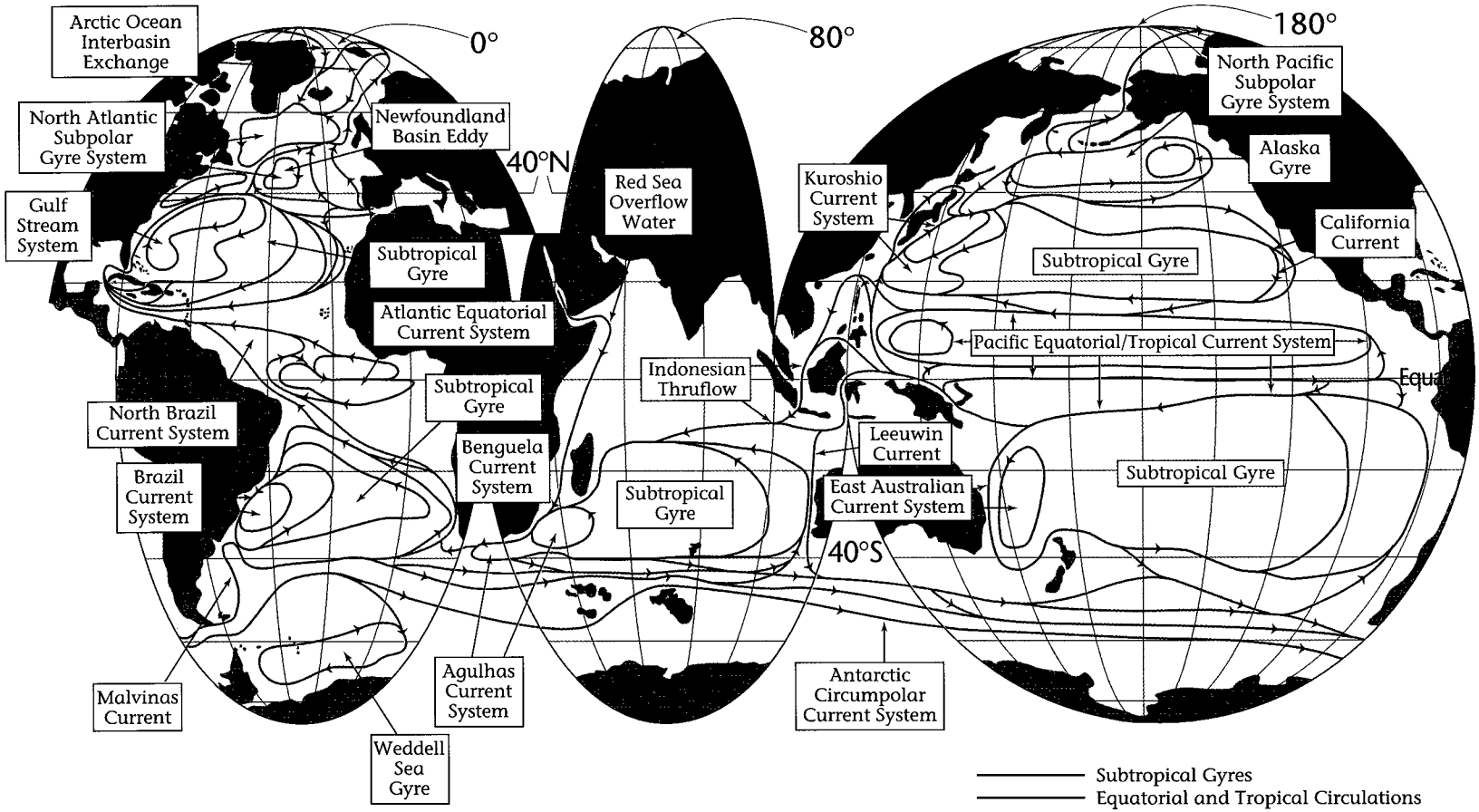

Figure I-1: A global map schematically identifying the location and nomenclature for most major upper ocean flow patterns and the connections between these current systems. Subtropical gyre circulations are in red, polar and subpolar flows in blue, equatorial and tropical current patterns in purple, and intergyre or interbasin exchanges are in green.

Table I-1: Water mass abbreviations used in the text

Abbreviation	Full Name
AABW	Antarctic Bottom Water (generic)
AAIW	Antarctic Intermediate Water (generic)
CDW	Circumpolar Deep Water (generic)
DSOW	Denmark Straits Overflow Water
LNADW	Lower North Atlantic Deep Water
LSW	Labrador Sea Water
MOW	Mediterranean Outflow Water
MNADW	Middle North Atlantic Deep Water
NACW	North Atlantic Central Water (generic)
NADW	North Atlantic Deep Water (generic)
NSOW	Nordic Seas Overflow Water (generic)
SACW	South Atlantic Central Water (generic)
SPMW	Subpolar Mode Water
UNADW	Upper North Atlantic Deep Water

gyres, equatorial undercurrents, and eastern boundary currents. Intergyre and interbasin flows will be a focus of my report, especially Volume III. A discussion of basins other than the North Atlantic will be contained in future volumes of this report, and each will start with an updated version of Figure I-1.

Subtropical Gyres are composed of strong narrow currents in their western reaches involving poleward and eastward net flow, an "interior flow" returning water equatorward, to some extent in "eastern boundary currents," with an "equatorial" or southern branch flowing primarily westward. Subtropical Gyres, although existing on basin-scale longitudinally, also tend to have sub-basin-scale gyres (recirculations) in their western reaches (Figure I-1) and be populated by energetic eddies, including current rings. Recirculations and mesoscale eddies can be interrelated, as discussed in

more detail below. The nomenclature WBCS (Western Boundary Current System) includes the main boundary current(s) plus recirculations (quasi-stationary eddies), and "energetic" mesoscale features by implication. In the North Atlantic, we have the Gulf Stream System (GSS), composed of the Gulf Stream itself, a recirculation to the south, a northern recirculating gyre, and a very energetic mesoscale eddy field. Subtropical Gyres may interchange water with Subpolar Gyres as well as with Tropical Current Systems. For example, in the North Atlantic, the upper layer replacement flow for NADW formation has to move through low and subtropical latitudes and thence to a Subpolar Current System.

There are also subpolar, polar (latitudes above, say, $\sim 40°$), tropical (at low latitudes, *i.e.*, less than 20° latitude), and equatorial current systems along with intergyre and interbasin exchanges in Figure I-1. Figure I-1 does not contain a tropical upper layer gyre in the North or South Atlantic Oceans for simplicity. Flow patterns right at the equator are an important research area in their own right (*e.g.*, Leetmaa *et al.*, 1981). In my opinion, deep as well as upper ocean circulation systems in the vicinity of the equator are strong candidates for future research priority, particularly with respect to vertical exchanges/transformations of water masses transiting this regime (see for example, Friedrichs *et al.*, 1994, and Schmitz, 1995). The polar circulation patterns in the southern hemisphere, denoted by blue lines in Figure I-1, will be called the Antarctic Circumpolar Current System (ACCS). Figure I-1 does not contain all of the polar gyres "associated with" the ACCS.

The largest horizontal scale temperature (and other property) structures associated with most of the currents shown in Figure I-1 are laid out in the atlas produced by Levitus (1982). This atlas contains global- and basin-scale hydrographic features of the oceans, and such figures need not be reproduced here. It should be noted that mesoscale features may tend to be smoothed out or distorted in the Levitus atlas (Lozier *et al.*, 1994, 1995). A significant point is that the broad range ($-1.5° \rightarrow 29.5°C$) of temperatures encountered at the sea surface in figure 12 of Levitus (1982) is also the vertical temperature range for the ocean (approximately), with circulations carrying water of these temperatures and other properties from the mixed layer down through the ocean depths to lower latitudes (Iselin, 1939), approximately along isopycnal surfaces (Montgomery, 1938). This is a zero-order explanation (advective) of the *T/S* (temperature/salinity) curve at many ocean locations. Water mass (or water type)

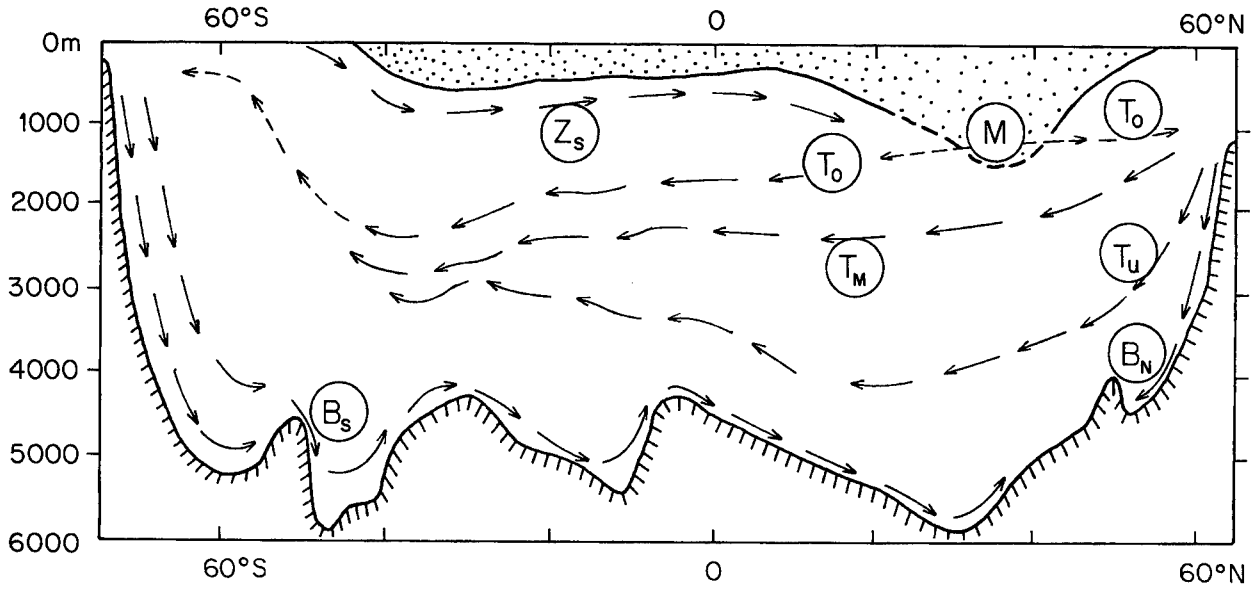

Figure I-2: A meridional–vertical section of the subthermocline general (thermohaline) circulation in the Atlantic Ocean, simplified from Wüst (1935) by Schmitz (1995). Z_S denotes Subantarctic Intermediate Water, B_S and B_N bottom water south and north, T_O, T_M, T_U denote upper, middle and lower deep water (North Atlantic Deep Water, NADW), M Mediterranean Water. The stippled layer is the warm-water sphere. Depths in meters.

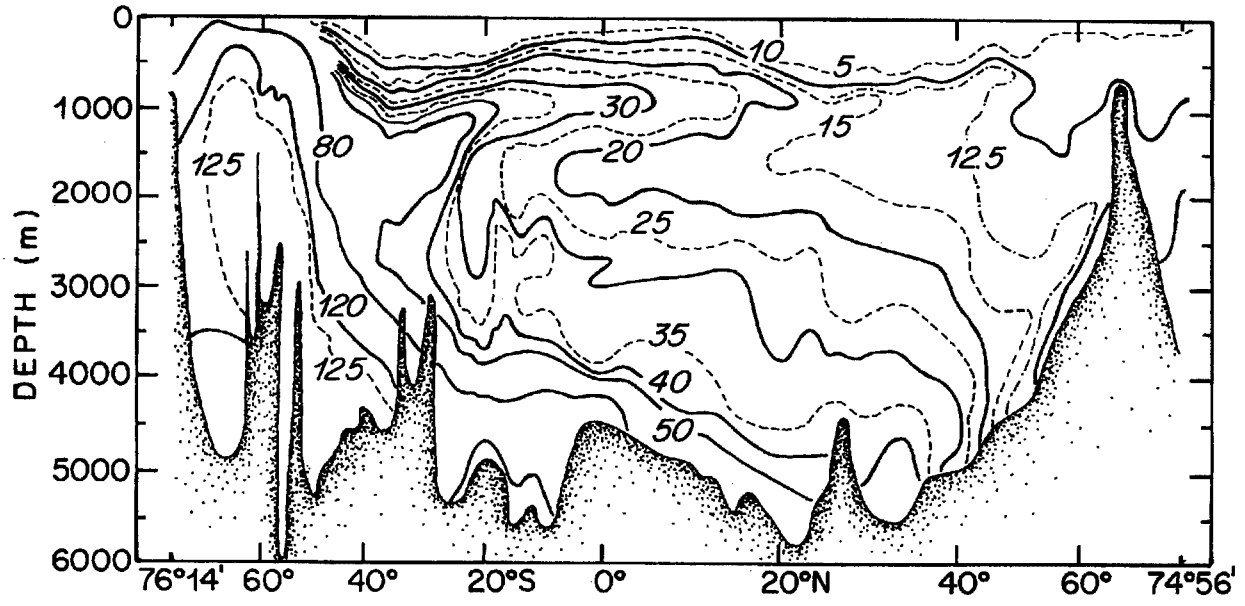

Figure I-3: A meridional silicate section across the Atlantic Ocean, adapted (smoothed and simplified) from Reid (1994, his figure 5g). Silica contours in μmol kg^{-1}.

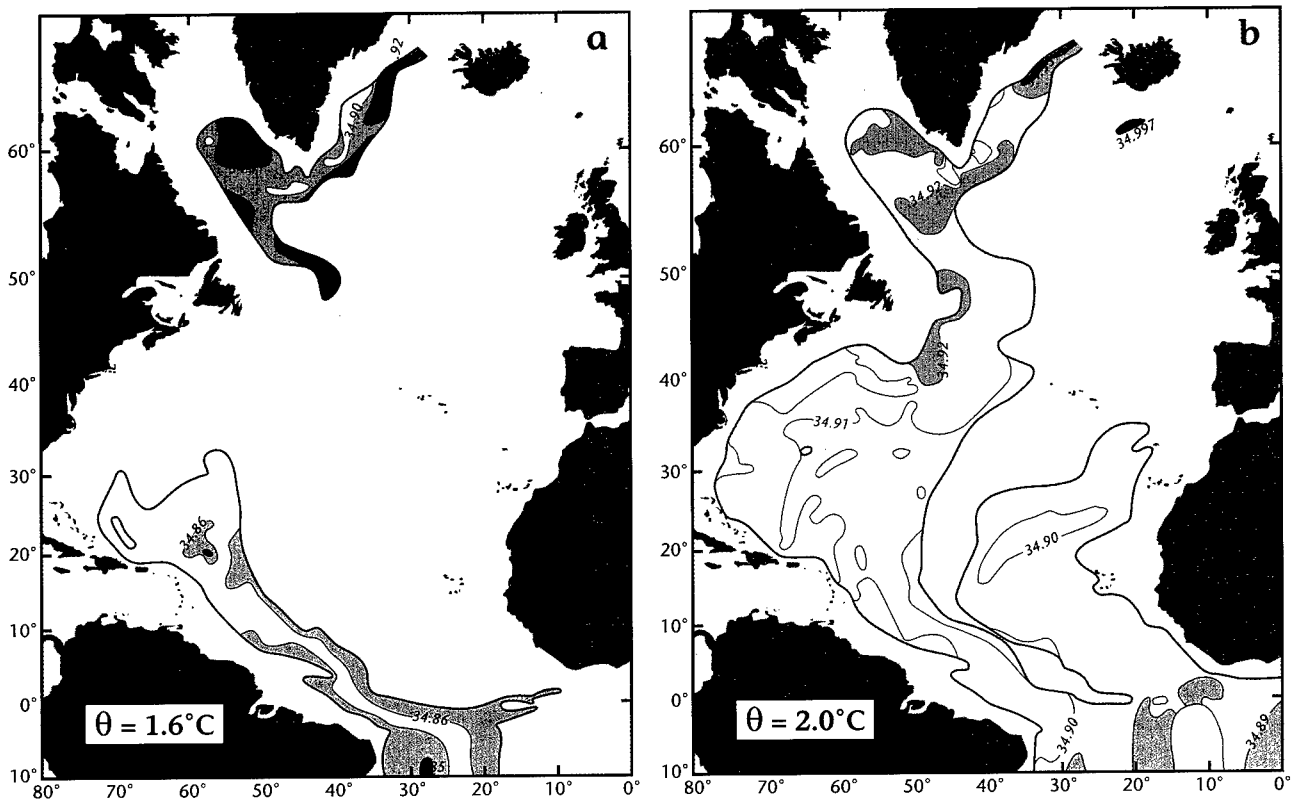

Figure I-4: Salinity contours (psu) on the $\theta = 1.6°$ (a) and 2.0°C (b) surfaces, adapted from Worthington and Wright (1970), here taken to represent LNADW.

conversion processes (formation, sinking, upwelling, mixing) may be significant mostly in special areas. The classic picture of large-amplitude, uniform, large-scale upwelling in the ocean interior has not been verified observationally (Toole *et al.*, 1994), especially when this upwelling is supposed to occur across the thermocline (Garrett, 1993; Schmitz, 1995).

Various schematic charts and sections for some of the subthermocline global scale flow elements not shown in Figure I-1 are contained in Figures I-2 through I-10. There are interbasin exchanges in these figures, some of which may be associated with Figure I-1. The classic thermohaline circulation picture based on an interpretation of data from the *Meteor* Expedition is shown in Figure I-2 (taken from Wüst, 1935, as simplified by Schmitz, 1995). Many elements of this schematic prevail as state-of-the-art thinking in general terms to this day, a remarkable achievement. Figure I-2 even includes indications of Mediterranean Outflow Water (MOW) influence on Upper North

Atlantic Deep Water (UNADW) as well as "upwelling" of Lower North Atlantic Deep Water (LNADW) (see Table I-1 for a review of water mass names) to Middle North Atlantic Deep Water (MNADW) near and beyond the equator (Friedrichs *et al.*, 1994; McCartney, 1996; Schmitz, 1995) and subsequent incorporation into a generic NADW approaching the ACCS. The definitions of the various brands of NADW may vary depending upon author and data location. Generic NADW incorporated into the ACCS, a complex process, is here taken to primarily become part of Circumpolar Deep Water (CDW) with minor exception. The connection of NADW to CDW and CDW to the deep circulation in the Pacific and Indian Oceans is a crucial point (Lynn and Reid, 1968; Mantyla and Reid, 1983, 1995; Reid and Lynn, 1971). Joe Reid's contributions dominated my initial global perspective of the subthermocline ocean circulation. Figure I-2 contains subthermocline characteristics of the largest scale meridional cell in the Atlantic Ocean, but the replacement path(s) for the renewal of NADW are not shown.

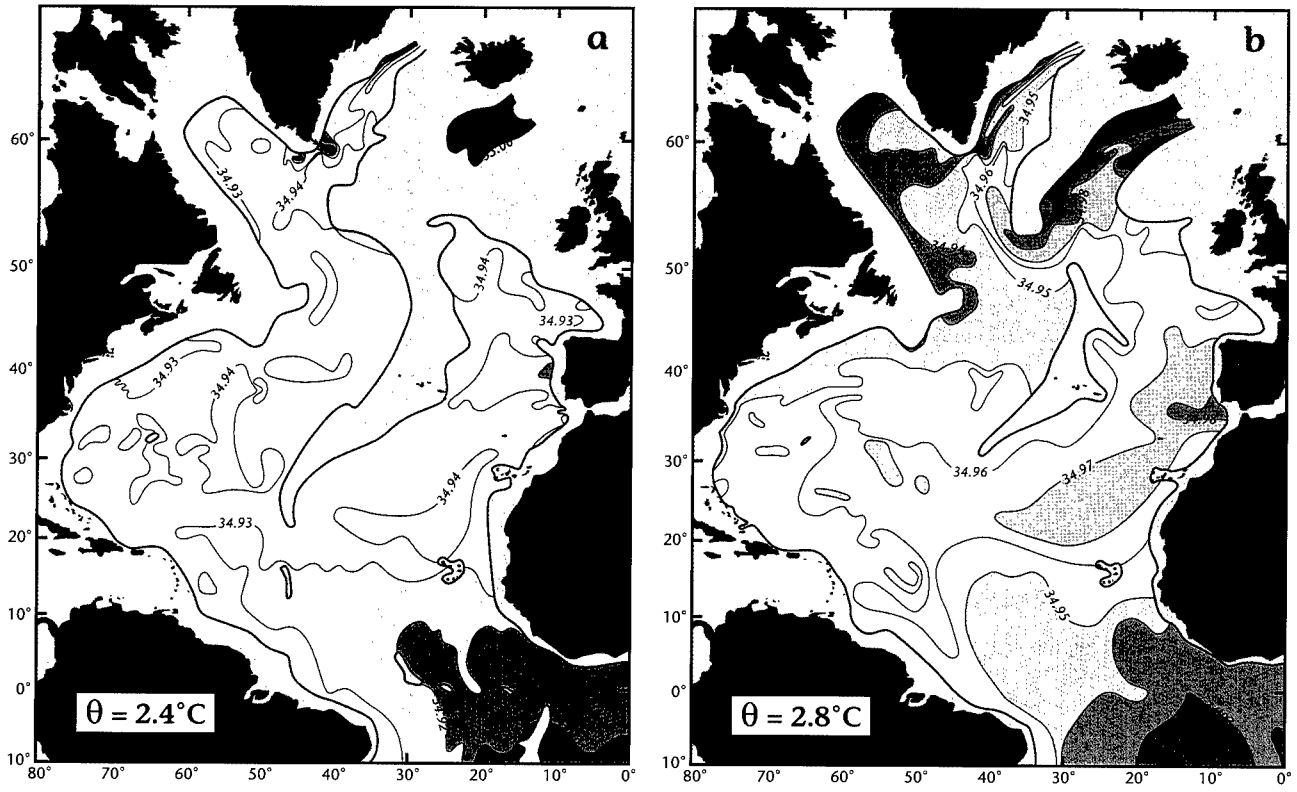

Figure I-5: Salinity contours (psu) on the θ = 2.4° (a) and 2.8°C (b) surfaces, adapted from Worthington and Wright (1970), here taken to represent MNADW.

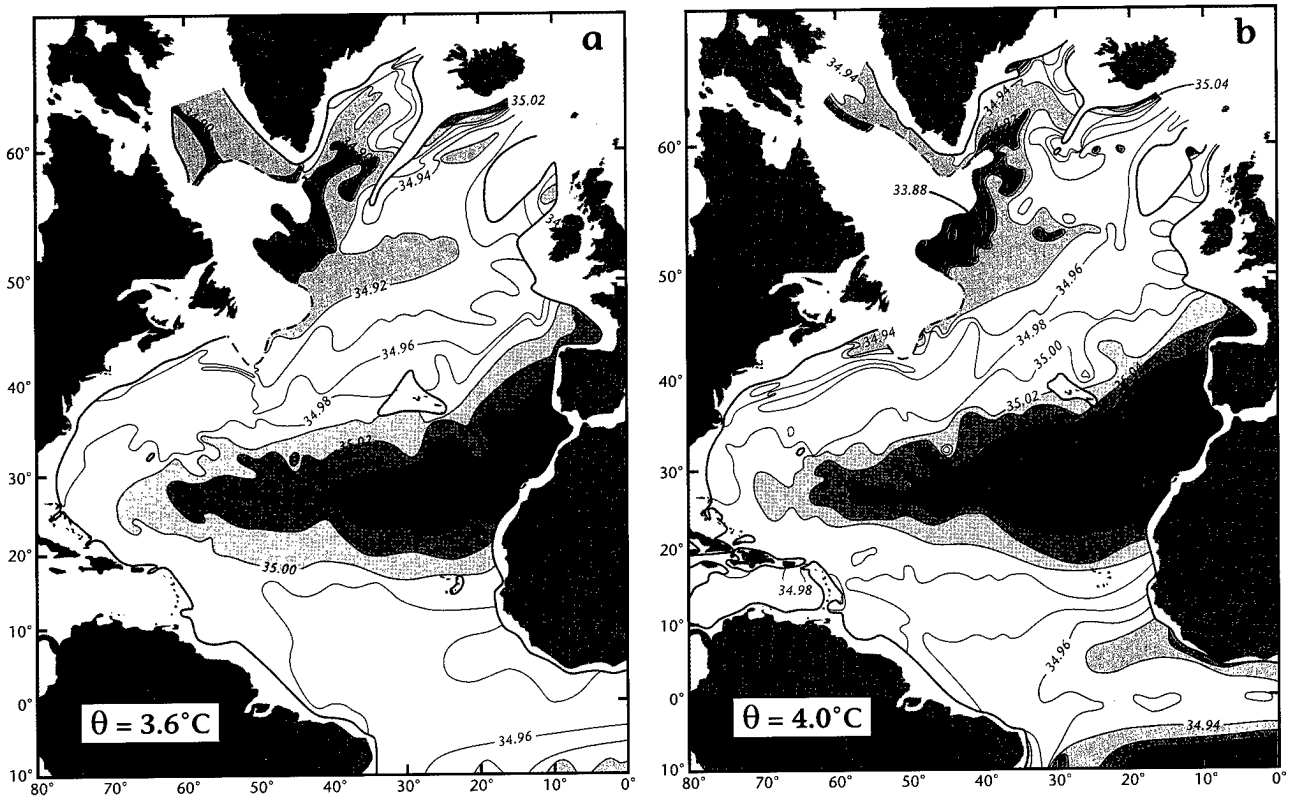

Figure I-6: Salinity contours (psu) on the $\theta = 3.6°$ (a) and 4.0°C (b) surfaces, adapted from Worthington and Wright (1970), here taken to represent UNADW.

A meridional section of silicate through the Atlantic Ocean is shown in Figure I-3, taken from Reid (1994). The deeper pathways in Figure I-2 and those implied in Figure I-3 are also exhibited in Figures I-4 through I-6, which depict selected Salinity (S) contours on potential temperature (θ) surfaces, taken from the Worthington and Wright (1970) atlas. These plates are organized from lower to higher θ in three groups with correspondence to the brands of NADW indicated in Figure I-2. Lower NADW is here taken to be the combination of Antarctic Bottom Water (AABW) entering the western North Atlantic from the south ($34.90 \leq S \leq 34.93$ psu, practical salinity units) and the densest element of Denmark Straits Overflow Water (DSOW) entering the North Atlantic from the polar ocean ($34.85 \leq S \leq 34.90$ psu), as characterized by the θ, S distributions in Figures 4a and b. Figures 4a and b are for $\theta = 1.6$ and 2.0°C respectively, and are taken to be representative of the range $1.0 \leq \theta \leq 2.2$°C. According to McCartney (personal communication, 1996) this LNADW joins the DWBC after executing a path down the east flank of the Bermuda Rise. Note that Pickart's (1992) sections

across the DWBC in the Slope Water region have a minimum θ of about 2°C, so not much LNADW is present there on the definition used here. This point is discussed further in Section 7, this volume of my report. Middle NADW ($2.2 \leq \theta \leq 3.4$°C) is here taken to be a combination in the North Atlantic of overflow across the Iceland-Scotland Ridge, as characterized by the ($\sim$ 35.00 psu) S values in the northeast corner of Figure 5, with modified AABW moving north on the eastern side of the Mid-Atlantic Ridge; see also McCartney *et al.* (1991). Middle NADW is also influenced by the least dense DSOW and modified AABW west of the Mid-Atlantic Ridge. Upper NADW ($3.4 \leq \theta \leq 4.6$°C) may be characterized by the S distributions on $\theta = 3.6$° and 4.0°C in Figure 6. Labrador Sea Water (LSW) and MOW contribute to UNADW in Figure 6. Some MOW could contribute to LNADW and/or MNADW formation by incorporation into the North Atlantic Current and eventually, perhaps, either entering the nordic seas or in entrainment

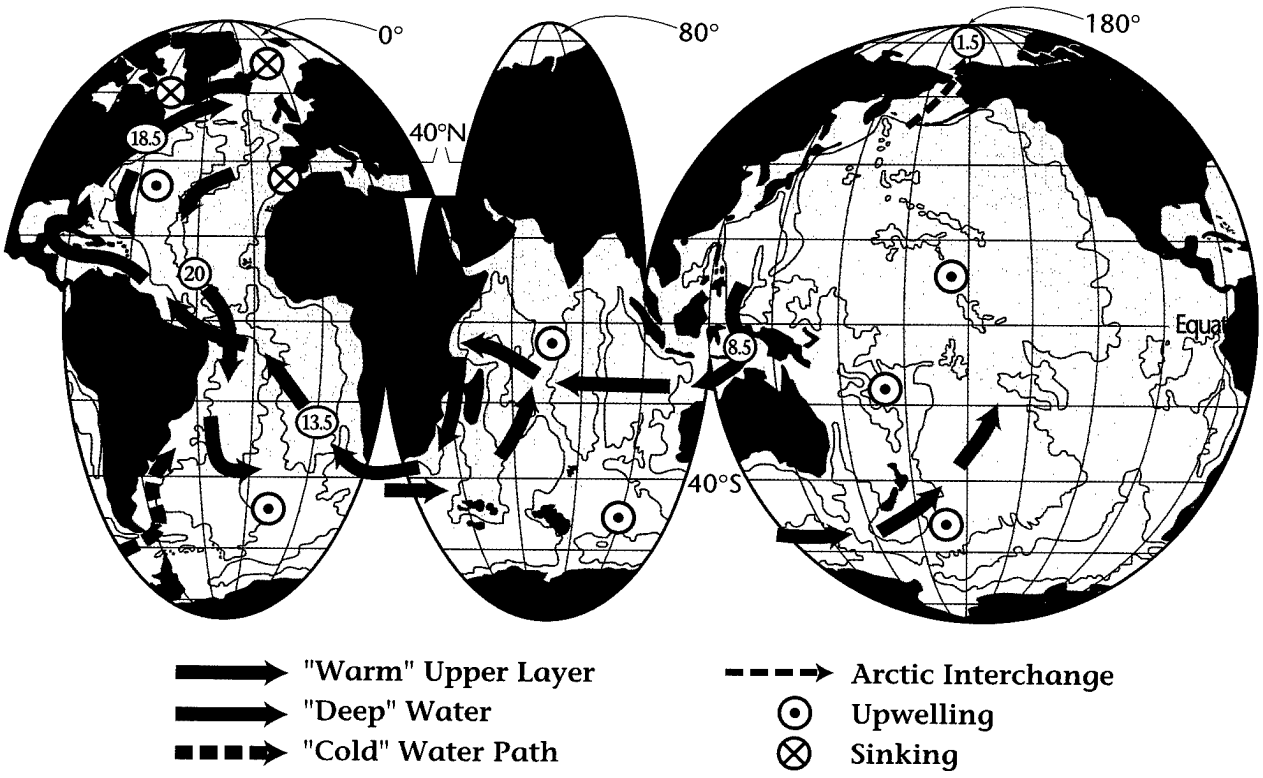

Figure I-7: A map of the pathways and transports for NADW formation and renewal, adapted and modified from Gordon (1986) by Schmitz (1995). Transports in circles in Sverdrups.

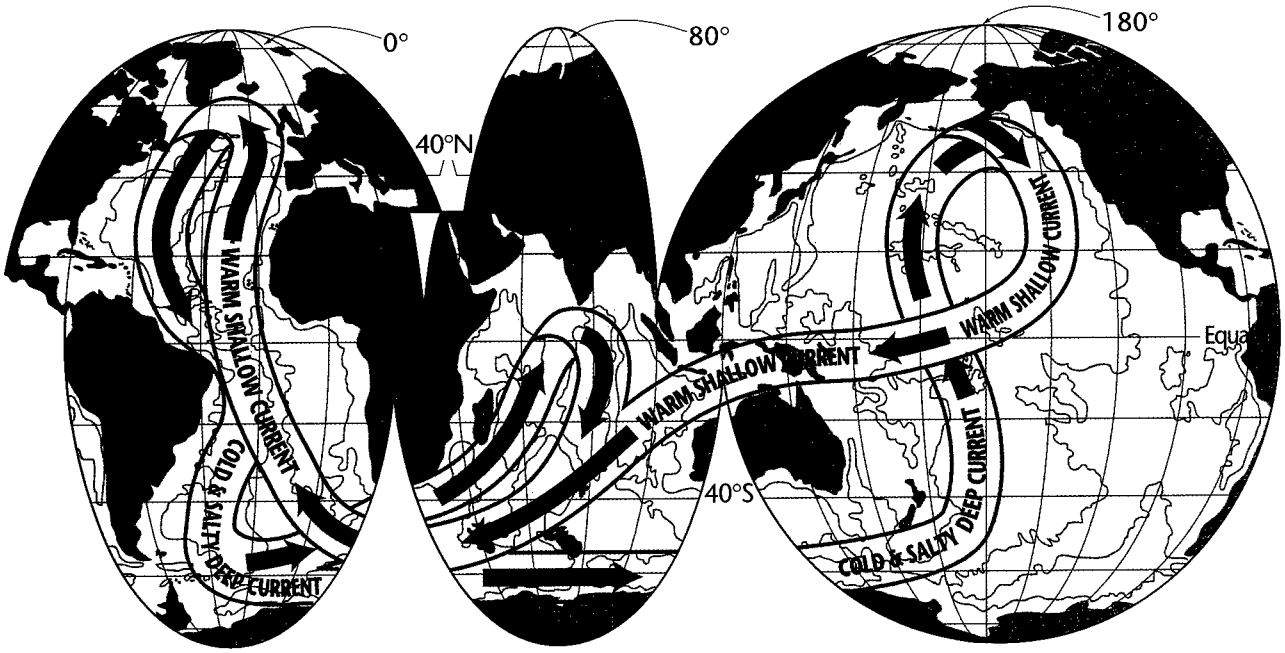

Figure I-8: A two-layer thermohaline conveyor belt summary taken schematically from Broecker (1987, 1991) by Schmitz (1995).

Table I-2: Typical potential density ranges for various layers

Layer	σ Range (kg m^{-3})
Upper	$\sigma_\theta < 26.8$
"Upper Intermediate"	$27.0 \geq \sigma_\theta \geq 26.8$
"Total Intermediate"	$27.5 \geq \sigma_\theta \geq 26.8$
Deep	$27.8 \geq \sigma_\theta \geq 27.5$
Bottom	> 27.8

as the overflow waters plunge down the slope (discussed in following sections of this report).

Early versions of various global pathways for the replacement of NADW are shown in Figures I-7 and I-8. Figure I-7 is taken from an adaptation of Gordon (1986) by

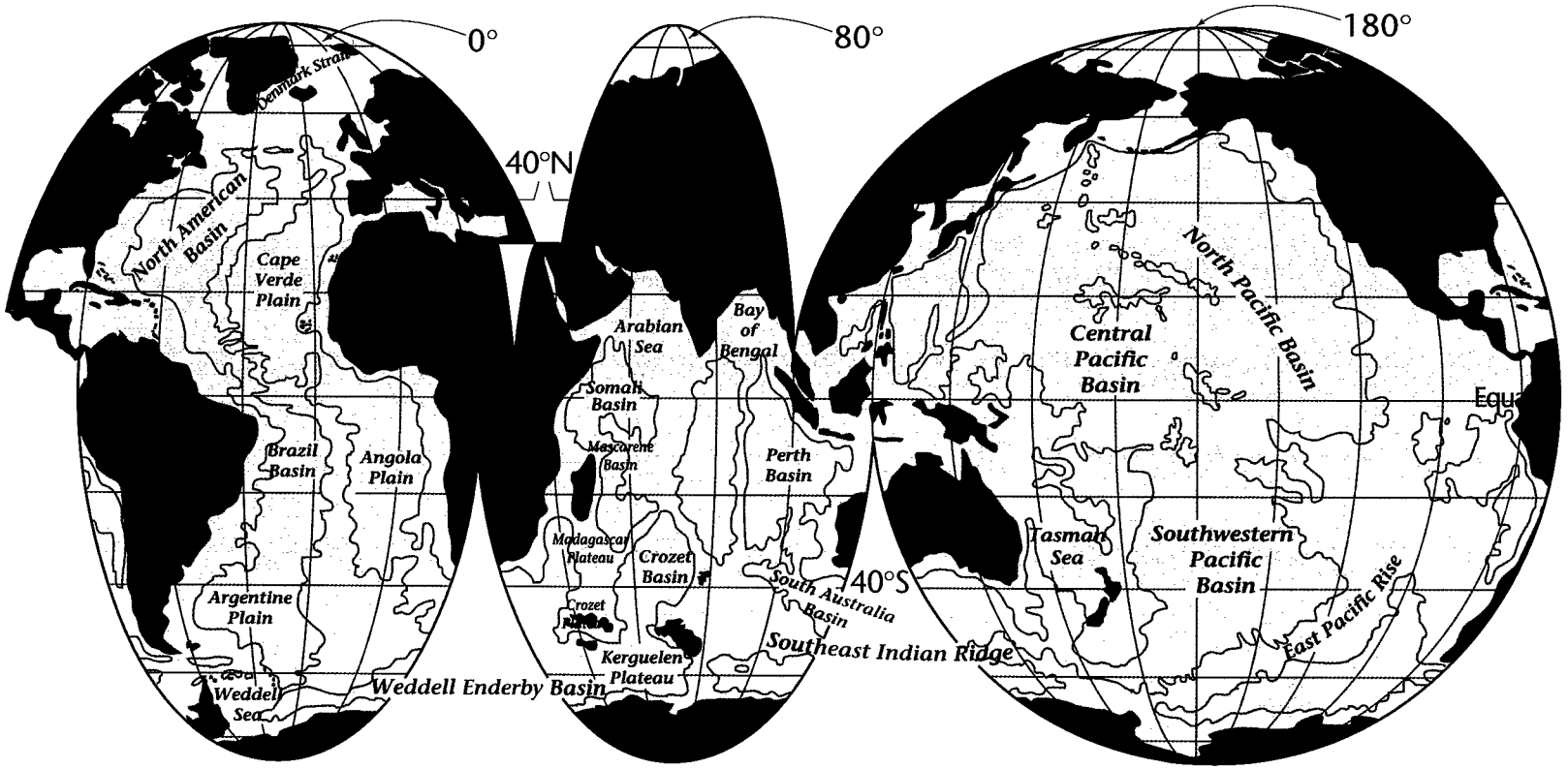

Figure I-9: The standard global base map used in this report, with the 4000-m isobath and topographic feature names.

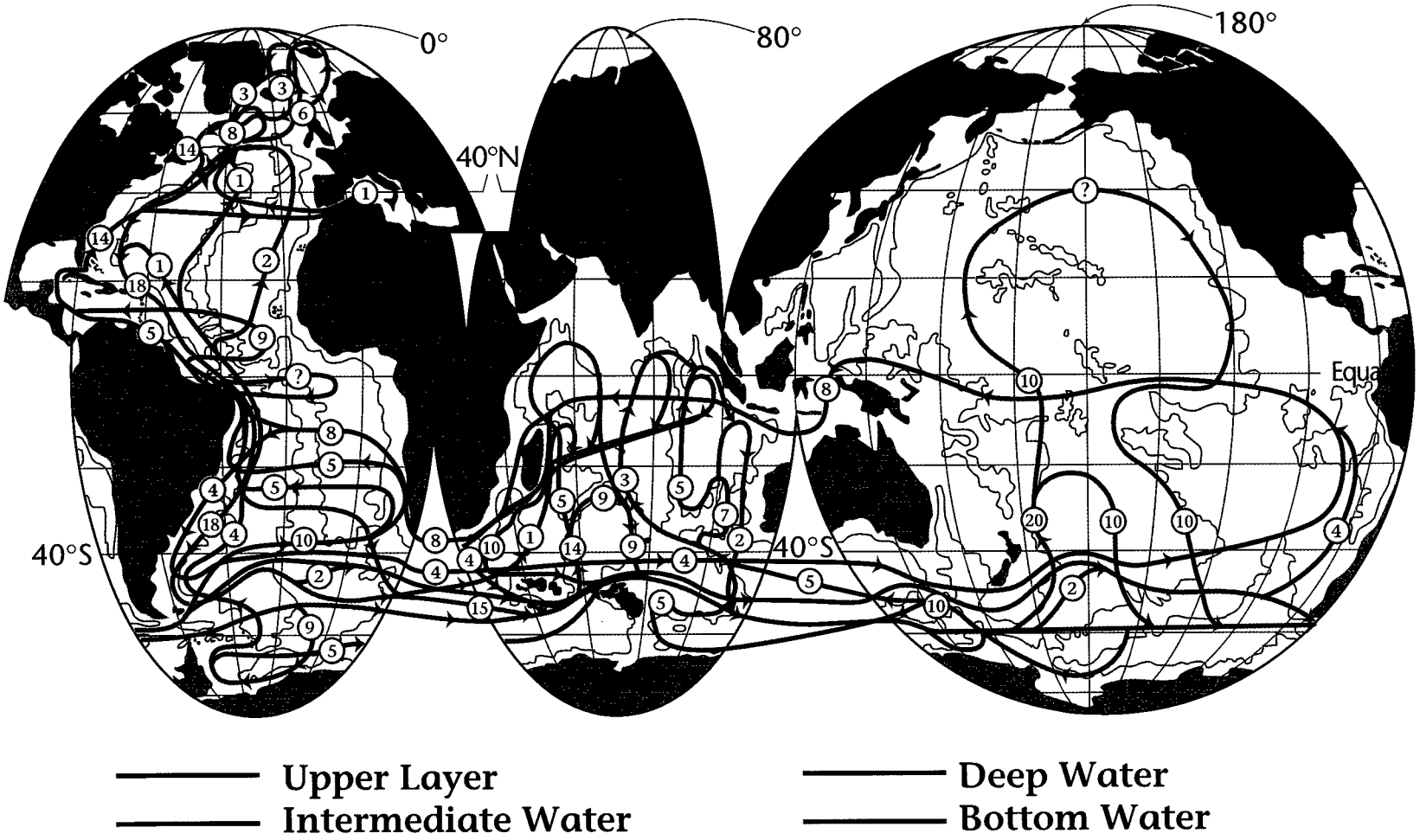

Figure I-10: A four-layer version of the deep and abyssal global thermohaline circulation and its upper level compensation flows. Bottom water is shown by a blue line, deep water by a green line, a red line is used for intermediate depth flows, and purple denotes the uppermost layer. Volume transport estimates (in Sverdrups) are in circles associated with the key path segments, and color changes indicate water mass conversion.

Schmitz (1995), and I-8 is the conveyor belt schematic by Broecker (1987, 1991), as used by Schmitz (1995). Figure I-9 is a standard global base map with some bathymetric features labeled; pink areas denote plateaus at key locations (choke points) in the southern Indian/Antarctic Oceans. Figures I-10 and I-11 contain more recent versions (using the vertical layers in Table I-2) of the composite global thermohaline circulation by Schmitz (1995), with fundamental differences from Figures 7 and 8, especially with regard to ideas about the replacement path(s) for NADW. Note that the upper layer compensation path(s) for NADW renewal has (have) multiple branches with upwelling and/or water mass conversion occurring in many regions in Figures I-10 and I-11. There is, however, more or less general agreement that the ACCS is the conduit for transporting NADW to the Indian and Pacific Oceans, either as CDW (a notion pioneered by Joe Reid, see *e.g.*, Lynn and Reid, 1968; Reid and Lynn, 1971; Mantyla and Reid, 1983) or perhaps in small amounts as more pristine NADW (especially for the western Indian Ocean; please see Mantyla and Reid, 1995, their figure 6). Figures I-10

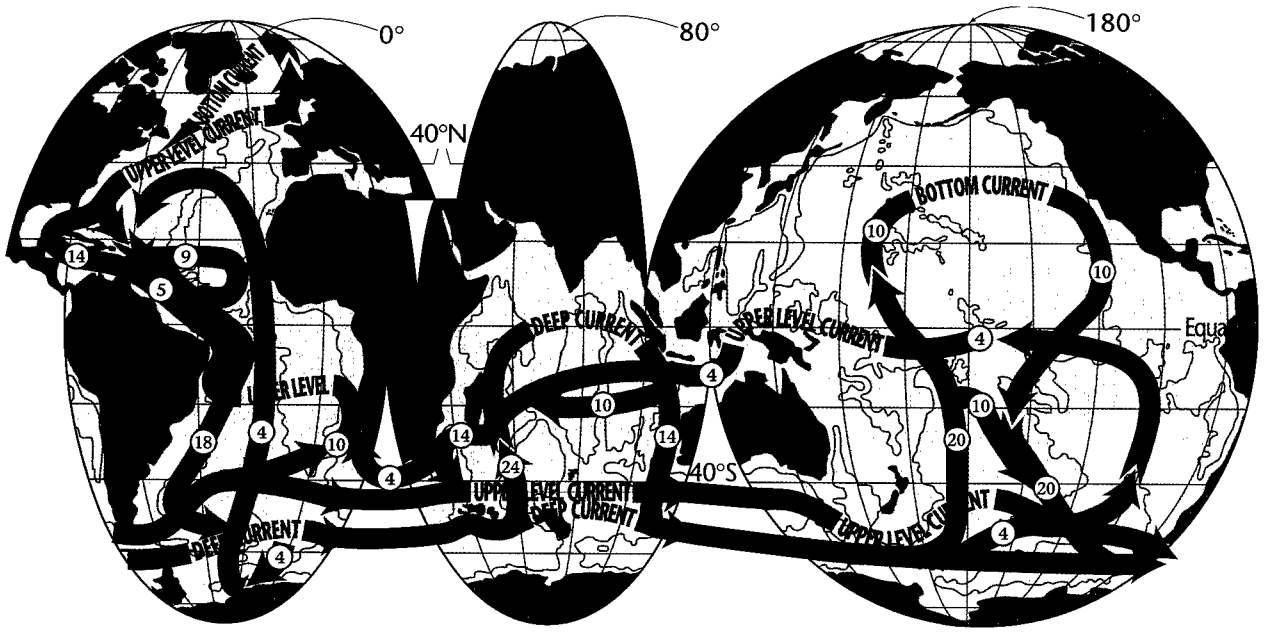

Figure I-11: A three-layer, interbasin-scale, thermohaline conveyor belt based on a condensation of the four-layer picture in Figure I-10, adapted from Schmitz (1995). Here red lines characterize both upper ocean and intermediate layers, green lines denote deep transports, blue bottom circulation. Volume transport estimates (in Sverdrups) are in circles associated with the key path segments, and color changes indicate water mass conversion.

and I-11, including the question mark in the North Pacific abyssal layer, will be discussed in more detail in Volume III.

An update or modern version of Figure I-2 that is new with this report is shown in Figure I-12, which has a global feature (CDW) in the southern oceans, and also includes the upper layer replacement flows for the formation of NADW. This is my first attempt at a "single" and "simple" global two-dimensional meridional section type of representation for NADW distribution and replacement (in response to a challenge from my theoretically-inclined colleague next door, Dr. Xin Huang). Circumpolar Deep Water is a water mass initially formed from NADW, but homogenized (possibly participating in many circuits of the ACCS) by a complex global circulation process, involving transit from the northernmost North Atlantic to the ACCS and thence to northern Pacific and northern Indian Oceans and back to the ACCS as deep water with modifi-

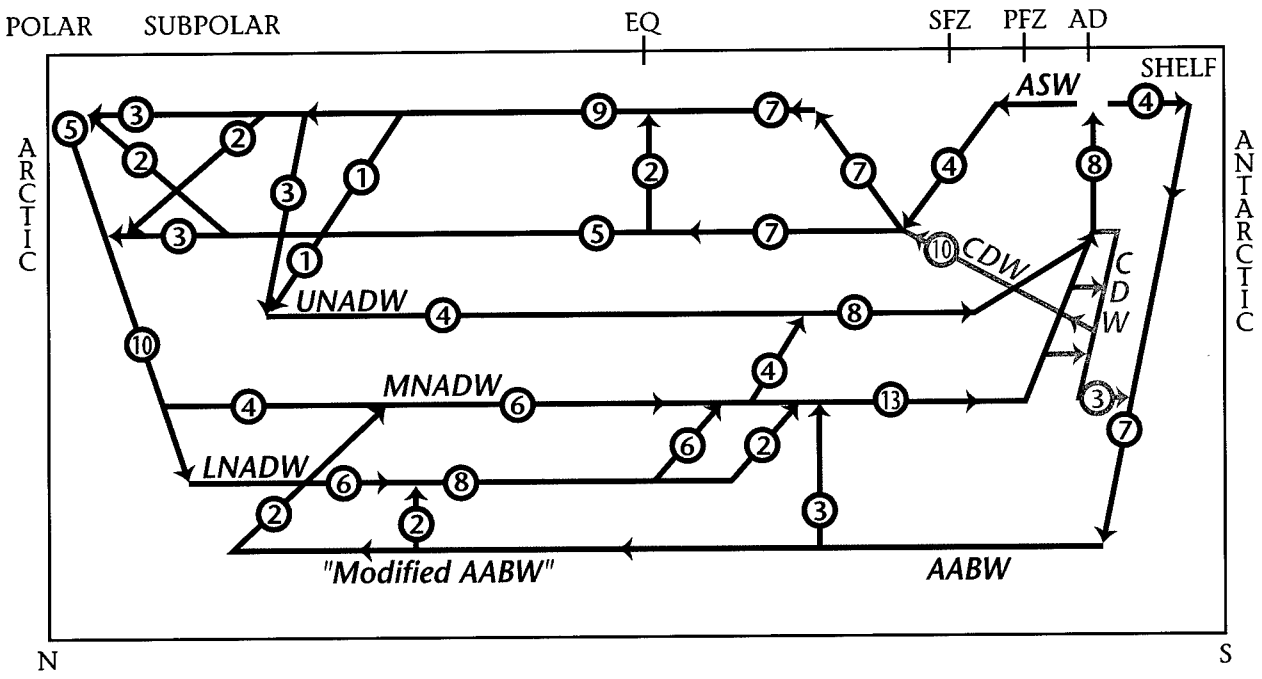

Figure I-12: A six-vertical-element meridional section for the thermohaline flow in the "North Atlantic," with a "simplified global linkage (CDW)." Purple denotes upper layer, red intermediate, green deep, and blue bottom. Circumpolar Deep Water is set off in light blue lines. There are three branches for deep water. Various geographical and oceanographic features are inserted around the border of the figure. EQ denotes the equator, SFZ is Subpolar Frontal Zone, PFZ is Polar Frontal Zone, AD is Antarctic Divergence. Transports (in Sverdrups) in circles. This type of meridional section for interbasin flow is new with this report.

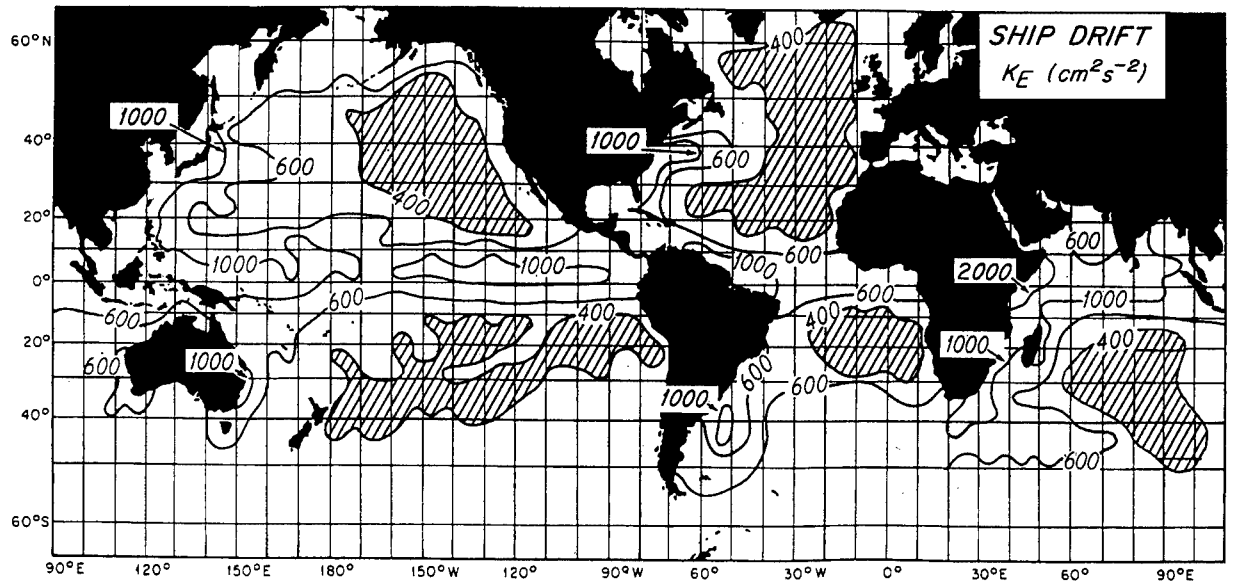

Figure I-13: The global distribution of eddy kinetic energy at the sea surface, as adapted from Wyrtki *et al.* (1976), Schmitz *et al.* (1983), and Schmitz (1996). K_E is defined in the text.

cation by mixing along the way. So the few light blue lines characterizing CDW in Figure I-12 are a (very) condensed representation of a (very) global process.

In Figure I-12, 3 Sv of upper layer water and 2 Sv of ("upper") Intermediate Water, with the upper layer water having been converted from North Atlantic Central Water (NACW) to Subpolar Mode Water (SPMW) by convection along its path in the subpolar region (McCartney, 1996), enter the polar seas of the North Atlantic from the eastern-most branch of the North Atlantic Current and are modified in the Arctic (Mauritzen, 1993) and exit the Denmark Straits (3 Sv) and Iceland-Scotland Gap (2 Sv) as overflow waters. Two Sverdrups of upper layer water (having been modified in situ in the subpolar gyre as noted above for the branch entering the polar seas) and 3 Sv of "upper" intermediate water are entrained into the 5 Sv Nordic Seas Overflow Water (NSOW) as it plunges downslope into the northern North Atlantic. The 3 Sv of DSOW plus its 3 Sv entrained from the subpolar gyre are joined by 2 Sv of modified "western" AABW to form 8 Sv of "fresh LNADW," that is in fact bottom water north of 40–45°N. The 2 Sv of Iceland-Scotland Overflow water plus its 2 Sv entrained from the subpolar gyre join the 2 Sv of modified AABW moving north up the eastern Atlantic (Figures 4 and 5 here and McCartney *et al.*, 1991) to form 6 Sv MNADW. There are 4 Sv of UNADW in Figure I-12, formed from LSW (itself formed by convection as the densest element of SPMW), by

mixing with MOW, and entrainment of ambient subpolar gyre water. Convection in the subpolar gyre may also influence the θ/S characteristics of the ambient subpolar gyre water that is entrained into the overflows as they plunge down the slope.

The 8 Sv of LNADW moves south of 40°N along the eastern side of the Blake-Bahama Outer Ridge and then joins the DWBC (at that point carrying primarily MNADW and UNADW north of ~ 20–30°N, prior to being joined by LNADW) at ~ 20–30°N (M. McCartney and R. Curry, personal communication, 1996). All "brands" of NADW upwell or step up "1 brand" at the equator and in the South Atlantic in Figure I-12. So the grand transport totals of NADW before crossing the equator into the South Atlantic are 8 Sv LNADW, 6 Sv MNADW, 4 Sv UNADW having originated as 4 Sv modified AABW, 8 Sv NACW (being modified to SPMW and LSW), 5 Sv upper AAIW, and 1 Sv MOW. Speer and McCartney (1991) estimate that 10 ± 3 Sv of LNADW crosses the equator along with 14 ± 2 Sv of combined UNADW and MNADW, approximately.

The largest scale features of the ocean circulation at the sea surface were first determined quantitatively by estimates of currents based on ships' navigational data (Duncan and Schladow, 1981). These surface current estimates will collectively be referred to as ship drift data. These observations are typically based on 24-hour differences in position and often assembled by averaging over 5 degrees of latitude/longitude (sometimes 1- or 2-degree areas) so the resulting currents can be highly smoothed. But the variances in these data were used to get the first global picture of the eddy field (at the sea surface, Wyrtki *et al.*, 1976). A smoothed picture of the intensity (energy) of the global eddy field (discussed and defined below) at the sea surface based on "ship drift" data is contained in Figure I-13.

3. Introduction to the North Atlantic Circulation

A composite smoothed speed contour and direction (arrow) plot of the surface currents in the North Atlantic based on one particular set of ship drift data is shown in Figure I-14. Many of the major circulation features of the upper layer flow in the North Atlantic Ocean are contained in Figure I-14, *i.e.*, a strong Gulf Stream penetrating to the longitude of the Grand Banks, and some other features that have been known in general terms for a few hundred years. On the other hand, several important characteristics of the upper layer circulation (basically those on smaller spatial scales)

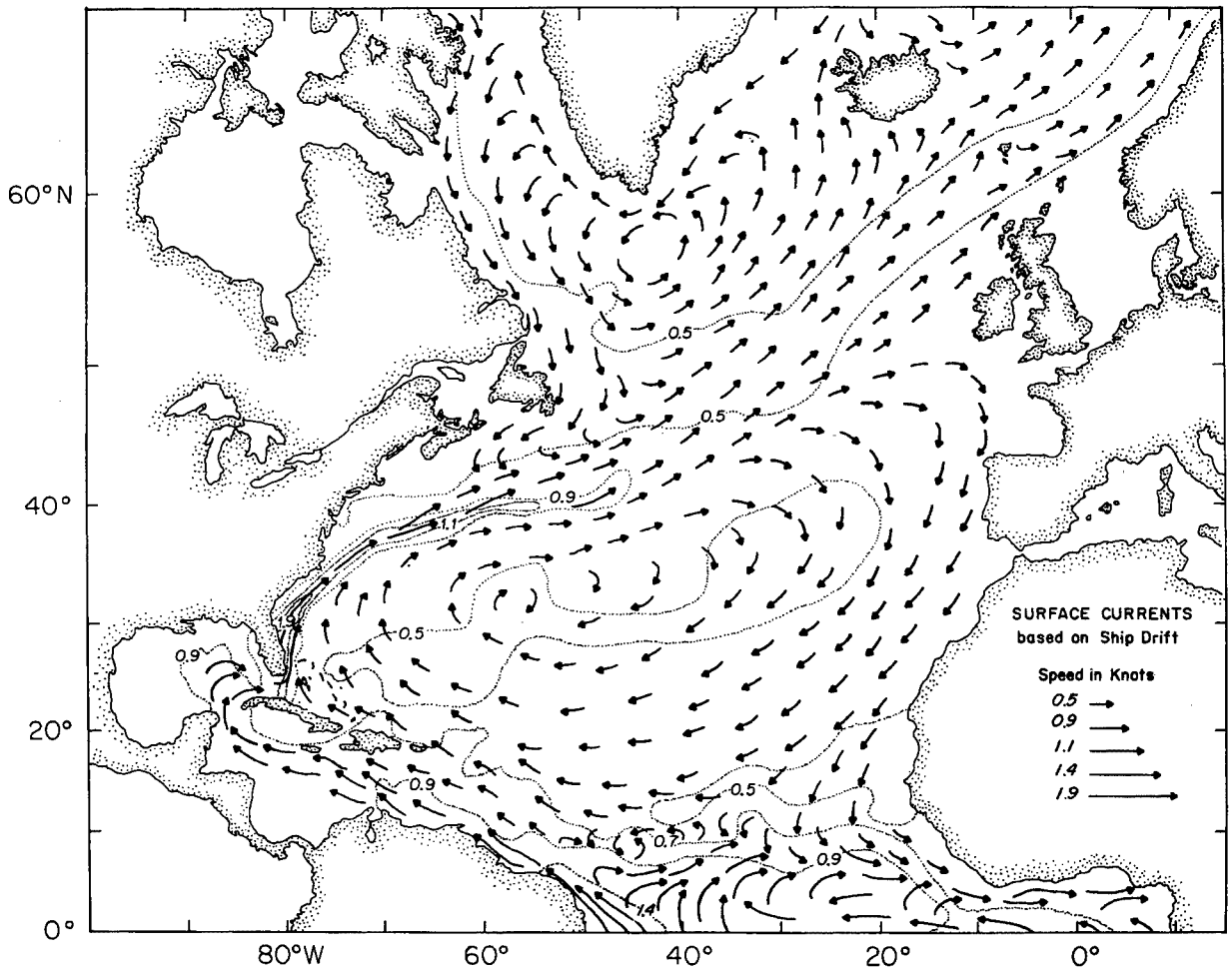

Figure I-14: A smoothed map of averaged surface currents for the North Atlantic, adapted from a map of surface currents for the North Atlantic based on ship drift data for the summer (figure I-5, p. 24 in U.S. Naval Oceanographic Office Publ. 700, 1965). Arrows indicate flow direction, contours and arrow length indicate flow strength (magnitude, in knots).

are not clearly present in Figure I-14. Examples would be the Northern Recirculation Gyre of the Gulf Stream (or Slope Water Gyre), as well as the southern recirculation of the Gulf Stream, although there is an Antilles Current in Figure I-14. Note the cross-equatorial flow. Figure I-14 also contains a subpolar gyre in more or less modern-day form including a North Atlantic Current (NAC) with flow into the polar seas as is the state-of-the-art picture today. Figure I-15 is an early version (Sverdrup *et al.*, 1942) of upper layer transports for the North Atlantic circulation. This presentation (I-15) includes the Slope Water Gyre (or northern recirculation of the Gulf Stream) as well as

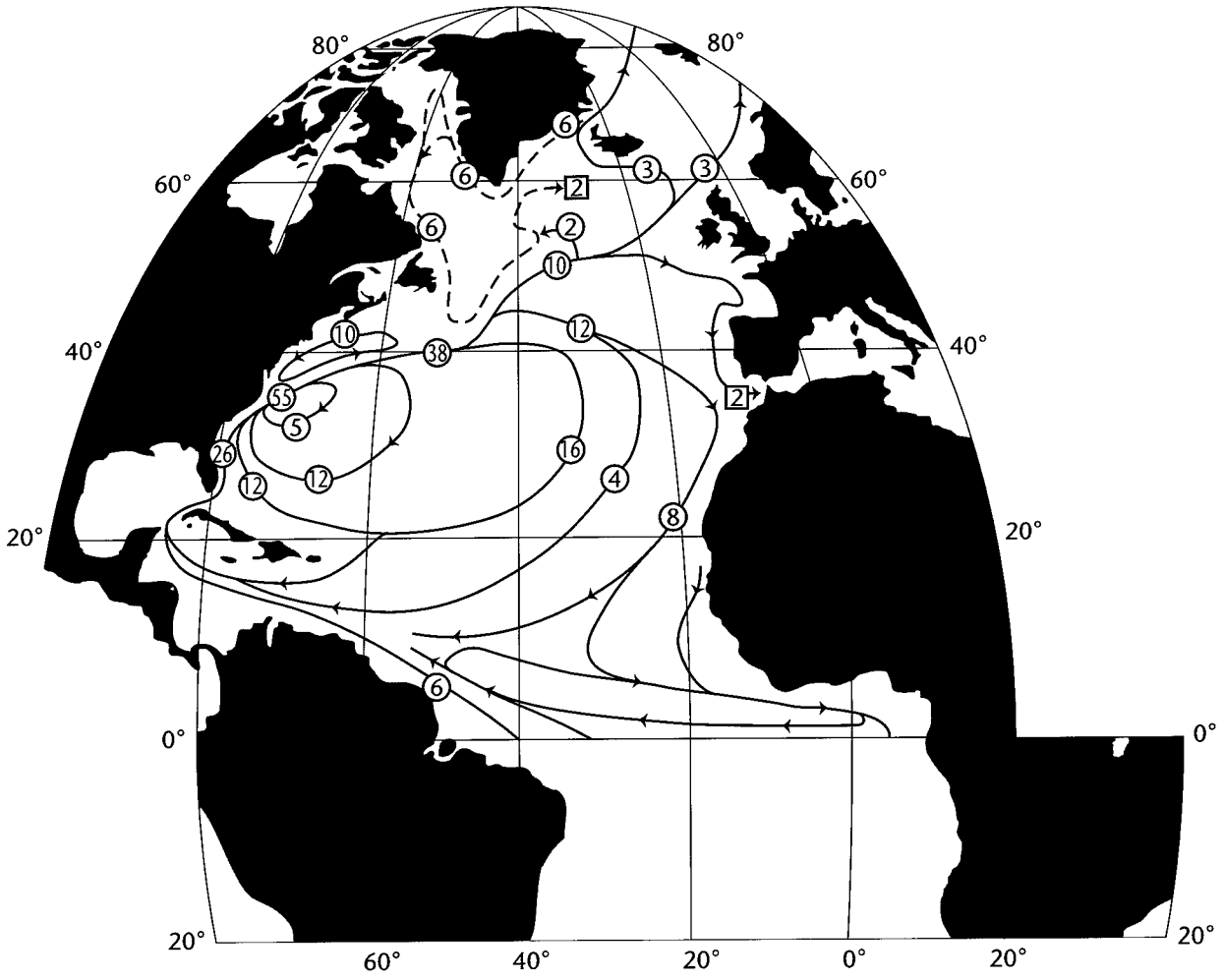

Figure I-15: Transports (numbers in Sverdrups in circles attached to lines with arrows, numbers in squares indicate sinking) for the upper layers in the North Atlantic Ocean, adapted from Sverdrup *et al.* (1942, figure 187, their p. 684).

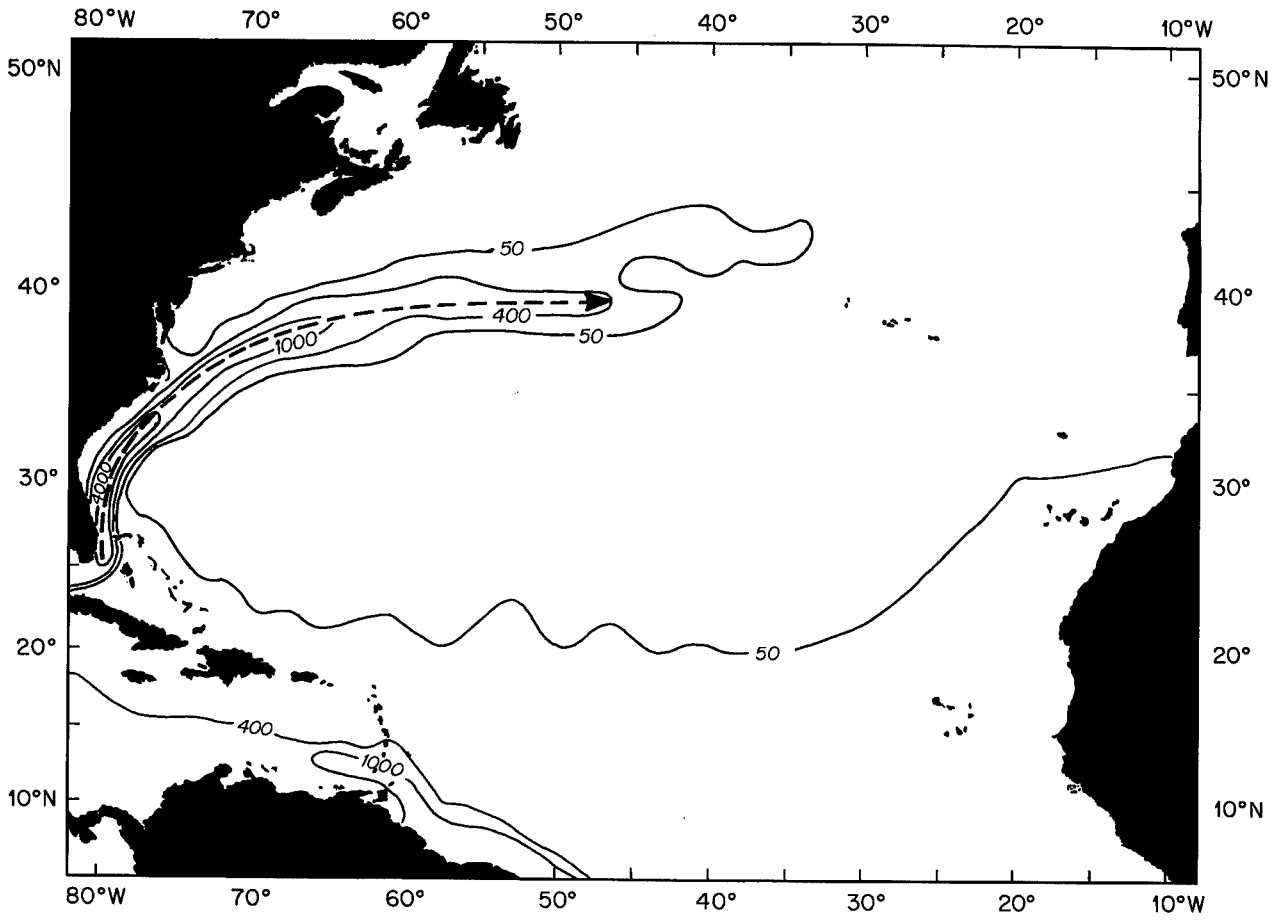

Figure I-16: Kinetic energy of the mean flow (K_M, in cgs units) in the North Atlantic at the sea surface, based on ship drift data. Adapted from Wyrtki et al. (1976) and Schmitz et al. (1983). K_M is defined in the text in standard fashion.

a recirculation south of the Gulf Stream, cross-equatorial flow, Labrador and Irminger Currents and a subpolar gyre.

The kinetic energy (per unit mass, hereafter understood) of the mean flow ($K_M = \bar{u}^2 + \bar{v}^2/2$) at the sea surface for the North Atlantic is shown in Figure I-16 ($\bar{u}$ and $\bar{v}$ are the mean zonal and meridional currents). The kinetic energy of the eddy field ($K_E = \overline{u'^2} + \overline{v'^2}/2$) for the North Atlantic at the sea surface is shown in Figure I-17 ($u' + v'$ are the deviations from the temporal (or combined space-time) means, $\bar{u}$ and $\bar{v}$). Figures I-13, I-16 and I-17 are all based on ship drift data and have been described and discussed in various forms by Wyrtki *et al.* (1976), Schmitz *et al.* (1983) and

Schmitz (1996). Many other surface currents based on ship drift data (and "similar measures" of surface currents with surface drifters) have been published (for example, Richardson, 1981, 1989; Richardson and McKee, 1984; Richardson and Walsh, 1986). Peter Niiler and colleagues used especially accurate surface drifters over the last 10–20 years (*e.g.*, Niiler *et al.*, 1987 and 1996; Poulain *et al.*, 1996). Maps of eddy kinetic energy at subsurface depths in the North Atlantic Ocean are located in Section 9 of this volume of my report.

Portions of a very influential map of the general circulation of the western North Atlantic according to Iselin (1936) are shown in Figure I-18. Stommel's (1957) idealized two-layer circulation for the entire Atlantic Ocean is shown in Figure I-19. The general elements of I-19 are contained in the similar, but observationally based, maps

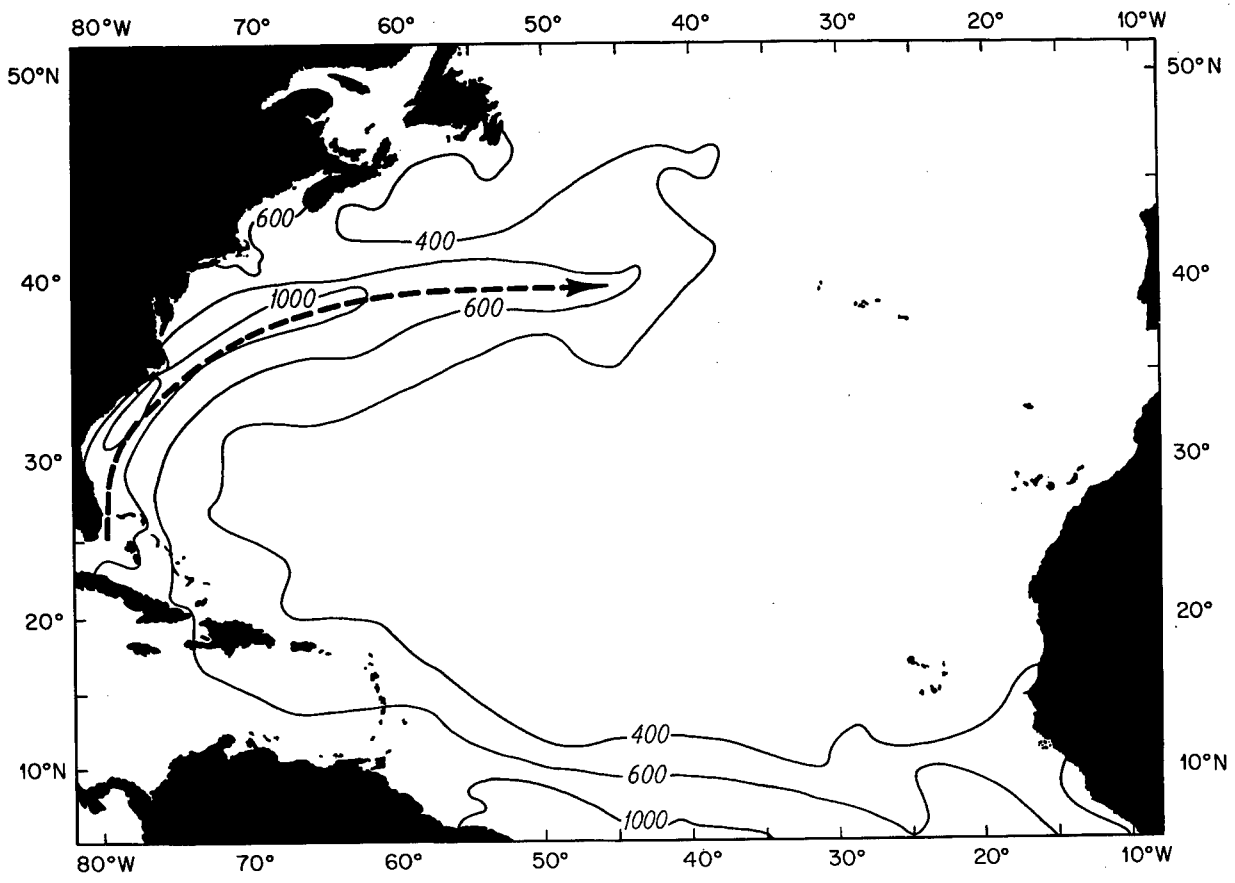

Figure I-17: Kinetic energy of the eddy field (K_E, in cgs units) at the sea surface in the North Atlantic. Adapted from Wyrtki *et al.* (1976) and Schmitz *et al.* (1983). K_E is defined in the text in standard fashion.

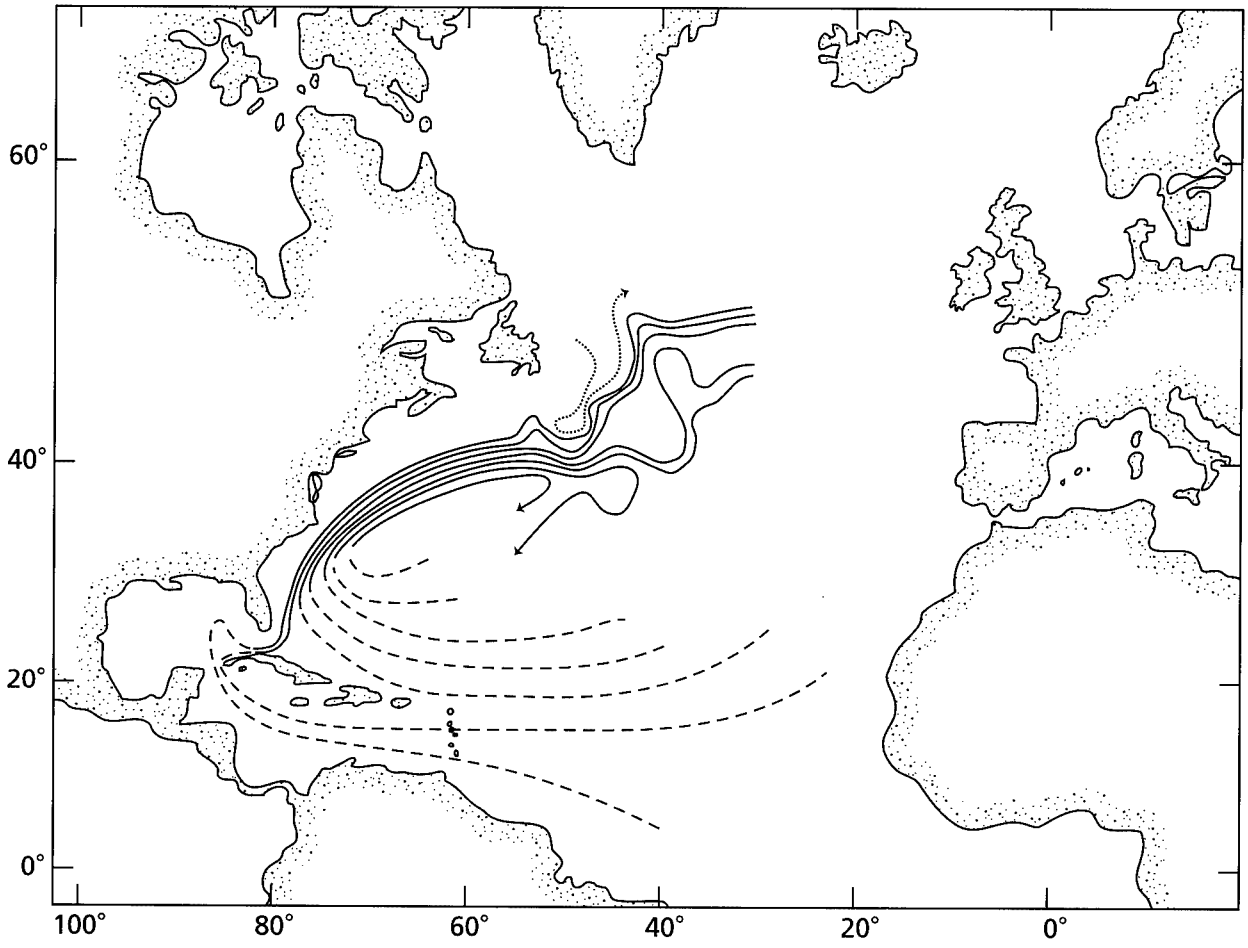

Figure I-18: A map of the quasi-permanent western North Atlantic Circulation associated with the 0–2000 m depth range, adapted from Iselin (1936).

of Schmitz and McCartney (1993, hereafter SM93) and their updates in the following. In my opinion, as discussed later in this report, Figure I-19 along with the work and ideas that went into it, including his books on the Gulf Stream (Stommel, 1958, 1965), are the major results from a generation of physical oceanography. Fuglister (1960, 1963) published the seminal collection of hydrographic data in the Atlantic for the early post-World War II era. A more recent treatise on the North Atlantic Circulation (Worthington, 1976) contains, for example, total transport streamlines (Figure I-20) for the entire North Atlantic. This treatise is overly restrictive of intergyre and interbasin exchanges both within the North Atlantic and between the South and North Atlantic Oceans (Clarke *et al.*, 1980; Schmitz and Richardson, 1991, hereafter SR91; Schmitz, 1995; SM93). I feel that Worthington's most interesting contributions to the North

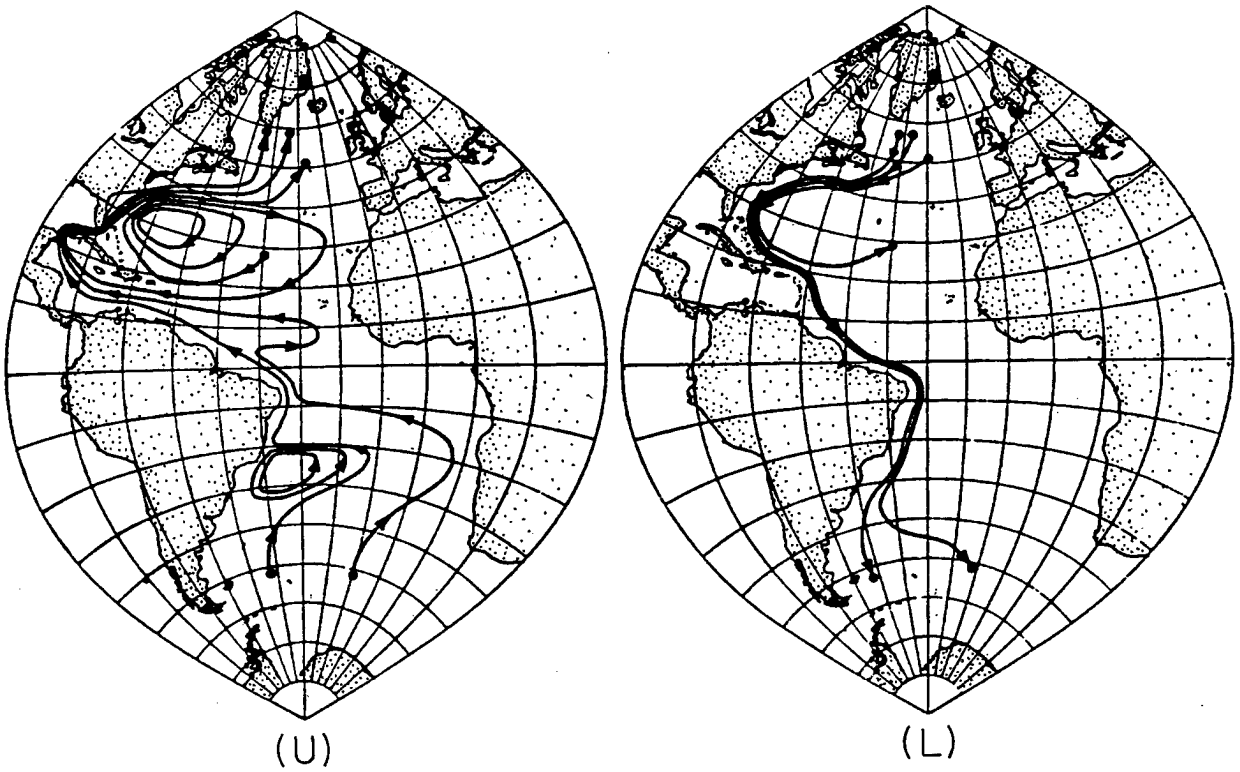

Figure I-19: A two-layer transport streamline field (~10 Sv contour interval) schematically taken from Stommel (1957); (U) denotes upper layer and (L) denotes lower. Small circles denote the sinking of NADW in the northern North Atlantic, upwelling elsewhere.

Atlantic circulation are contained in his hydrographic and water mass atlases (Wright and Worthington, 1970; Worthington and Wright, 1970). In particular, several plates from these atlases were used as illustrative figures (I-4 through I-6) earlier in this report. The atlases by Fuglister and Worthington are most useful, and very high quality. Dietrich's (1969a, 1969b) atlas of the northern North Atlantic contains a wealth of important information as does his textbook (Dietrich *et al.*, 1980). More recent atlases of hydrographic data for the Atlantic have been published by Levitus (1982, also global) and Lozier *et al.* (1994, 1995).

An updated version of a transport schematic (adapted from SM93, their figure 8) for the upper layer general circulation of the North Atlantic Ocean (~ 0 to 800 m in the subtropical gyre; temperatures > 7°C, say) is contained in Figure I-21, and for selected deep currents (~ 2000–4000 m depth, say) in Figure I-22. One feature of the "update" in Figure I-21 involves a modified path (Reid, 1978, 1981, 1994; Tsuchiya,

1989) for Mediterranean Water (~ 1 Sv at the source according to Bryden and Kinder, 1991). The 1 Sv of MOW entrains at least 1 Sv from the ambient water present as it plunges down the slope so that the net circulation (Price and Baringer, 1994) is at least 2 Sv, but only 1 is taken in Figure I-21 to flow north, primarily joining the North Atlantic Current (NAC). The other 1 Sv or so of MOW is assumed to be part of a gyre-like circulation of intermediate water (see below). The major new features are related to the circulation in the northern North Atlantic, discussed in more detail later. Note, however, that Figure I-21 (as well as figure 8 from SM93) does not contain a subpolar gyre, both for simplicity and because the part of the subpolar gyre not connected to the replacement flow in the NAC is typically colder than 7°C. A "new" (color) scheme, relative to SM93, for different pathway components is used here. Red indicates the

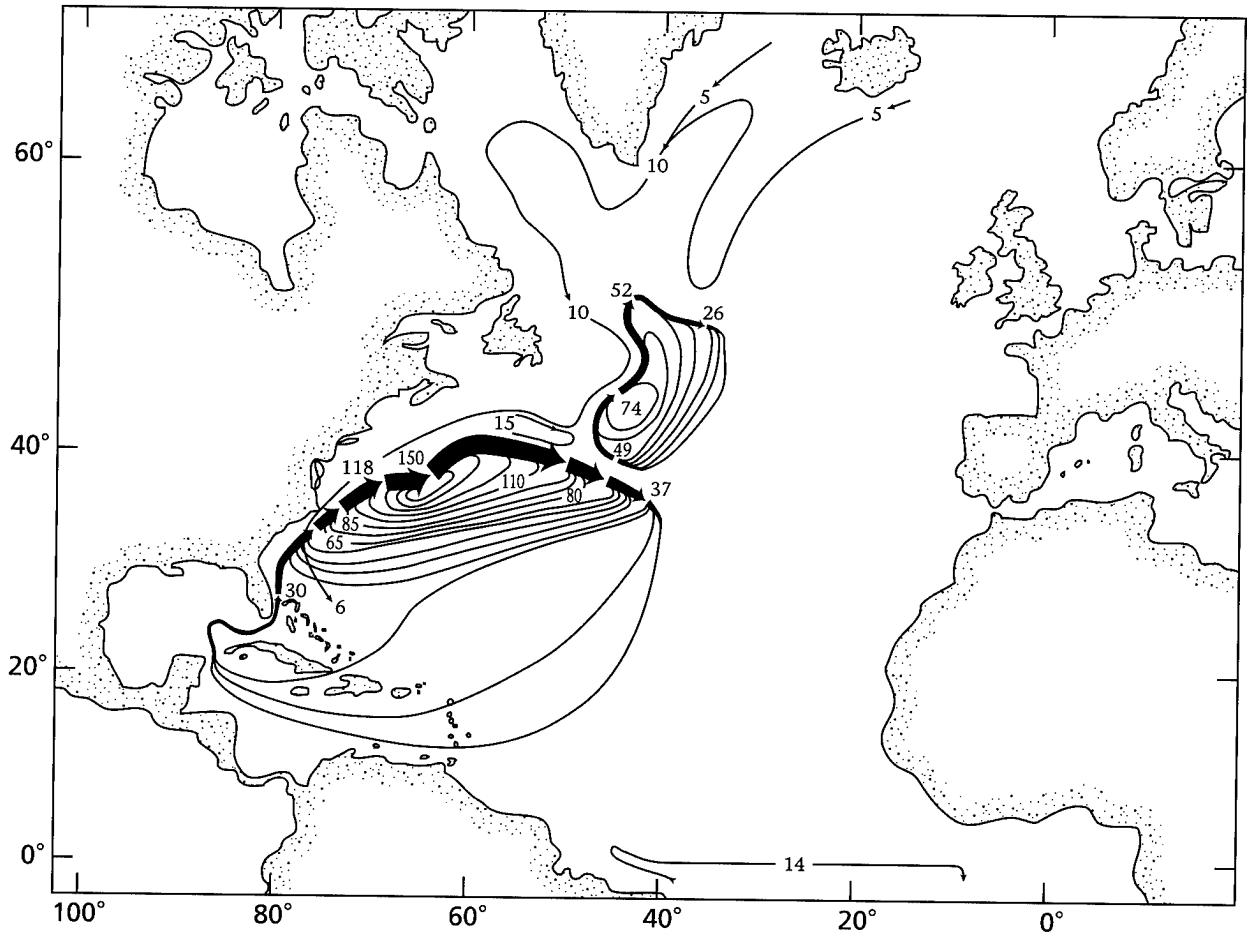

Figure I-20: Total transport streamlines (in Sverdrups) for the North Atlantic Circulation, adapted from Worthington (1976).

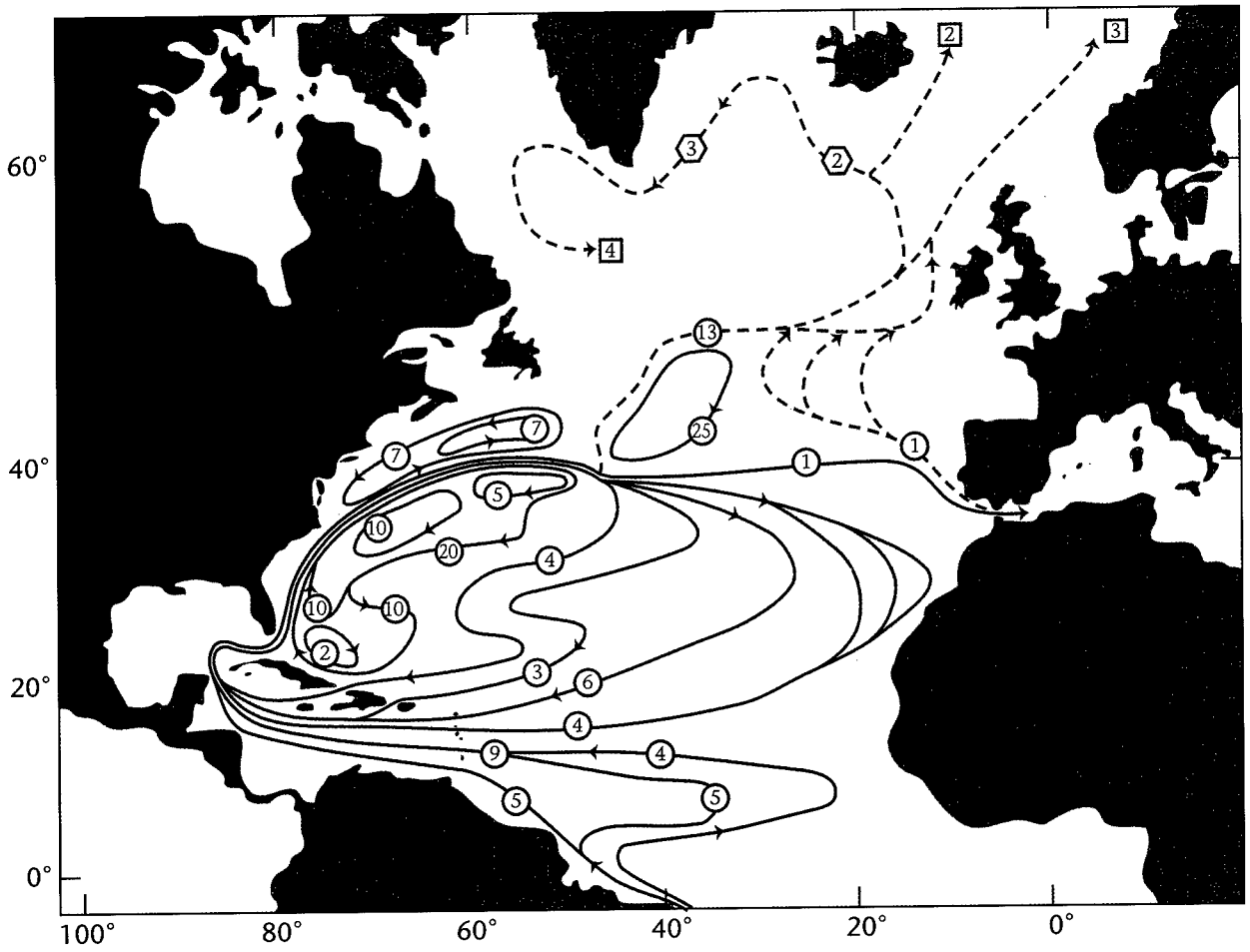

Figure I-21: Upper layer (temperatures greater than ~ 7°C) transports for the North Atlantic (Schmitz and McCartney, 1993; this is an update of their figure 8). Transports in circles are in Sverdrups. Transports (Sv) in squares denote sinking and a hexagon denotes entrainment. Red lines denote the replacement flow for the meridional cell involving NADW, the latter formation being shown in blue boxes attached to dashed red lines, which indicate that significant cooling may take place. Solid green lines characterize the subtropical gyre and recirculations as well as the Newfoundland Basin Eddy. Dashed blue lines denote the addition of Mediterranean Water to the system.

path of the upper layer flow ($T \geq 7°C$) that participates in deep water formation, with the solid line denoting subtropical flow and the dashed lines subpolar and polar flow, the latter denoted by blue squares. Hexagons indicate entrainment of the upper layer replacement flow by the overflows. Green solid lines indicate closed, "non-thermohaline," flows, which include the Slope Water Gyre(s), the Newfoundland Basin Eddy (the southern recirculation of the North Atlantic Current) and the Antilles Current as part of the southern recirculation of the Gulf Stream. Dashed blue lines indicate that part of

the path of Mediterranean Water that contributes (primarily) to UNADW formation, although some MOW influence is possibly present in the replacement flows entrained by the overflows, and in SPMW, or even to the component of the NAC entering the polar seas. I haven't tried to show all of this because I'm not dealing with fractions of a Sverdrup transport-wise, and frankly I don't have a quantitative picture of the fractional splits anyway.

Some major topographic features of the North Atlantic, which strongly affect the deep currents in Figure I-22, are depicted in Figure I-23. My exposure to the character-

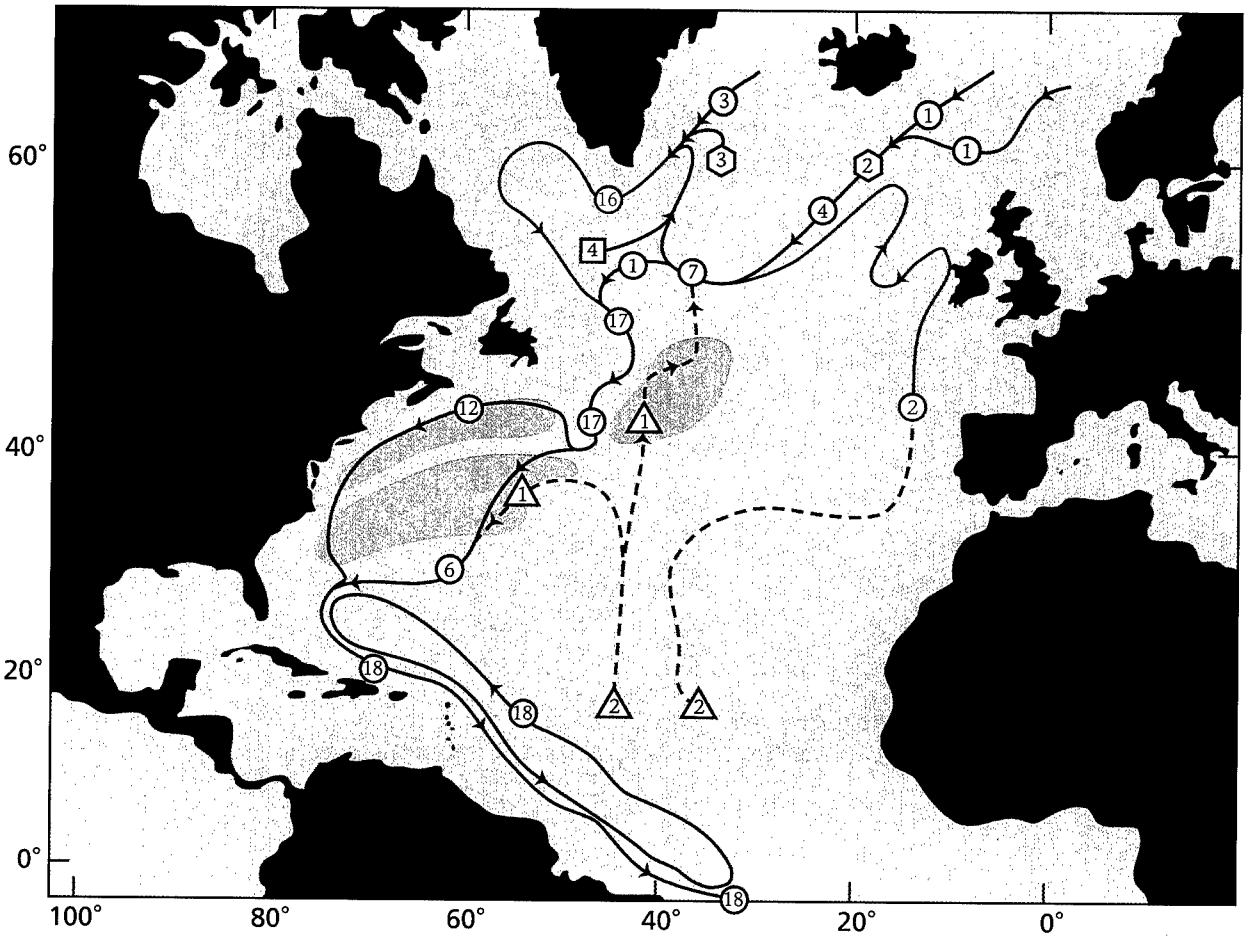

Figure I-22: Circulation schematic for NADW (1.6° – 4°C), based on SM93 figure 12a. The deep recirculating gyres in figure 10 of SM93 were added in the form of areas colored light blue. Green denotes NADW, dark blue is bottom water, light blue lines are used when NADW is also bottom water, red hexagons indicate entrained AAIW (modified) or SPMW or perhaps even NACW. Squares represent sinking and triangles represent upwelling. Transports are in Sverdrups.

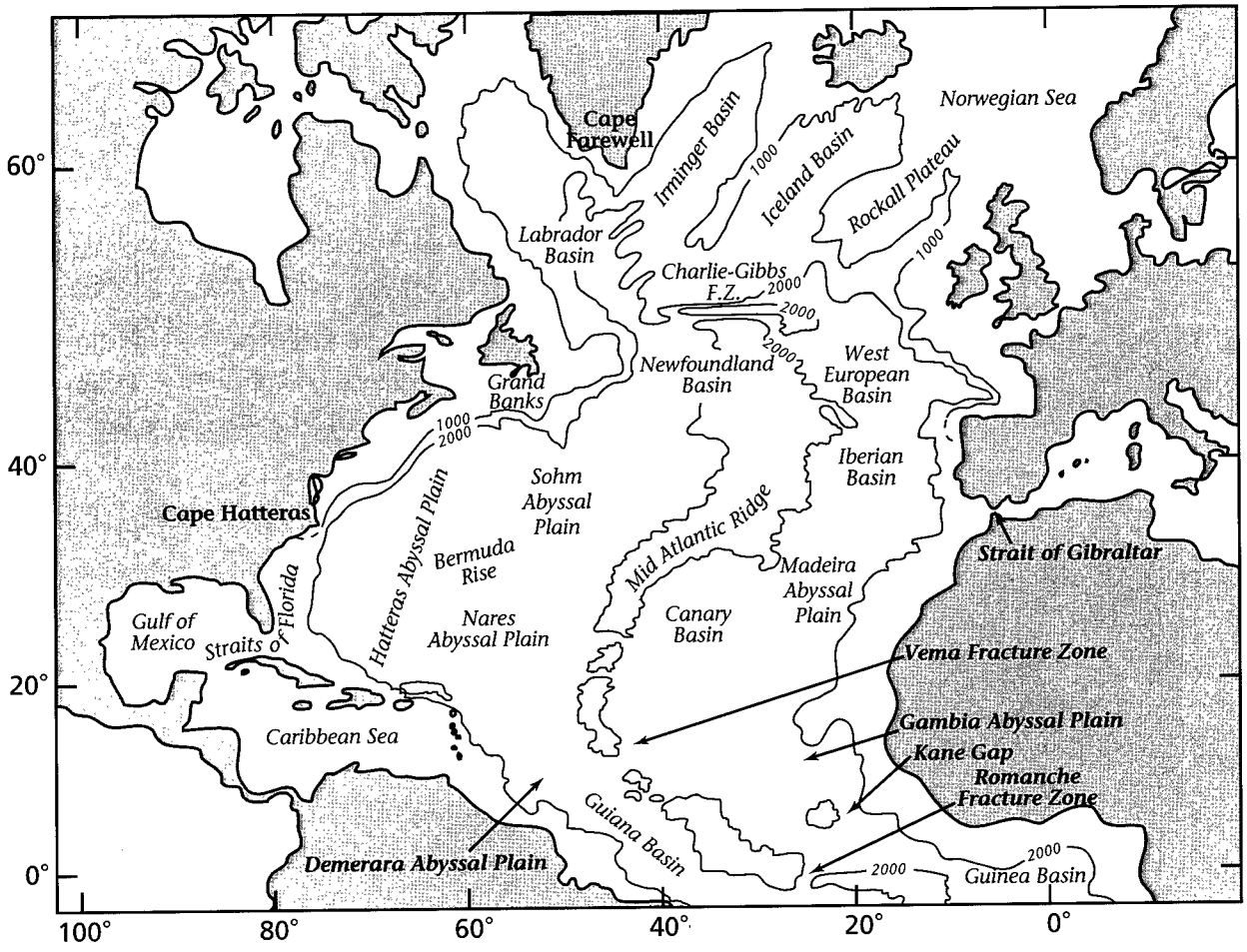

Figure I-23: A topographic and feature nomenclature map for the North Atlantic.

istics of the deep circulation of the North Atlantic, as contained for example in Figure I-22, which is also an update of a similar figure by SM93, has been strongly influenced by interactions with my colleague Mike McCartney, and in my opinion McCartney (1992) wrote a prominent recent article in that regard (see also McCartney, 1996), especially in the context of deep recirculations. Figure I-22 is intended to depict the circulation involving NADW formation, not all of the deep and bottom circulation in the North Atlantic. Swallow and Worthington (1957) published the first measurements of a deep western boundary current. Reid's (1994) Atlantic Ocean total transport streamlines are shown schematically in Figure I-24. I have modified this figure somewhat in the vicinity of the equator and selected fewer contours.

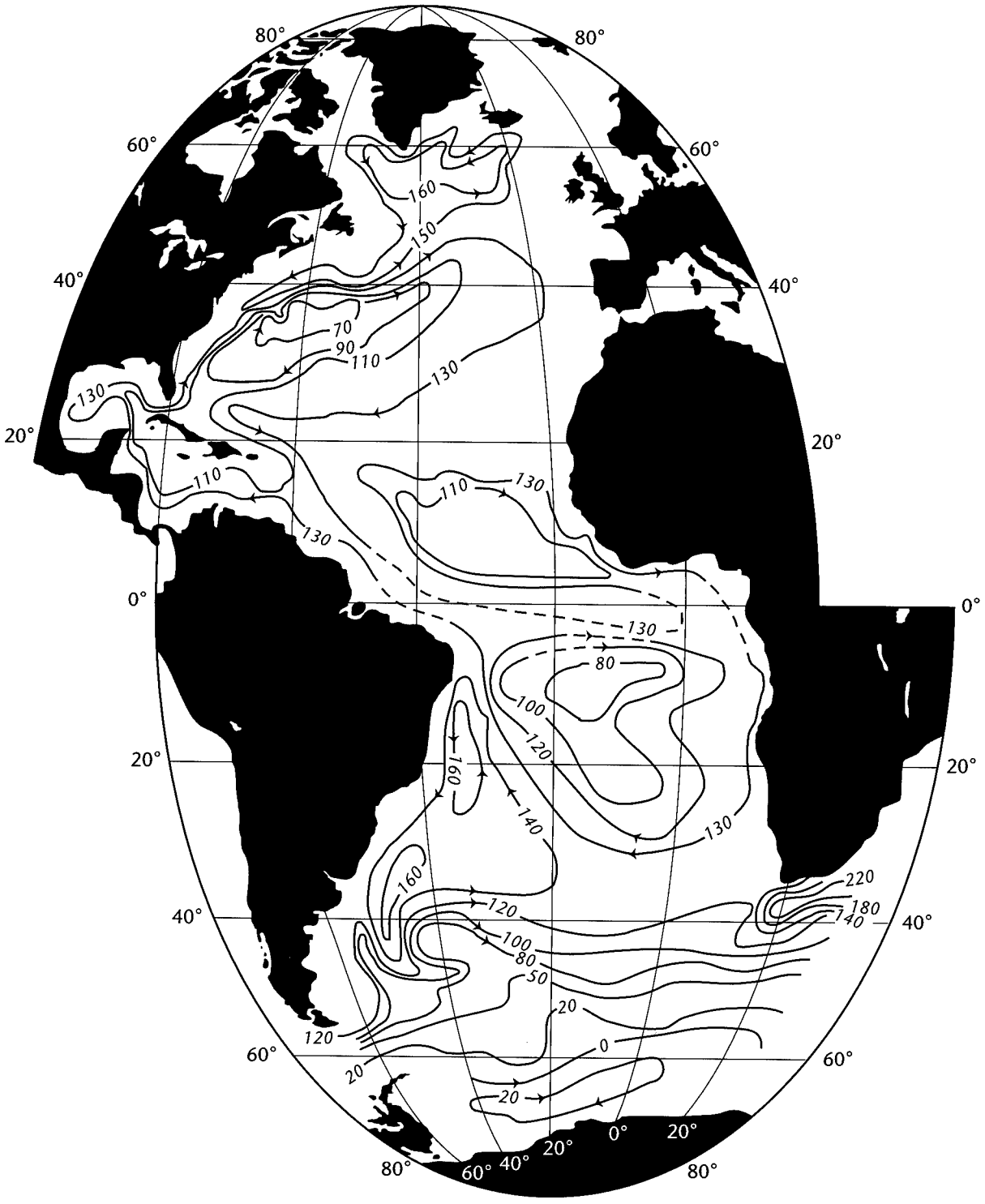

Figure I-24: Transport streamlines (in Sverdrups) for the Atlantic, adapted from Reid (1994).

4. The North Atlantic Subtropical Gyre

As noted above, every closed ocean basin except for the North Indian has a quasi-permanent clockwise (counterclockwise in the southern hemisphere) circulation at mid-latitudes, primarily but not entirely in the upper 1000 m or so depth range. Deeper penetrations of wind-driven currents occur in Western Boundary Current Regions like the Gulf Stream System (GSS) and may be associated with recirculation(s). Subtropical Gyres exist at mid latitudes, say between 15 and 40°N, moving water poleward in the west and equatorward in the east; they occupy roughly the area from the east coast of continents (the west side of ocean basins) to the west coast of the next continental land mass (the east side ocean basins). A prominent feature of subtropical gyres that shows up clearly in surface current maps (like Figures I-1 and I-14) and/or transport maps like Figures I-18 through I-21 is that they are not symmetrical. Particularly strong currents occupy the westward 25–50% or so of these flow patterns, *i.e.*, currents in subtropical gyres are westward-intensified (first explained by Stommel, 1948). Western boundary currents are also maintained or even strengthened while existing as free "zonal jets" when they are the northwestern limb of subtropical gyres (*i.e.*, the downstream increase in transport of the Gulf Stream, see Stommel, 1958, 1965; Worthington, 1976, or Knauss, 1969, for example). Actually, subtropical gyres in the North Atlantic and North Pacific Oceans

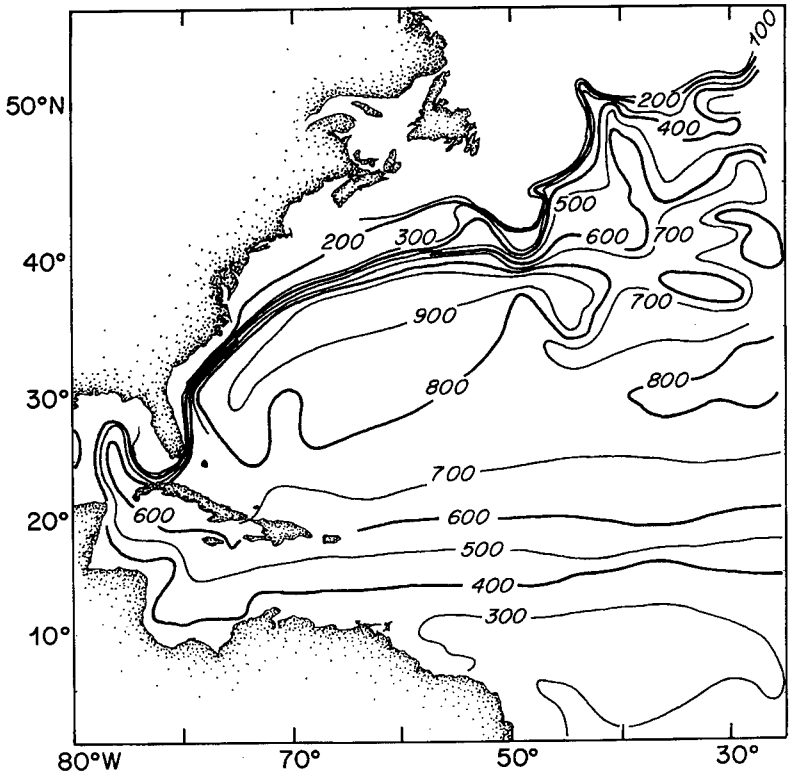

Figure I-25: 10° isotherm depths (in meters) in the western North Atlantic according to Iselin (1936).

are basically northwestward-intensified, especially in the North Atlantic, where strong currents extend quite far eastward (zonal jets), even at depths to the ocean bottom. The Agulhas Current System (ACS) in the South Indian Ocean has upper layer transport and density structure similar to the GSS (Schmitz, 1996). Westward intensification is a general global feature of all large-scale current systems at all depths, but there are global asymmetries in subtropical gyres involving weaker systems in the South Pacific and South Atlantic Oceans, as discussed in later volumes of this report.

The earliest definitive map (to my knowledge) with a recirculation south of the Gulf Stream is due to Iselin (1936), Figure I-18; please also note Figure I-15. Worthington (1976) strongly emphasized this feature (see also Stommel *et al.*, 1978). Schmitz (1977, 1978, 1980) directly observed and discussed portions of the southern recirculation, as well as the westward flowing segments at 55° W and 70° W of a Slope Water Gyre or recirculation north of the Gulf Stream. It was also clear early on (Schmitz *et al.*, 1970; Schmitz, 1976, 1978, 1980; Wyrtki *et al.*, 1976) that current fluctuations or eddies are most energetic in the vicinity of strong, large-scale currents at *all* depths. Sub-basin scale recirculating gyres, along with large and spatially very inhomogeneous eddy kinetic energies (K_E), were shown (Holland, 1978, 1979; Schmitz, 1978; Schmitz and Holland, 1982) to be related to eddies in numerical general circulation models (GCMs) that simulated the Gulf Stream System. Some type of mean westward flow suggesting a cyclonic gyre (certainly the westward flow component thereof) in Slope Water was indicated by early current meter data (Webster, 1969, his figure 4; Luyten,

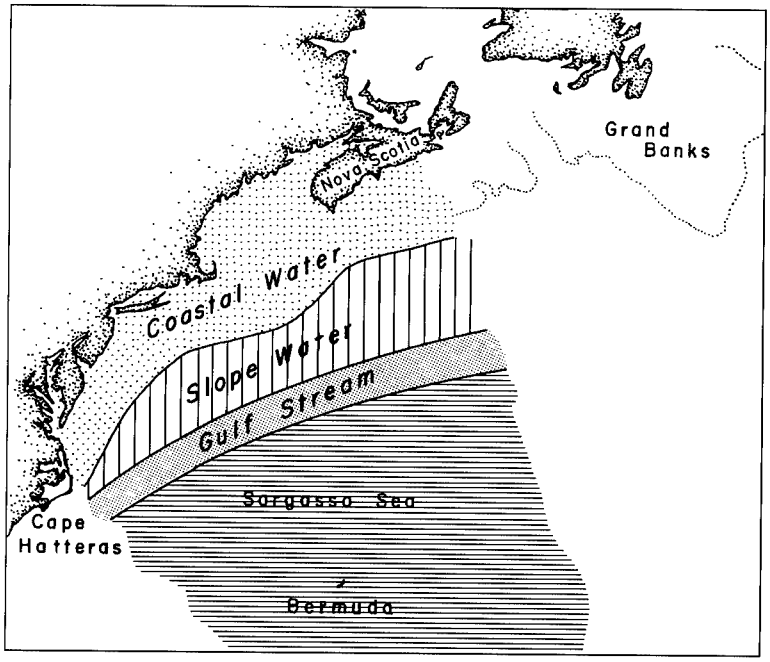

Figure I-26: Water mass location and nomenclature in the western North Atlantic, according to Iselin (1936).

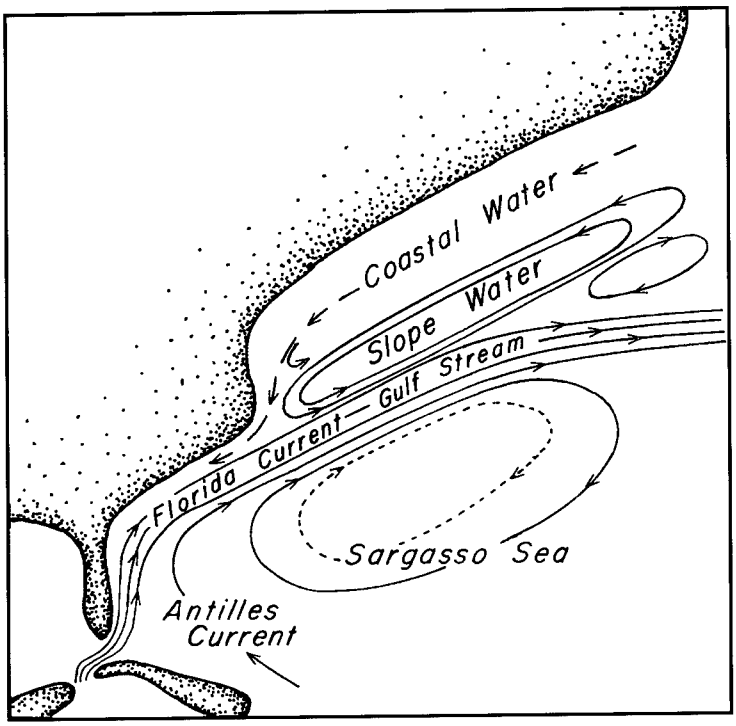

Figure I-27: Current and water mass nomenclature and location in the western North Atlantic, according to Sverdrup *et al.* (1942).

Both recirculations and energetic eddies are prominent features of the western segments of ocean basins at all depths (Schmitz *et al.*, 1983; McCartney, 1992; SM93; Hogg and Johns, 1995). As indicated above, the combination of the Gulf Stream, its recirculations, and associated eddy field is called here the Gulf Stream System (GSS). The recirculations (defined to be that part of the flow field added to the Florida Current) both north and south of the Gulf Stream contain the

1977, his figure 10; Schmitz, 1977, his figure 6 and p. 26; 1978, his figure 1), and more definitively by Hogg (1983) using current meter data as well as dynamical arguments (see also Pickart and Hogg, 1989). The northern recirculation gyre(s) has (have) now been defined in considerable detail (Hogg, 1983; Hogg and Stommel, 1985; Hogg *et al.*, 1986; Pickart and Hogg, 1989; SM93).

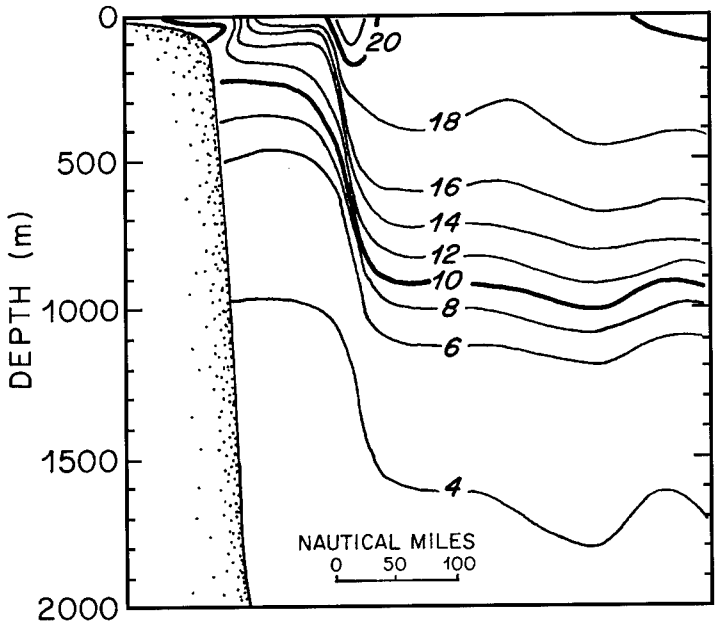

Figure I-28: A temperature (°C) profile across the Gulf Stream System from Chesapeake Bay to Bermuda, adapted from Sverdrup *et al.* (1942).

downstream increase in transport of the Gulf Stream, and include deep gyres (Figure I-22) that penetrate to the ocean bottom. In the upper ocean, the eddy field in the GSS is dominated by meanders plus ring formation and passage (Hogg, 1994; Hogg and Johns, 1995). The very strong current fluctuations (amplitude roughly a knot) in the abyssal GSS first observed directly by Schmitz *et al.* (1970) may be related to current meanders, either of the Gulf Stream and/or its recirculations, and/or associated with deep thermohaline currents. Energetic deep fluctuations, some associated with meanders of Deep Western Boundary Currents (DWBCs), have now been observed at a variety of locations in the vicinity of the DWBC (*e.g.*, Lee *et al.*, 1990, 1996; Pickart and Watts, 1990). In this report, DWBCs will be mostly, but not entirely, discussed independently of what I refer to as subtropical gyre circulations, which may also contain the upper layer replacement flow for DWBCs (and do so in the North Atlantic), completing "meridional cells."

Figure I-25 is an early map of the depth of the 10° isotherm in the western North Atlantic from Iselin (1936), defining the basic structure of the associated circulation. Figure I-26 defines the approximate boundaries of the water masses that preoccupied students of the circulation of the western North Atlantic. Figure I-27 is another "nomenclature" and schematic current pattern map of this area, from Sverdrup *et al.* (1942), and I-28 is a temperature section from the same source for the Chesapeake Bay to Bermuda line. Figure I-29 is an interesting first cut at partitioning the transport on the Chesapeake Bay to Bermuda section, an initial attempt to rationalize the source and structure of some of the downstream increase in transport of the Gulf Stream. Area A in Figure 29 includes only water with $T > 20°C$, and Area B only water

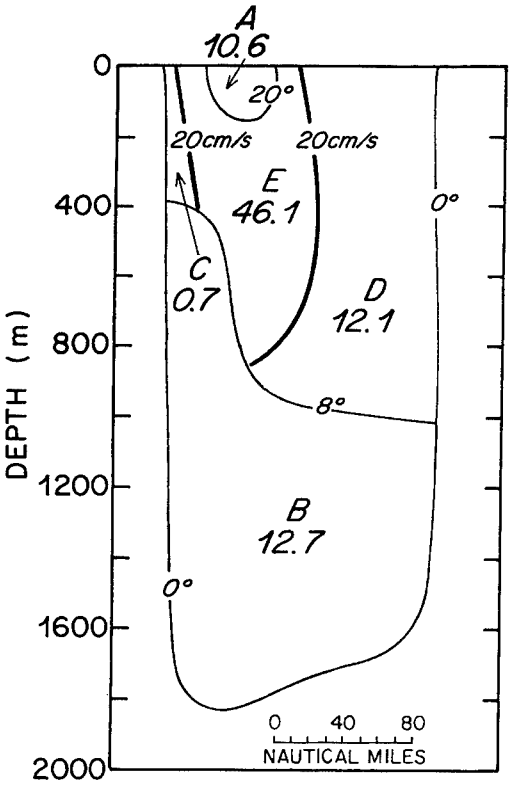

Figure I-29: A transport partitioning section across the Chesapeake Bay to Bermuda line, from Iselin (1936). Each of the areas A–E were assigned a transport (in Sv) as shown on the figure under the letter, and as discussed in the text.

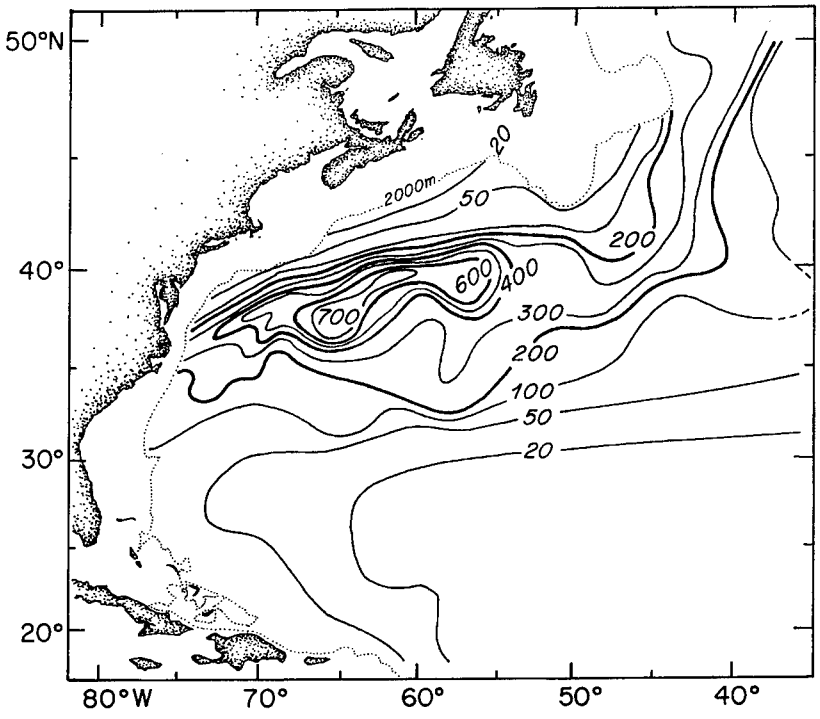

Figure I-30: A map of eddy kinetic energy per unit mass (K_E, units $cm^2\ s^{-2}$) near 700 m depth in the western North Atlantic, adapted from Owens (1984, 1991) and Richardson (1993).

colder than 8°C. Area D encompasses water having recently joined the Florida Current from the Sargasso Sea, and Area E is the "core" of the Current. Area C is a nearshore regime.

The zero-order discussion and rationalization of the large-scale flow in the entire Atlantic Ocean at both thermocline and abyssal depths (Stommel, 1957, 1958, 1965), as summarized in Figure I-19, does gloss over to some extent the role played by intermediate and bottom water, something that cannot as easily be done in other oceans. The two editions of *The Gulf Stream* (Stommel, 1958, 1965) formed for me the essential basis for what was known about the Atlantic Ocean and even the WOC prior to the observational surge of the last, say, 30 years. One of the main qualitative advances of the past few decades of ocean exploration is the clear identification of and emphasis on recirculations or sub-basin scale gyres along with mesoscale eddies throughout the world's oceans, especially for the North Atlantic Subtropical Gyre (Schmitz *et al.*, 1983; SM93; Schmitz, 1996), and the GSS is now recognized as the prototypical area of this type (Hogg and Johns, 1995). Thermohaline and interbasin circulations (Gordon, 1986; Schmitz, 1995) are now on the "front burner" in physical oceanography.

Schmitz and McCartney (1993) have presented several summary maps of the North Atlantic Circulation that include the transport structure of the Subtropical Gyre for a variety of layers. The North Atlantic subtropical gyre circulation, although dominated by a 100–150 Sv quasi-horizontal cell, can't really be closed satisfactorily with-

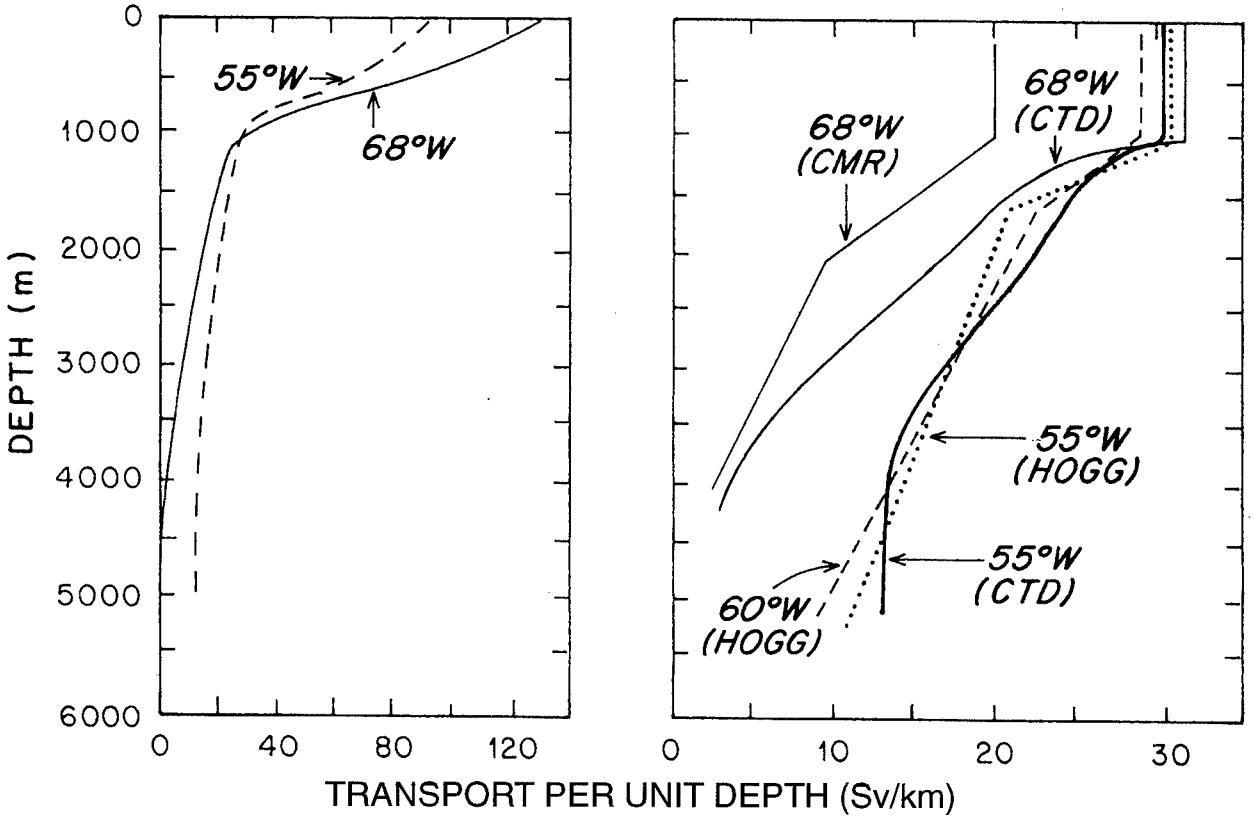

Figure I-31: The downstream development (from 68°W to 55°W) of the vertical structure of the transport of the Gulf Stream, adapted from figure 5 by Hall and Fofonoff (1993). Transport per unit depth (Sv/km); left frame from CTD stations at 68° and 55°W, right frame including in addition the current meter results (CMR) at 68°W (Hall, 1986; Hall and Bryden, 1985), at 60°W (Hogg, 1993), and current meter and CTD results at 55°W (Hogg, 1992).

out knowing the pathways of the ~ 20 Sv meridional cell that connects the South Atlantic and Subpolar North Atlantic. The modern identification of these pathways, now generally accepted but with details still to be determined, was contained in SM93, with the path cleared for this by SR91. Two of these maps (with some updates) were included in the introduction here as Figures I-21 and I-22 (please see also Figure I-12). Please note that Figures I-21 and I-22 do not contain a subpolar gyre circulation because of the definitions of the flows that are mapped (see below). Most of the general circulation maps and tables presented in this report will be for transport in various layers.

Wyrtki *et al.* (1976), Schmitz *et al.* (1983), and Schmitz (1996) have presented maps of K_E at the sea surface, two used above as Figures I-13 and I-16. A recent map of K_E for the mid-latitude western North Atlantic at 700-m depth (Owens, 1984, 1991; Richardson, 1993) is contained in Figure I-30. Over the last several years, a promising zero-order description and rationalization of the mesoscale eddy field has become available. Eddy energy is largest near strong flows (intensification not only in western boundary currents, but along their mid-latitude open-ocean extension), roughly as indicated by gyre-scale numerical models where eddies develop as a result of instability processes in the mid-latitude jet and then propagate into the ocean interior. My point of view is that mesoscale eddies in subtropical and subpolar gyres act as at least one of the energy sources for recirculations but do not play a crucial role in the dynamics of the mean flow in the ocean interior (in the North Atlantic, for example, the idea is that the downstream increase in transport of the Gulf Stream is at least partially eddy-driven but not the flow through the Florida Straits). The fluctu-

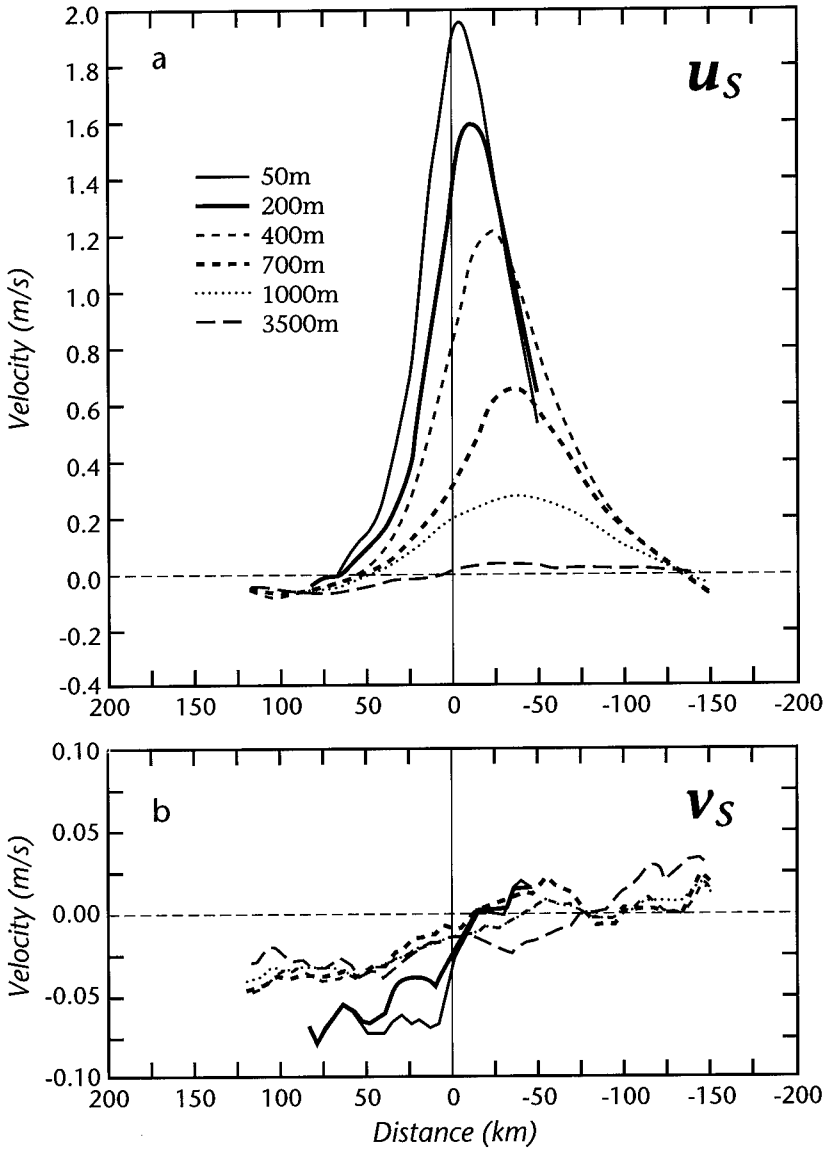

Figure I-32: Cross-stream profiles of averaged Gulf Stream currents at 68°W, from Johns *et al.* (1995); (a) along-stream current component u_s (cm s^{-1}) and (b) cross-stream current component v_S (cm s^{-1}).

ating response to forcing by variable winds might be perceived as forming the roughly horizontally homogeneous background signal in subtropical gyre interiors.

Subtropical gyres tend to have a directly wind-forced upper layer circulation transporting 20–40 Sv. This may be augmented by a thermohaline replacement flow component of 10–20 Sv. For strong WBCs like the GSS, a mixed instability develops that is the primary energy source for mesoscale eddies. These eddies in turn feed back to the mean flow resulting in recirculations that penetrate into abyssal layers. These recirculations are involved with a "downstream increase in transport" of around 50–100 Sv. Of course, dynamics other than eddy rectification may be important for these recirculations. My guess is that recirculations are more inertial in their westward segments where they are developing into "strong currents" and eddy-driven in their eastward regions where they are forming and the main "eastward jet" is decaying, the hot region for the instability process and where recirculations are initiated (see also Spall, 1996c). In this report (see Sections 6 and 7) it is also suggested, for the first time I think, that there exists a similar but not identical configuration for the North Atlantic Current System (or Subpolar Gyre Current System).

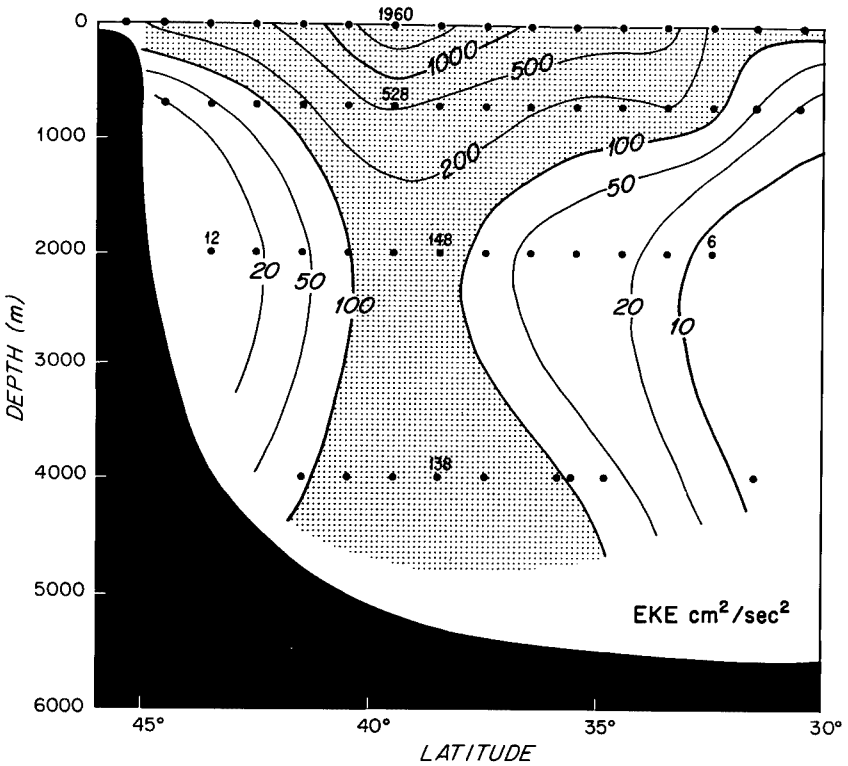

Figure I-33: A meridional section of K_E (contours in cm² s⁻²) across the GSS in the vicinity of 55°W, adapted from Richardson (1983).

There exist several interesting review articles on the GSS (Bane, 1994; Fofonoff, 1981; Hogg and Johns, 1995; Worthington, 1976). The article on western boundary currents by Hogg and Johns (1995) is a very valuable summary, not only for the GSS, but for WBCs at all depths throughout the global ocean. Hall and

Table I-3: Transport in 16 potential density anomaly classes at 68° and 55°W, along with area-averaged velocity of water in each class; also shown for each location are net transports for larger subclasses, from Hall and Fofonoff (1993).

	68°W			55°W		
σ_θ (kg m^{-3})	Transport (10^6 m^3 s^{-1})		$\bar{u}$ (m s^{-1})	Transport (10^6 m^3 s^{-1})		$\bar{u}$ (m s^{-1})
<26.00	7.03	15.17	0.90	—		—
26.00–26.25	8.14		0.85	—		—
–26.50	23.78		0.49	10.69		0.66
–26.75	11.53	45.88	0.52	21.10	44.44	0.53
–27.00	10.57		0.42	12.65		0.34
–27.20	6.98		0.38	6.12		0.32
–27.40	5.87		0.29	5.58		0.28
–27.60	5.07	35.28	0.22	5.53	36.86	0.20
–27.70	5.16		0.15	5.47		0.16
–27.74	5.07		0.13	6.10		0.14
–27.77	7.13		0.11	8.06		0.13
–27.80	7.38		0.09	10.33		0.13
–27.825	5.33	22.71	0.08	7.98	33.69	0.11
–27.850	5.07		0.07	8.28		0.10
–27.875	4.93		0.05	7.10		0.09
>27.875	6.15		0.02	24.10		0.07
Total	125			139		

Fofonoff (1993) describe the state of the art in our knowledge (Figure I-31 and Table I-3) of the downstream increase in the Gulf Stream transport. For orientation purposes, profiles of mean currents and a section of K_E across the Gulf Stream System are contained in Figures I-32 and I-33.

Several hydrographic sections and attendant results have been used (Hall and Bryden, 1982; Rintoul and Wunsch, 1991; Roemmich and Wunsch, 1985) to give us a

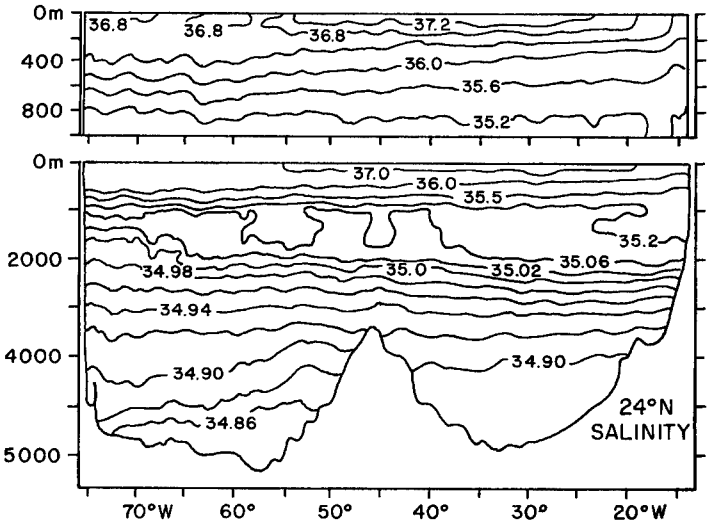

Figure I-34: A salinity (psu) section along 24°N in the Atlantic adapted from Roemmich and Wunsch (1985).

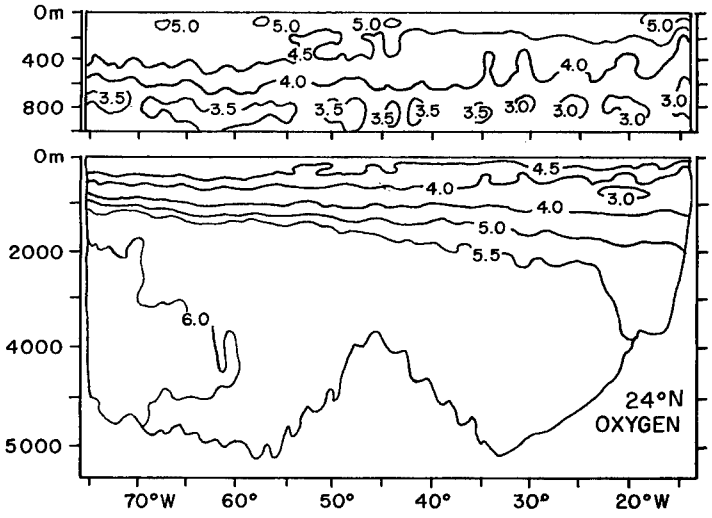

Figure I-35: An oxygen (ml L^{-1}) section along 24°N, adapted from Roemmich and Wunsch (1985).

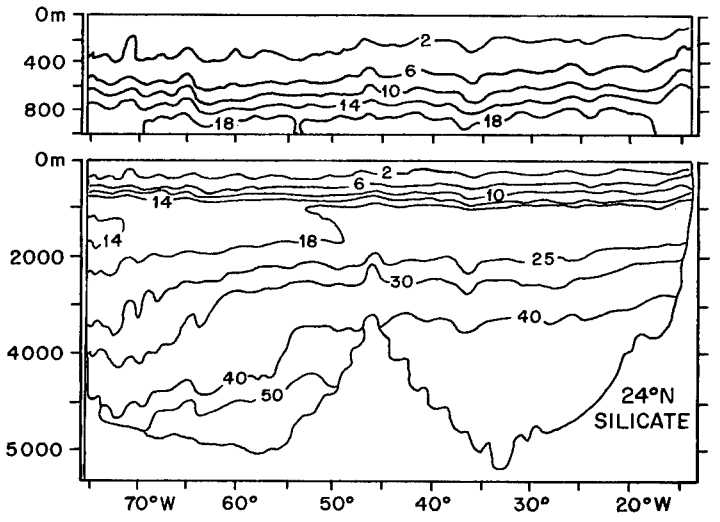

Figure I-36: A silicate (µg-at. L^{-1}) section along 24°N, adapted from Roemmich and Wunsch (1985).

comparatively sharp picture of the gyre interior across 24°N. Selected salinity, oxygen, and silicate contours are displayed in Figures I-34 through I-36. Results from this work along 24°N as well as data from the Caribbean Passages and Florida Current (Stalcup and Metcalf, 1972; Schmitz and Richardson, 1968) were used by SR91 and Schmitz *et al.* (1992) to connect clearly the tropical, subtropical and subpolar upper layer circulations of the North Atlantic with the South Atlantic for the first time. Their results are very supportive of the Stommel (1957) picture shown here as Figure I-19. Stommel's book (1958, 1965) is really a very nice introduction to the interior circulation of the North Atlantic as well as to the book's titular subject (*The Gulf Stream*). Stramma's (1984) maps of the circulation in the eastern North Atlantic are summarized here in Figure I-37. This paper by Stramma is a part of the basis of the circulation in Figure I-21.

Each "piece" of the North Atlantic Subtropical Gyre will now be briefly discussed separately. Other ocean basins will be discussed in Volumes II and/or III.

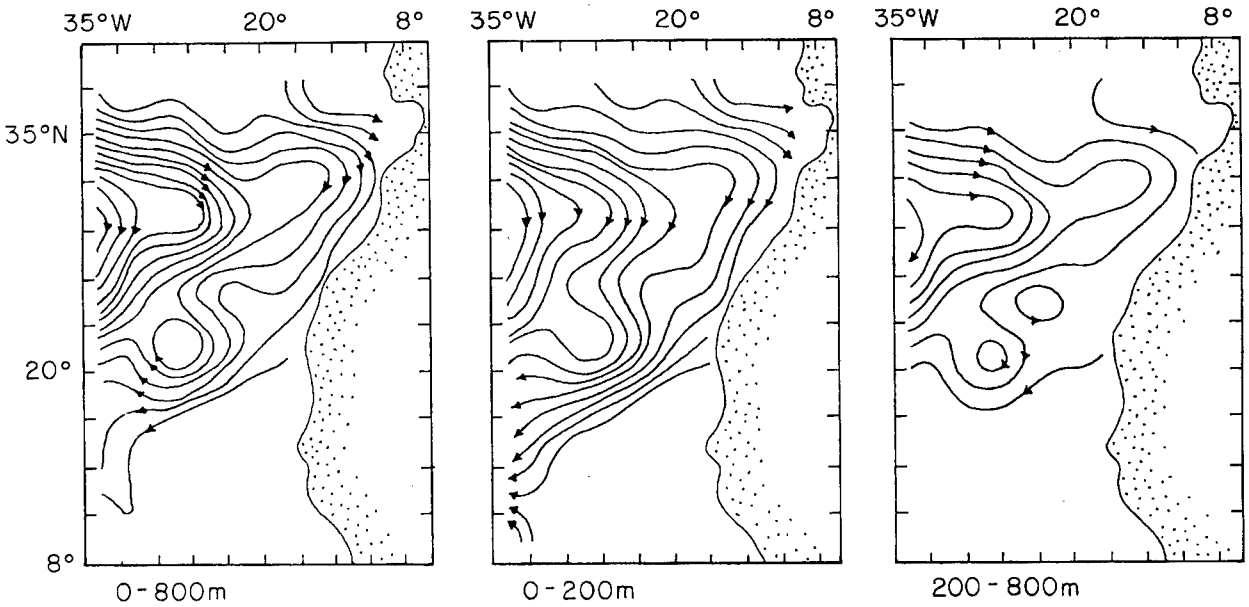

Figure I-37: Transport streamlines for the eastern North Atlantic, adapted from Stramma (1984). This is a combination of Stramma's figures 7, 8 and 9, for the indicated depth ranges. For 0–800 m, each flow line represents 1 Sv, for 0–200 m, 0.5 Sv, and for 200–800 m, 1 Sv. The total transport between 35°W and the coast is ~ 10 Sv.

4a. The Florida Current

Here the name "Florida Current" denotes that part of the GSS between the Gulf of Mexico and Cape Hatteras, probably the best documented component of the North Atlantic Circulation, particularly while in the Straits of Florida. General maps of pronounced current features and topography for the northern portions of this general area are shown in Figures I-38 and I-39, adapted from John Banes's (1994) review article.

There are lots of hydrographic sections across the Straits of Florida in the vicinity of Miami. Temperature (T), Salinity (S), Oxygen (O_2), and Silicate contours for one of the latest are displayed in Figure I-40. There are four prominent characteristics of the salinity distribution in Figure I-40b that indicate hydrographic origin. The S_{max} ($S \geq 36.6$ psu) on the eastern or offshore side of the Straits is typically associated with subtropical underwater. At the base of this maximum, for salinities 36.4 to 36.6 psu, and $17.9 \leq T \leq 18.2$°C, there is a comparatively thick layer of 18° Water

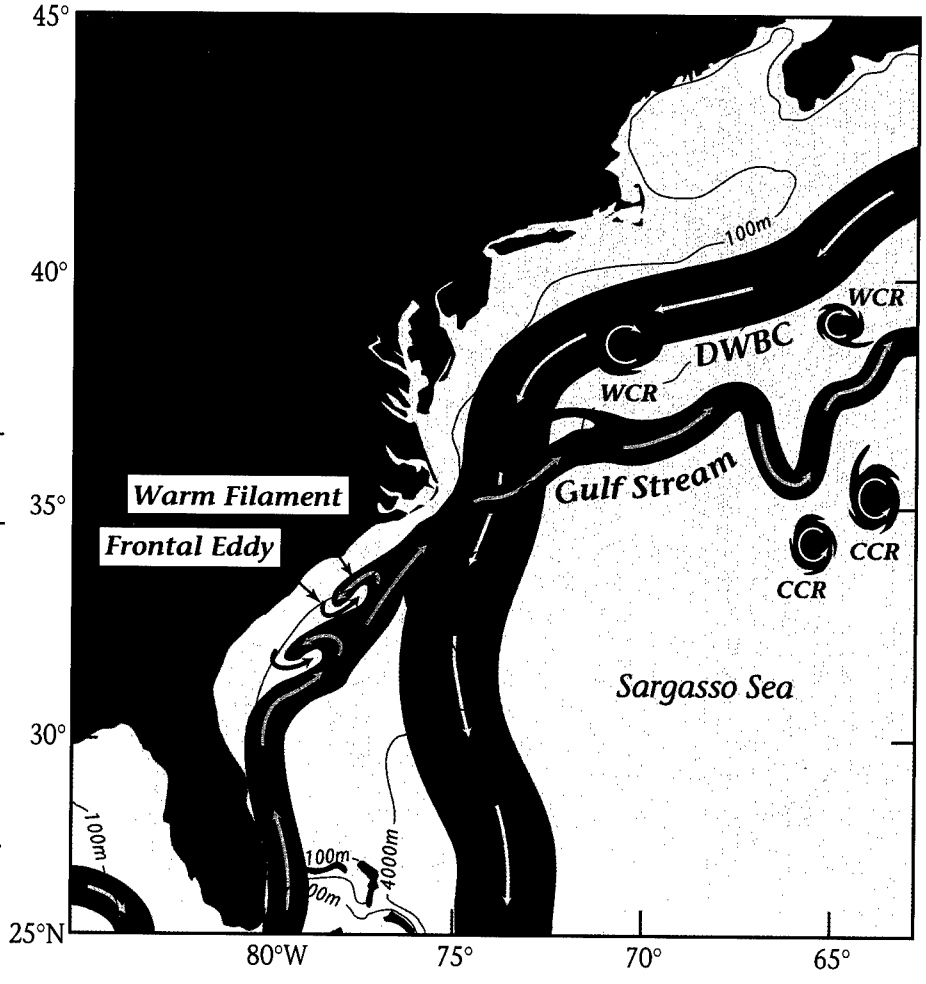

Figure I-38: The major current features in the westernmost North Atlantic, according to Bane (1994). CCR denotes cold core ring, WCR warm core ring, DWBC Deep Western Boundary Current. Depth contours in meters.

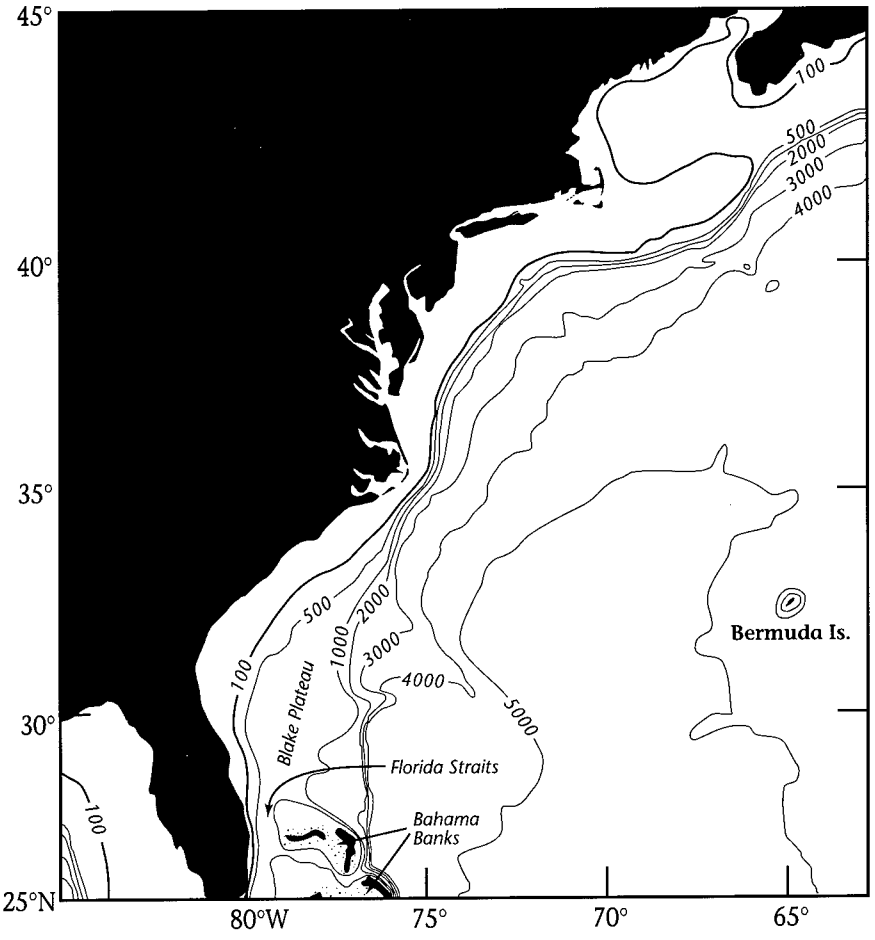

Figure I-39: Bathymetry in the region of Figure I-38, adapted from Bane (1994). Depth contours in meters.

(Worthington, 1959). Both of these components originate in the North Atlantic. Above the 36.6 isohaline (above the S_{max}) there is a comparatively fresh, thin upper layer. This layer occupies roughly the topmost 100 m depth of the Florida Current with salinities ~ 36.0 psu. These comparatively low salinities (for a surface layer, compared to the open North Atlantic) are primarily of South Atlantic origin (SR91) and include an Amazon River discharge influence. Below all this, there is a comparatively fresh "deep" layer ($6° \leq T \leq 15°$) with, in particular, a layer of $S < 35.0$ psu near the bottom, the latter often referred to as AAIW. But most of this water is above the salinity minimum and will be typically referred to in this report as "upper" intermediate water. These deep and bottom layers also have low O_2 and high silicate (Figures I-40c and I-40d). The hydrography of this layer (and others as well) in the Caribbean has been described by Morrison and Nowlin (1982). According to SR91 (see also Atkinson, 1983; Iselin, 1936; and Richardson, 1977), "upper intermediate water" with $T \sim 7$–$12°C$, $S \sim 34.88$–35.2 psu, and $\sigma_\theta \sim 27.0$–27.3 kg m^{-3} (along with perhaps some S_{min} AAIW with T < 7°C near the bottom) contains ~ 5 Sv (Tables I-3 and I-4) of South Atlantic origin within the Straits of Florida that also flows onto the Blake Plateau.

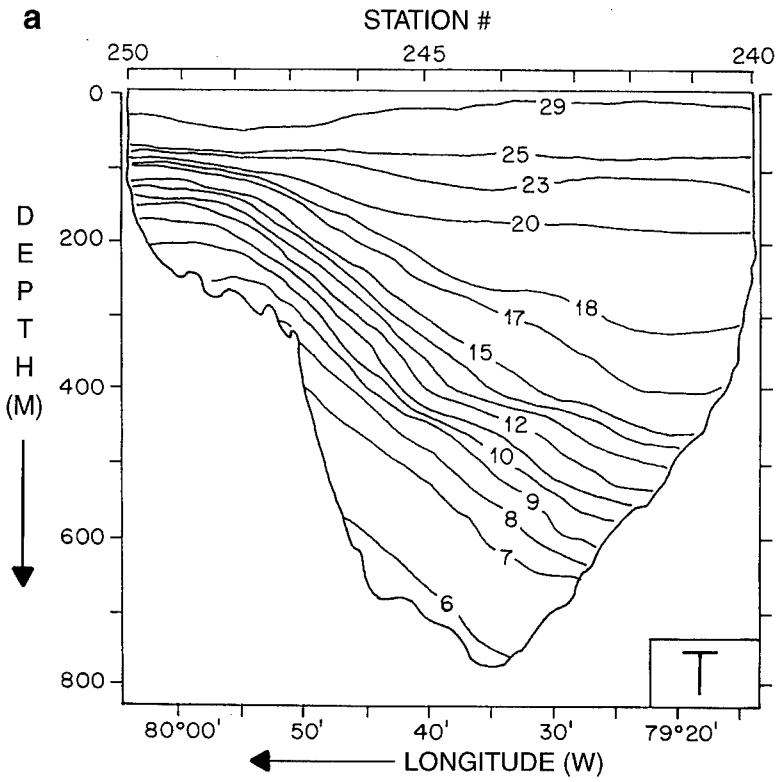

Figure I-40a: Selected contours for a section across the Florida Straits near Miami, as adapted from Roemmich and Wunsch (1985); Temperature (T, °C).

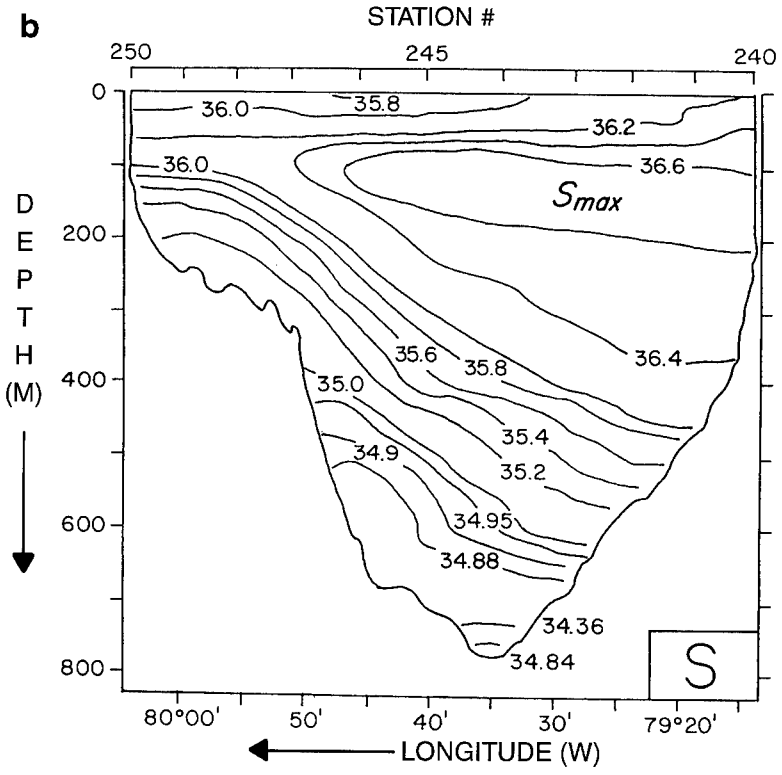

Figure I-40b: Selected contours for a section across the Florida Straits near Miami, as adapted from Roemmich and Wunsch (1985); Salinity (S, psu).

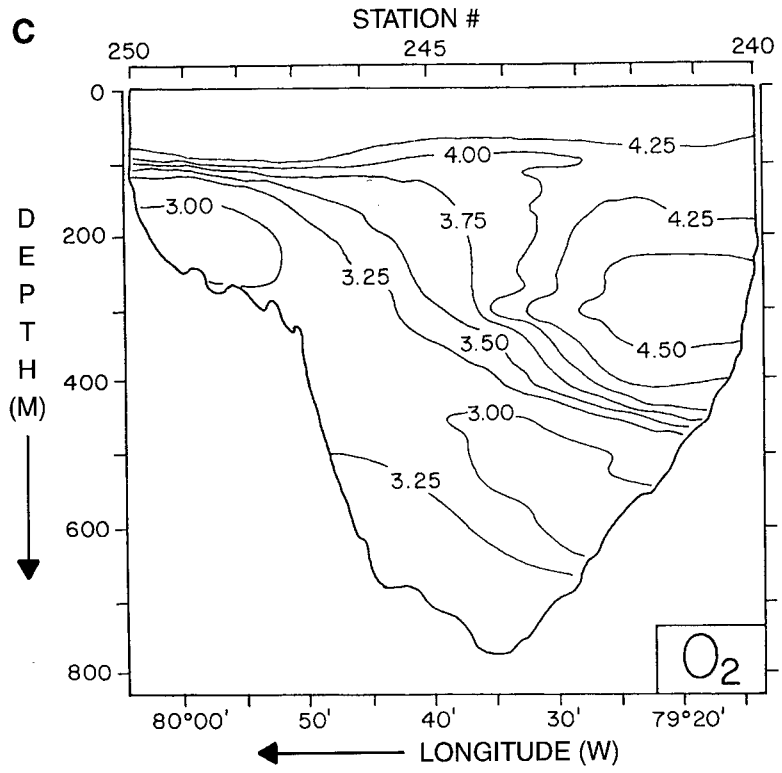

Figure I-40c: Selected contours for a section across the Florida Straits near Miami, as adapted from Roemmich and Wunsch (1985); Oxygen (O_2, ml L^{-1}).

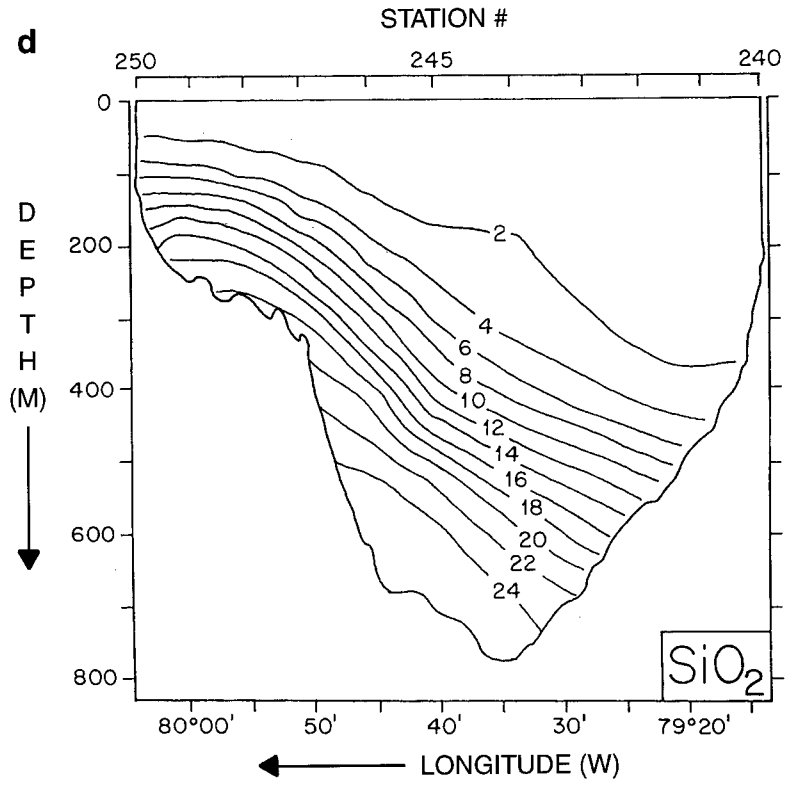

Figure I-40d: Selected contours for a section across the Florida Straits near Miami, as adapted from Roemmich and Wunsch (1985); Silicate (SiO_2, µg-at. L^{-1}).

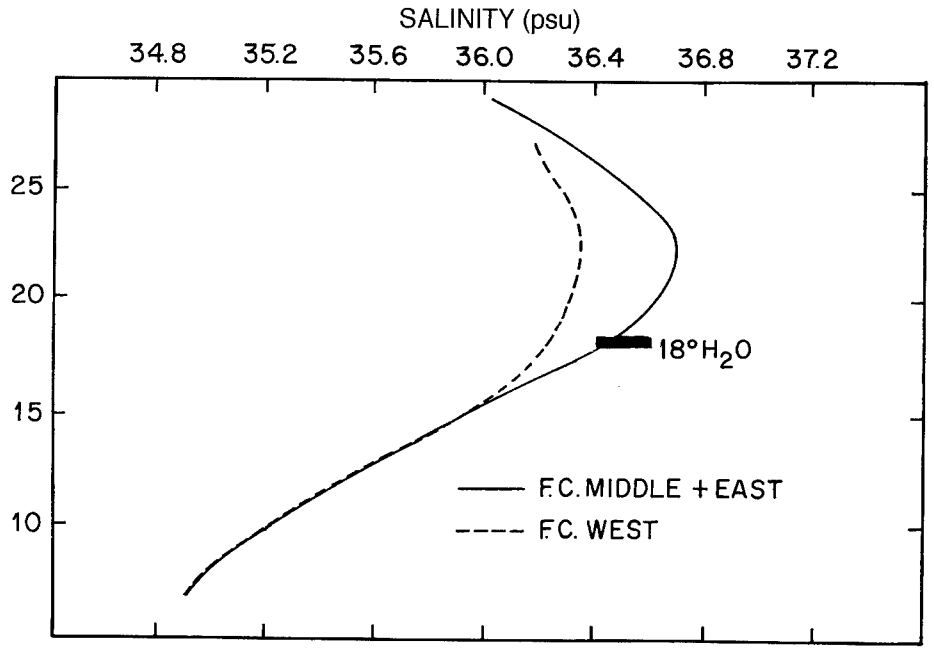

Figure I-41: Two generalized *T/S* curves for the Florida Current in the Straits of Florida in the vicinity of Miami, with the range of 18° Water according to Worthington (1959) superimposed.

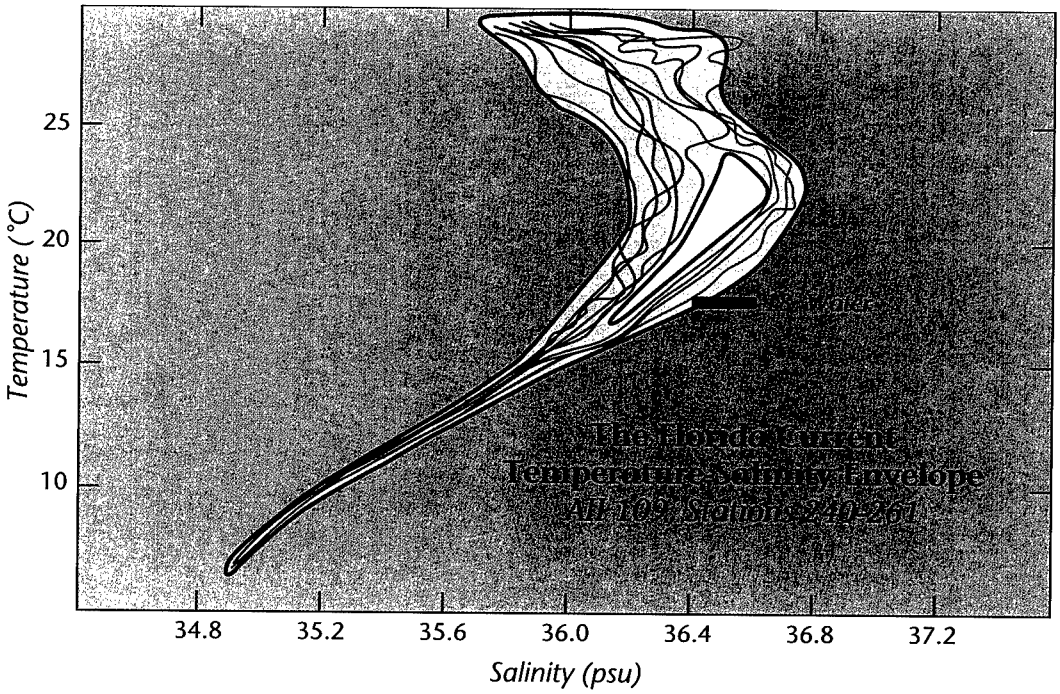

Figure I-42: The Florida Current *T/S* Envelope based on data collected by Roemmich and Wunsch (1985), adapted from Schmitz *et al.* (1993).

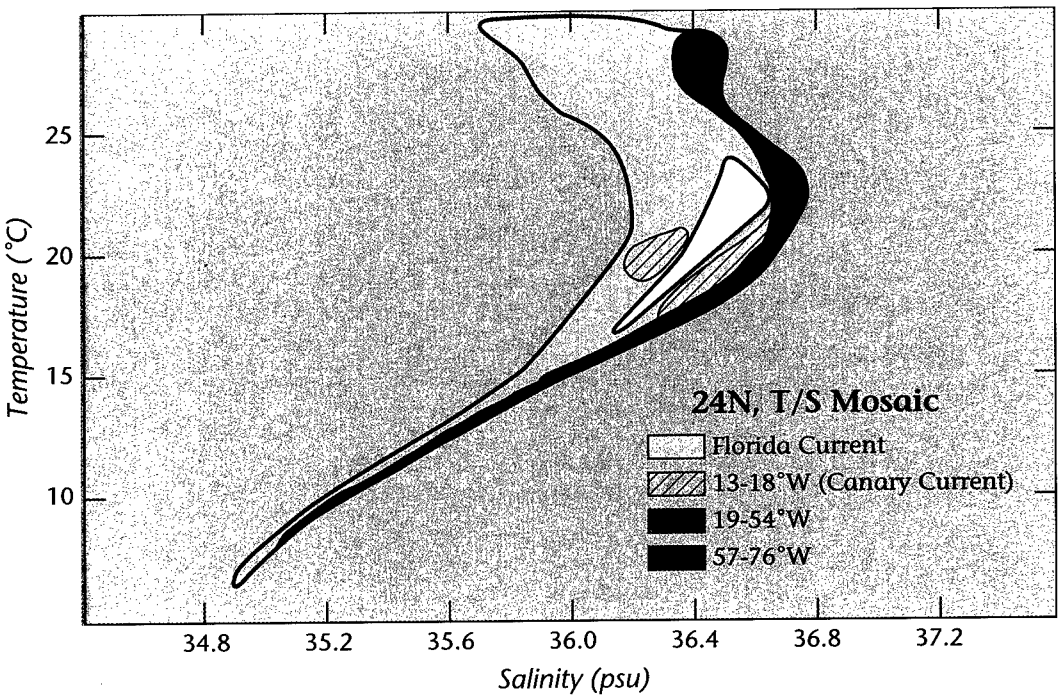

Figure I-43: The *T*/*S* envelope along the interior segment of 24°N, from data obtained by Roemmich and Wunsch (1985), adapted from Schmitz *et al.* (1993).

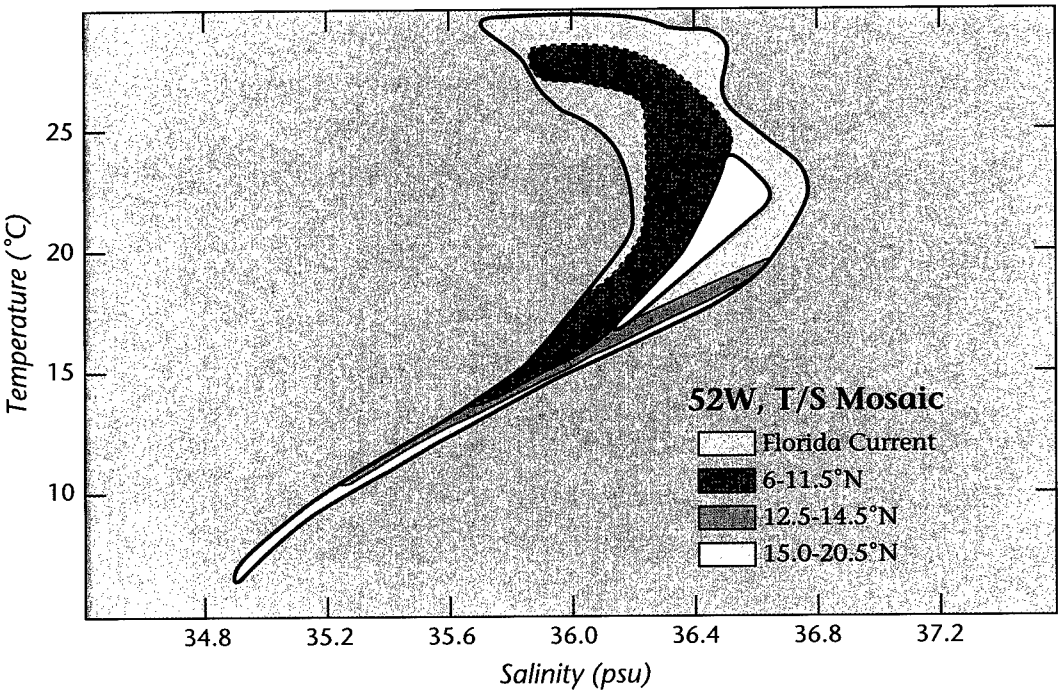

Figure I-44: The *T*/*S* envelope along 52°W, from the coast of South America north to about 20°N, adapted from Schmitz *et al.* (1993).

Table I-4: Average Florida Current transports in selected temperature intervals (ΔT) at 27°, 29°N and Cape Hatteras, adapted from Leaman *et al.* (1989)

Temperature interval	STACS (27°N)		FACTS (29°N)		Cape Hatteras	
	Absolute transport	Mean velocity	Absolute transport	Mean velocity	Absolute transport	Mean velocity
ΔT (°C)	T_s (x10^6 m^3 s^{-1})	$\bar{v}$ (m s^{-1})	T_F (x10^6 m^3 s^{-1})	$\bar{v}$ (m s^{-1})	T_{CH} (x10^6 m^3 s^{-1})	$\bar{v}$ (m s^{-1})
27.0–29.5	0	—	0.8	0.83	0	—
24.5–27.0	8.6	1.15	6.9	0.64	3.2	1.03
22.0–24.5	3.1	1.12	4.5	0.55	8.5	0.61
19.5–22.0	3.0	1.12	4.2	0.52	7.8	0.68
17.0–19.5	4.5	0.86	5.4	0.38	19.1	0.57
14.5–17.0	3.8	0.77	4.4	0.36	10.4	0.57
12.0–14.5	2.8	0.61	3.3	0.31	7.7	0.48
9.5–12.0	2.3	0.45	2.5	0.21	6.3	0.38
7.0–9.5	1.7	0.38	1.2	0.11	5.8	0.27
4.5–7.0	0.1	0.23	0	—	8.5	0.12
2.0–4.5	0	—	0	—	16.4	0.04
Total	29.0		33.2		93.7	

STACS: Sub-Tropical Atlantic Climate Studies FACTS: Florida Atlantic Coast Transport Study

Table I–5: Transport–temperature range partitioning along 24°N prior to SR91

Temperature range (°C)	Florida Current transport (Sv)*	Florida Current transport (Sv)†	Caribbean interior transport (Sv)‡	24°N transport (Sv)*
>17	17.4	19.3	17	–9.5
12–17	6.6	6.7	6	–2.9
7–12	5.0	3.9	6	1.9
<7	0.5	—	—	–19.0
Sum	29.5	29.5	29	–29.5

*Hall and Bryden (1982). †Leaman *et al.* (1989). ‡Roemmich (1981).

The *T/S* curves in the Florida Current vary from one general type on the inshore edge of the current to another near the Bahamas (Parr, 1937; SR91; Wenneckens, 1959). The offshore or eastern type of *T/S* curve contains Subtropical Underwater and 18° Water and the inshore type of *T/S* curve does not. Subtropical Underwater and 18° Water are North Atlantic phenomena. A very general summary plot of these two *T/S* types using data taken in 1985 is shown in Figure I-41 (adapted from SR91), also indicating the location of 18° Water (Worthington, 1959). Canonical Florida Current *T/S* envelopes with various stations superimposed are contained in Figure I-42 (from Schmitz *et al.*, 1993). These curves are very stable in time. Schmitz *et al.* (1993) used this stability in comparing and contrasting various segments of the Florida Current *T/S* curves with those along 24°N in the interior North Atlantic (Figure I-43) and along 52°W (Figure I-44), as an aid in identifying the probable origin of various *T/S* ranges or classes. Basically, low salinity water is of South Atlantic and high salinity water is of North Atlantic origin. For the "lower layer" of 7–12° water, high silicate (see below) is a crucial supportive identifier. As one example, Figure I-45 compares silicate curves for the Florida Current vs the open Atlantic along 24°N, where SiO_2 values for the Florida Current are noticeably higher for $\sigma_\theta > 26.8$, approximately.

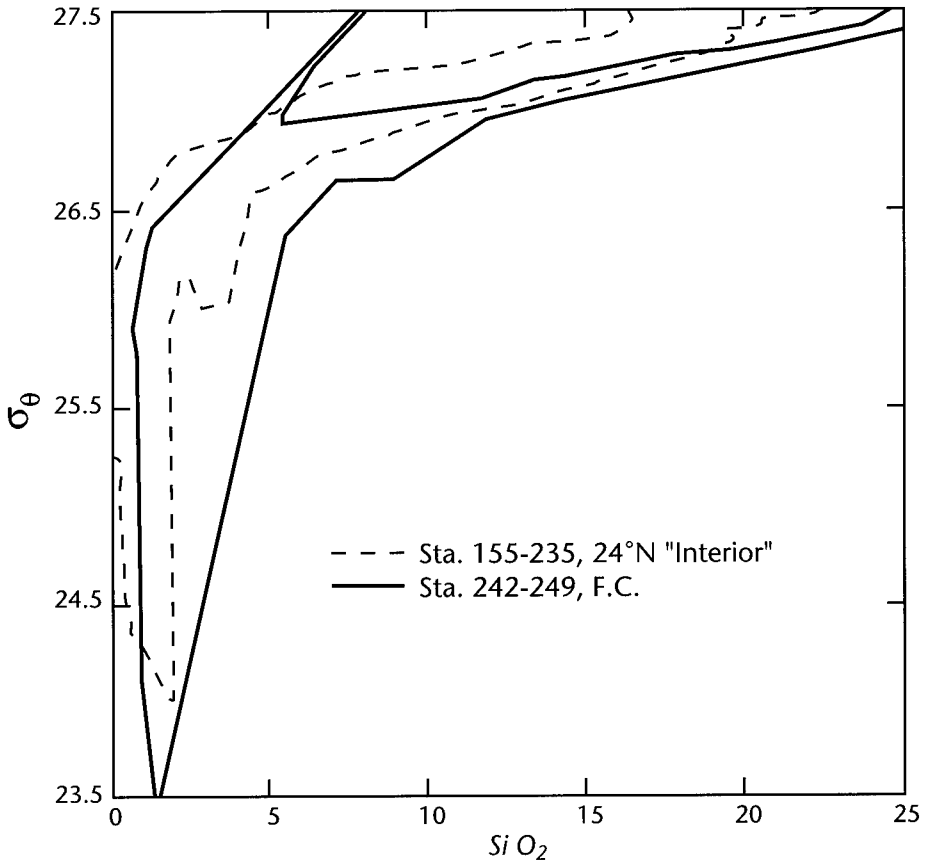

Figure I-45: Silicate (SiO_2) vs σ_θ curves for the Florida Current and for the open Atlantic along 24°N.

"Mean" velocity sections across the Florida Current are also abundant, relatively speaking, with several shown in Figure I-46. A few cross-stream transport distributions are contained in Figures I-47 through I-49. There is a lot of temporal stability (to within ±2 Sv) implied by Figure I-47, over a 70-year time interval. All in all, the transport of the Florida Current while within the Straits of Florida is probably better known than that for any oceanic area, as is the hydrography (Larsen, 1992; Leaman *et al.*, 1987; Parr, 1937; Roemmich and Wunsch, 1985; Schmitz and Richardson, 1968; SR91; Schmitz *et al.*, 1993; Wenneckens, 1959). The transport of the Florida Current roughly triples between the Straits of Florida and Cape Hatteras (Leaman *et al.*, 1989; Richardson *et al.*, 1969; Richardson and Knauss, 1971; SM93). A summary of transports from 27°N to Cape Hatteras (Leaman *et al.*, 1989) is presented in Table I-4.

Stommel's (1957) picture of the thermohaline circulation in the Atlantic Ocean had about 20 Sv (1 Sv = 10^6 m^3 s^{-1}) of abyssal flow crossing the equator and entering the South Atlantic, with a corresponding cross-equatorial return transport to the North Atlantic in the upper ocean. This guess (Stommel, personal communication), partially motivated by observations of the strong southward-flowing abyssal currents along the western boundary of the Atlantic, slipped from prominence until recently, when SR91 presented evidence that about 45% of the transport of

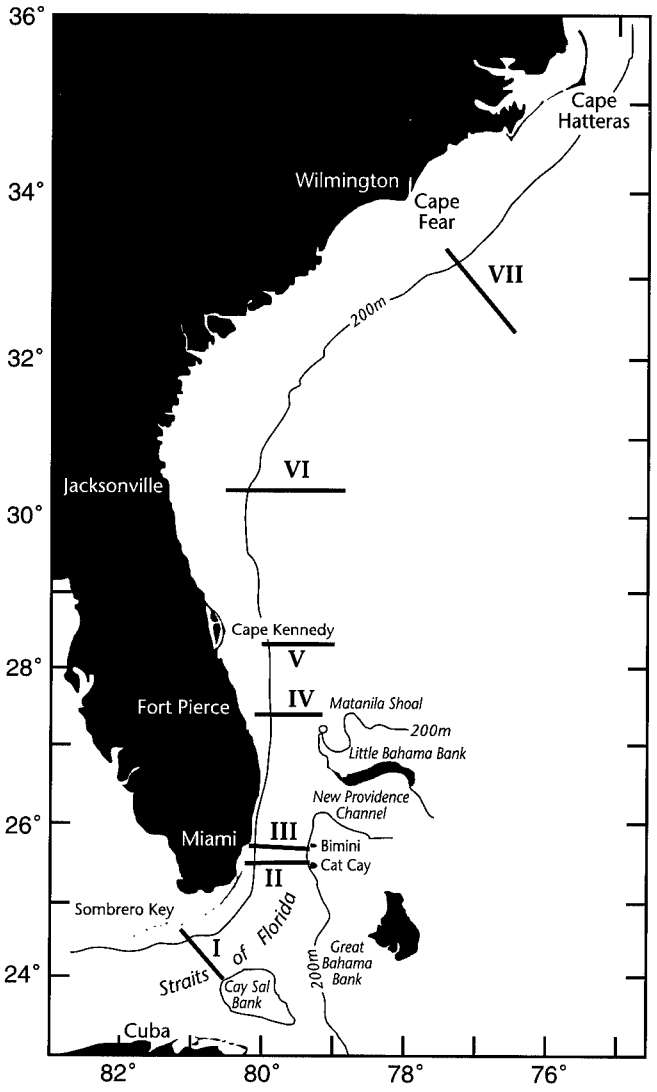

Figure I-46a: Locations of sections of downstream speed contours across the Florida Current, based on dropsonde data, adapted from Richardson *et al.* (1969).

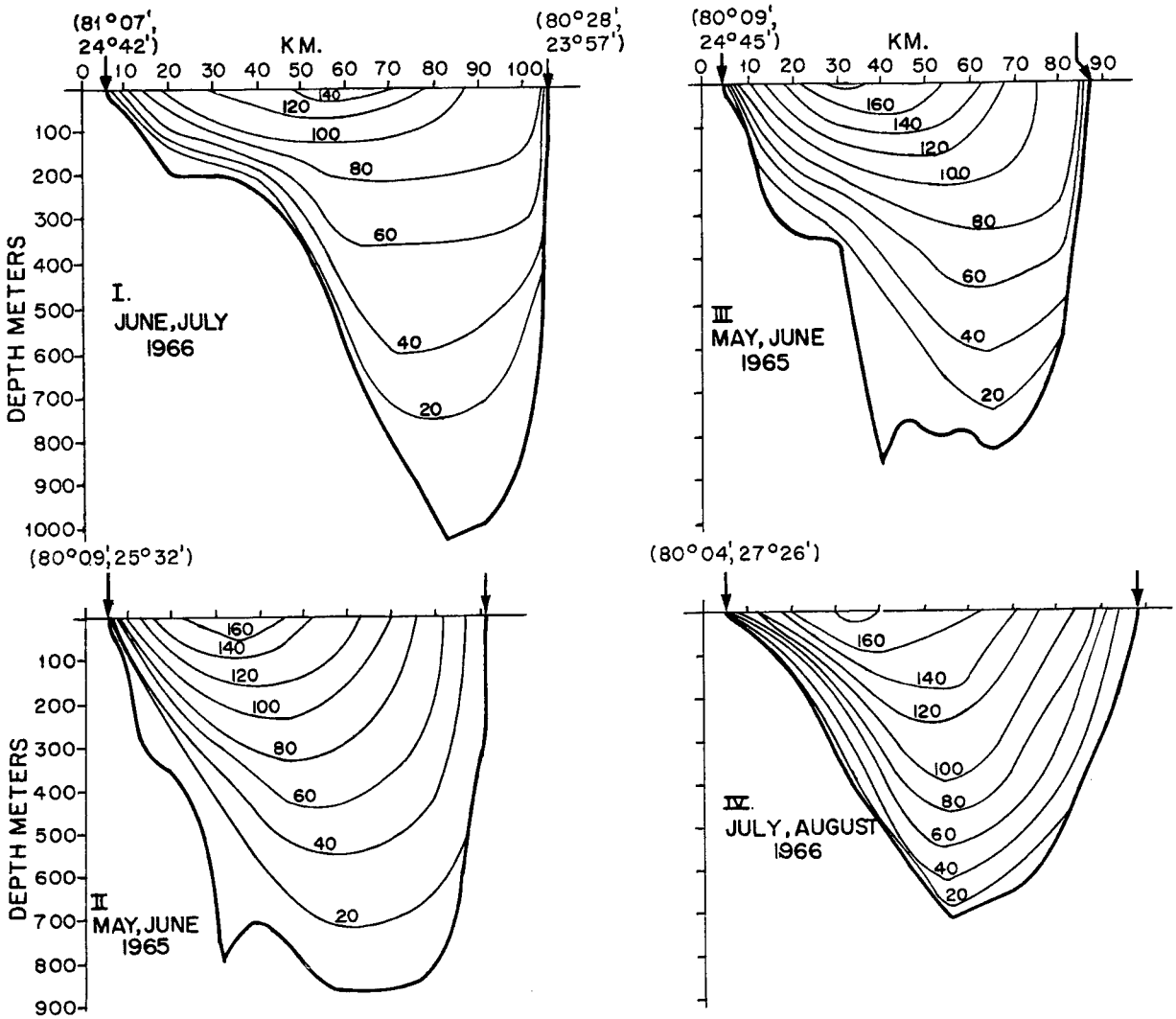

Figure I-46b: Sections of downstream speed contours across the Florida Current, based on dropsonde data, adapted from Richardson *et al.* (1969), in cm s^{-1} for the southernmost sections.

the Florida Current could be of South Atlantic origin. The source(s) of the well-established Florida Current transport had not yet been clearly sorted out, with Worthington (1976) and Leetmaa *et al.* (1977) postulating a North Atlantic origin for more or less the entire 30 Sv. Schmitz and McCartney (1993) published maps of the transports for the North Atlantic that basically provided the first purely observationally based endorsement (updated in Figures I-21 and I-22 above) of the Stommel (1957) picture (Figure I-19 above). Schmitz and McCartney (1993) and Schmitz (1995) have

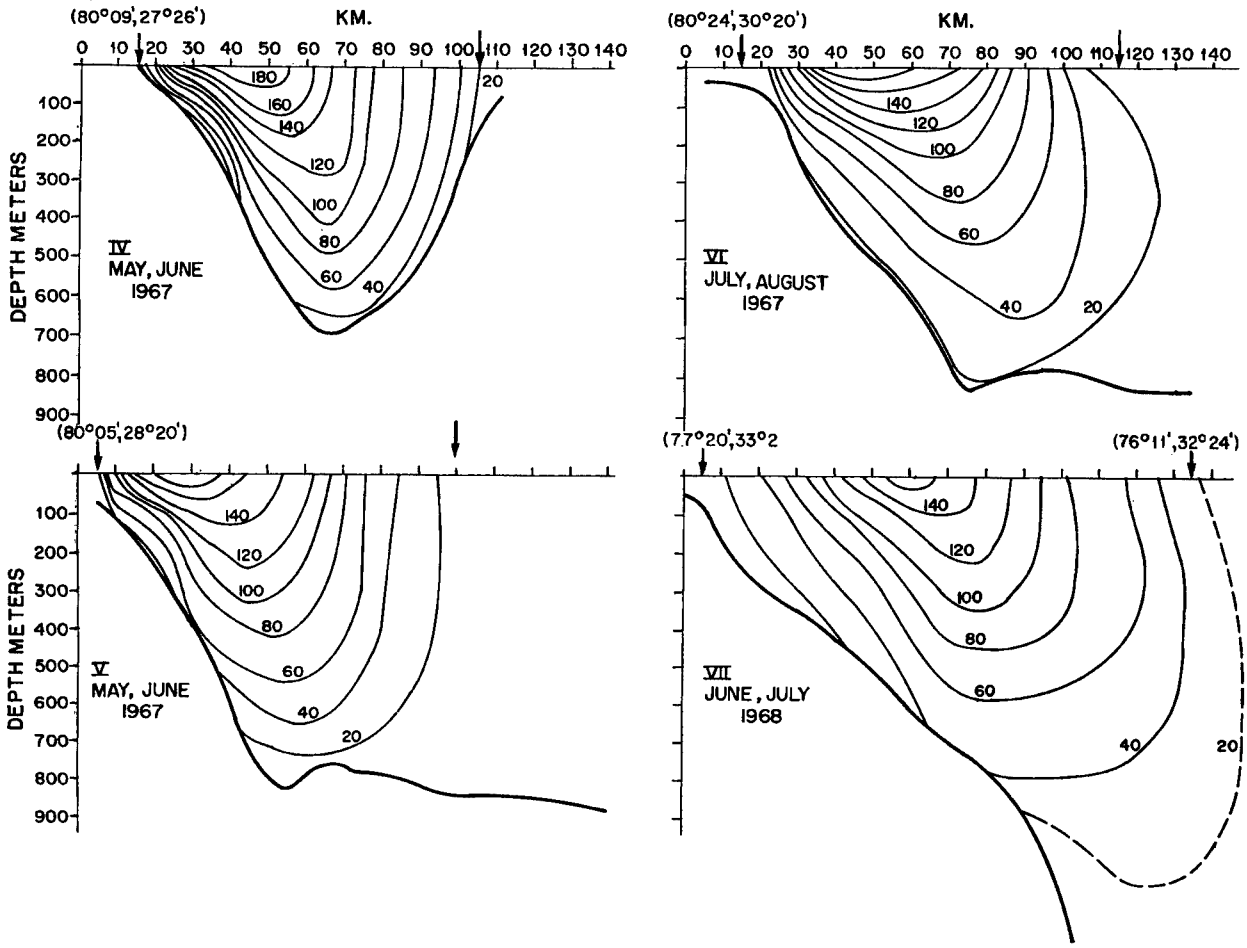

Figure I-46c: Sections of downstream speed contours across the Florida Current, based on dropsonde data, adapted from Richardson *et al.* (1969), in cm s^{-1} for the northernmost sections.

also emphasized the role of the Florida Current in interbasin/intergyre exchange on global scale.

According to SR91 and Schmitz *et al.* (1993), one may think of the transport of the Florida Current as "originating" from basically two areas: the interior of the North Atlantic subtropical gyre and the tropical South Atlantic. The latter contribution is envisioned to be part of a globally linked replacement flow for NADW (Gordon, 1986; Schmitz, 1995), whereas the North Atlantic contribution to the Florida Current is primarily the wind-driven segment of the subtropical gyre, although composed of a significant component of 18° Water. Each of these contributions is characterized by a distinct niche (Tables I-5 and I-6) in property space (SR91, Schmitz *et al.*, 1993;

Stalcup and Metcalf, 1972). The general agreement (~ 1–2 Sv) between diverse authors in Tables I-5 and I-6 is noteworthy. Most of the water entering the Caribbean and Straits of Florida in the 16–23°C temperature range is characterized by a special (North Atlantic) temperature–oxygen curve in comparison with water of South Atlantic origin. Below 16°, water of South Atlantic origin, often referred to as AAIW, is characterized by low salinity and high silicate. Above 25°C, which is roughly above 100 m depth in the Florida Current, salinities off Miami, for example, are too fresh (Figure I-40b) to have come advectively from the mid-latitude (24°N) North Atlantic (SR91). A recent summary of total transport breakdowns for the subtropical North Atlantic (Lee *et al.*, 1995; their figure 17) is presented in modified form in Figure I-50, apparently in good agreement with SR91 and SM93. Lee *et al.* (1995) have, in Figure I-50, 26 Sv of Sverdrup interior flow, of which about 19 Sv

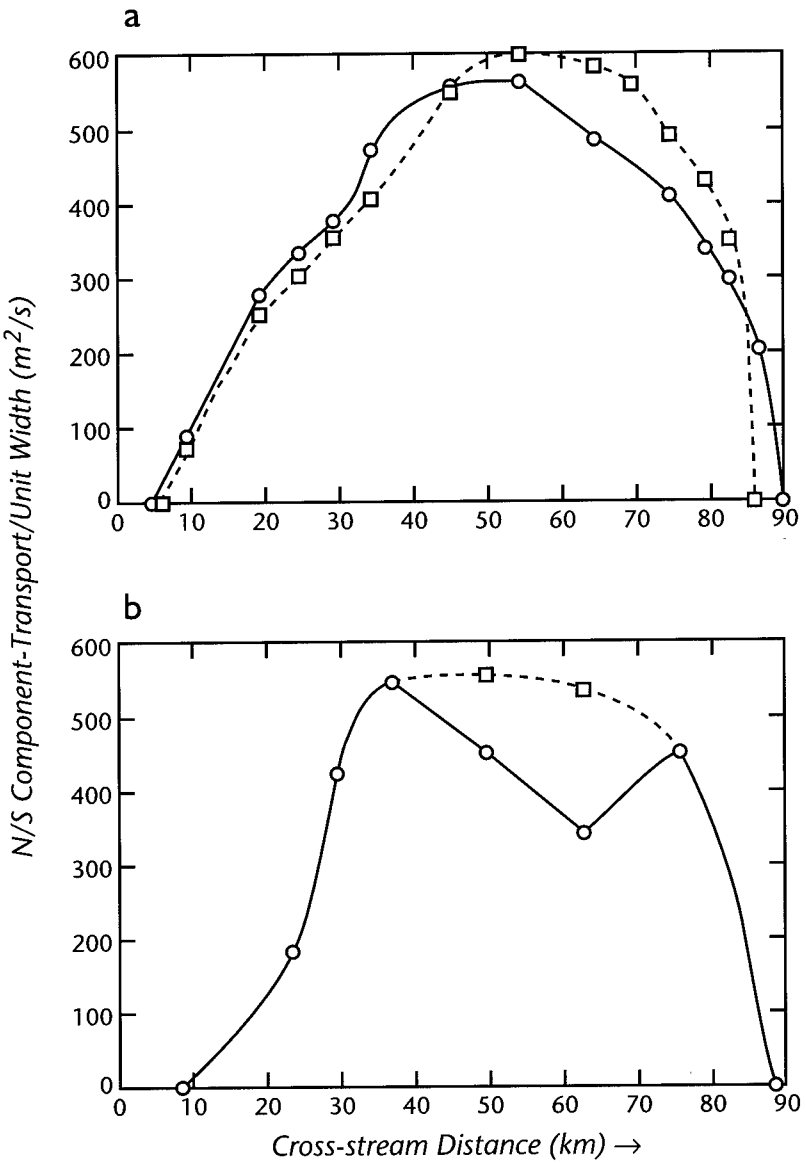

Figure I-47: Transport per unit width as a function of cross-stream distance for the Florida Current off Miami, adapted from Schmitz and Richardson (1968). (a) For two dropsonde sections near Miami, and (b) using Pillsbury's (1890) values extrapolated in depth as he did (○) as compared to the extrapolation (□) indicated in (a).

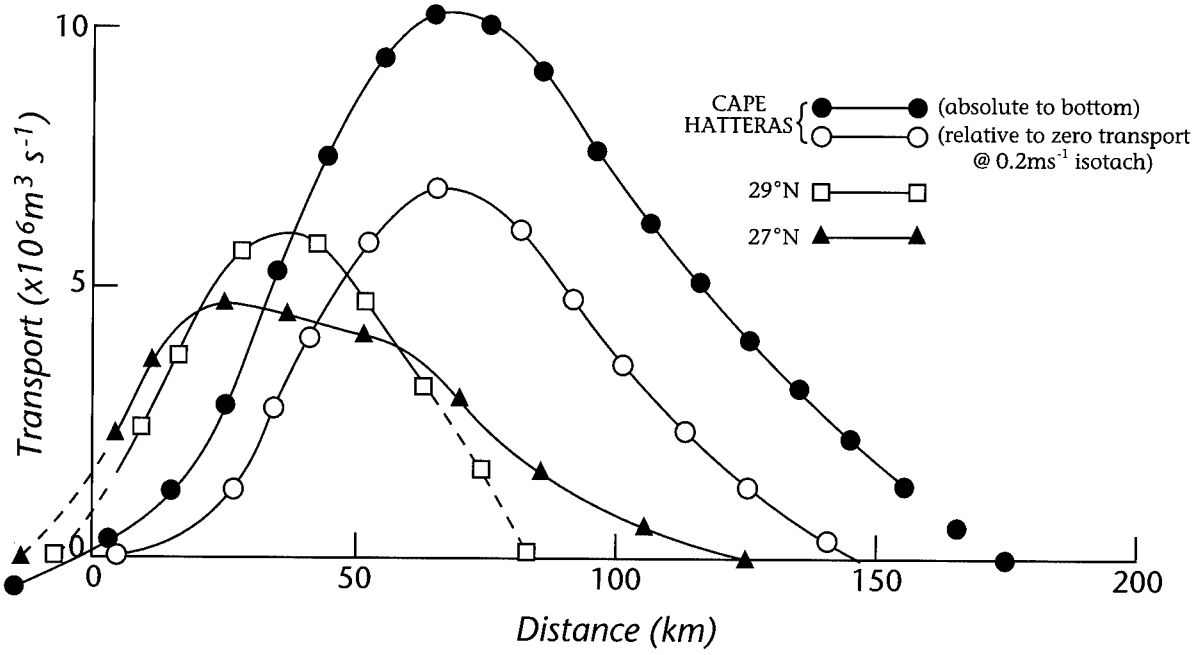

Figure I-48: Transports along a variety of sections across the Florida Current from the Straits of Florida to Cape Hatteras, adapted from Leaman *et al.* (1989).

Table I-6: Transport–temperature range breakdowns for the Florida Current, Caribbean inflow and along 24°N according to SR91

Temperature range (°C)	Florida Current transport (Sv)*	Florida Current transport (Sv)†	Caribbean inflow transport (Sv)‡	24°N transport (Sv)*
>24	8.1	9.2	8.9	–1
17–24	9.3	10.0	8.4	–8.5
12–17	6.6	6.7	5.4	–2.9
7–12	5.0	3.9	6.1	1.9
<7	0.5	—	—	–19.0
Sum	29.5	29.8	28.8	–29.5

*Hall and Bryden (1982, recalculated). †Leaman *et al.* (1989, recalculated).
‡New (recalculated).

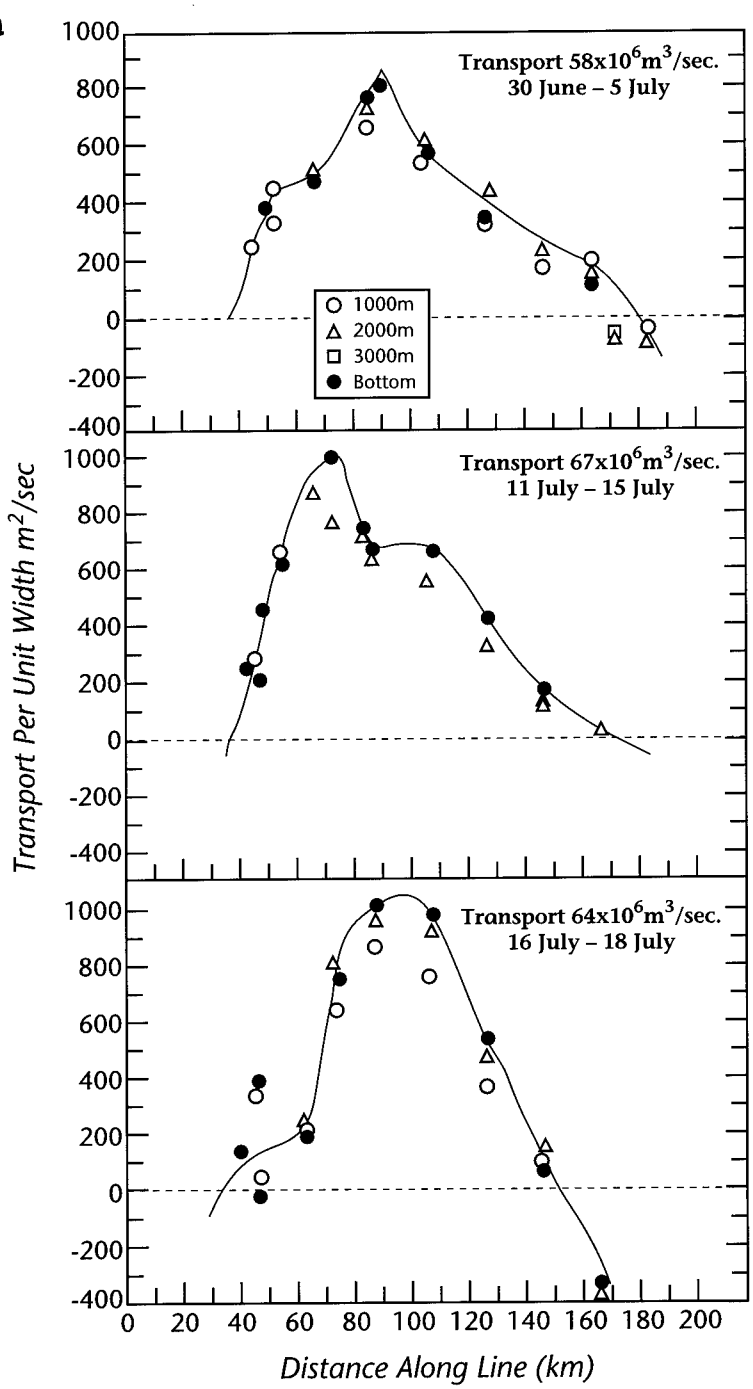

Figure I-49: Transports per unit width near Cape Hatteras, adapted from Richardson and Knauss (1971): (a) as a function of cross-stream distance.

(which includes the approximately 2 Sv flow into the Florida Current through Northwest Providence Channel) is in the Florida Current. My view (see Schmitz *et al.*, 1992), and please refer to Figure I-21, is the extra 7 Sv is part of an Antilles Current that is part of the southern Gulf Stream recirculation.

Perhaps the most straightforward South Atlantic component in the GSS to track hydrographically is "upper intermediate water." This water was first "noticed" over the Blake Plateau by Iselin (1936). This point, and the fate of this water as it transits the North Atlantic, is illustrated in three figures. Figure I-51 is reconstructed from Atkinson (1983), superimposed on the SR91 and Schmitz *et al.* (1993) *T/S* envelope. Figure I-52 is adapted from Richardson (1977), and Figure I-53 is modified from Tsuchiya (1989). Schmitz and Richardson (1991) identified a transport of about 3–6 Sv for

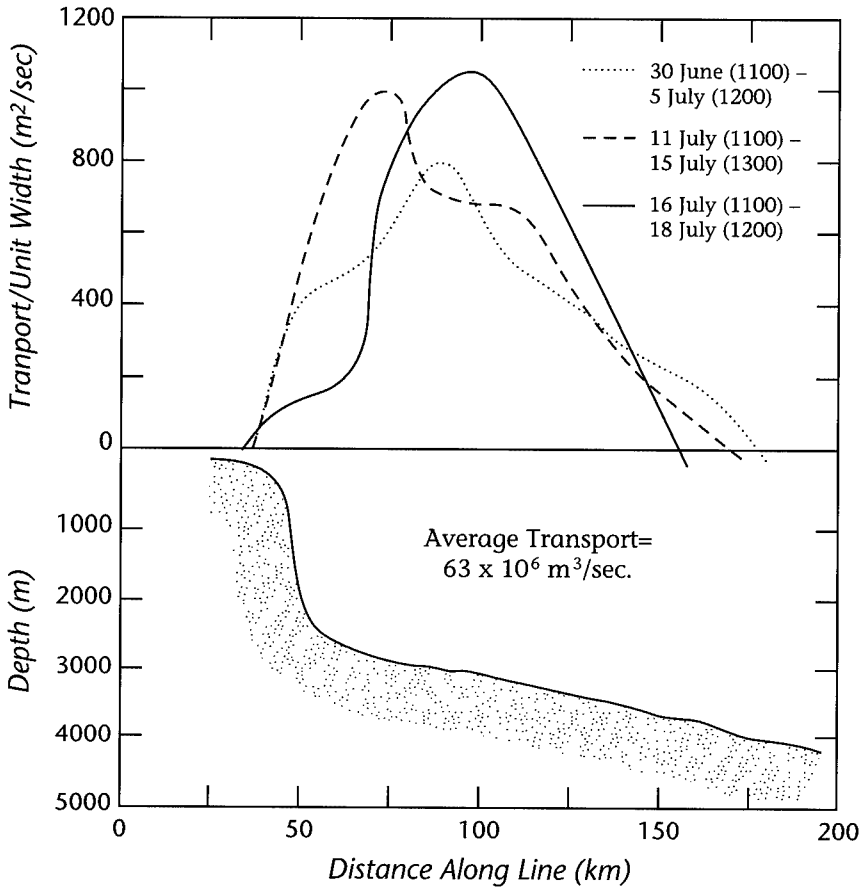

Figure I-49 (continued): Transports per unit width near Cape Hatteras, adapted from Richardson and Knauss (1971): (b) a summary and (c) section location.

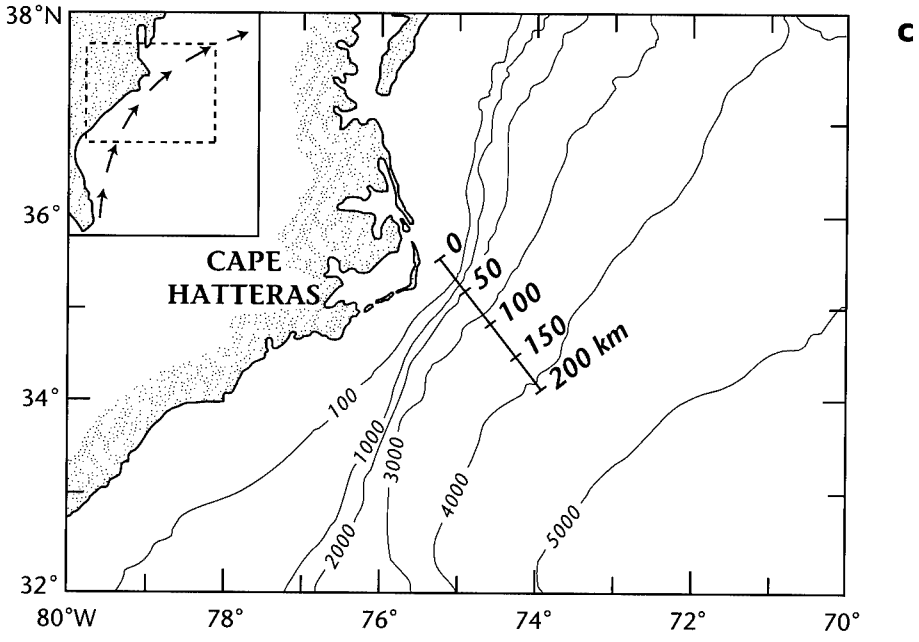

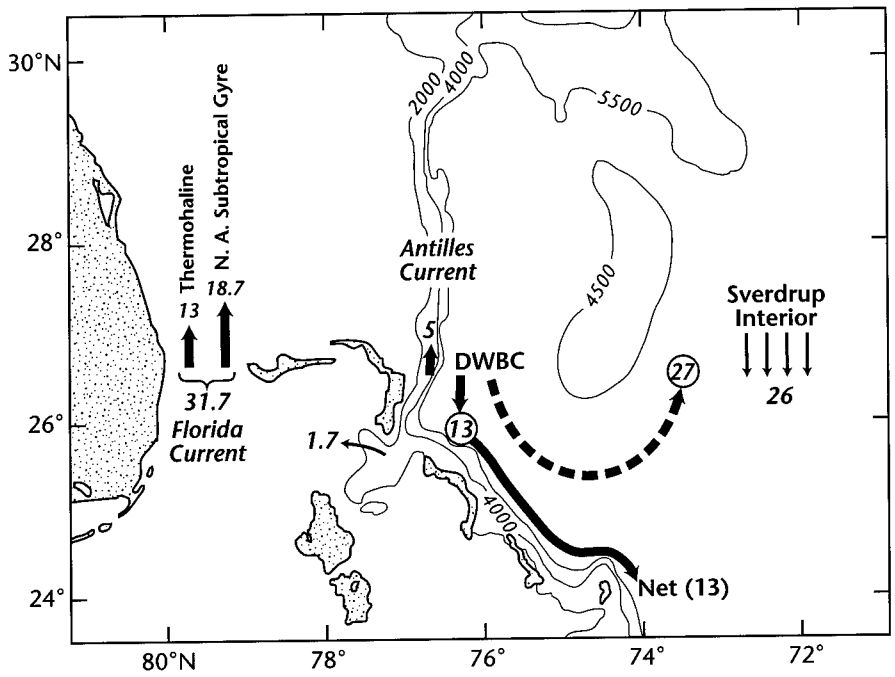

Figure I-50: Transport summary for the Subtropical Atlantic along 26.5°N, adapted from Lee *et al.* (1996).

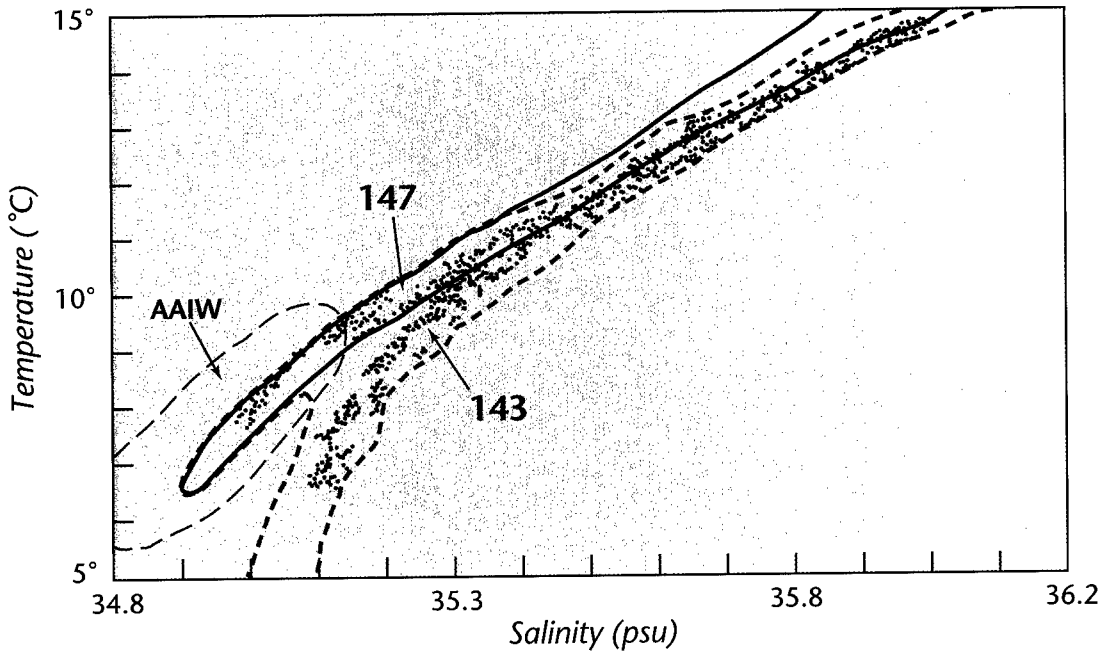

Figure I-51: *T*/*S* curves for the Florida Current as it emerges from the Straits of Florida, based on data (within the θ/S envelope denoted by dashed green lines) collected by Atkinson (1983, his figures 2 and 3) and using the standard *T*/*S* envelope (solid red line) for the Florida Current while in the Straits of Florida (Figure I-42). The red dots are from station 147, on the inshore edge of the current, in "AAIW." The green dots are for station 143, offshore of the main core of the Florida Current.

this water type in the Florida Current off Miami, consistent with estimates of 7–12° water transport by Hall and Bryden (1982), Roemmich and Wunsch (1985), and Leaman *et al.* (1989); see Tables I-3 and I-4. Based on Atkinson's and Tsuchiya's figures, quite a bit of "mixing" of this water type may occur on the Blake Plateau, and throughout the GSS and North Atlantic Current. Perhaps this also occurs upstream of the Blake Plateau, within the Straits of Florida and throughout the system of topography leading from the equator to the Straits. Figure I-51 shows how "AAIW" looks as it exits the Straits of Florida and flows onto the Blake Plateau, and Figure I-52 contains the "AAIW remnants" near Cape Hatteras. Tsuchiya's results in Figure I-53 are the clearest picture I am aware of that shows "AAIW" traversing the GSS, the North Atlantic Current, and finally entering the polar seas as well as the subpolar gyre, while at the same time apparently "mixing with" or entraining Mediterranean Water (see also Reid, 1978, 1981, 1994).

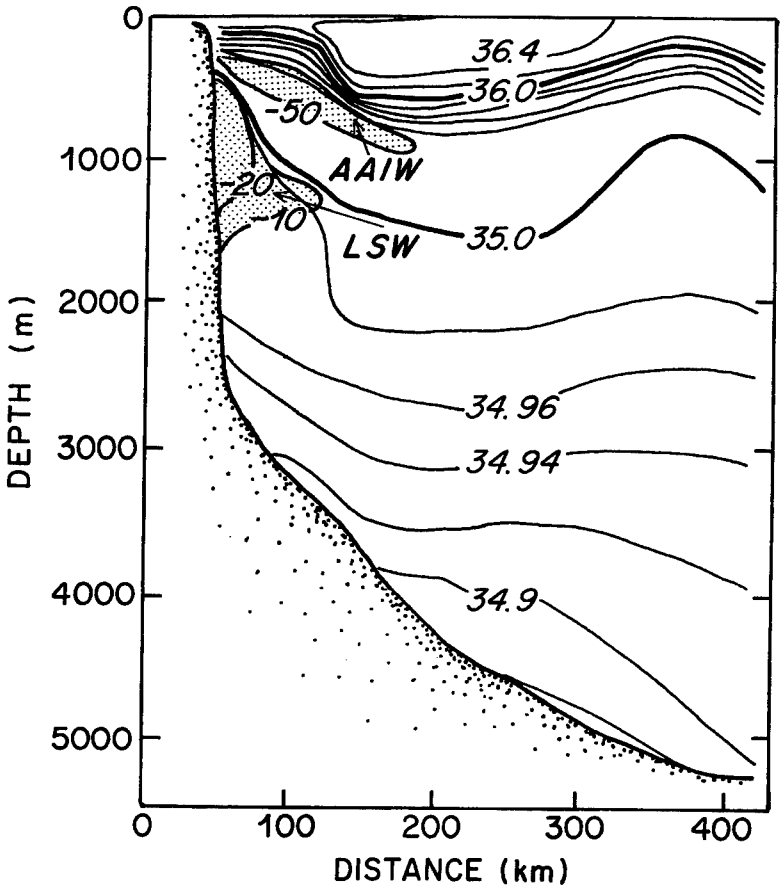

Figure I-52: A salinity (psu) section at Cape Hatteras, adapted from Richardson (1977); Labrador Sea Water indicated by LSW and Antarctic Intermediate Water by AAIW.

Time variations in the transport of the Florida Current, particularly in or near the Straits of Florida, have also been extensively studied (*i.e.*, Lee and Williams, 1988; Greatbatch *et al.*, 1995; Johns and Schott, 1987; Larsen, 1992; Leaman *et al.*, 1987; Lee *et al.*, 1985; Molinari *et al.*, 1985; Montgomery, 1941; Niiler and Richardson, 1973; Parr, 1937; Schmitz and Richardson, 1968; Schott *et al.*, 1988; Wertheim, 1954).

a

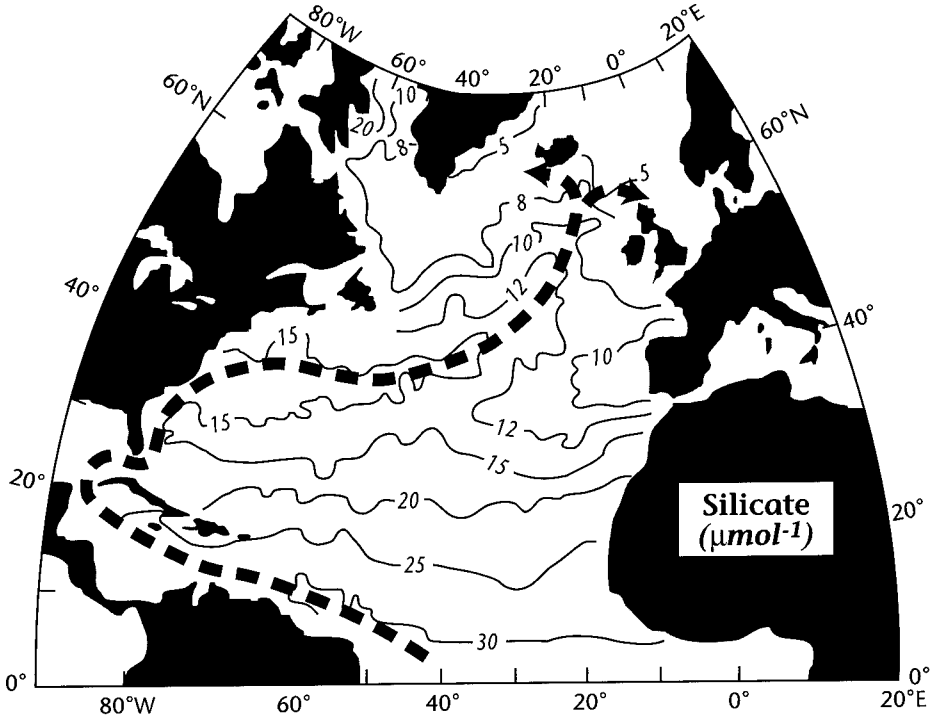

Figure I-53: Silicate (a) and salinity (b) contours on an isopycnal surface located in AAIW, with the heavy dashed line being a hypothetical locus of flow. Adapted with modification from Tsuchiya (1989); silicates in μmol L−1, salinities in psu.

b

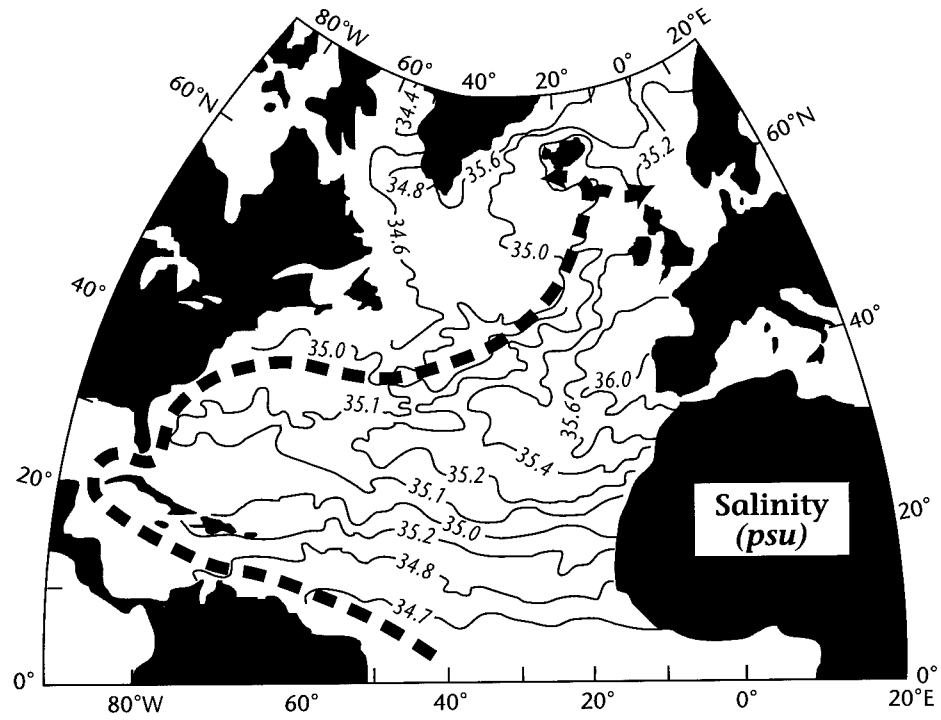

Larsen (1992) finds a seasonal amplitude of 2.5 Sv and an interannual transport amplitude of 1.5 Sv (comparatively a very small number!) in the presence of a mean of 32 Sv for the Florida Current. This is essentially identical to results (mean transport 30 Sv, seasonal amplitude ± 3 Sv) presented by Schmitz and Richardson (1968). Niiler and Richardson (1973) reported a somewhat higher seasonal variation (± 4 Sv) than either Larsen (1992) or Schmitz and Richardson (1968). The extra 2 Sv in the estimate of the mean by Larsen (1992) relative to Schmitz and Richardson (1968) is due to the location of Larsen's measurements north of Northwest Providence Channel, where the inflow has been estimated to be ~ 2 Sv by Finlen (1966) and Richardson and Finlen (1967). All in all, the Florida Current is about as stable as any ocean current, especially in transport. Off Miami, essentially any "complete" direct measurements of "time-averaged" transport find about 30 Sv

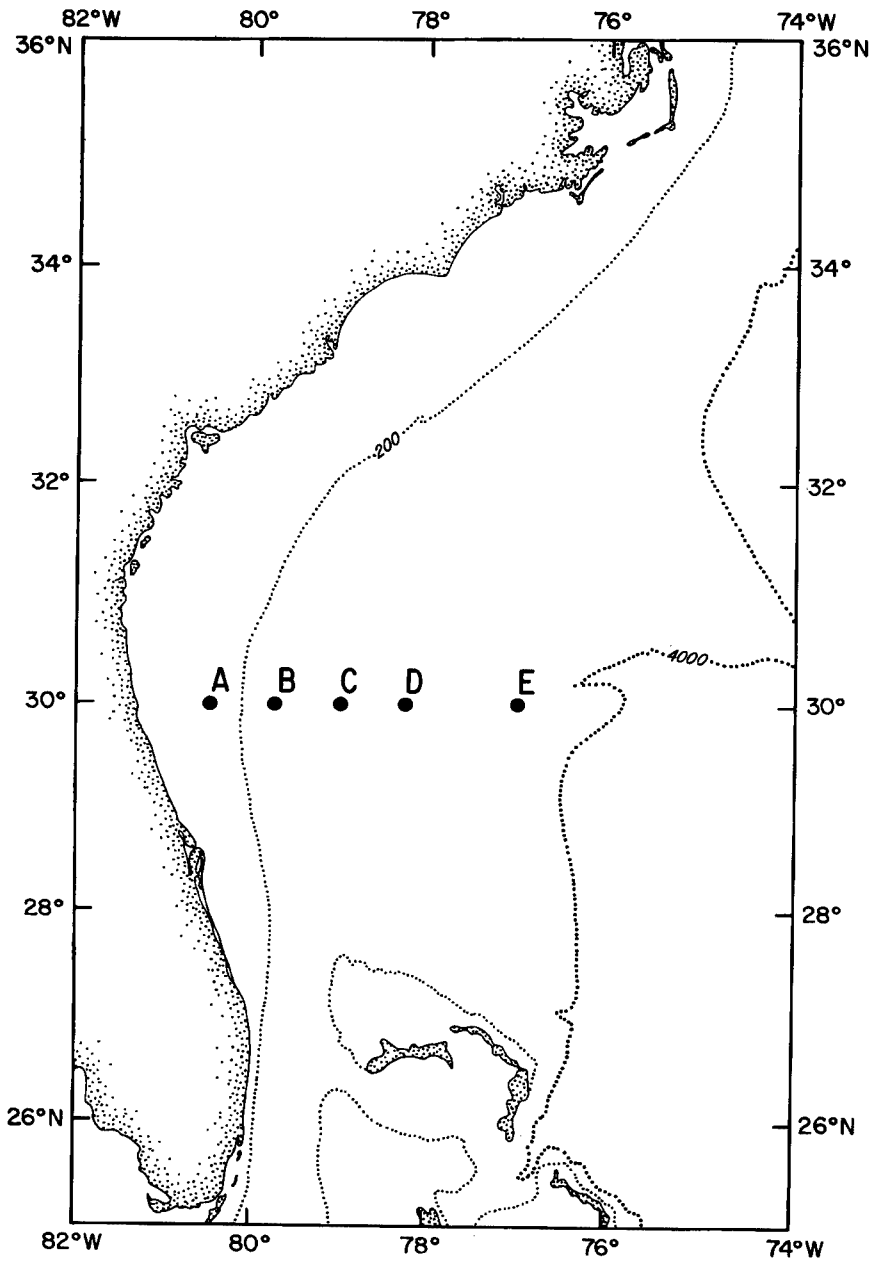

Figure I-54: Location of anchor stations across the Blake Plateau along approximately 30°N.

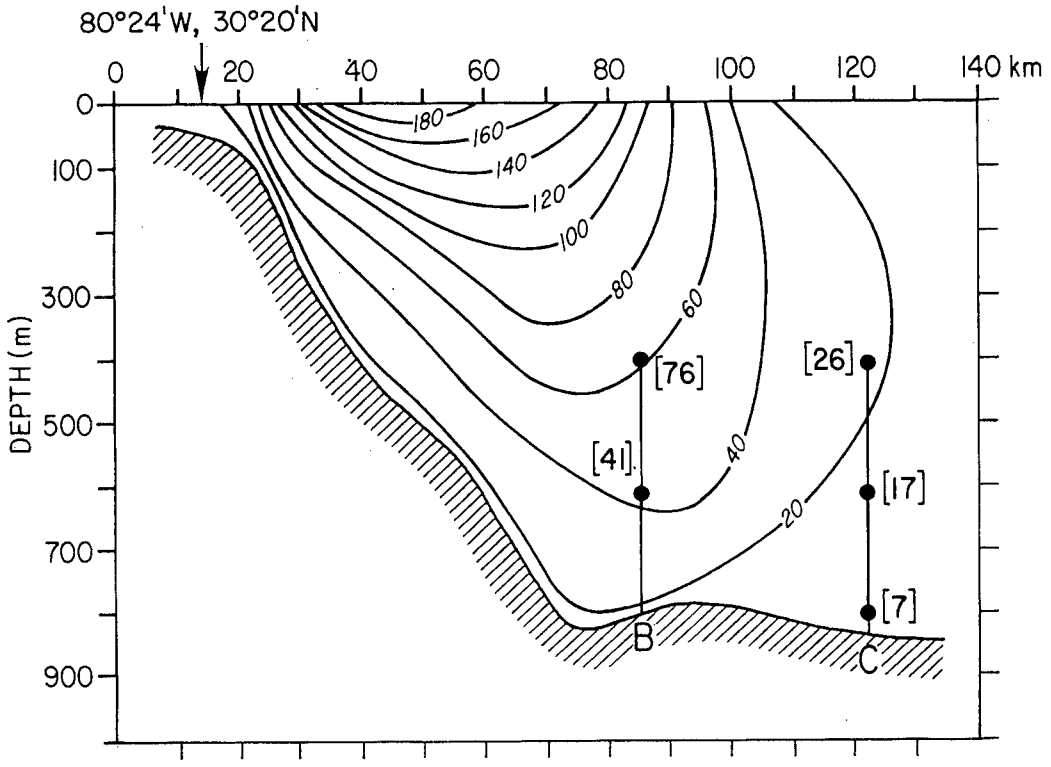

Figure I-55: A comparison of time averages of downstream current components (cm s^{-1}) from the current meter array in Figure I-54 with dropsonde results (downstream speed component contours in cm s^{-1}) from Figure I-46.

(Leaman *et al.*, 1987; Niiler and Richardson, 1973; Schmitz and Richardson, 1968). Temporal stability appears to hold even over the Blake Plateau (Figures I-54 and I-55). So the real message from the composite data base is that the low-frequency variability of the transport of the Florida Current is of comparatively low amplitude relative to the mean.

Recently, a variety of very nice investigations have addressed the details of the flow in regions associated with the Florida Current Regime (Leaman *et al.*, 1995; Lee *et al.*, 1995). This kind of activity was completed early on in Northwest Providence Channel by Finlen (1966) and Richardson and Finlen (1967).

4b. The Gulf Stream as a Zonal Jet with Recirculations

As the Florida Current leaves the Blake Plateau and becomes the Gulf Stream, the flow in this "boundary current" turns from predominantly meridional to mostly zonal, near Cape Hatteras and beyond. This separation of the Gulf Stream from the coast has historically been a challenging research area (*i.e.*, Richardson, 1977; Stommel, 1958, 1965; Thompson and Schmitz, 1989). The depth changes rather quickly from ~ 1000 to ~ 4–5000 m, the current starts to meander at large amplitude (but much more so farther downstream in the vicinity of the New England Seamounts; Cornillon, 1986; see Figure I-56) and form rings (Richardson, 1993). There are large downstream increases in transport, notably at depths deeper than that of the Blake Plateau (~ 1000 m). Historically, there has been a huge interest in the downstream increase in transport of the Gulf Stream System (Iselin, 1936; Knauss, 1969; Stommel, 1958, 1965; Worthington, 1976), an issue that is now nearly sorted out (Hall and Fofonoff, 1993; Hogg and Johns, 1995; Schmitz and McCartney, 1993). Recently, altimetric data have proven useful in describing various properties of the upper level Gulf Stream (Kelly, 1991; Kelly and Gille, 1990).

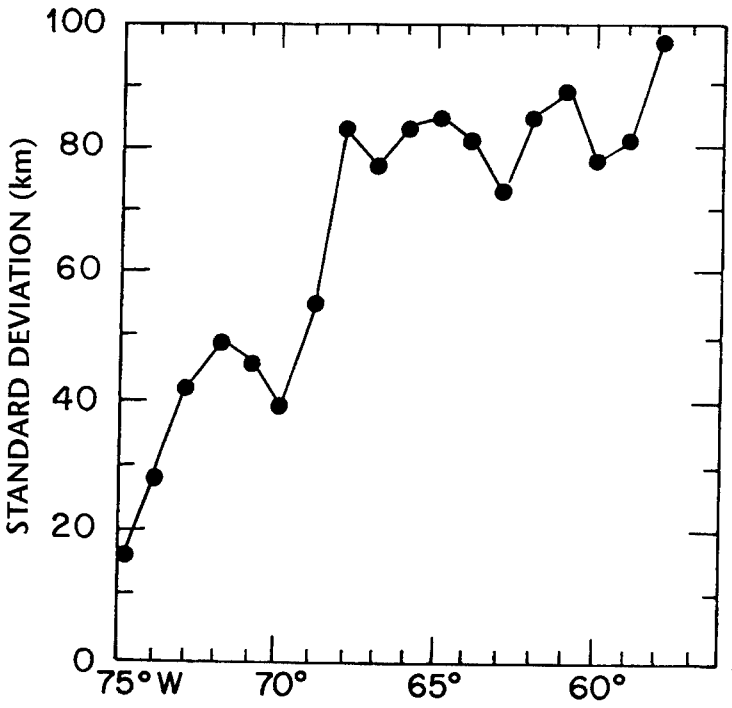

Figure I-56: Standard deviation of Gulf Stream meander paths (normal to the Stream axis) downstream of Cape Hatteras, adapted from Cornillon (1986).

Existing review articles more than adequately discuss this regime, and Hogg and Johns (1995) are state of the art (see also Hall and Fofonoff, 1993), so my report will be inordinately brief on this topic. Meander statistics are described in Figure I-56. Selected hydrographic distributions across the Gulf Stream at 68°W and 55°W, taken from Hall and Fofonoff (1993), are shown in Figures I-57 and I-58. Figure I-59 contains their curves of transport in

temperature classes for a variety of sections across the Gulf Stream System. Table I-3 contains the associated breakdown of transports at 68°W (see also Hall, 1986) and 55°W in density classes, according to Hall and Fofonoff (1993). Various vertical sections of speed contours across the fully developed Gulf Stream are shown in Figures I-60 to I-62, organized so as to move downstream in the GSS, and sources are, respectively, Halkin and Rossby (1985), Johns *et al.* (1995) and Richardson (1985). The difference between Eulerian and Lagrangian views of the transport of the Gulf Stream is illustrated in Figure I-63, adapted from Johns *et al.* (1995). A contemporary picture

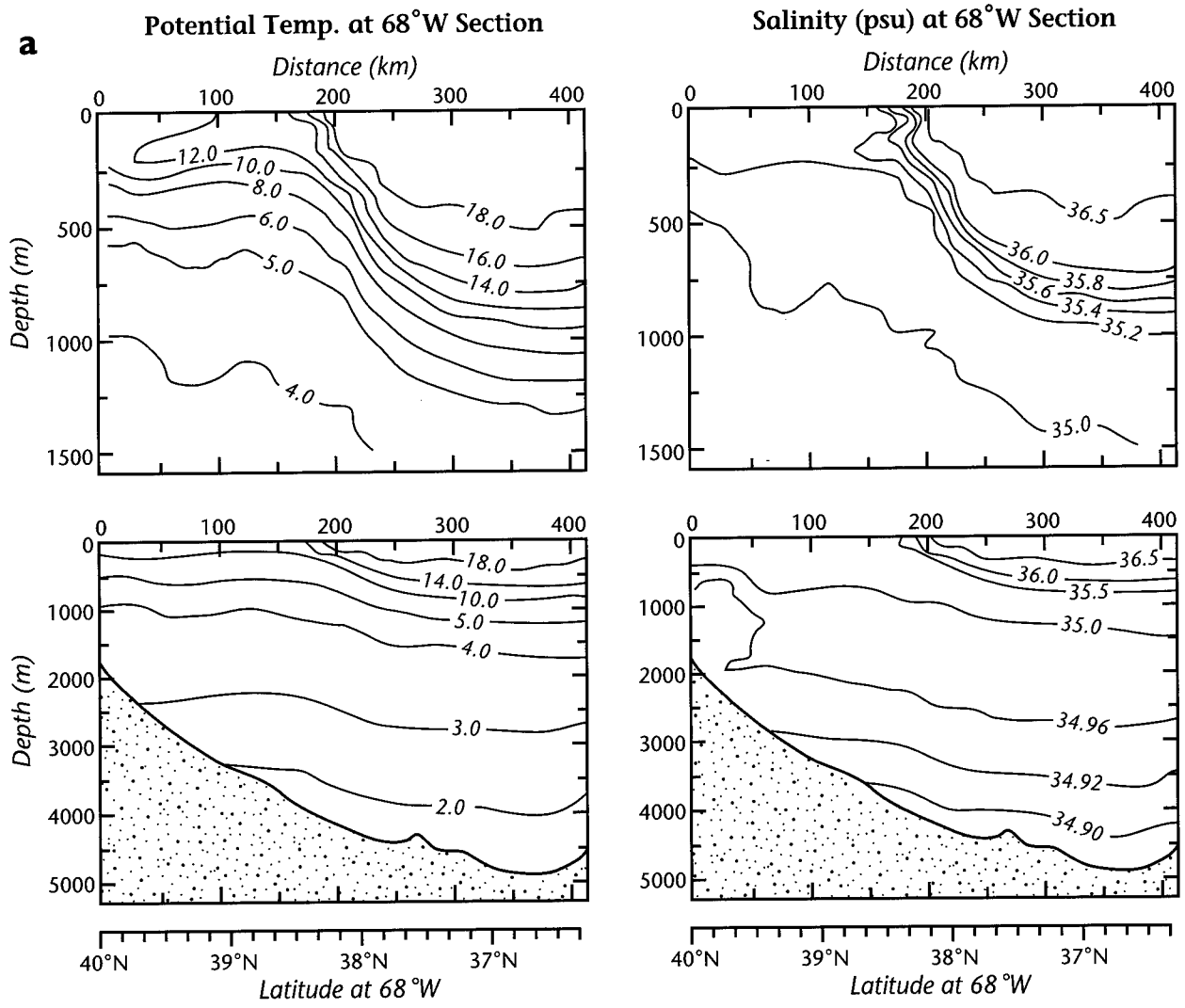

Figure I-57a: Potential temperature (°C) and salinity (psu) sections (contours) across the Gulf Stream at 68°W, adapted from Hall and Fofonoff (1993).

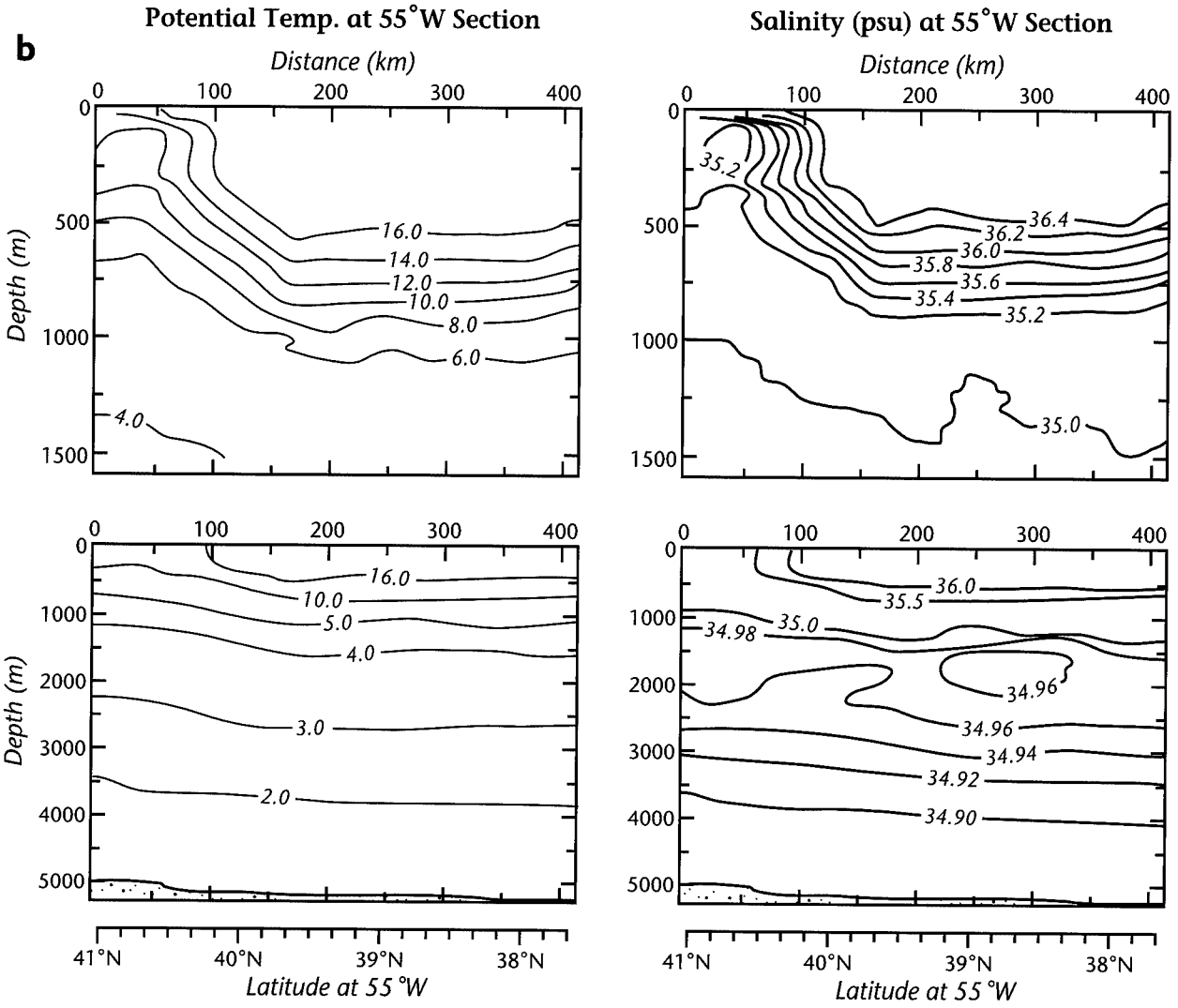

Figure I-57b: Potential temperature (°C) and salinity (psu) sections (contours) across the Gulf Stream at 55°W, adapted from Hall and Fofonoff(1993).

of the transport structure of the GSS including downstream increase and modification is contained in Figure I-64, adapted from Johns *et al.* (1995); see also Hogg (1992) and Hogg and Johns (1995).

Somewhere in the vicinity of 50°W, say between 55 and 45°W, the Gulf Stream decreases in transport and branches. The decrease in transport is associated with divergence from the eastward zonal jet into its recirculations and return flow and continuation as the North Atlantic Current. There are four principal branches of the

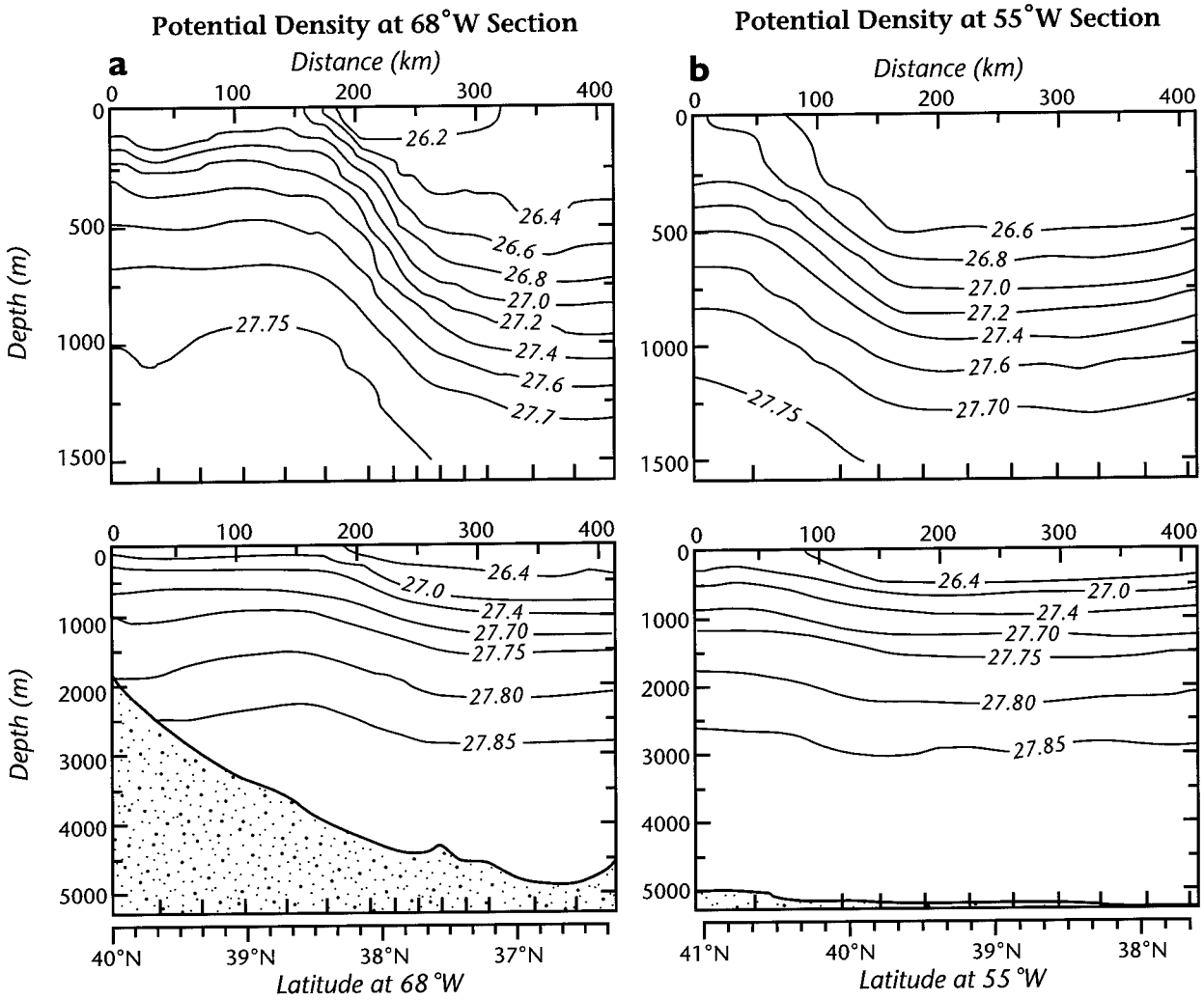

Figure I-58: Potential density (kg m^{-3}) sections across the Gulf Stream at 68°W (a) and 55°W (b), adapted from Hall and Fofonoff (1993).

Gulf Stream in the upper ocean (Figure I-21), the North Atlantic Current (NAC), the Azores Current (which eventually supplies the wind-driven component of the Florida Current), a southern recirculation, and a northern recirculation. The NAC is discussed in the section on subpolar circulations. The Azores Current, a name I use in a generalized sense to mean all of the flow east and south from the Gulf Stream that does not recirculate north of the Caribbean, is discussed in the next section, along with the gyre interior. Recirculations are discussed throughout this report, and there is also a contribution of ~ 1 Sv into the Mediterranean Sea from the generalized Azores Current.

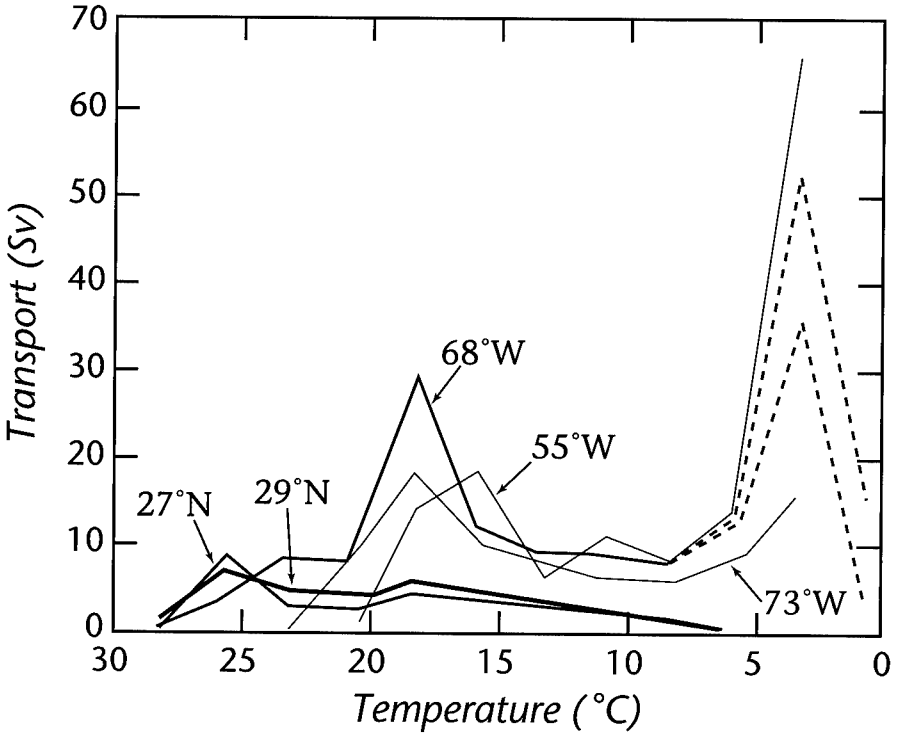

Figure I-59: Gulf Stream transport (x10^6 m^3 s^{-1}) in temperature (°C) classes at a variety of sections, adapted from Hall and Fofonoff (1993).

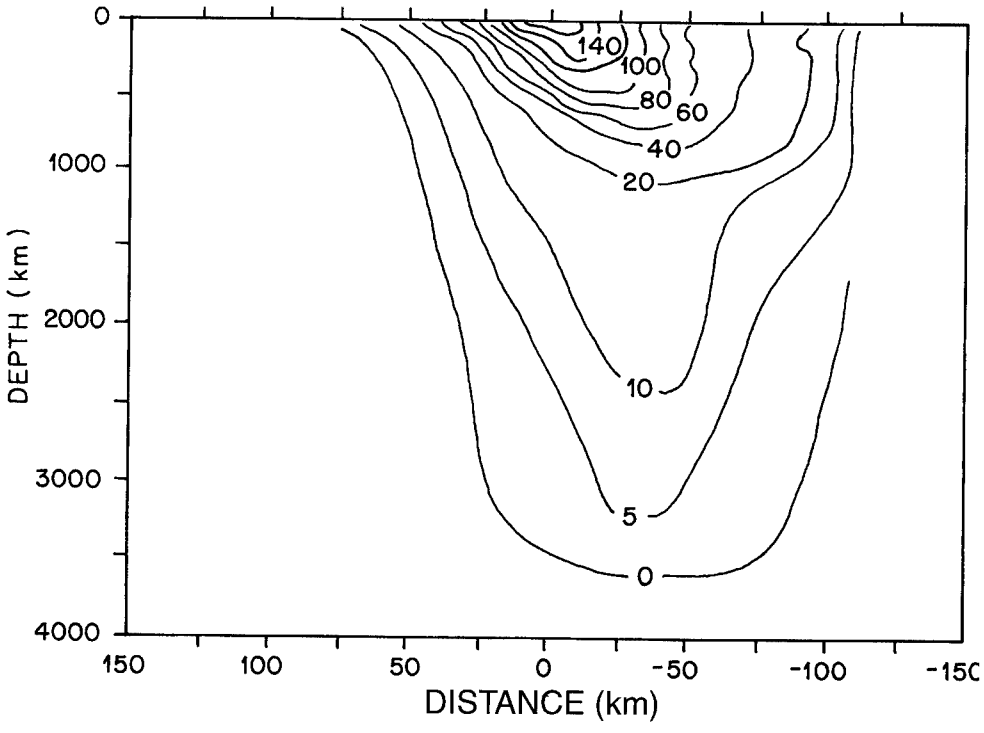

Figure I-60: Downstream speed (in cm s^{-1}) contour figures for the Gulf Stream at 73°W, adapted from Halkin and Rossby (1985).

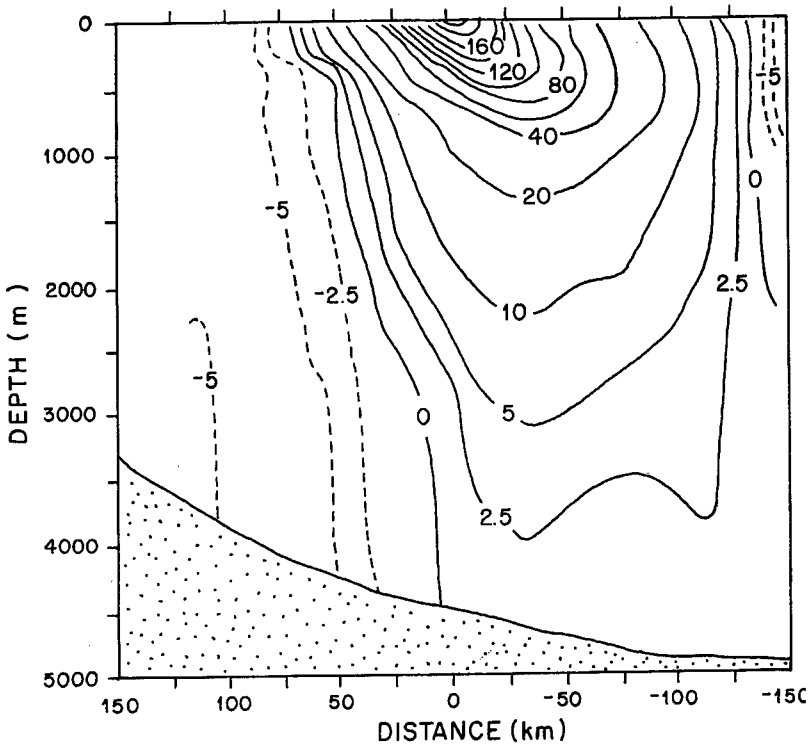

Figure I-61: Downstream speed (in cm s^{-1}) contour figures for the Gulf Stream at 68°W, adapted from Johns *et al.* (1995).

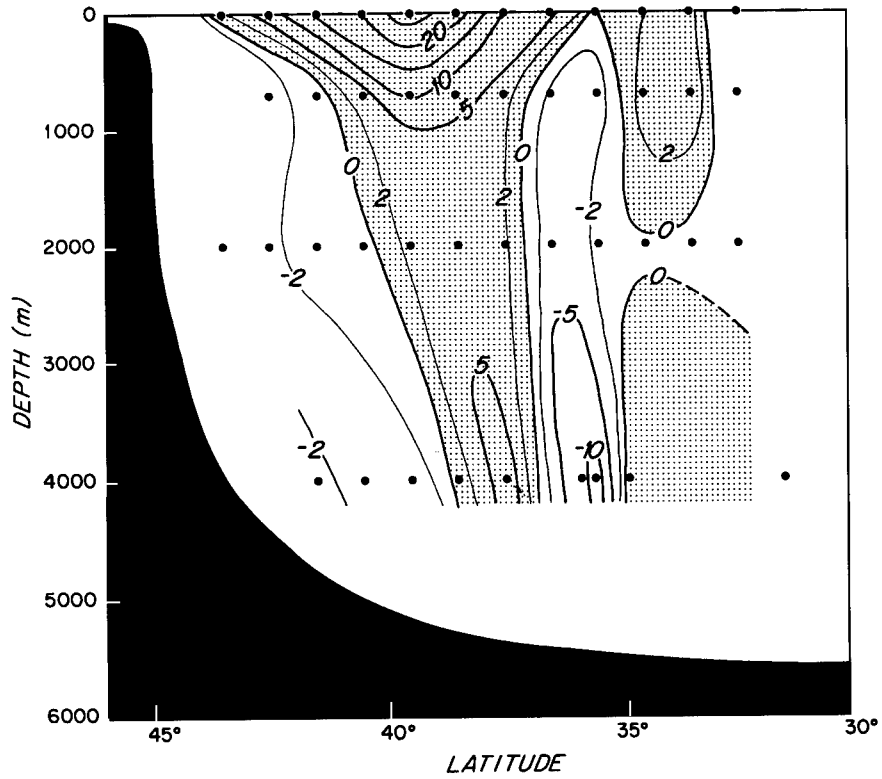

Figure I-62: Downstream speed (in cm s^{-1}) contour figures for the Gulf Stream at 55°W, adapted from Richardson (1985).

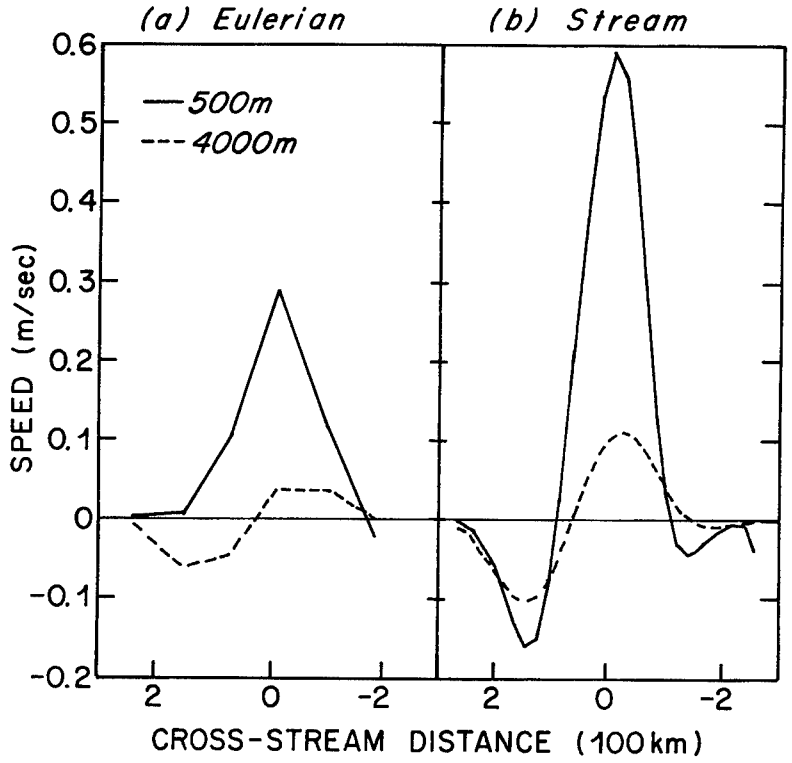

Figure I-63: An illustration, at two depths (500 and 4000 m) of Eulerian and Langrangian views of the Gulf Stream, adapted from Johns *et al.* (1995).

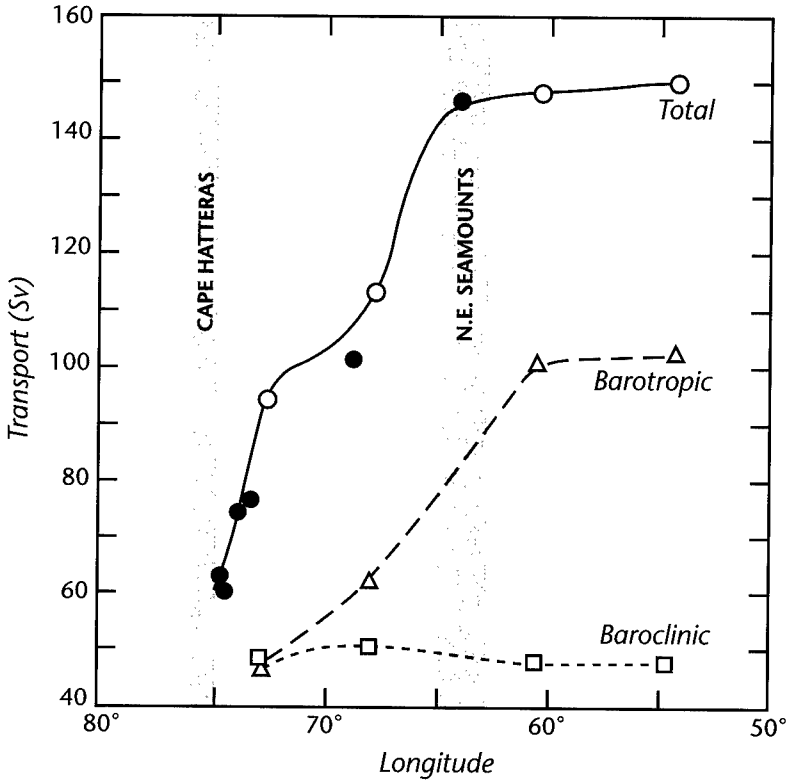

Figure I-64: Summary of observations of the downstream increase in transport of the Gulf Stream from Cape Hatteras to 55°W, adapted from Johns *et al.* (1995). Solid circles are from Knauss (1969), open circles are from Leaman *et al.* (1989), Johns *et al.* (1995), and Hogg (1992). The open triangles and squares are from Hogg (1992, 73°, 60° and 55°W) and Johns *et al.* (1995, 68°W).

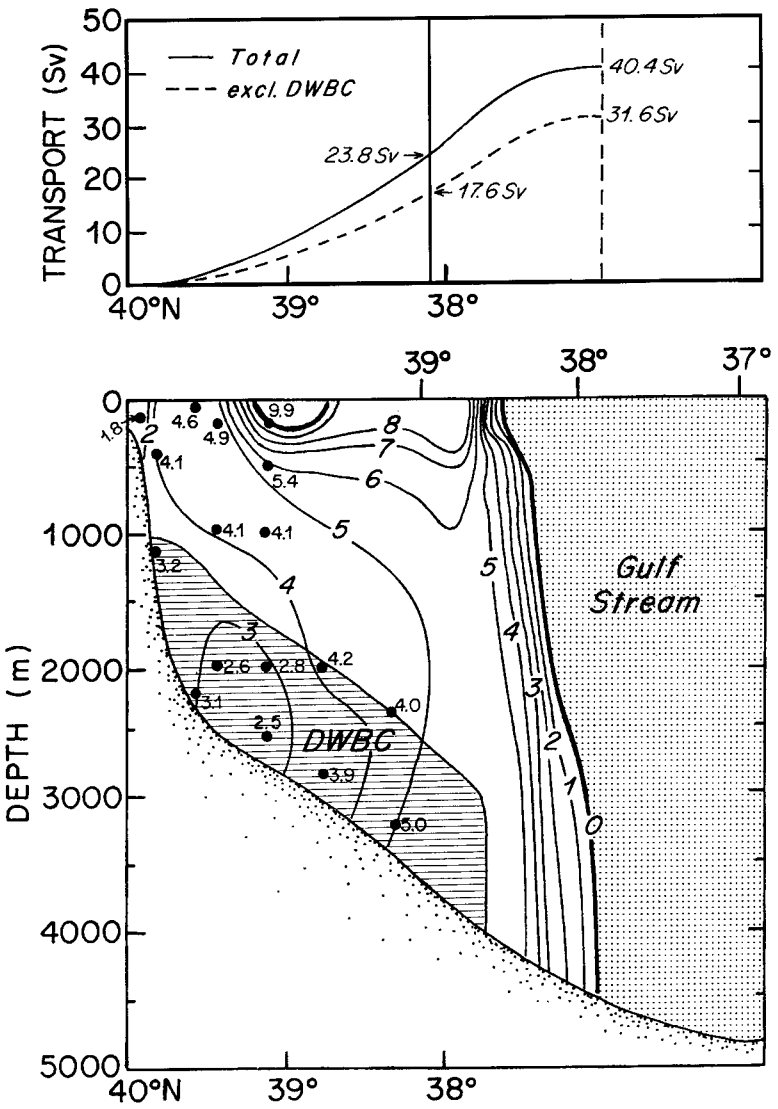

Figure I-65: (top) Cumulative westward transport from the shelf break to the edge of the Gulf Stream. The solid line shows the total transport; the dashed line excludes the shaded area denoted DWBC. (bottom) Cross section of mean zonal flow (in cm s^{-1}) north of the Gulf Stream near 68°W. Solid lines denote westward flow, adapted from Johns *et al.* (1995, their figure 14).

The structure of the flow regime in Slope Water at 68°W (Johns *et al.*, 1995; Shay *et al.*, 1995) is shown in Figure I-65. This figure clearly shows both the DWBC and the northern recirculation gyre. Note that the DWBC is also observed to meander (Johns and Watts, 1986). The northern (slope water) and southern recirculations of the Gulf Stream have received a lot of attention, being "responsible" for the downstream increase in transport of the GSS. In Figure 64, the baroclinic transport of the Gulf Stream from Cape Hatteras to 55°W is basically constant at about 50 Sv. However, relatively depth-independent, at least partially eddy-driven, recirculations are responsible for a barotropic transport that doubles from ~ 50 to ~ 100 Sv between Cape Hatteras and 55°W.

4c. The Gyre Interior

Historically, investigations of the upper layers (above 1000 m or so, say, or above $\sigma_\theta \doteq 27.4$) of the subtropical gyre interior tended to be dominated by questions about the applicability of the Sverdrup relation (Leetmaa *et al.*, 1977; Roemmich and Wunsch, 1985; Schmitz *et al.*, 1992; Stommel, 1958, 1965), the existence and strength of any Antilles Current (Olson *et al.*, 1984; Owens *et al.*, 1988; Rosenfeld *et al.*, 1989; Stommel, 1958, 1965), the role of eddies in the mean circulation (Stommel, 1958, 1965; Schmitz *et al.*, 1983), transports across, say, 24°N (Hall and Bryden, 1982; Roemmich and Wunsch, 1985), the source and transport of the Azores Current (Gould, 1985; Stramma, 1984; Siedler *et al.*, 1992), and the structure and time dependence of flows near the eastern boundary (Käse *et al.*, 1985; Müller and Siedler, 1992; Pollard and Pu, 1985; Saunders, 1982; Schmitz *et al.*, 1988; Stramma, 1984; Zenk and Müller, 1988; Zenk *et al.*, 1991). Hank Stommel was fond of analyzing hydrographic data in special ways to determine currents, and in the interior another of his neat ideas was the Beta Spiral (e.g., Stommel and Schott, 1977).

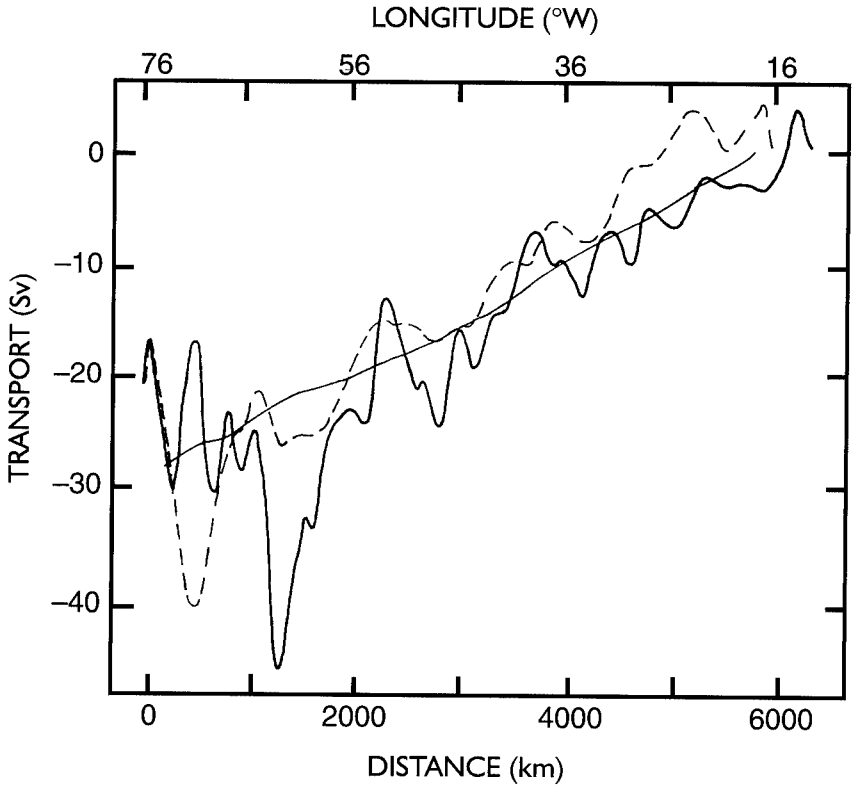

Figure I-66: Transports calculated from the Sverdrup relation with the "Ekman Component" subtracted (thin line), compared with geostrophic transports calculated using hydrographic data along 24°N, solid line denotes data taken in 1981, dashed line indicates earlier IGY data-based results from Leetmaa *et al.* (1977), adapted from Roemmich and Wunsch (1985); see also Schmitz *et al.* (1992).

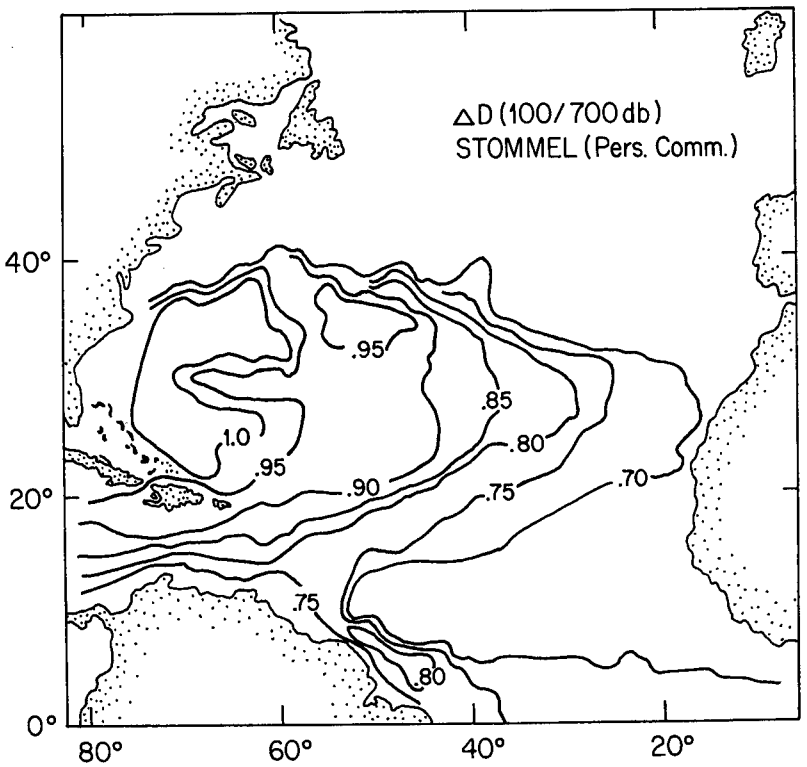

Figure I-67: The ΔD pattern (100/700 dbar, in dynamic meters) in the subtropical North Atlantic based on the hydrographic data set used by Leetmaa *et al.* (1977) and Stommel *et al.* (1978); see Schmitz *et al.* (1992), their figure 6.

Debate (Hautala *et al.*, 1994) over the validity of Sverdrup balance in the North Atlantic was initiated by Leetmaa *et al.* (1977), who demonstrated that this balance is generally consistent with hydrographic data in the eastern 4000 km of the subtropical gyre. The Sverdrup relation was also compared with data along 24°N (Figure I-66) by Roemmich and Wunsch (1985). Dynamic height variation (ΔD) curves are shown in Figure I-67 for the upper layers of the subtropical and tropical North Atlantic, adapted from Stommel (personal communication), see also Schmitz *et al.* (1992) and Böning *et al.* (1991a). Sverdrup transport contours are superimposed on selected dynamic height contours in Figure I-68. Sverdrup balance over the North Atlantic along 24°N up to the eastern edge of the Florida Current requires that the subtropical circulation (above a σ_θ of $\doteq$ 27.4, say) consists of a 30-Sv horizontal circulation cell composed of southward Sverdrup flow in the interior and northward flow in the Florida Current (Roemmich and Wunsch, 1985). However, such a "closed" shallow horizontal circulation cell in the subtropical North Atlantic is clearly inconsistent with the required net northward transport of a sizable quantity of surface water to be converted to deep water in the polar and Labrador seas. Roemmich and Wunsch (1985) noted that the actual basin-

wide integral of the observed geostrophic transport was 19 Sv southward, a number more consistent with the existence of the thermohaline cell but implying that Sverdrup balance cannot be "valid" all the way to the eastern edge of the Florida Current. Their study suggests that the observed and wind-derived geostrophic transports begin to disagree systematically about 2000 km east of the western boundary, roughly one third of the distance across the subtropical Atlantic. The total Sverdrup transport in the eastern two thirds of the Atlantic basin (17 Sv) is then consistent with the purely wind-driven component of the Florida Current, with the remaining 13 Sv of Florida Current transport returned southward at depth in the (DWBC) thermohaline cell (Schmitz and Richardson, 1991; Schmitz *et al.*, 1992). I feel (Figure I-21) that there is an order 10 Sv, partly wind-driven, component to the southern Gulf Stream recirculation that appears as an "Antilles Current."

In the western segment of the gyre interior, particularly near 24°N, considerable attention has been focused on both the Antilles Current and on the DWBC. Sections through this area are shown in Figure I-69. Surface dynamic heights are shown in

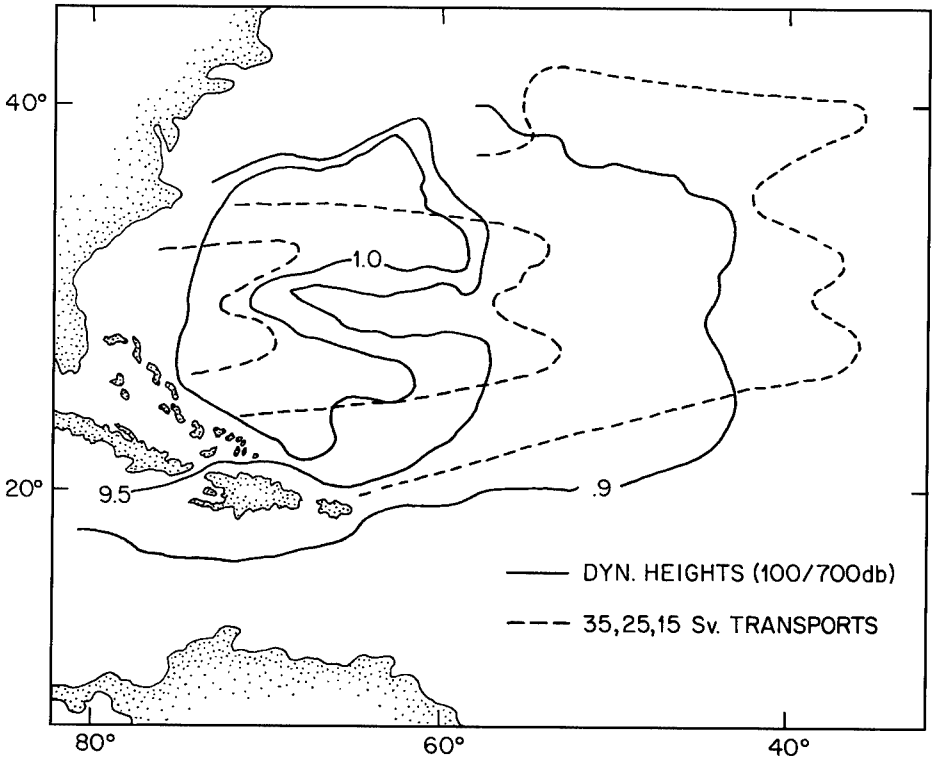

Figure I-68: Sverdrup transport curves superimposed on selected ΔD contours taken from Figure I-67, adapted from Schmitz *et al.* (1992).

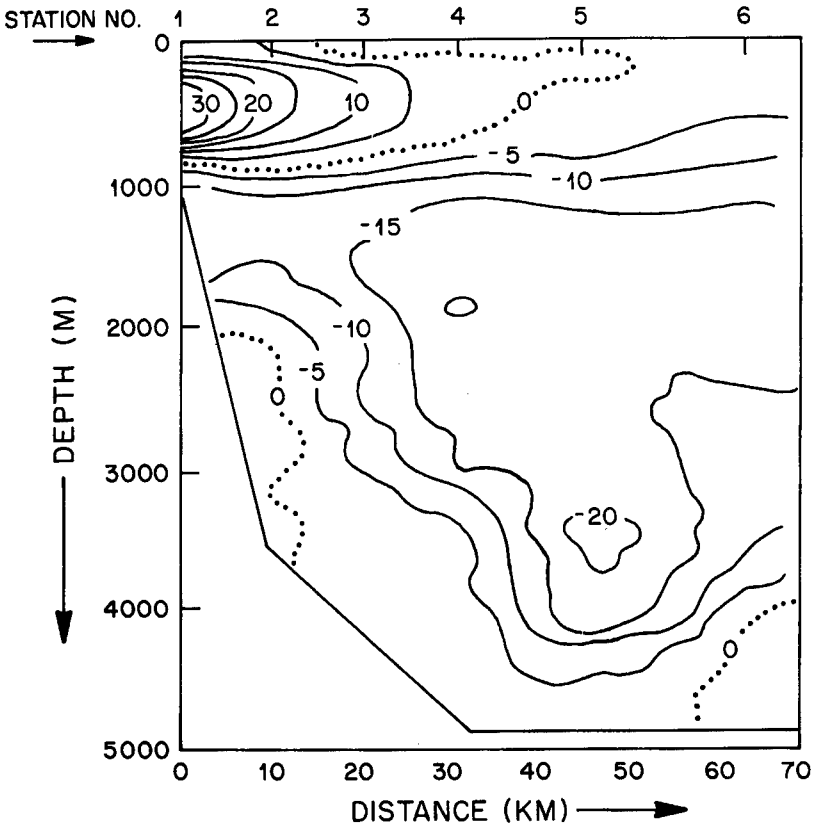

Figure I-69: Time-averaged northward speed contours (cm s^{-1}) for a section off Abaco, Bahamas, adapted from Rosenfeld *et al.* (1989).

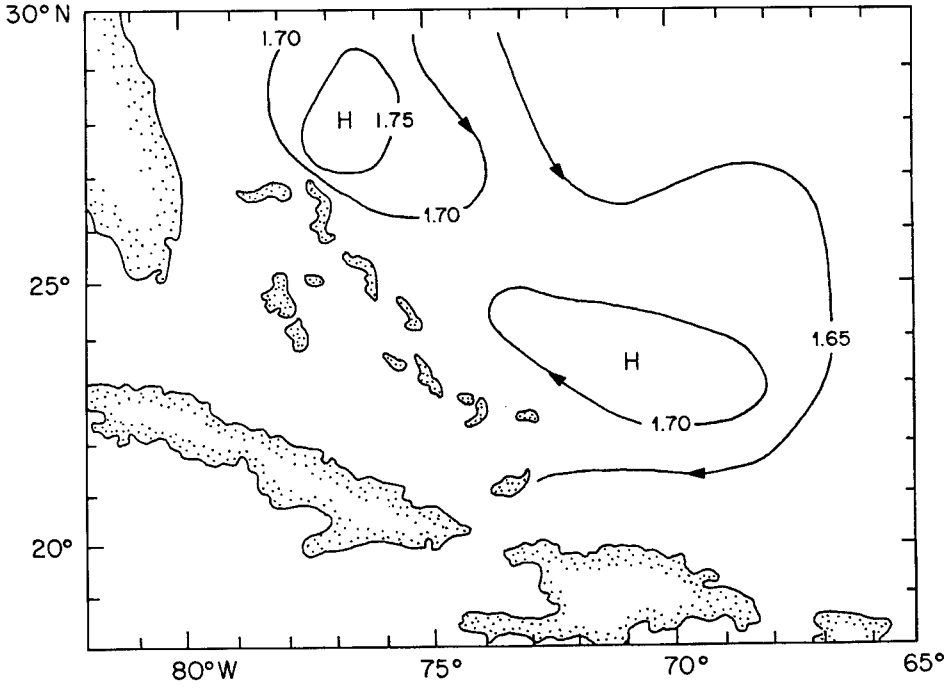

Figure I-70: Surface dynamic topography (dynamic meters) relative to 1000 m in the western subtropical North Atlantic, taken from Schmitz *et al.* (1992).

Figure I-70. The DWBC is well defined in Figure I-69, from about 1000 m depth to near the bottom. There is a possible "Antilles Current" concentrated on the inshore edge of the section with a northward speed maximum at ~ 500 m depth. However, this current appears to be part of a closed circulation pattern on regional scale (*e.g.*, Figure I-70).

The role of eddies in the dynamics of the gyre interior will be discussed in more detail in Section 8 and in Volume III. Generally speaking, my opinion is that eddies do not play a particularly important role in the dynamics of the ocean interior (see Schmitz *et al.*, 1983). Two large field programs (MODE and POLYMODE), primarily emphasizing mesoscale eddies, were carried out in the 1970s near 28° and 31°N in an area centered (nominally) on 70°W, in the gyre interior (but west and near the subtropical front) and on the edge of the southern Gulf Stream recirculation (The MODE Group, 1978; Owens *et al.*, 1982; Owens, 1985). The spectral characteristics of the MODE Site have been summarized by Schmitz (1989). In addition, a large air–sea interaction program was conducted near the same area in the mid 1980s (Weller, 1991). In the east, key observational articles are by Gould (1983), Müller and Siedler (1992), Schmitz *et al.* (1988), and Zenk and Müller (1988).

For the Azores Current, and flows near the eastern boundary, along with the North Equatorial Current east of ~ 50°N, I have relied on Gould (1985), Käse and Siedler (1982), Käse *et al.* (1985), Klein and Siedler (1989), Pollard and Pu (1985), Siedler *et al.* (1985), Stramma (1984), Sy (1988), Zenk and Müller (1988), and Zenk *et al.* (1991). Klein and Siedler (1989) have discussed the origin of the Azores Current very nicely, and Saunders (1982) has described a circulation pattern in the northern North Atlantic consistent with the Klein and Siedler (1989) results. The circulation pattern east of the Mid-Atlantic Ridge by Stramma (1984), which was used as a basic reference by SM93, was shown above in Figure I-37.

4d. Eddies and the Gulf Stream System

In Section 7 below, eddies will be discussed extensively. In this section, I will briefly summarize the kinematics of eddies close to the Stream itself. Gulf Stream meanders will appear as an eddy (periods 20–200 days, say) signal in an Eulerian time-series frame of reference. Meander statistics are summarized in Figure I-56. Gulf Stream Rings (Figures I-71 and I-72) were the first type of mesoscale eddy to be extensively studied (Fuglister, 1971; Fuglister and Worthington, 1951; Iselin, 1940; Richardson *et al.*, 1973, 1978; Richardson, 1976, 1993). As indicated above, to a cur-

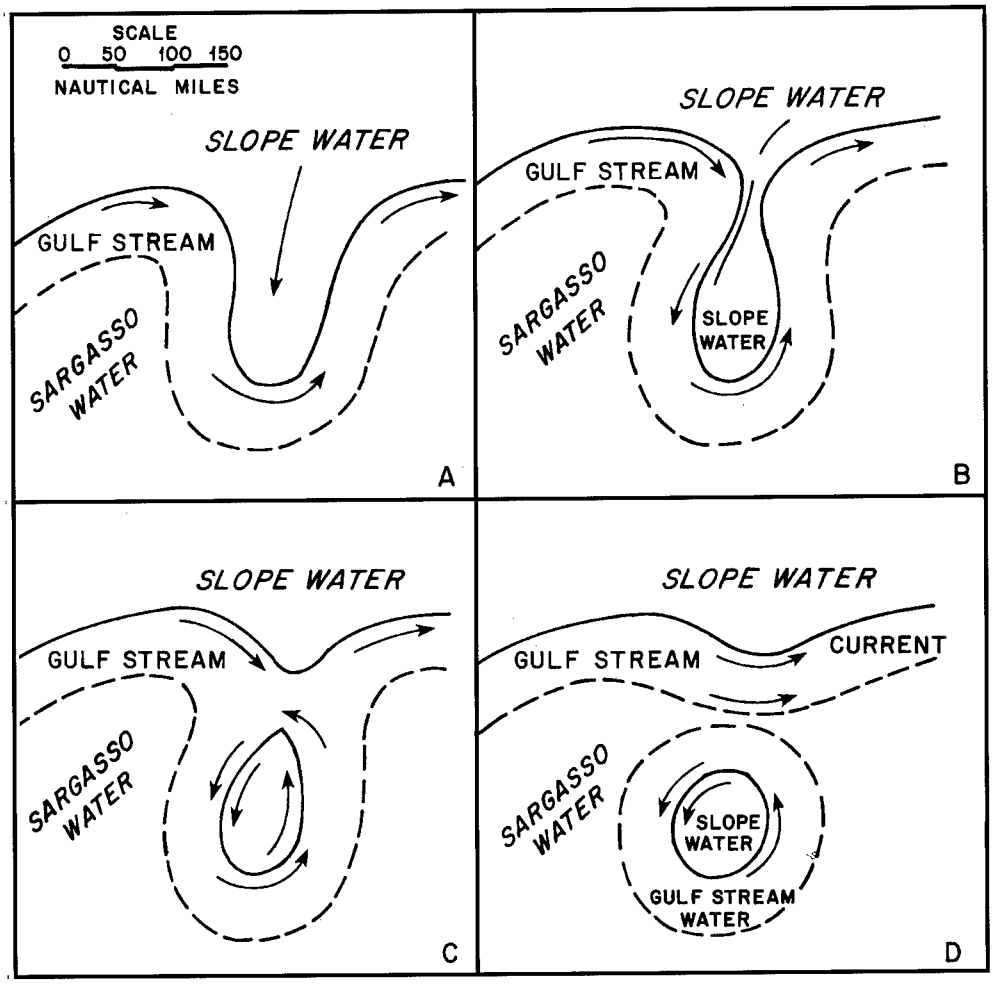

Figure I-71: The kinematics of Gulf Stream warm ring formation, from P. Richardson (personal communication, 1995).

rent meter, Gulf Stream meanders register as eddies as do Gulf Stream Rings when they pass through a site (Hogg, 1994; Hogg and Johns, 1995).

Gulf Stream Rings and meanders have been fairly easy to get at kinematically (synoptic scale) in the upper reaches of the Gulf Stream (the 10° isotherm and above, say), as evidenced by the material in the papers noted at the start of this section and in various review articles. The deep variability and mean flow for rings as well as the Gulf Stream System itself have historically been difficult to describe (Schmitz *et al.*, 1970; Schmitz, 1977). The overall transport structure of both rings and the GSS has also required a lot of effort to define, with breakthroughs in one or more of these areas being accomplished by Hogg (1983), Hall and Bryden (1985), Johns and Watts (1986), Hall and Fofonoff (1993), Hogg (1994), Hogg and Johns (1995), and Johns *et al.* (1995).

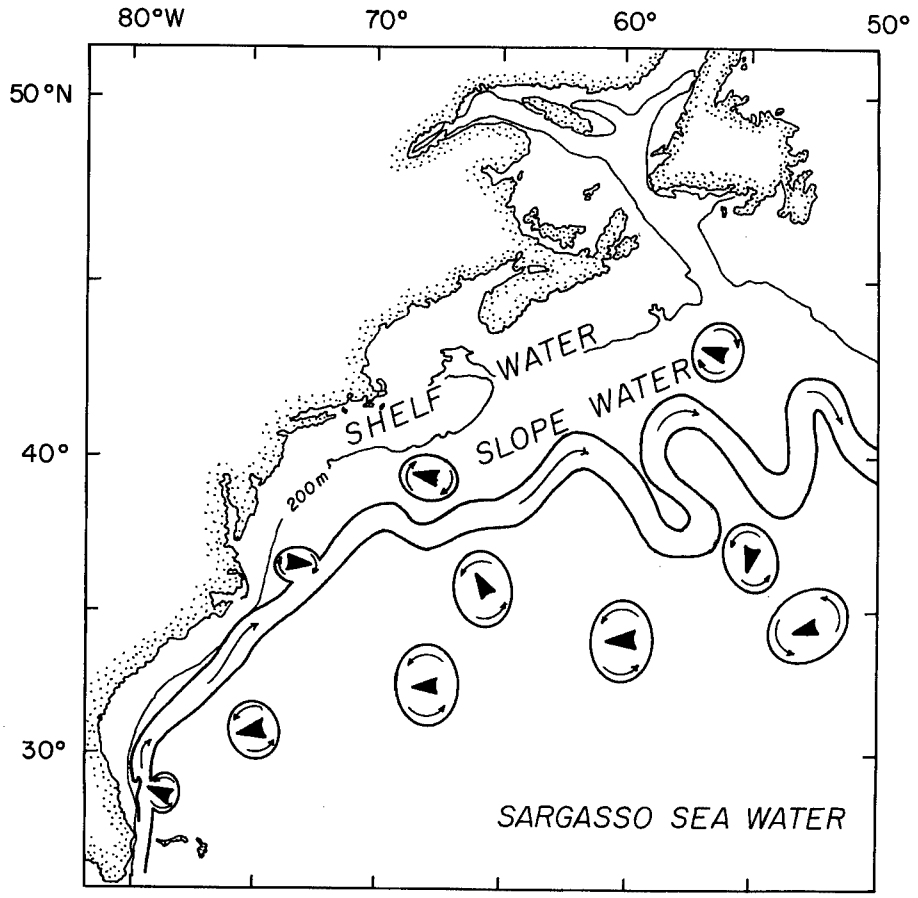

Figure I-72: A map of the western North Atlantic with a schematic representation of the Gulf Stream path, and having a typical number of both cold and warm core rings present, taken from Richardson (1976).

5. On the Tropical Atlantic

Although many investigations of the western tropical Atlantic and Caribbean Sea (Figure I-73) have shed light on the circulation there and on the exchange between the South and North Atlantic, it is an extremely complicated area (Bruce *et al.*, 1985; Cochrane, 1969; Cochrane *et al.*, 1979; Flagg *et al.*, 1986; Mazeika, 1973; Mazieka *et al.*, 1980; Metcalf, 1968, 1976; Metcalf and Stalcup, 1967; Model, 1950; Pillsbury, 1890; Richardson and Reverdin, 1987; Roemmich, 1981; Stalcup and Metcalf, 1972). However, the North Brazil Current System and lately the Caribbean passages have been studied extensively in recent years (Brown *et al.*, 1992; da Silveira *et al.*, 1994; Johns *et al.*, 1990; Richardson, 1994; Richardson *et al.*, 1994; Schott *et al.*, 1995; SR91; Wilson and Johns, 1996; Wilson *et al.*, 1994), so that a clearer picture is emerging. One schematic of the upper level currents at low latitudes in the North Atlantic is shown in Figure I-74.

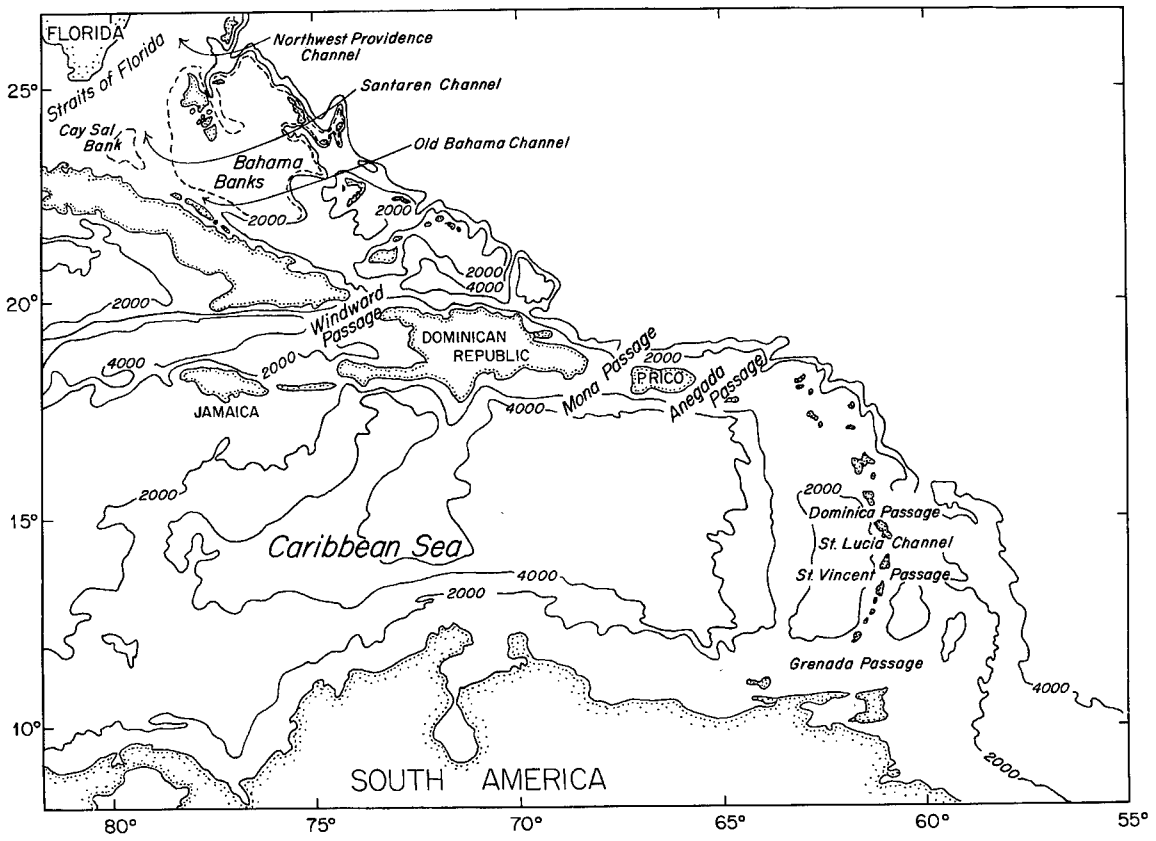

Figure I-73: A map of the Caribbean Sea area, showing key passage names.

Table I-7: Summary of Windward Island Passages monitoring program cruises (Wilson and Johns, 1996)

	Dates	Ship	Stations	Grenada	St. Vincent	St. Lucia	Dominica
WI-1	12–20 Dec 1991	*HMBS Trident*	14	A	A	A	
WI-2	04–09 May 1992	*HMBS Trident*	14	A	A	A	
WI-3	18–22 Sep 1992	*HMBS Trident*	14		A	A	A
WI-4	08–14 Dec 1992	*HMBS Trident*	17	A	A	A	
WI-5	07–12 Feb 1993	*HMBS Trident*	8	C			
WI-6	24–28 Mar 1993	*HMBS Trident*	14		B	B	B
WI-7	08–10 Jun 1993	*Malcolm Baldrige*	21	D	D	D	D
WI-8	01–09 Apr 1994	*Malcolm Baldrige*	27	D	D	D	D
WI-9	18–28 Jul 1994	*Malcolm Baldrige*	42	D	D	D	D
WI-10	06–09 Dec 1994	*HMBS Trident*	6			D	
Total			177	7	9	9	5

A Full depth CTD and upper ocean (< 300 m) ADCP
B Full depth CTD only
C Upper ocean (< 300 m) ADCP only
D Full depth CTD and full depth lowered ADCP

Wilson and Johns (1996) have recently carried out the most extensive transport measurement program ever in the (southern) Caribbean passages. Results are summarized in Tables I-7 through I-9 and Figure I-75. Table I-7 is a list of the cruises made and location of lines of stations across passages. In Table I-8, there are transport estimates for each of these cruises along with some statistics. The most remarkable feature of Table I-8 is the very large amplitude, long-term variability in the measured transports. This feature was originally noted by Pillsbury (1890) and Model (1950, using Pillsbury's results, Table I-10), but made much clearer by Wilson and Johns (1996). Pillsbury (1890) actually found no net transport through Grenada Passage and surroundings. Another feature (Table I-10) emphasized by Model (1950) was the broad distribution (see also Schmitz *et al.*, 1993) of net transport through many passages, not just the southern passages. Table I-9 lists mean transports for temperature layers, adapted from Wilson and Johns (1996) and SR91. The SR91 estimates were based on

Table I-8: Total transport (in units of 10^6 m^3 s^{-1}) by cruise and passage (Wilson and Johns, 1996)

Cruise		Grenada	St. Vincent	St. Lucia	3 PSG Total	Dominica
1 cm s^{-1} =		0.27 Sv	0.20 Sv	0.17 Sv		0.3
WI-1	(12/91)	6.9	5.9	0.1	12.9	
WI-2	(5/92)	0.1	2	0.5	2.6	
WI-3	(9/92)		4.9	1.4		0.5
WI-4	(12/92)	2.6	2.2	2.2	7	
WI-5,6	(2, 3/93)	no complete deep transport sections				
WI-7	(6/93)	11.2	4.9	0.8	16.9	–0.2
WI-8	(4/94)	2.2	–0.2	0.9	2.9	1.9
WI-9	(7/94)	4.9	4.3	1.9	11.1	–0.3
WI-10	(12/94)			–0.4		
Mean		4.7	3.4	0.9	(9.0) 8.9	0.5
Std Err		1.6	0.8	0.3	(1.8) 2.3	0.5
Direct Obs. Only		5.4	3	0.8	9.2	0.7
SR 91		9.5	9.7	5.9	25.1	2.6
Std. Dev		3.2	2	1.2	4	

Table I-9: Mean transport temperature layers for indicated passages (Wilson and Johns, 1996)

Passage	<7°C	>7°C	7–12°C	12–17°C	17–24°C	12–24°C	>24°C	Total
Grenada	0.1 (0.1)	4.6 (1.5)	1.2 (0.8)	0.7 (0.3)	0.6 (0.4)	1.3 (0.5)	2.2 (0.4)	4.7 (1.6)
St. Vincent	–0.1 (0.1)	3.5 (0.8)	0.5 (0.3)	0.6 (0.2)	0.7 (0.1)	1.4 (0.3)	1.5 (0.4)	3.4 (0.8)
St. Lucia	–0.1 (0.1)	1 (0.3)	–0.2 (0.1)	0.1 (0.1)	0.3 (0.1)	0.4 (0.1)	0.8 (0.1)	0.9 (0.4)
Total	–0.1 (0.2)	9.1 (1.7)	1.5 (0.8)	1.4 (0.3)	1.6 (0.4)	3.1 (0.6)	4.5 (0.6)	9.0 (1.8)
SR91								
Grenada	1.8	7.7	2.2	0.6	2.1	2.7	2.8	9.5
St. Vincent	1.8	7.8	1.6	2.2	1.8	4	2.3	9.7
St. Lucia	2.1	3.8	1.3	0.9	0.8	1.7	0.8	5.9
Total	5.7	19.4	5.1	3.7	4.7	8.4	5.9	25.1

Table I-10: Caribbean Passage transports (in Sv.) according to Pillsbury (1890) and Model (1950)

Passage Boundaries	Transport
Paria–Grenada–St. Vincent	0
St. Vincent–St. Lucia	3.2
St. Lucia–Martinique	3.1
Martinique–Dominica	4.8
Dominica–Guadalupe	2.7
Guadalupe–Antigua	5.1
Antigua–Barbuda	0.2
Barbuda–St. Martin, Anguilla	2.2
St. Martin, Anguilla–Anegada, Virgin Gorda	2.9
Anegada, Virgin Gorda–Puerto Rico	0
Puerto Rico–Haiti	3.0
Haiti–Cuba	0.8
	28.0

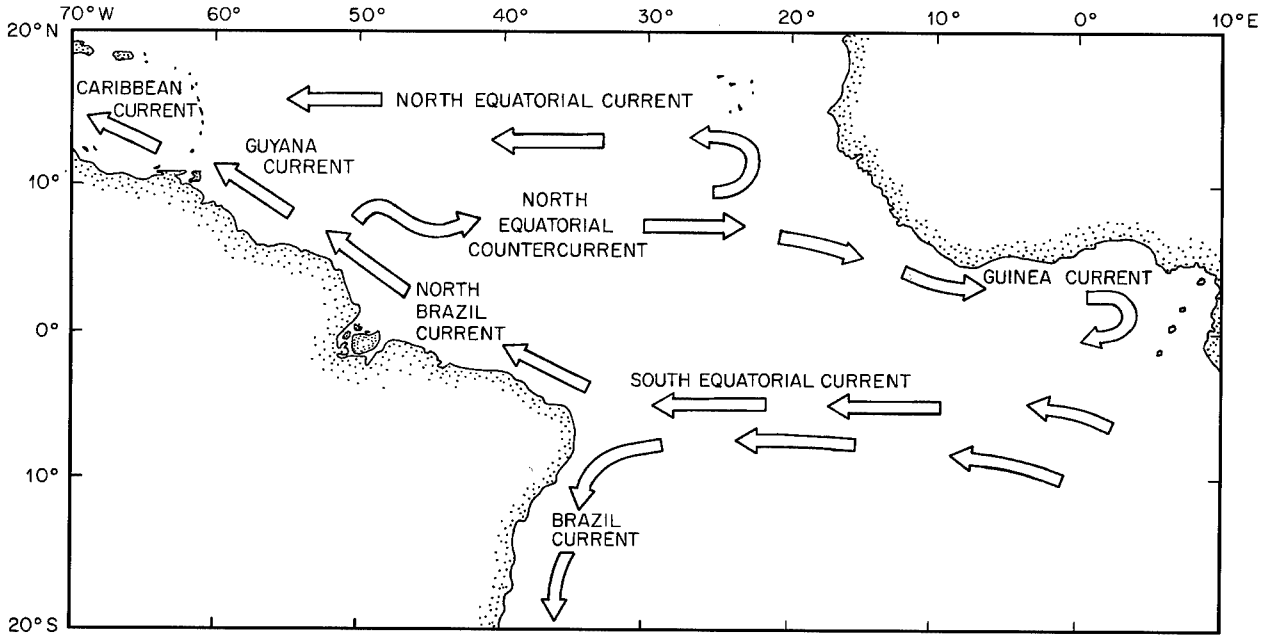

Figure I-74: The pattern, location and nomenclature of the principal upper layer currents in the tropical Atlantic, adapted from Richardson and Walsh (1986).

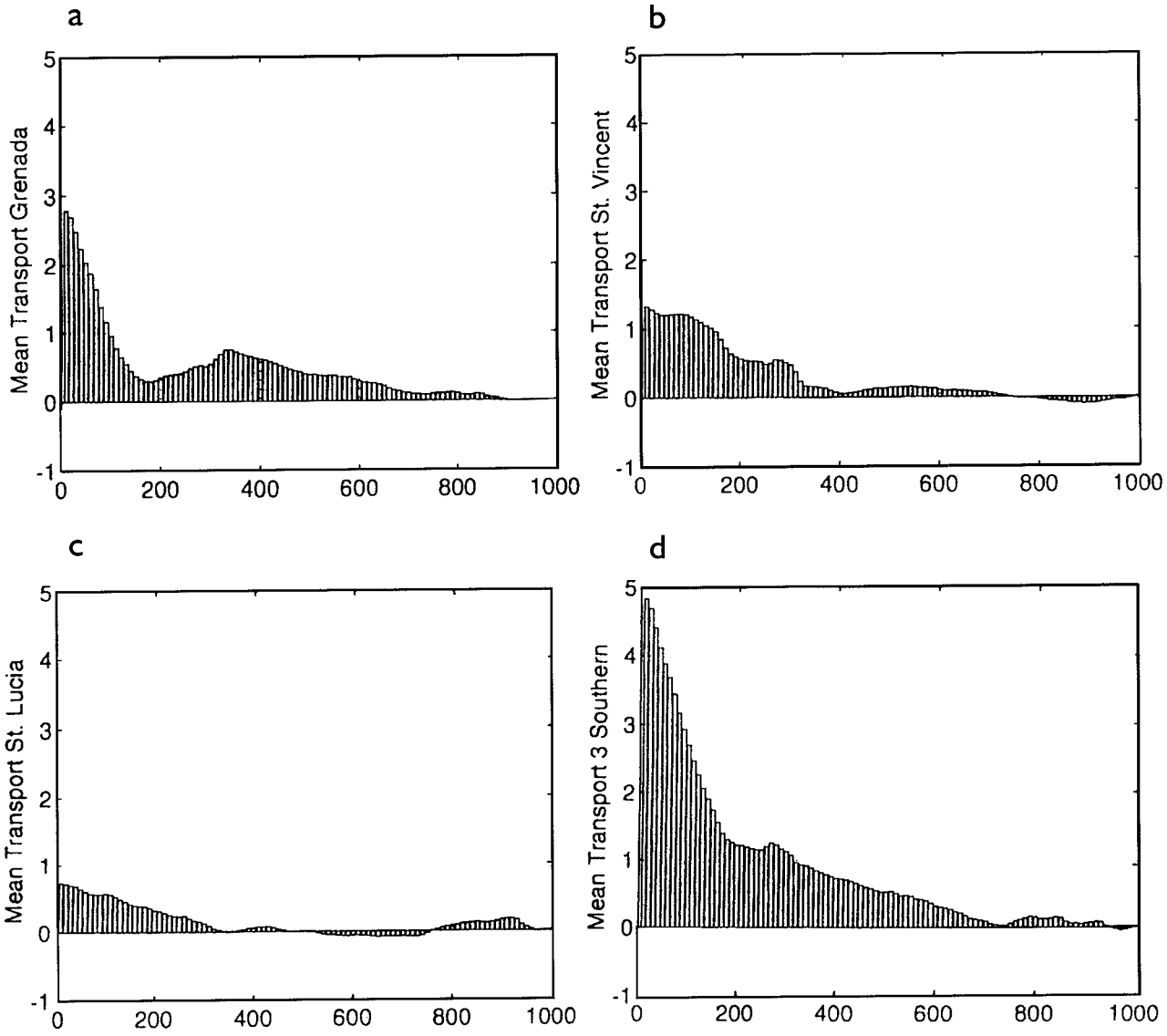

Figure I-75: Transport per unit depth (in 10^4 m^2 s^{-1}) by 10-meter vertical bins: (a) Grenada Passage, (b) St. Vincent Passage, (c) St. Lucia Passage, and (d) sum of the three southern passages, adapted from Wilson and Johns, 1996.

only 1 month of lowered current meter data (Table I-11) acquired by Stalcup and Metcalf (1972).

The retroflection area is well defined by surface drifters (Figure I-76), presented by Richardson and Reverdin (1987) and Richardson *et al.* (1994). Summary schemat-

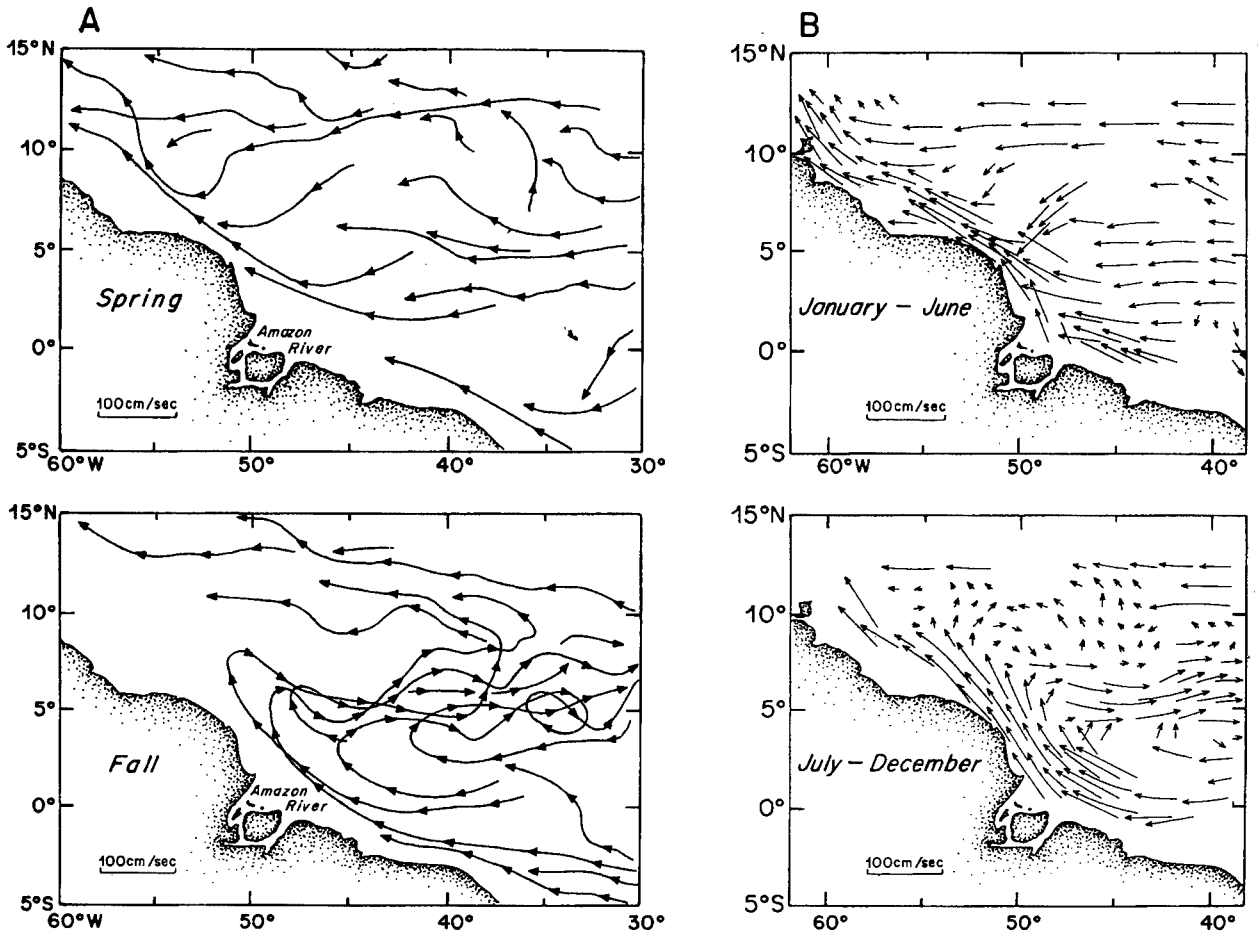

Figure I-76: A compilation of surface drifter data in the North Brazil Current Retroflection area, 1983–1985, adapted from Richardson and Reverdin (1987); (a) selected individual tracks, and (b) averaged or mean velocity.

ics for North Brazil Retroflection Eddies (Richardson, 1994) with the larger scale circulation in their area of occurrence are shown in Figure I-77, and a detailed case study in I-78. These features have now been modelled with some relevance (Fratantoni *et al.*, 1995), as has seasonal variability (Böning *et al.*, 1991b).

SOFAR floats have recently been used to study the deep flow in the vicinity of the equator (Richardson and Schmitz, 1993). Two possible syntheses of the general flow pattern observed at 1800 m are shown in Figure I-79. McCartney and colleagues have focused on the deep flow at low latitudes in the past several years (McCartney, 1993; McCartney *et al.*, 1991; McCartney and Curry, 1993). The exchange of water between

the South and North Atlantic has long been a central topic in tropical oceanography. Table I-12, for example, is taken from Sverdrup *et al.* (1942). Even today this table looks good to me, at both the equator and perhaps at 30°S. The specific numbers by layers compare to within a few Sverdrups with SM93 and SR91. Recent measurements of the origins of the NBCS in the South Atlantic (da Silveira *et al.*, 1994; Schott *et al.*, 1995; Stramma, 1991; Stramma *et al.*, 1990, 1995), are also consistent with Table I-12, SR91 and SM93 to within a few Sverdrups, in terms of net (not including retroflected transports) flow into the North Atlantic.

Table I-11: Westward transport through the Grenada, St. Vincent and St. Lucia Passages as measured with a lowered current meter (Sverdrups)

Date	>36	O_2 minimum	<34.8	Total
Grenada Passage				
16 March	3.8	1.8	2.0	7.6
20 March	2.6	2.2	1.7	6.5
14 April	4.8	3.6	1.9	10.3
17 April	8.9	4.1	2.9	15.9
18 April	6.6	2.3	1.4	10.3
18 April	3.3	2.8	1.2	7.3
Mean	4.9	2.8	1.8	9.6
St. Vincent Passage				
22 March	4.1	5.4	3.2	12.7
23 March	4.6	5.8	1.7	12.1
26 March	3.5	3.6	1.7	8.8
10 April	3.8	2.7	1.2	7.7
12 April	4.3	2.6	1.2	8.1
13 April	4.7	2.6	1.7	9.0
Mean	4.1	3.8	1.8	9.7
St. Lucia Passage				
3 April	1.3	1.8	1.9	5.0
5 April	2.0	2.6	2.2	6.8
Mean	1.6	2.2	2.1	5.9
Grand means	10.6	9.0	5.7	25.2

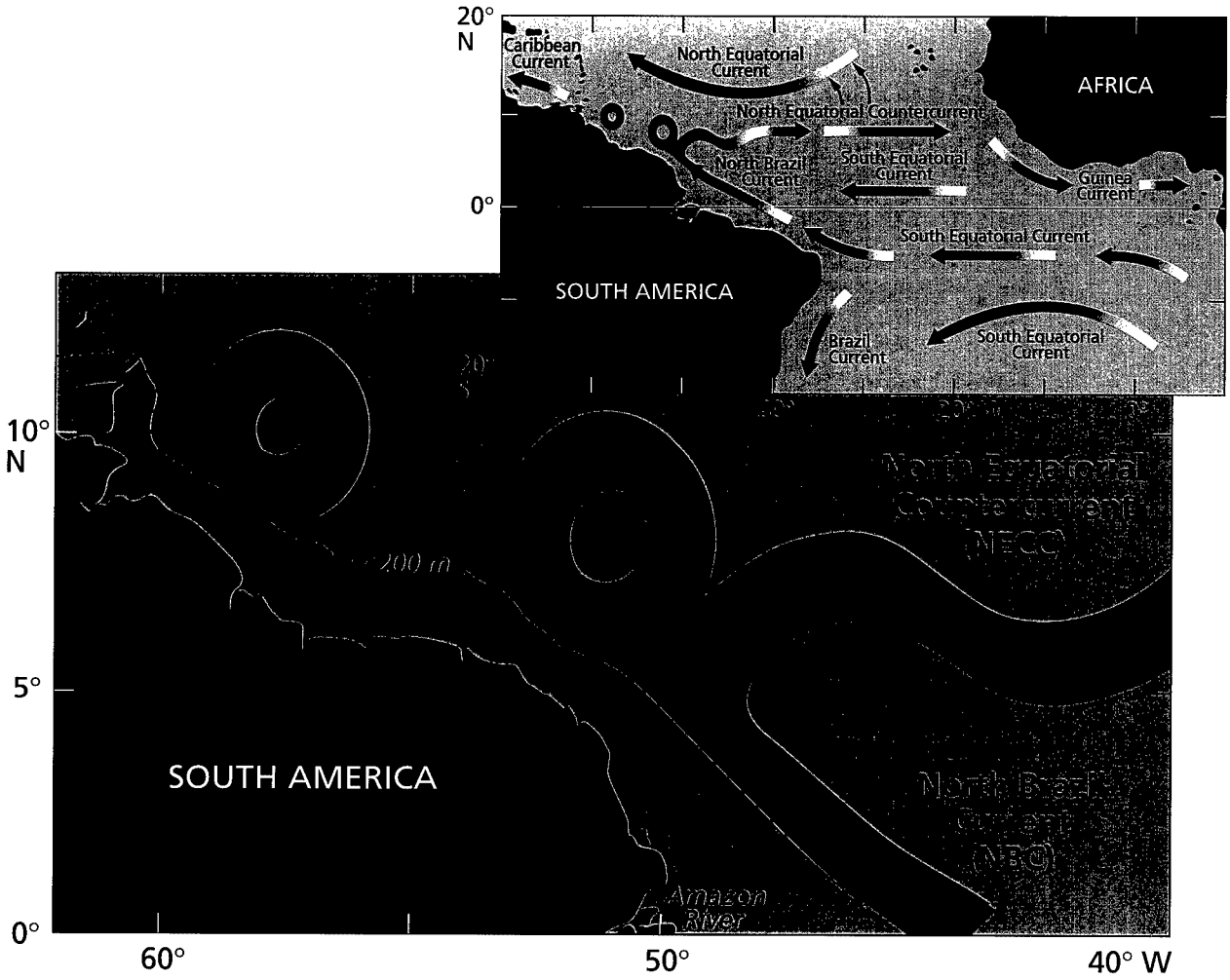

Figure I-77: Large scale schematic diagram for North Brazil Current retroflection eddies and their environment, adapted from Richardson (1994).

Of course, the equatorial Atlantic is a major research area in its own right (Gouriou and Reverdin, 1992; Leetmaa *et al.*, 1981; Philander, 1973; Philander and Pacanowski, 1986a and b). Numerical models developed by Philander and Pacanowski (1986a, b) have been shown to agree with the ocean surface data base to within a factor of about 2 by Richardson and Philander (1987). Gouriou and Reverdin (1992, their figure 18) identify 7 Sv of surface layer water crossing into the North Atlantic, in reasonable agreement with Schmitz and Richardson (1991) and Figure I-21 (which has 9 Sv).

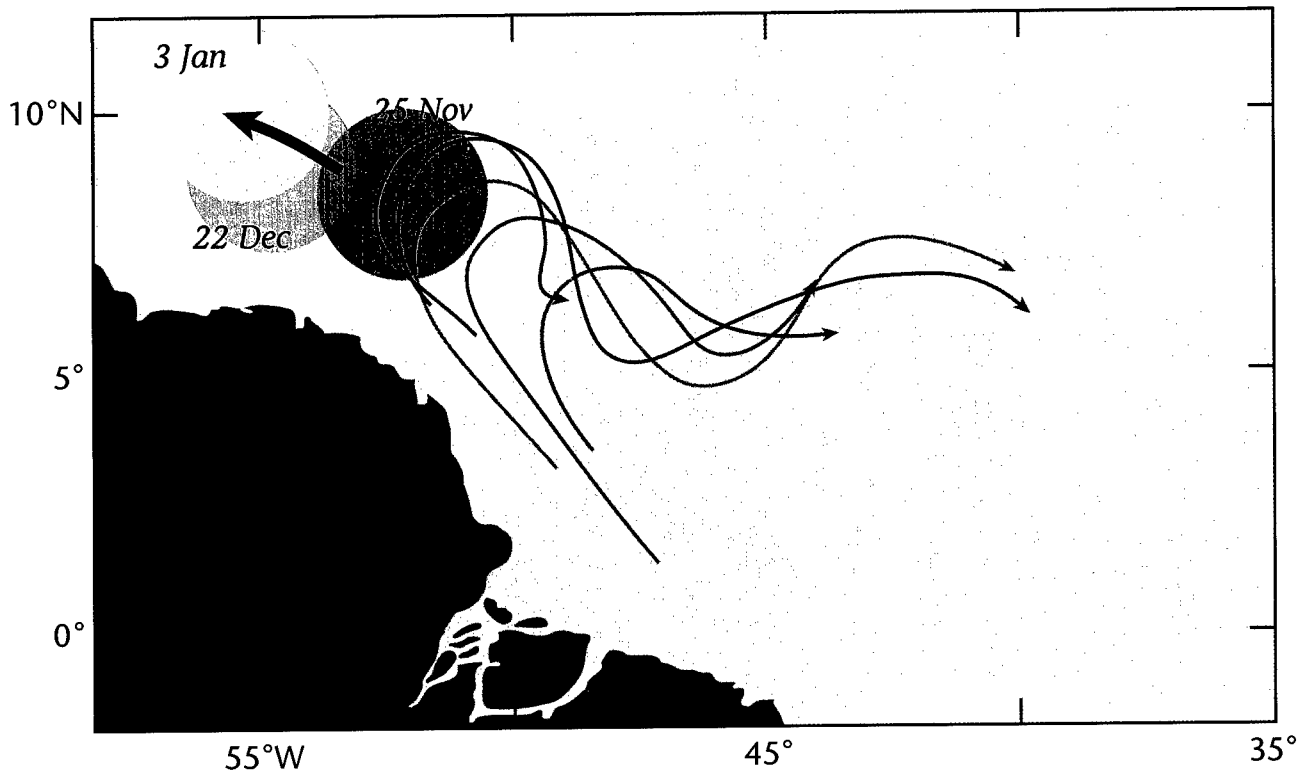

Figure I-78: North Brazil Current retroflection eddies and associated surface drifter tracks, 1979.

Table I-12: Transport of water across Latitude 30°S and across the equator, adapted from Sverdrup *et al.* (1942, their table 76)

		Transport in million m^3/sec toward	
Latitude	Water Mass	North	South
30°S	Upper water	16	
	Intermediate water	9	
	Deep water		18
	Bottom water	3	
0°	Upper water	6	
	Intermediate water	2	
	Deep water		9
	Bottom water	1	

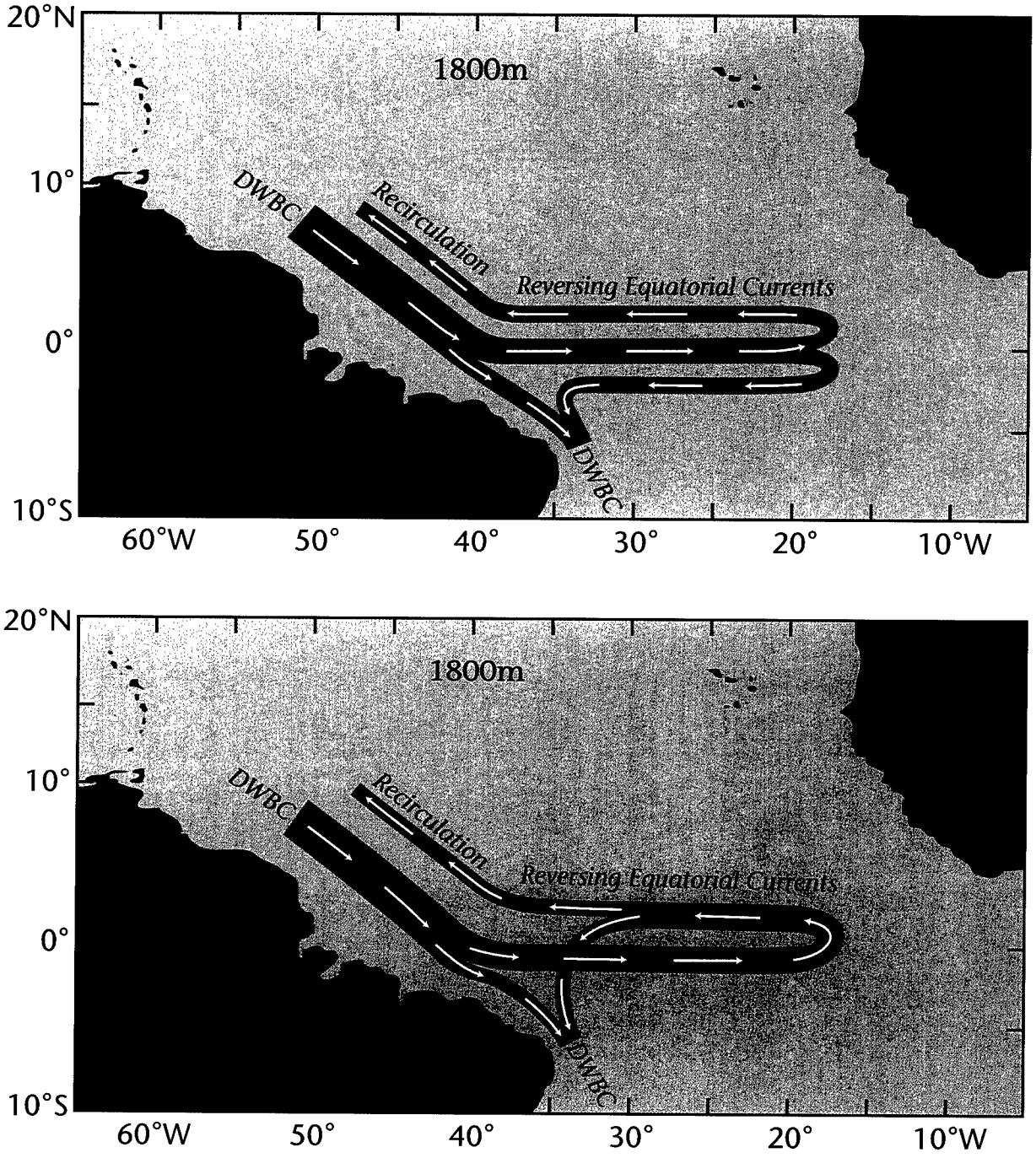

Figure I-79: Schematic diagrams for the flow patterns implied by SOFAR float trajectories at 1800 m.

6. The Subpolar North Atlantic

This area, with its proximity to Europe and Canada, has been the focus of a lot of attention historically. My own experience with the northern North Atlantic has not been extensive, so this treatment of the topic will be restricted, but not because the area is not important. Emphasis will be on intergyre or interbasin exchange. The "upper layer" water used to form NADW must enter subpolar latitudes (> ~ 40°N) from the subtropics (≥ 20° and ≤ 40°N). One version of such an exchange was shown earlier in this report in Figures I-21 and I-22, which are modifications (updates) of figures 8 and 14 in SM93.

A recent schematic of the part of the largest scale meridional cell involving DSOW (Denmark Straits Overflow Water) in the North Atlantic is shown in Figure I-80 (M.

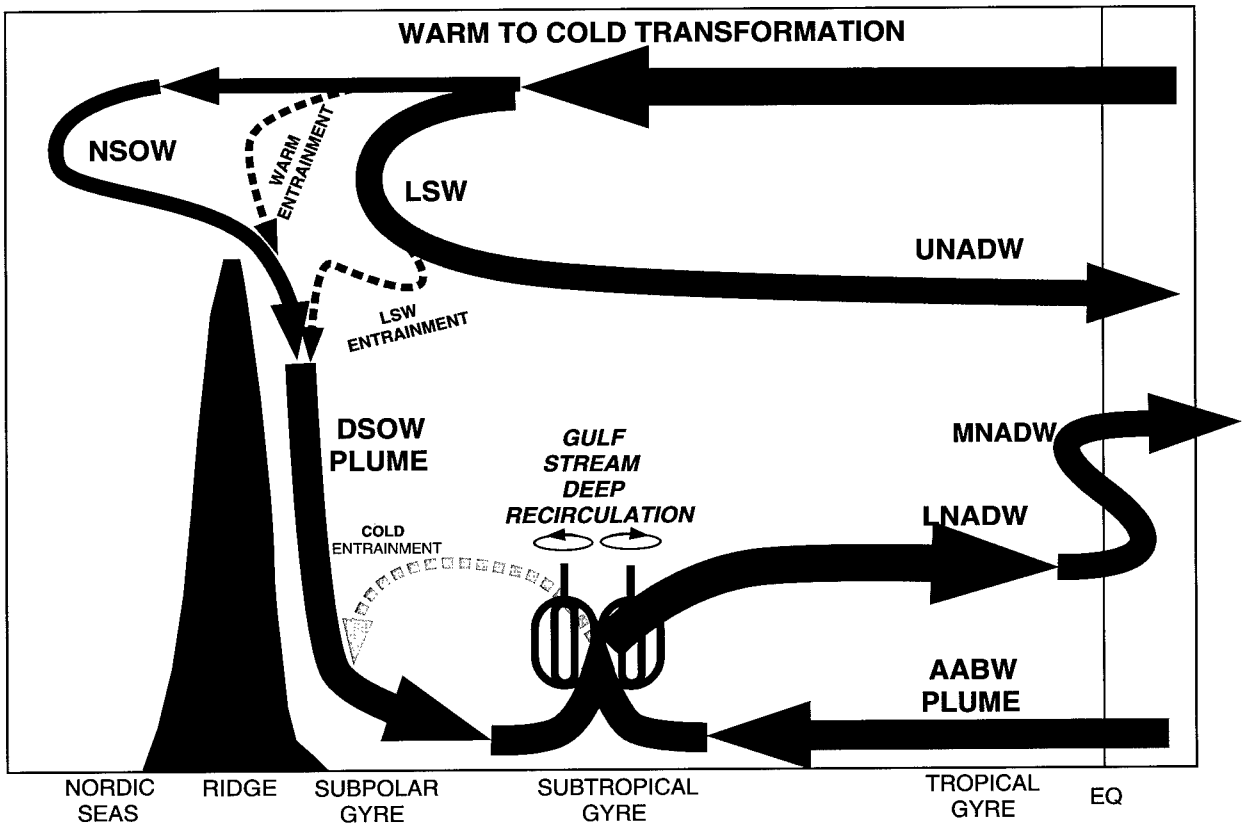

Figure I-80: A meridional schematic section of the largest-scale overturning (thermohaline) cell in the North Atlantic, including a possible mixing mechanism, according to M. McCartney and R. Curry (personal communication, 1996). See text (especially Table I-1) for water mass nomenclature.

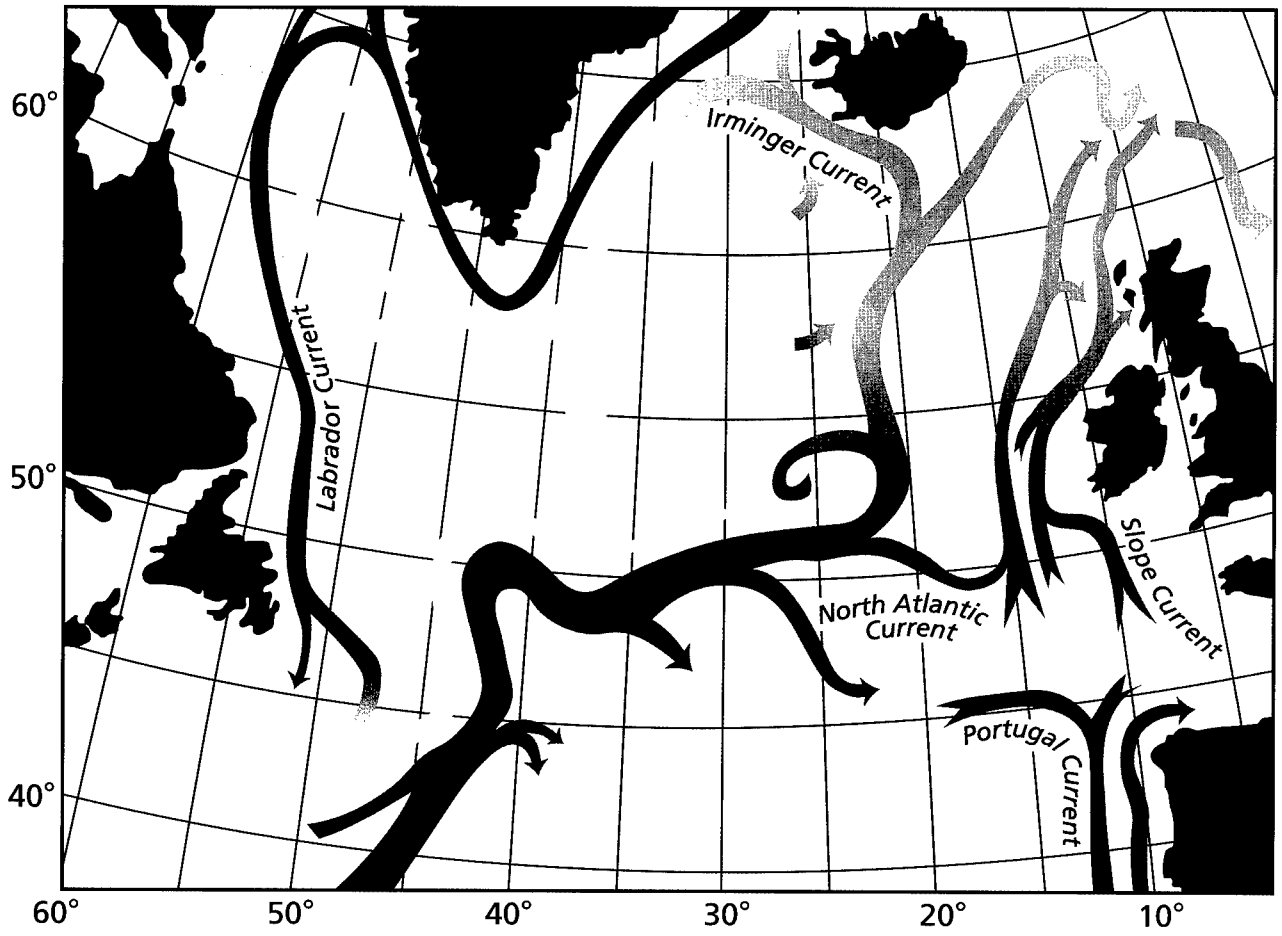

Figure I-81: A circulation scheme for the northern North Atlantic according to McCartney (1995, personal communication), adapted from Heywood *et al.* (1994), Ellett (1993), and Krauss (1986). Red lines denote water ~ 15°C, yellow ~ 4°C and blue ~ 0°C, with shadings of oranges or greens indicating intermediate temperatures. The small curled or spiraling lines denote sinking.

McCartney and R. Curry, personal communication, 1996). Please note that this figure and my meridional cell (Figure I-12, which also contains overflow across the Iceland–Scotland ridge system, and forms MNADW directly in the northern North Atlantic) are somewhat different. In Figure I-80, comparatively warm (dark blue) water from the subtropics, while in the "subpolar gyre," (a) exits (solid pink line) into the nordic seas and returns after conversion to overflow water (NSOW, red line); (b) is also partially transformed by convection into LSW (brown line), some of which is in addition later entrained (dashed brown line) into NSOW, and is the source for UNADW; and (c) also gets directly entrained (dashed pink line) into NSOW. The DSOW plume that is formed

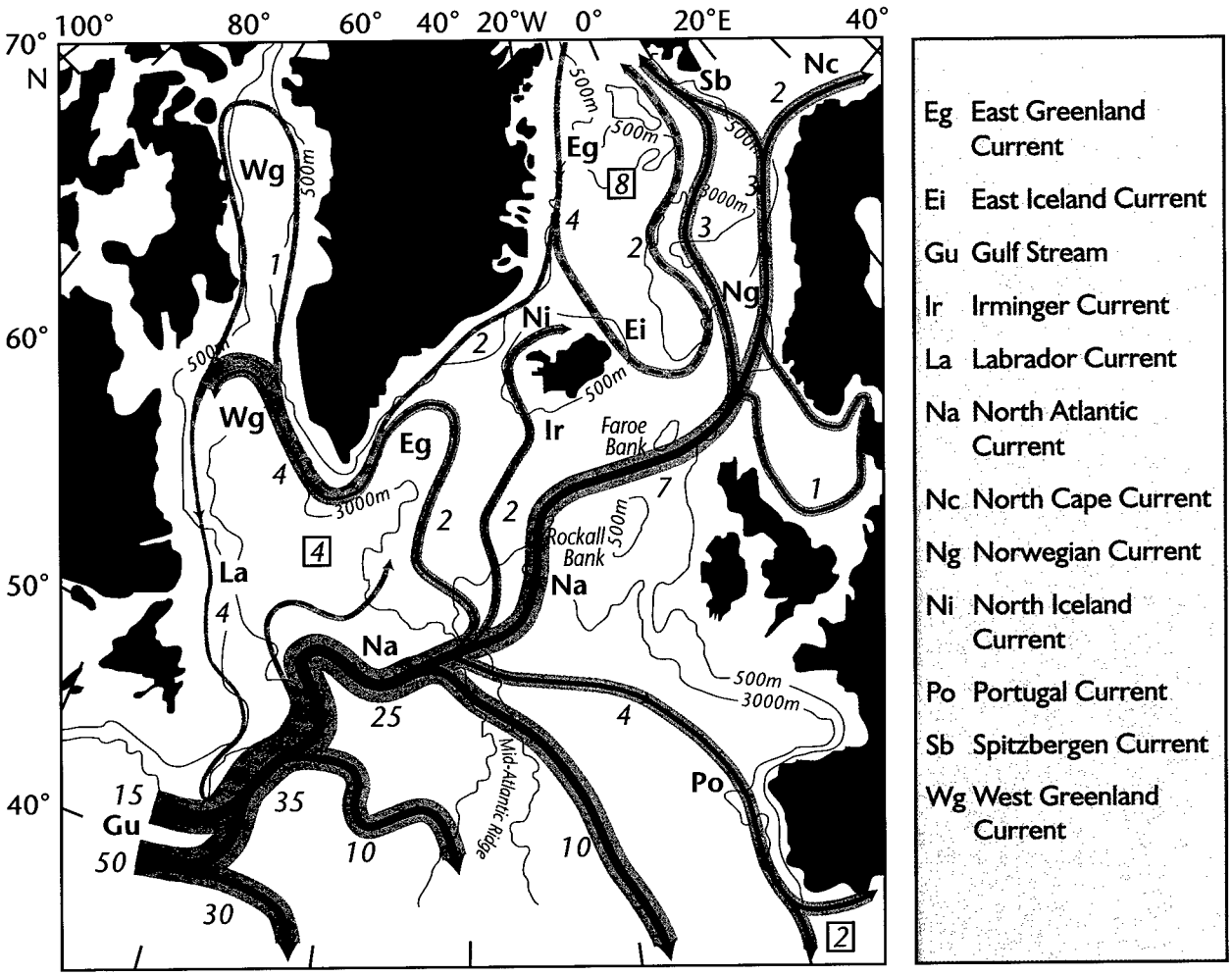

Figure I-82: The transports for the upper 1000 m of various currents in the northern North Atlantic, adapted from Dietrich *et al.* (1980); see also Dietrich (1969a, b) and Krauss (1986, 1995). See text for discussion. Transports next to various currents are in Sverdrups; squares denote descending water. Solid lines denote relatively warm currents, broken lines relatively cold.

from NSOW and both warm and LSW entrainment "mixes" with AABW (light blue line) and cold entrainment (yellow line) to form LNADW. The biggest difference between I-80 and my I-12 is that I-80 does not include the overflow across the Iceland–Scotland Ridge and the MNADW in Figure I-12.

Another recent schematic in a similar vein, of the associated horizontal circulation in the Subpolar Gyre Area, is shown in Figure I-81 (M. McCartney, personal communication, 1995; adapted from Ellett, 1993; Heywood *et al.*, 1994; and Krauss,

1986). The transports for the upper 1000 m of various currents in the Subpolar North Atlantic according to Dietrich *et al.* (1980) are shown in Figure I-82 (which also contains major topographic features); see also Dietrich (1969a, b) and Krauss (1986, 1995) and Wegner (1973). Beyond ~ 50°N in Figure I-82, the NAC (labeled Na in Figure I-82) and its northern branches are shown to transport 11–12 Sv, in comparison with 13–14 Sv in Figure I-21, hardly a significant difference. The sinking of 4 Sv in the Labrador Sea in Figure I-82 is identical to that in Figure I-21 (and its progenitor in SM93). The other branches of the NAC, those south of ~ 50°N, are different from those shown in Figure I-21. In particular, there is no Newfoundland Basin Eddy in Figure I-82, as opposed to the case presented by Mann (1967) and Clarke *et al.* (1980), adopted by SM93, and as in Figure I-21. On the other hand, the transports branching from the NAC south of ~ 50°N yield a summed transport of 20–25 Sv, about the strength as-

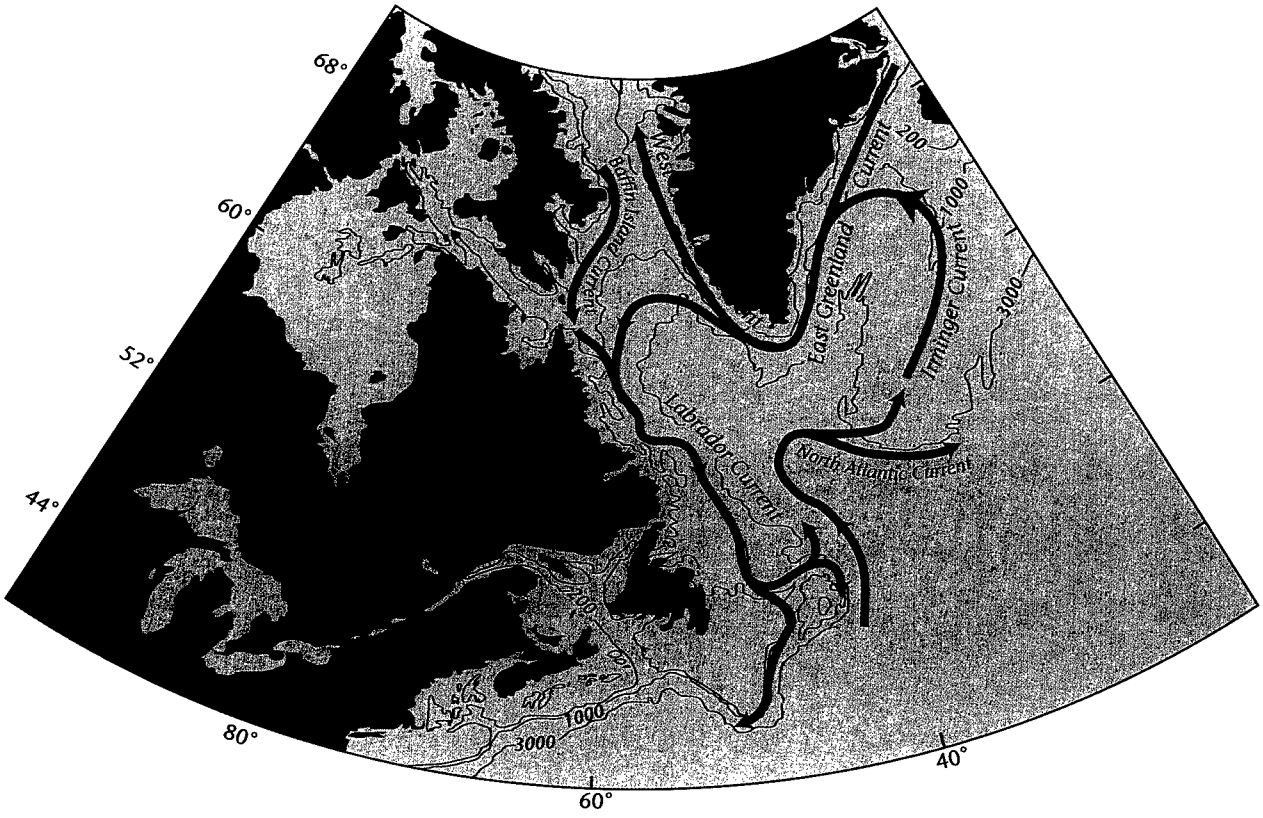

Figure I-83: The North Atlantic Subpolar gyre circulation, adapted from Lazier and Wright (1993). Red denotes warm water of subtropical origin, green water as it starts to cool in the Irminger Current, and blue denotes very cold water, basically LSW in the SPGS.

signed to the upper layers of the Newfoundland Basin Eddy in Figure I-21. The composite circulation in Figures I-81 and I-82 that is south of the polar seas and north of the GSS is here called the Subpolar Gyre Circulation System (SGCS).

The circulation in the western subpolar North Atlantic has been exceptionally well determined by Canadian oceanographers (Clarke, 1984; Clarke and Gascard, 1983; Clarke *et al.*, 1980; Lazier, 1973, 1982, 1994; Lazier and Wright, 1993; Mann, 1967), as indicated for example in Figure I-83, adapted from Lazier and Wright (1993). Lazier and Wright (1993) is a critical reference for establishing the contemporary picture of the Subpolar Gyre Circulation. Krauss and colleagues (Krauss, 1986, 1995; Krauss and Meinke, 1982; Krauss *et al.*, 1990) have also done a lot of work in the northern North Atlantic, especially on the North Atlantic Current; see also Saunders (1982), Sy (1988) and Sy *et al.* (1992). Figure I-84 is a picture of the eddy field (the first accurate EKE distribution) associated with the North Atlantic Current (Krauss, 1986). There have also been recent satellite-altimeter-data-based estimates of surface K_E there (Heywood *et al.*, 1994).

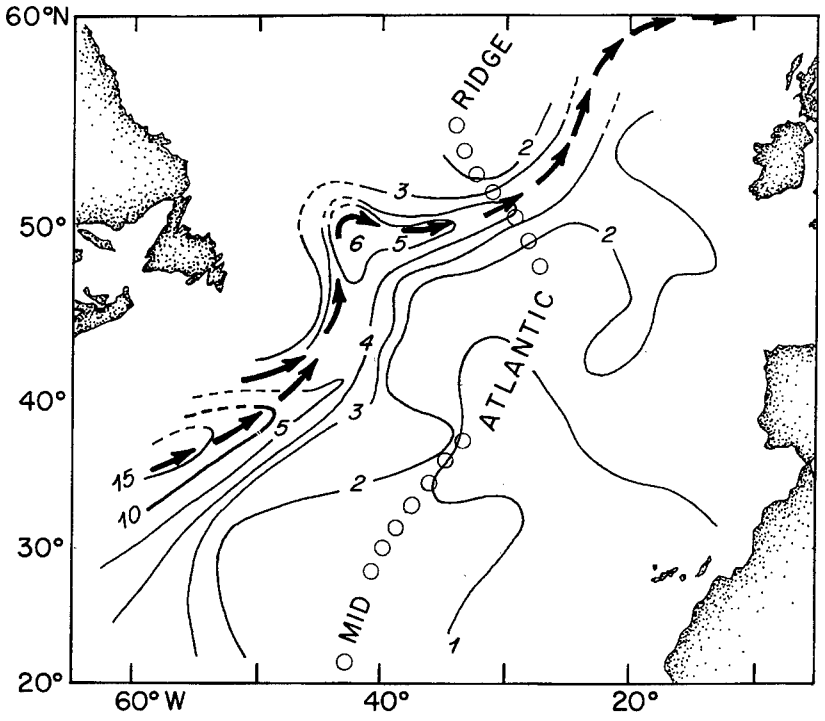

Figure I-84: EKE in the vicinity of the North Atlantic Current (NAC). Contours in units 100 cm^2 s^{-2}, solid arrows denote the path of the NAC system.

My starting point for the "upper layer circulation" in the northern North Atlantic is at the location where the Gulf Stream System splits near the Grand Banks. At this point the upper mixed layer flow in Figure I-21 from the South Atlantic into the GSS and subtropical gyre has hypothetically been converted to something like NACW, which I take

to include the upper layer convection resulting in 18° Water as well as subtropical underwater. A schematic diagram by SM93 comparing Mann (1967) and Worthington (1976) is shown in Figure I-85. Schmitz and McCartney (1993) basically agree with Mann (1967) and Clarke *et al.* (1980) concerning a connection between the GSS and the NAC, along with the existence of a Newfoundland Basin Eddy (Mann, 1967). The SM93 estimate of 13 Sv (increased to 14 here) of upper layer (12 Sv > 7°C directly from the GSS, 1 Sv Mediterranean Water; see Figure I-21) compensation flow in the NAC is the upper layer NADW replacement only, and does not include the upper layer of the predominantly wind- and thermodynamically-driven subpolar gyre proper (see Figure I-89 and accompanying discussion in the following). A scheme that has more than 14 Sv or so of upper layer water (T > 7°C) moving from the subtropics into the subpolar area needs to either return the excess relative to 14 Sv of this water south in the upper layer or provide correspondingly more (than 14 Sv) lower layer (T < 7°C) water formed or joining NADW. Schmitz and McCartney (1993) also have 4 Sv modified AABW joining NADW, as indicated in Figure I-86 (identical to Figure I-22, except

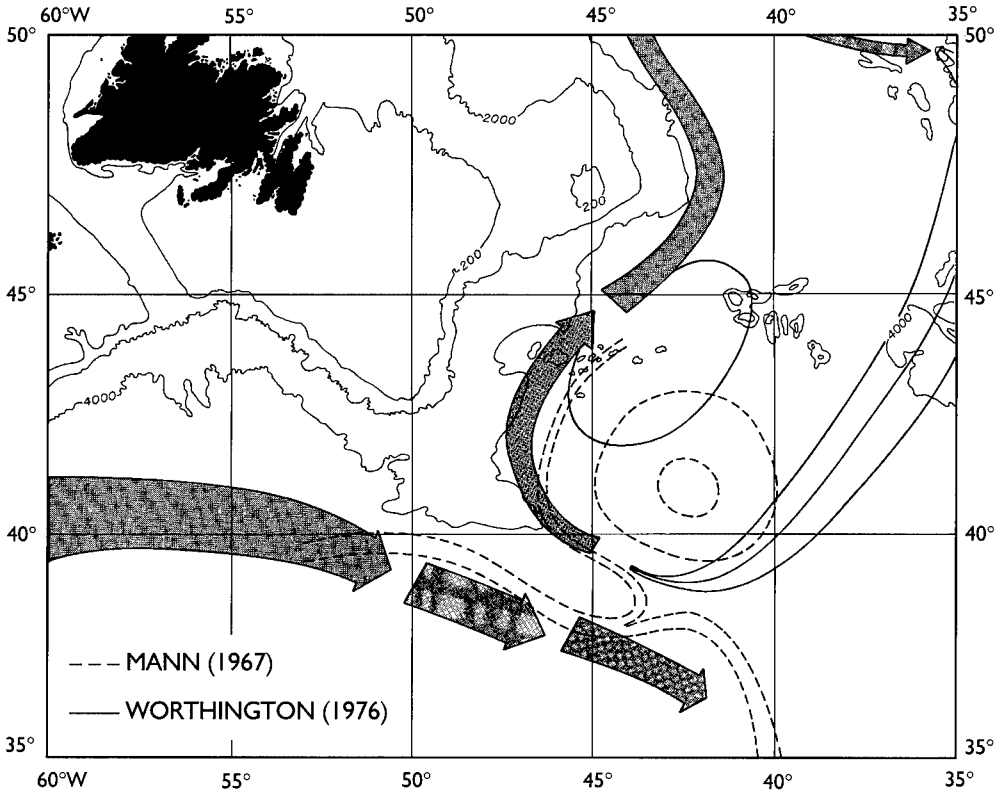

Figure I-85: A comparison between the path of the Gulf Stream and the Newfoundland Basin Eddy according to Mann (1967) and Worthington (1976), adapted from SM93.

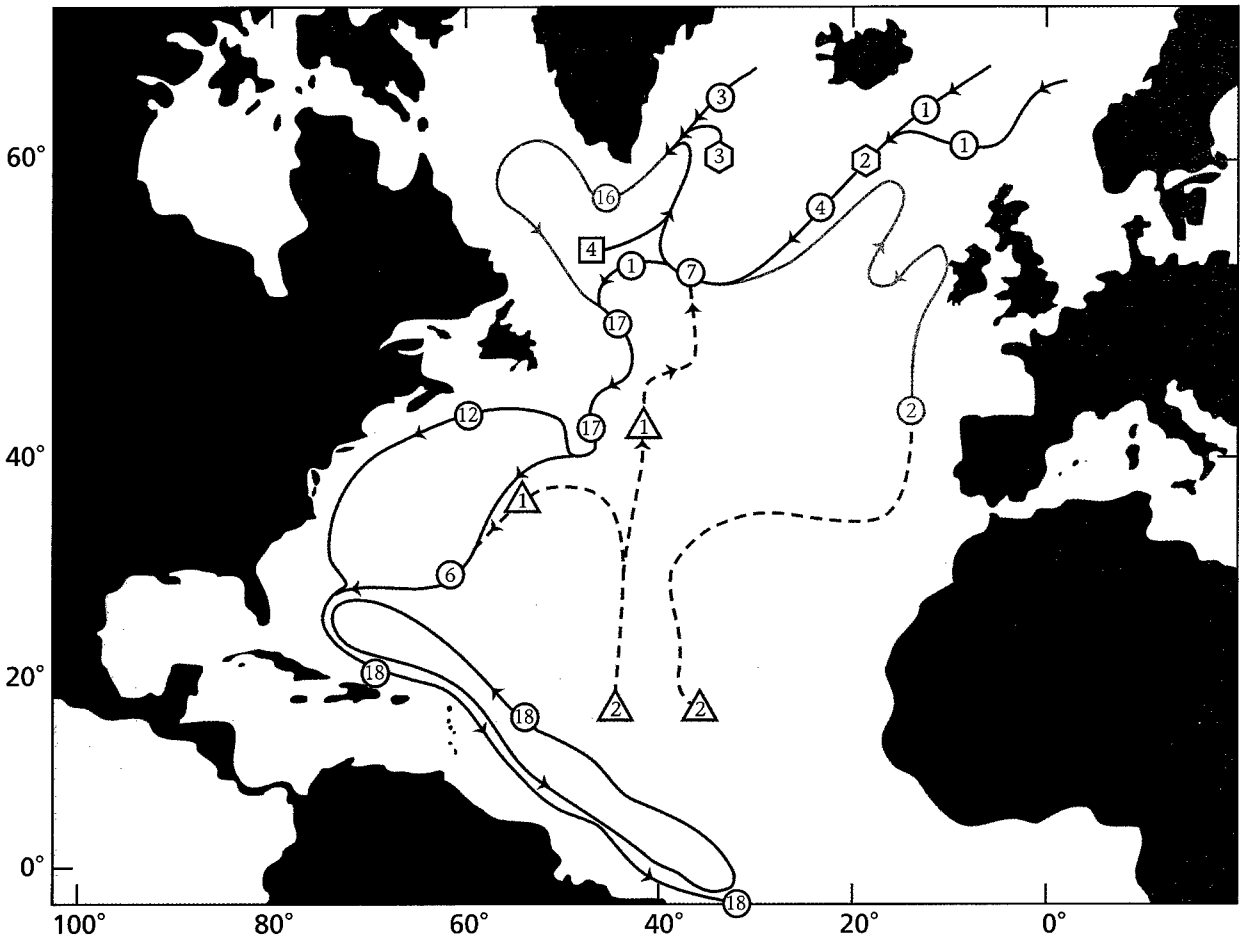

Figure I-86: Circulation schematic for NADW (1.6°–4°C), based on SM93 figure 12b. Green denotes NADW, dark blue is bottom water, light blue lines are used when NADW is also bottom water, red hexagons indicate entrained AAIW (modified) or SPMW or perhaps even NADW. Squares represent sinking, and triangles represent upwelling. Transports are in Sverdrups.

that the light blue deep recirculating gyres or eddies have been removed from I-22 for clarity), an update of their figure 12a, for $1.8° \leq \theta \leq 4.0°C$, nominal. This update (Figure I-86, which only considers flows associated with NADW) includes some of McCartney's latest ideas, as well as some of mine (see updated front cover illustration).

The NAC does not carry only subtropical water; it also entrains and recirculates (Figures I-81 and I-82) subpolar water to the north. The "northern recirculation" or Subpolar Gyre ("proper") is composed of the Irminger and West Greenland and Labrador Currents, including that part of the latter which joins the NAC (Figures I-81→I-83).

So the transport of the upper layer NAC is composed of (taking the lower extent of the NAC at 1500–2000 m, ~ 5°–7°C): (1) "Subtropical water" from the GSS, a total of 13 Sv, about 5 Sv of which is remnant upper AAIW, (2) 1 Sv "entrained" MOW, (3) ~ 25 Sv recirculation to the southeast of the NAC, within the Newfoundland Basin between about 40° and 45°N, located southeast of the Grand Banks and west of the Mid-Atlantic Ridge. This is the southern recirculation of the NAC, called by Mann (1967) the Newfoundland Basin Eddy, probably an eddy-induced flow as is the case for the northern recirculation of the GSS, and to some extent the southern recirculation of the GSS, (4) a northern recirculation (or "proper or classical subpolar gyre"), transporting about 30 Sv above 1500–2000 m. Both wind-forcing and thermohaline processes (Spall, 1992) are

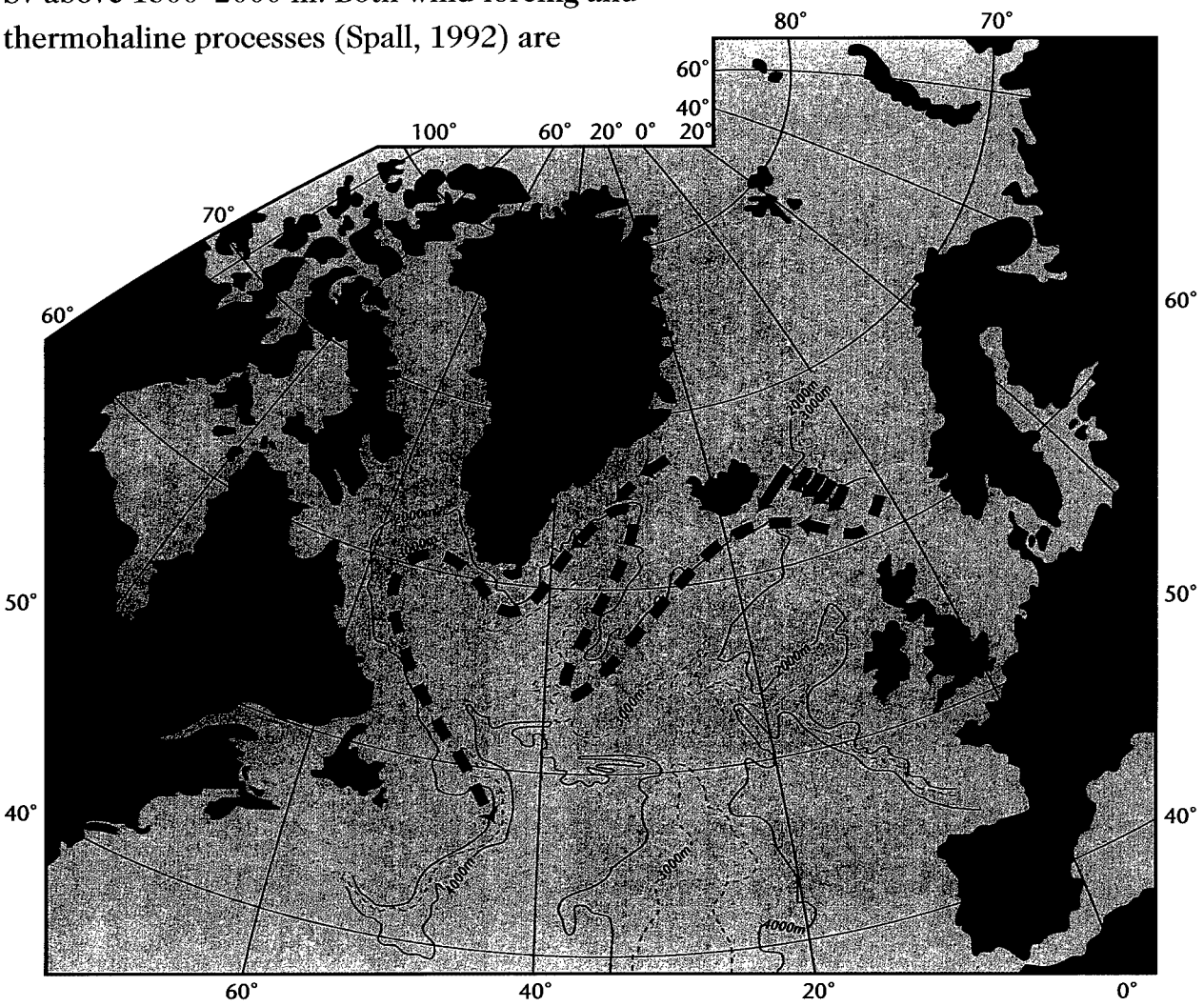

Figure I-87a: The deep circulation in the northern North Atlantic, adapted from Dickson *et al.* (1990).

important in the subpolar gyre proper, possibly dominating any eddy-forced rectification.

Warm water transformation does not occur in one large step at a single site in the subpolar area. Rather, upper layer waters are progressively cooled, sink by convection, and are modified by lateral and vertical mixing as they move around the northern recirculation of the NAC or classical subpolar gyre that is both wind-driven and a cooling spiral, converting NACW into SPMW into LSW. As the water of subtropical origin in the NAC turns northward and westward, about 5 Sv are lost first to the nordic seas (Mauritzen, 1993) and then another 5 Sv to entrainment into the overflows, plus 4 Sv involved in "open ocean convection" to

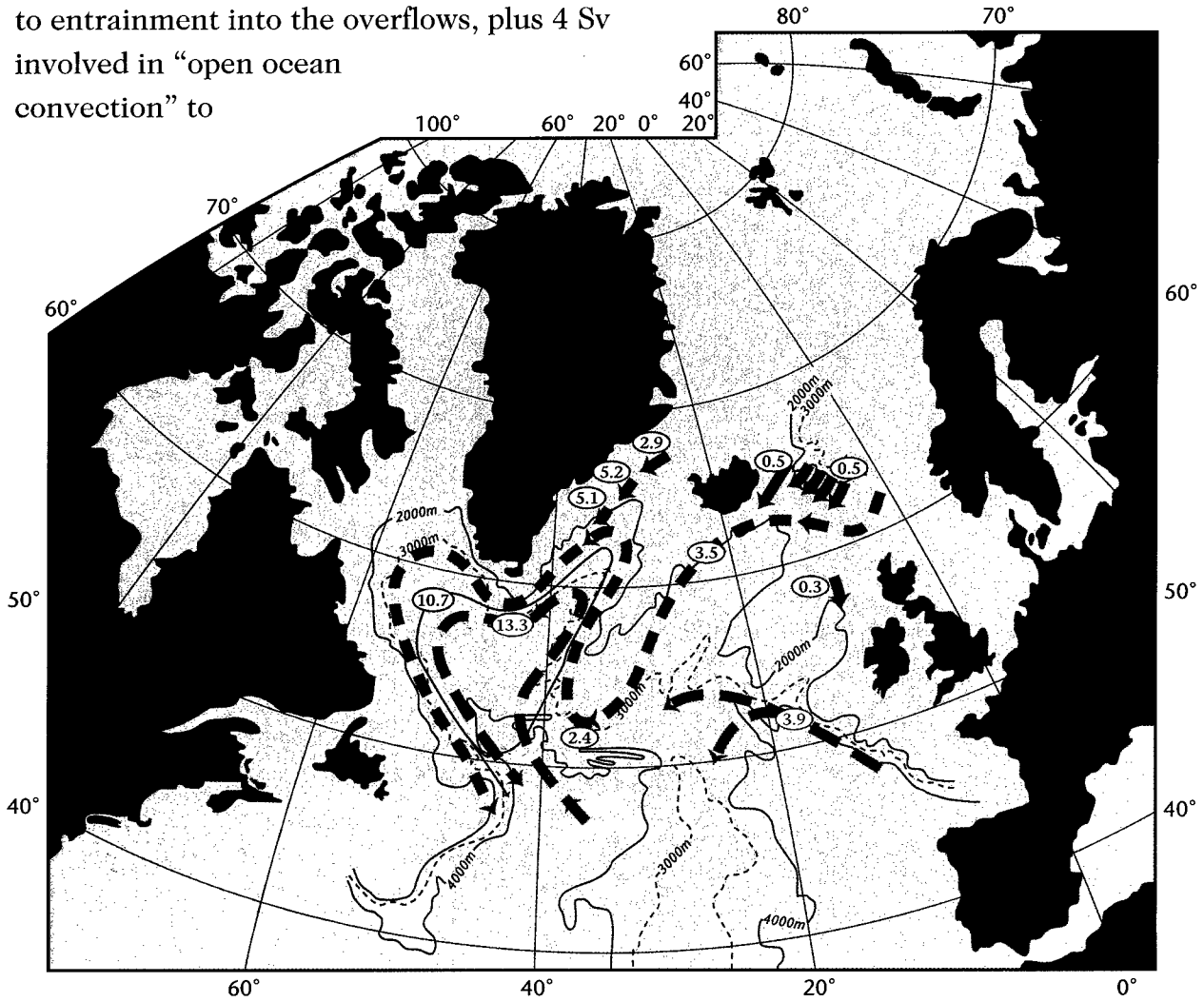

Figure I-87b: The deep circulation in the northern North Atlantic, adapted from Dickson and Brown (1994).

LSW. An observation of ambient subpolar gyre water being entrained into the overflow was reported early on (Müller *et al.*, 1974). In the upper layer subpolar gyre, air–sea heat loss cools a thick near-surface layer, the Subpolar Mode Water (Talley and McCartney, 1982), from 11°C to 3–4°C while precipitation and cross-frontal fluxes of runoff and ice-melt water freshen it from about 35.5 to 35.0. High latitude cooling and freshening drive the warm water transport progressively to colder, fresher and denser classes. The coldest of the thick surface layers is convected to about 1500 m in the Labrador Sea, forming LSW. There is a very new article on the origin of the warm inflow to the nordic seas (McCartney, 1996), which goes into much more detail than is done in this report. McCartney (1996) argues for conversion of NACW into SPMW.

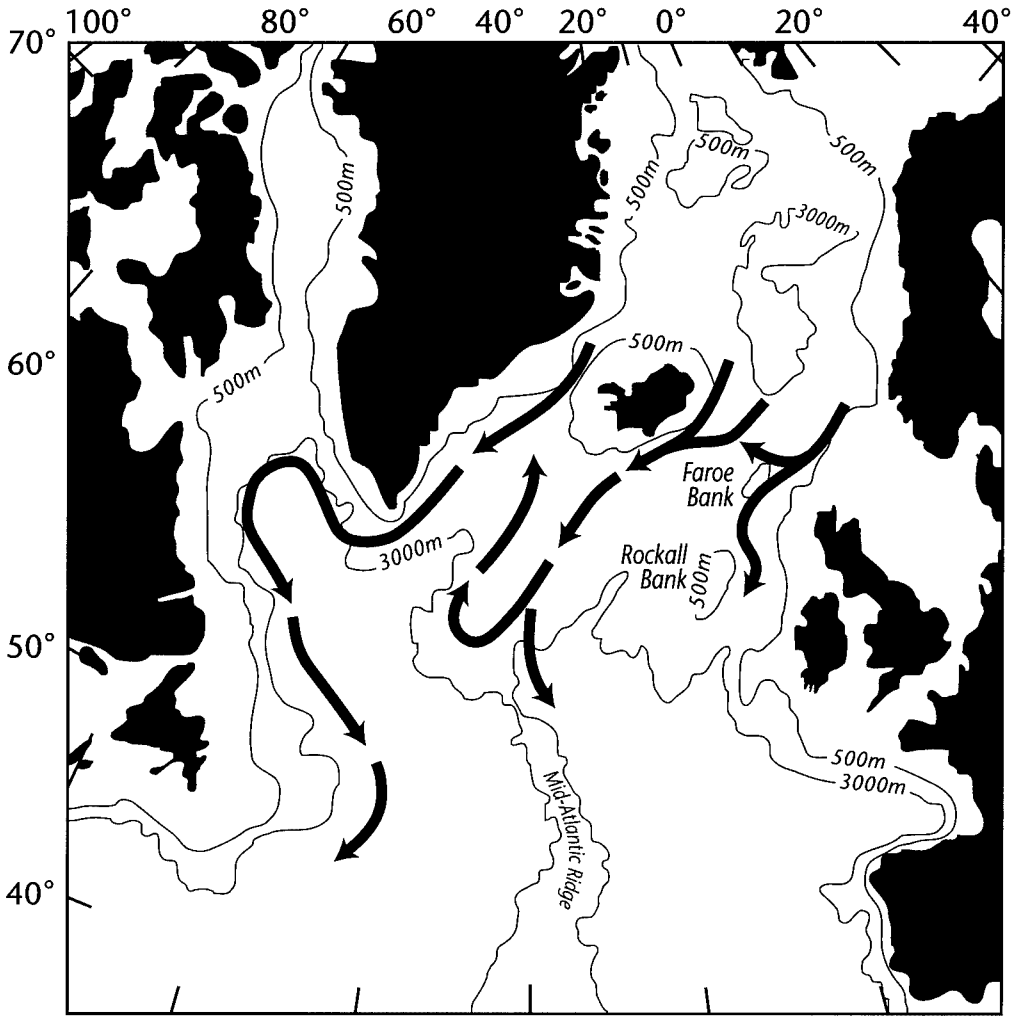

Figure I-88: Overflows from the polar North Atlantic and their fate in the subpolar North Atlantic, according to Lee (1974). This work anticipates much of the modern picture.

Perhaps the mixed-layer water flowing across the equator is converted to NACW in the North Atlantic Subtropical Gyre.

With respect to deep and bottom water circulation in the northern North Atlantic, Dickson's articles (Dickson and Brown, 1994; Dickson *et al.*, 1990) have been very influential (e.g., Figure I-87), along with publications by, for example, McCartney and Talley (1984), McCartney (1992), Reid (1994), and Lynn and Reid (1968). Figure I-87a is a picture of the fate of overflow water in the northern North Atlantic taken from Dickson *et al.* (1990). Figure I-87b is an update of Figure I-87a by Dickson and Brown (1994). There is a recent dissertation by Mauritzen (1993) which has focused our

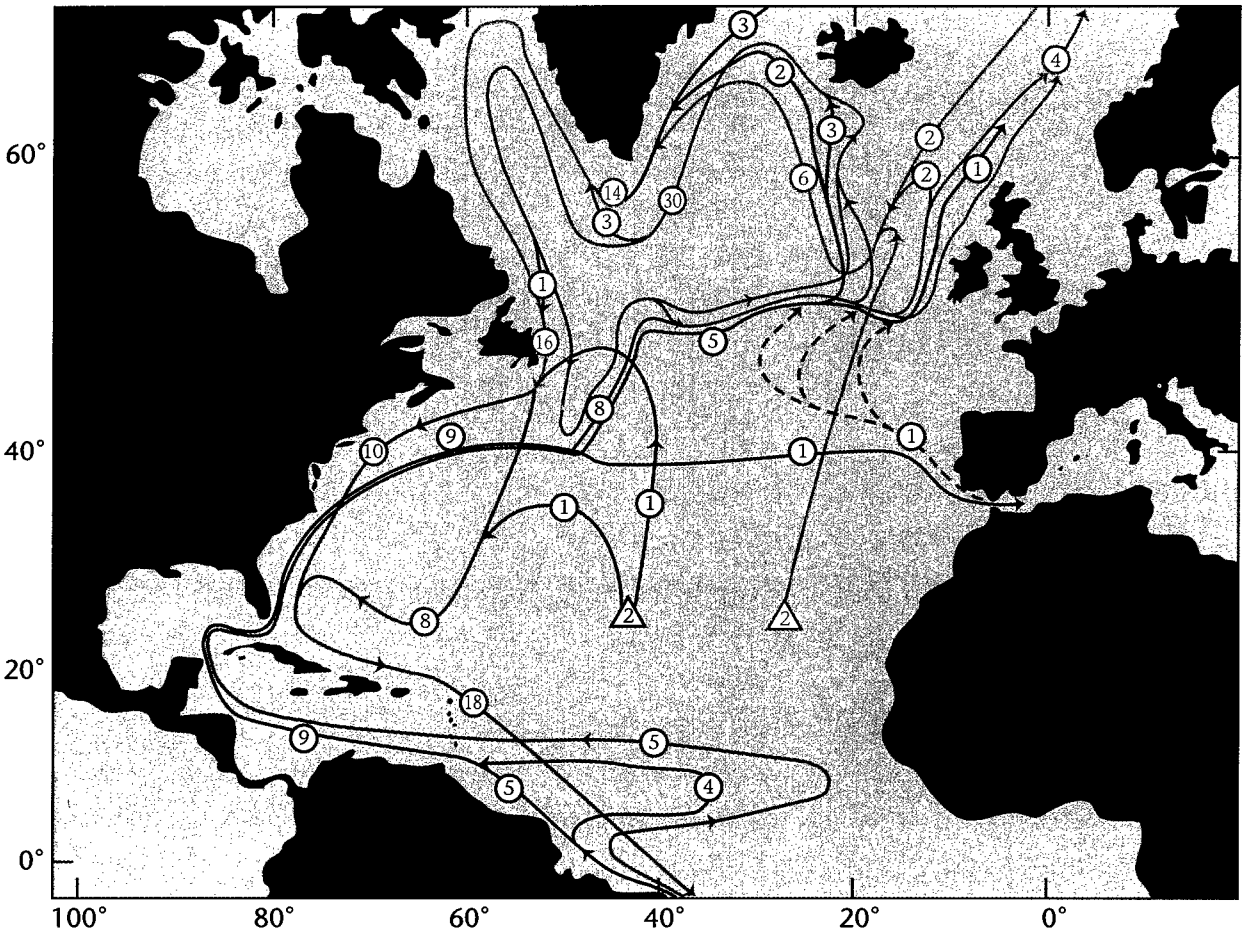

Figure I-89: A new schematic for the warm water interbasin and subpolar circulation in the northern North Atlantic. See text for an explanation of the colored lines. Transports in circles in Sverdrups, as usual, along with triangles denoting modified AABW.

attention on a "new" vision of NADW formation. This vision also affects what one might look for in the circulation patterns of the subpolar gyre, including the upper layer. A comparatively early version (Lee, 1974) of the path and location of the overflows is shown in Figure I-88, which anticipates rather well much of Figure I-87, and other overflow schemes.

A new general summary scheme associated with the above discussion of the general circulation in the subpolar North Atlantic (but excluding the Newfoundland Basin Eddy) as influenced by the subtropical and tropical North Atlantic is offered in Figure I-89, which also includes one version of a subpolar gyre. Figure I-89 is a depiction of the horizontal patterns of the flows associated with the NADW cell, excluding recirculation of NADW. In Figure I-89, 9 Sv of mixed layer (upper 50–100 m or so depth range) water with $T \geq 24°C$ enters the North Atlantic from the South Atlantic as a purple line. This 9 Sv is converted (red line) to NACW (perhaps first partly to 18° Water) in the subtropical gyre and exits through the NAC while to some extent joining the subpolar gyre (orange lines). The warmer segment of this flow (4 Sv) exits the subpolar gyre into the polar seas. The green line crossing the equator into the North Atlantic carrying 5 Sv is "upper" intermediate water that transits the subtropical gyre and also partly joins the subpolar gyre (orange). One Sverdrup of NACW is converted to MOW which joins the NAC. Part of this MOW plus some upper intermediate water enters the polar seas for a total of 1 Sv (green line). The rest of the MOW joins the subpolar gyre. Five Sverdrups in the NAC and subpolar gyre of subtropical origin is entrained into the overflows (light blue for ISOW and the "modified" AABW that joins it to become MNADW, dark blue for DSOW) to increase their transport from 5 to 10 Sv. Four Sverdrups of subtropical origin in the subpolar gyre (orange) joins the flow of NADW (light blue line) in the subpolar regions as SPMW and LDW and is eventually converted to UNADW with some MOW influence. The DWBC carrying 16 Sv NADW is joined by 2 Sv "western" AABW near the Grand Banks, and all this enters the subtropics as a green-line, two-branch DWBC that combines and exits to the South Atlantic carrying 18 Sv. All of the above is simply another (horizontal) version of the discussion around Figures I-12, I-22 and I-86. North Atlantic Deep Water in the context of the DWBC throughout the Atlantic will be discussed in more detail in the next section.

7. The NADW Meridional Cell and Deep Western Boundary Current

If we accept some version of the picture of NADW formation contained in earlier sections of this report [and according to Mauritzen (1993), McCartney (1992), McCartney and Talley (1984), Dickson and Brown (1994), Price and Baringer (1994), Schmitz (1995), and SM93], 5 Sv of "NAC upper layer" water with some MOW influence enters the polar seas on the easternmost side of the northernmost North Atlantic. In this context "upper layer" refers to water that has T ~ 5 → 15°C in the NAC and comes from the uppermost layer (~ 9 Sv, after having been converted to something like NACW) and upper AAIW (~ 5 Sv) flows that enter the tropical North Atlantic from the South Atlantic through the Equatorial Current System. The 5-Sv flow that enters the nordic seas exits after modification and entrains about 5 Sv of "ambient" Subpolar Gyre "upper layer" Water (including "upper" intermediate water) to form 10 Sv NADW. To form the DWBC (first clearly identified observationally by Swallow and Worthington, 1961), which extends all the way from the northern North Atlantic to the ACCS, we add 4 Sv of LSW that was formed by convection of "upper layer" water and ~ 4 Sv of "modified" AABW. A new version of the meridional structure of the "Atlantic" that includes the NADW cell was shown in Figure I-12; see also I-80. Figure I-89 (see also Figures I-22, 81 and 86) is a new map of the paths and transport amplitudes of the subtropical and tropical replacement flow for NADW in the northern North Atlantic, along with the paths of NADW and the Subpolar Gyre (schematically).

Some studies identify the formation of NADW and its flow as a DWBC in the Atlantic Ocean as being a "single" large-scale phenomenon. This is an oversimplifed representation of a complex of regional processes over the global ocean, although the formation process occurs predominantly in the northern North Atlantic. Figure I-89 shows some basic horizontal elements of the high-latitude processes: the warm-water source (NAC) branching from the Gulf Stream; the NAC transporting warm water into the subpolar gyre; the subpolar gyre acting as a recirculating cooling spiral for the subtropical waters brought in by the NAC, as well as the collecting point for a recirculating deep circulation; the eastern subpolar waters augmented by saline water from the Mediterranean invading the nordic seas; the overflows from the nordic seas entraining other waters to form the DWBC. Figure I-89 illustrates a number of complexities

brushed over in the simplicity of the single-cell "conveyor belt" picture of interbasin and intergyre flows. For example, there are three distinct pathways for warm-to-cold water transformation: (1) the nordic seas path where overflow waters (5 Sv) are formed; (2) upper-layer transformation by air–sea interaction in the cyclonic flow around the subpolar gyre that culminates in LSW formation (4 Sv); and (3) entrainment of ambient warmer waters (5 Sv) into the overflows. Entrainment into the North Atlantic Deep Water of even denser waters of Antarctic origin is also a critical factor in forming LNADW and MNADW. Other complicating factors are recirculations within the different basins. Additional three-dimensional global cuts at the composite global thermohaline circulation are shown in Figures I-90 and I-91. These figures are global representations of Figure I-12 and Figures I-86 and 89. Figure I-90 is from Arnold Gordon (personal communication), and I-91 is my update (with major modifications) of I-90, based on Schmitz (1995) and some new ideas. Figures I-90 and 91 will be discussed in a lot more detail in Volume III of this report.

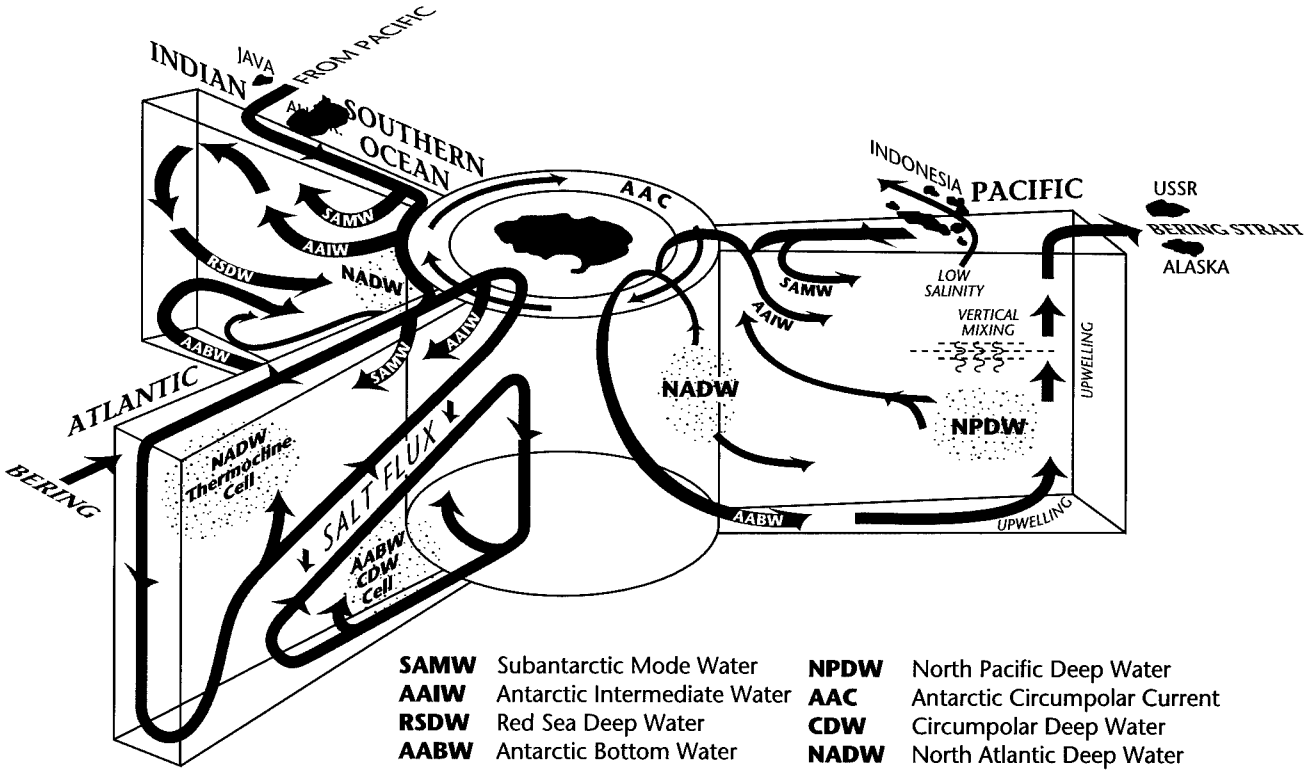

Figure I-90: Three-dimensional meridional global ocean slices that depict NADW formation and replacement, adapted with minor changes from A. Gordon (personal communication).

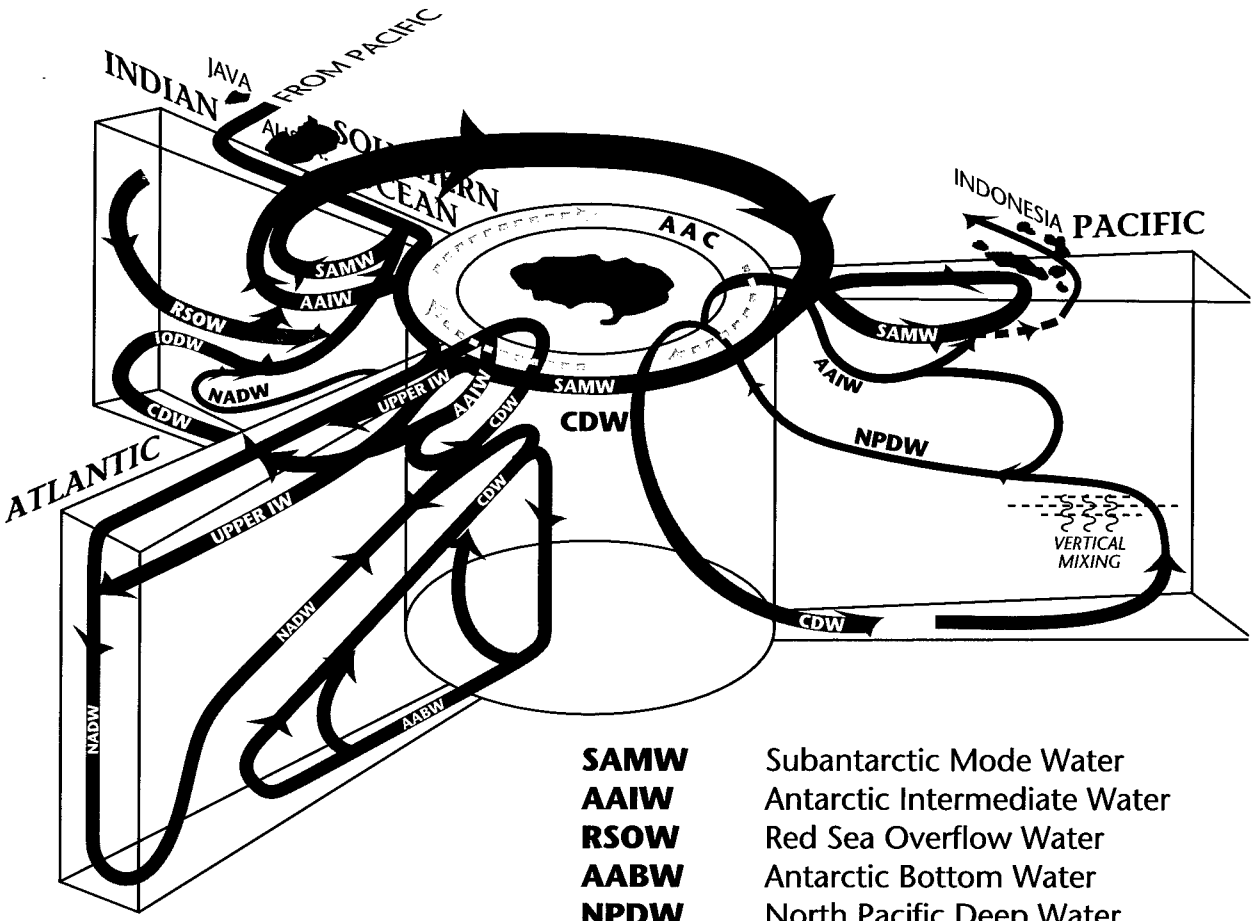

SAMW	Subantarctic Mode Water
AAIW	Antarctic Intermediate Water
RSOW	Red Sea Overflow Water
AABW	Antarctic Bottom Water
NPDW	North Pacific Deep Water
AAC	Antarctic Circumpolar Current
CDW	Circumpolar Deep Water
NADW	North Atlantic Deep Water
UPPER IW	$26.8 \leq \sigma_\theta \leq 27.25$
IODW	Indian Ocean Deep Water

Figure I-91: A new version of Figure I-90 with schematic meridional sections of interbasin flow for each ocean with their global linkages.

There is a recent review article on NADW (Fine, 1995) containing a schematic (reproduced here as part of Figure I-92) which exhibits the essentials of the general path of the DWBC in the North Atlantic, without recirculations. My take on McCartney's (personal communication, 1996) recent ideas (see also SM93) about the path of LNADW ($\theta \leq 2$°C, about) are added to Figure I-92 as a dashed line. One feature that I have not yet had the time to include in Figure I-92 involves newer data and ideas on the interaction of the path of the DWBC and deep Gulf Stream (Pickart, 1994a, b; Pickart and Smethie, 1993; Spall, 1996a, b). The flow of NADW (that is above LNADW,

above about $\theta = 2°C$) in a DWBC from formation region to low latitudes along the continental slope (Figure I-93) has been nicely documented by Pickart (1992), Pickart and Hogg (1989), Pickart and Watts (1990); see also Schmitz (1985), who observed SOFAR floats at 2000 m moving south around the Grand Banks. The path of the DWBC in Slope Water is shown in Figure I-93 and hydrographic properties there are contained in Figure I-94.

Recirculations of and time variability in the DWBC transport and path are now being addressed. The interaction between the Gulf Stream and the DWBC in the North

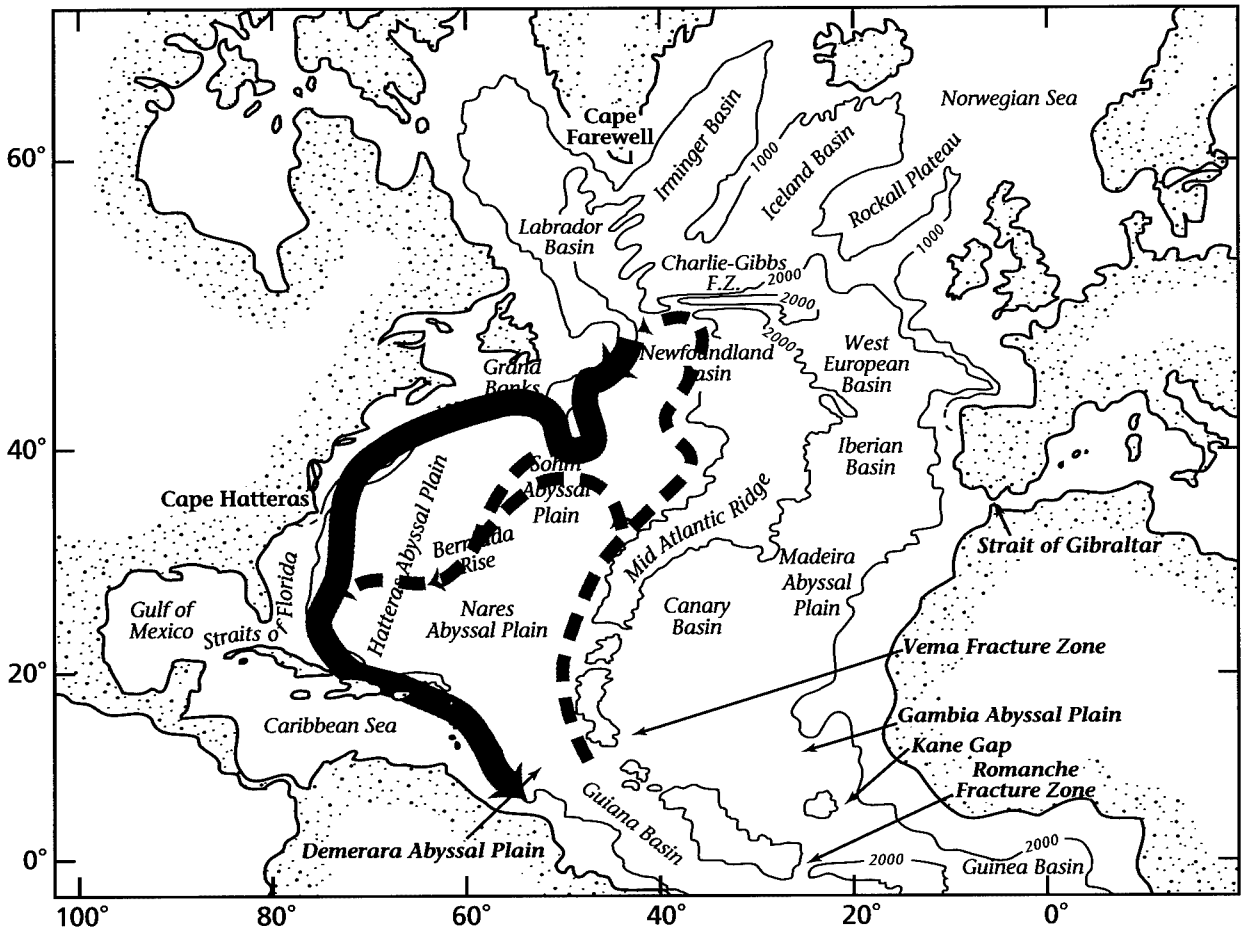

Figure I-92: The path of the DWBC, partly according to Fine (1995), and including my take on recent ideas by McCartney (personal communication, 1996); see also Figures I-86 and I-89. The solid line is the path taken by MNADW and UNADW; the dashed line is the path taken by modified AABW and LNADW.

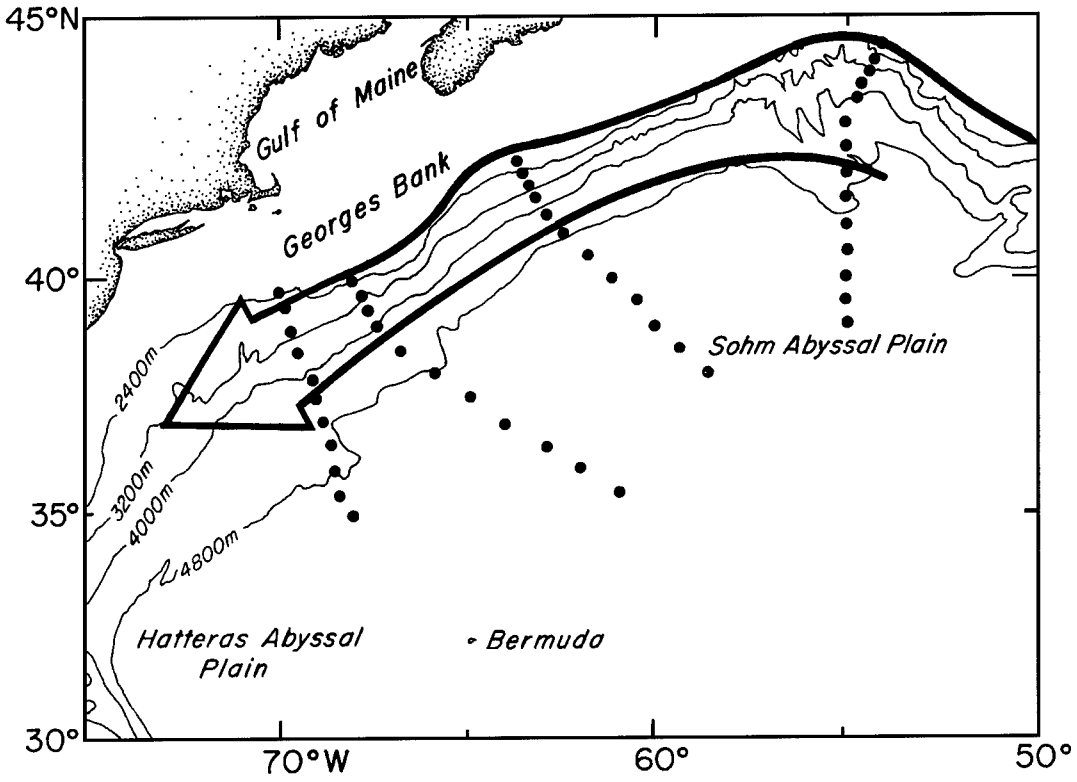

Figure I-93: A schematic of the path of the DWBC in the Slope Water Region, adapted from Pickart (1992). Dots indicate hydrographic station locations.

Atlantic is a topic of considerable interest (Thompson and Schmitz, 1989; Pickart and Smethie, 1993; Pickart, 1994a, b; Spall, 1996a, b). One area of particular emphasis has been with regard to influences on the path of the Gulf Stream, especially separation. Sections of mean flow across the DWBC along 26.5°N (Lee *et al.*, 1990) are contained in Figure I-95. It is at "low" latitudes that work on recirculations associated with the DWBC originated (McCartney, 1992, 1993). The transequatorial flow of NADW is at least as interesting (Friedrichs *et al.*, 1994) as the upper layer flows there.

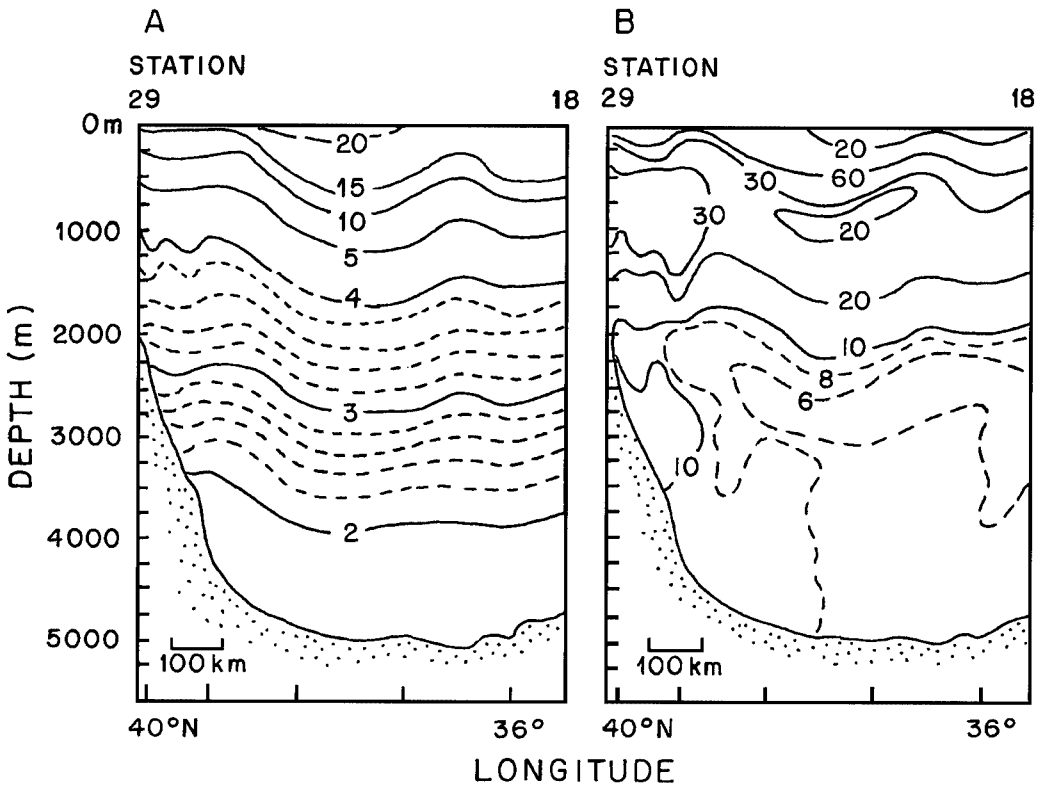

Figure I-94: Sections of θ (°C) (a) and F-12 (pM/kg x100) (b) across the DWBC, adapted from Pickart (1993); stations shown in Figure I-93.

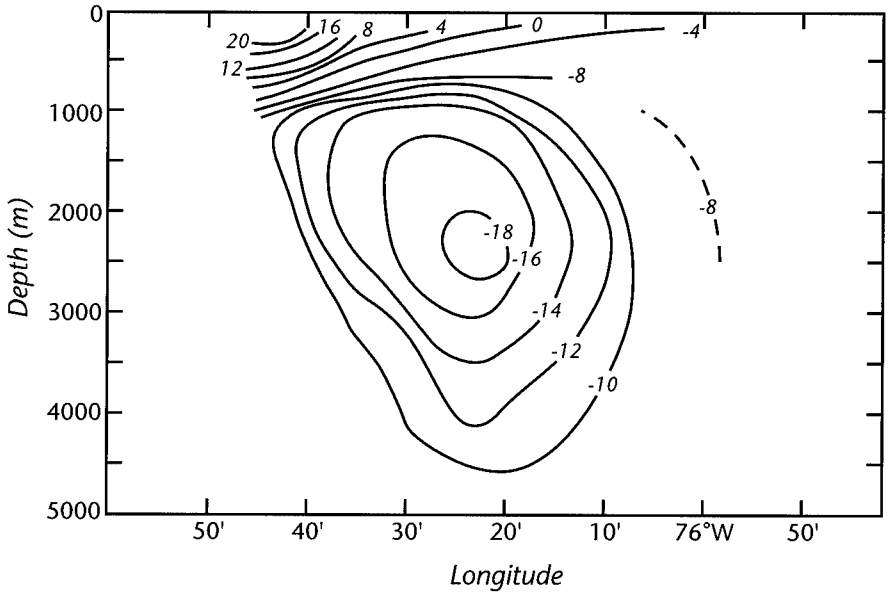

Figure I-95: Sections of mean flow (cm s^{-1}) across the DWBC near 26.5°N, adapted from Lee *et al.* (1990.)

8. A Few Comments on Intermediate Water

The history of investigations into the mid-depth flow patterns in the World's Oceans has been nicely summarized by Reid (1981). Early maps of the circulation of Intermediate Water are shown in Figures I-96 and I-97a, b. Throughout the World's Oceans, the circulation of intermediate water is not yet well documented in critical regions although important in the global picture (Reid, 1978, 1981; Schmitz, 1995).

In the Atlantic, it has long been recognized (*i.e.* Figure I-2, from 1935) that Mediterranean Water and AAIW are pervasive and contrasting components of the mid-depth

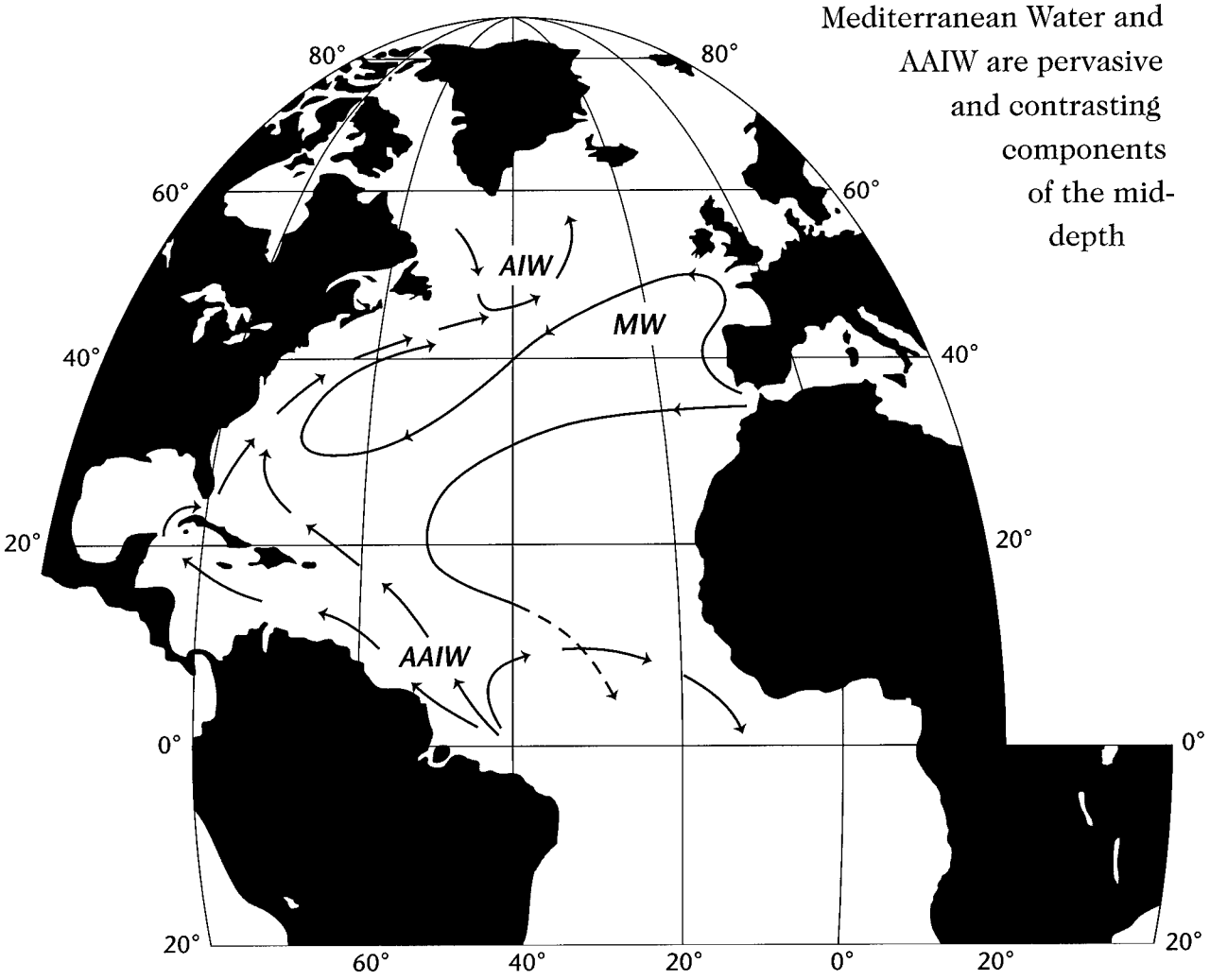

Figure I-96: The circulation of intermediate water in the North Atlantic, adapted from Sverdrup *et al.* (1942). AAIW denotes Antarctic Intermediate Water, AIW denotes Arctic Intermediate Water, MW Mediterranean Water.

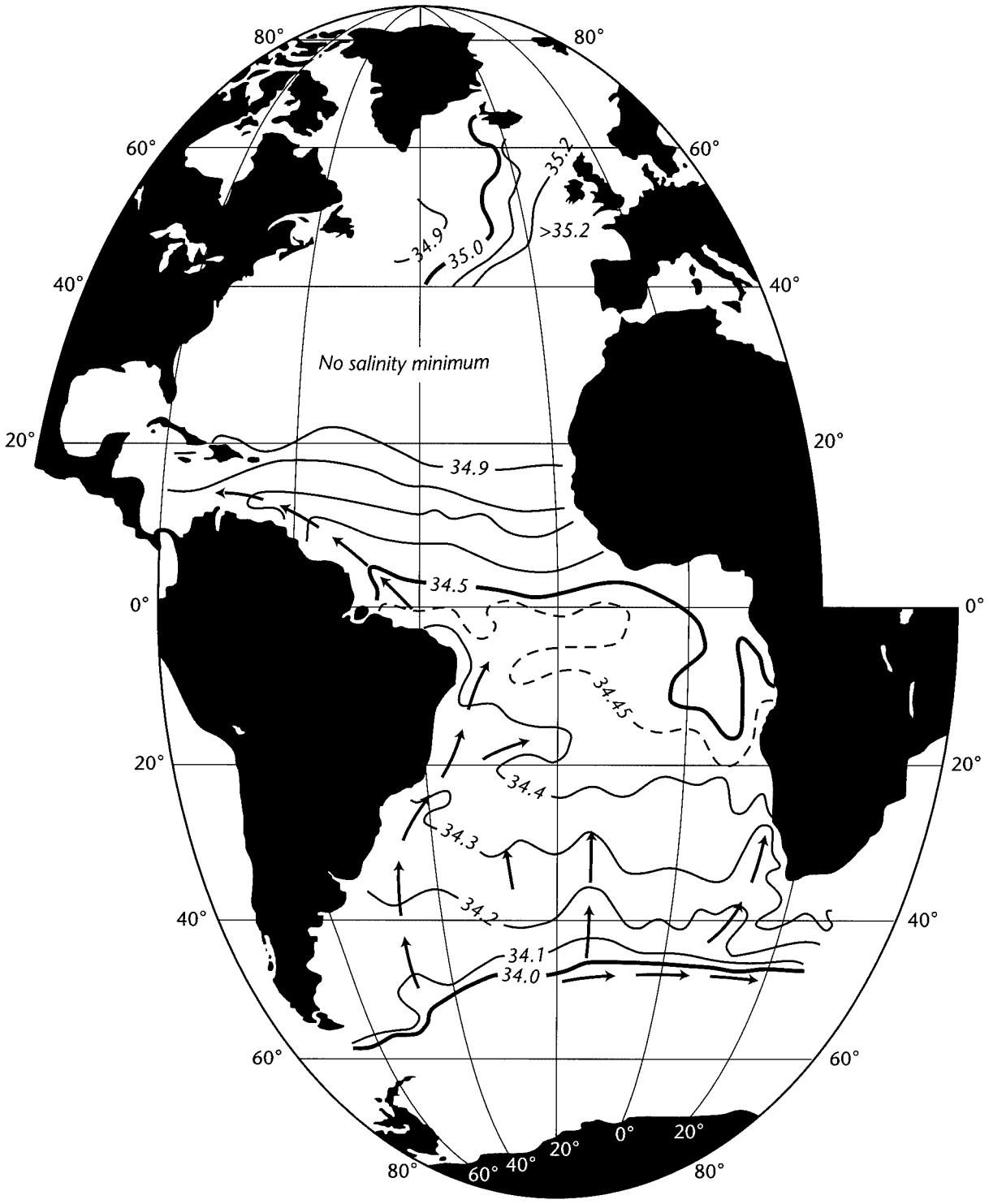

Figure I-97a: Intermediate water in the Atlantic Ocean, taken from Dietrich *et al.* (1980): salinity (psu) contours.

Figure I-97b: Intermediate water in the Atlantic Ocean, taken from Dietrich *et al.* (1980): current vectors.

water mass picture. This boundary in the interior of the North Atlantic is at about 20–25°N. But upper intermediate water transits the Gulf Stream System from the Caribbean to the nordic seas (Figures I-51–53). And Mediterranean Water (Worthington, 1976, figure 23) extends up the eastern side of the Atlantic as far as Iceland. A C-shaped pattern of σ_t surfaces in the North Atlantic, between, say, 27.0 and 27.6, was first published by Montgomery and Pollack (1942).

The outflow from the Mediterranean is about 0.7×10^6 m^3 s^{-1}. This seems like a small transport, but the salinity (38.4 psu) of the outflow is extremely high compared to any other waters in that depth and density range. This high S can be used to trace both a northward flow along the eastern boundary (into the North Atlantic Current and toward the Iceland–Scotland sill) and a westward flow across the Atlantic that presumably turns southward and northward along the western boundary and then perhaps eastward. As it nears the western boundary, it provides warm water of high salinity to the Gulf Stream. Maps of the spreading of Mediterranean Water have been presented by Arhan (1987; see also Käse and Zenk, 1987, and Talley and McCartney, 1982).

9. Mesoscale Eddies in the North Atlantic, and Globally

The name typically used for fluctuations in the period range 20–200 days, roughly, with horizontal dimensions of 100–500 km, say, is mesoscale eddies. One hundred kilometers is a prominent horizontal dimension in the ocean, being the approximate width of strong currents or half-width of current rings. Rings advecting at a few (1–5) centimeters per second (km day $^{-1}$) will therefore have a period of 40 to 200 days at a fixed instrument. The most robust observable spatial property of the mesoscale eddy field in the World's Oceans as well as the North Atlantic (*e.g.*, Schmitz *et al.*, 1983) is its order(s) of magnitude geographical inhomogeneity in K_E (and P_E). This pattern of geographical inhomogeneity (an overall factor of ~ 10 at the sea surface, and 100 at abyssal depths) is connected to the pattern of the general ocean circulation, in that the

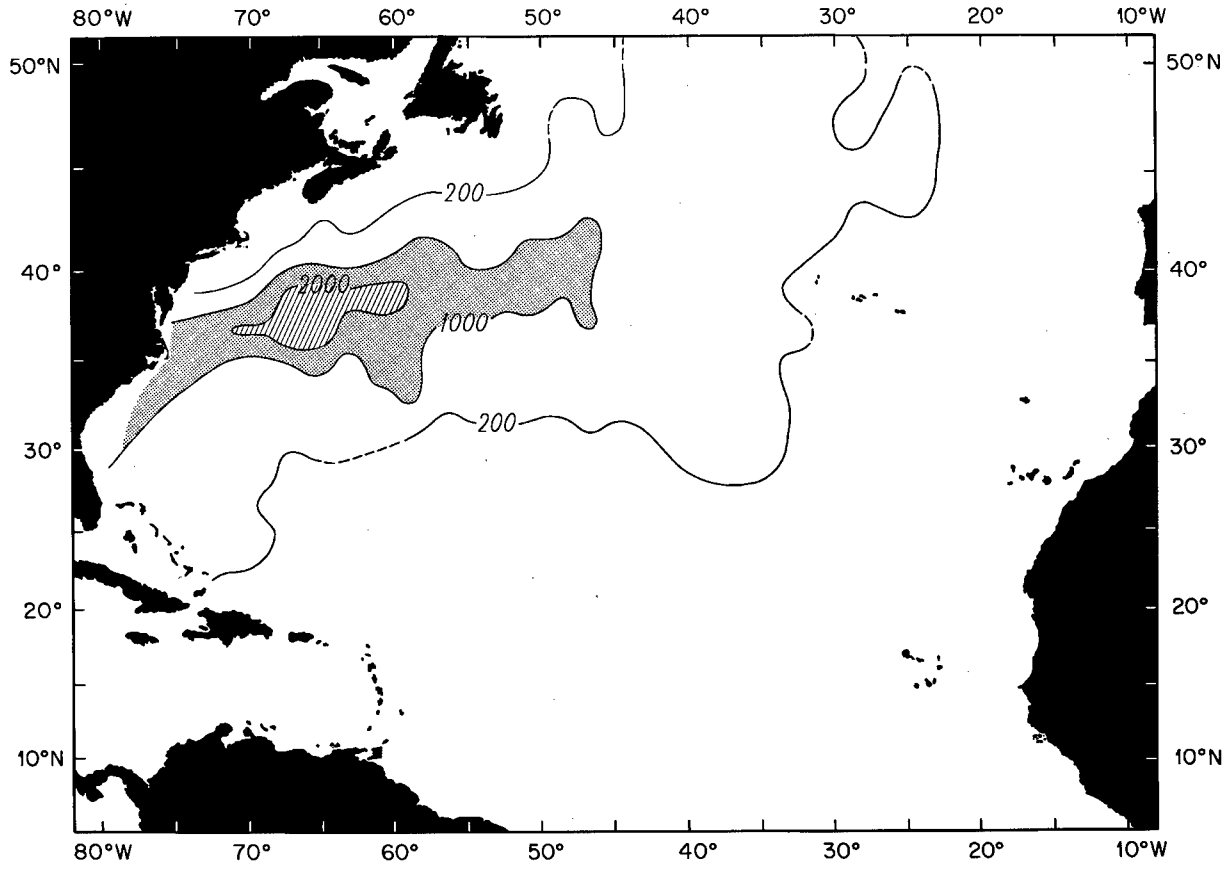

Figure I-98: Eddy kinetic energy (cm^2 s^{-2}) at the sea surface for the North Atlantic, adapted from Richardson (1985).

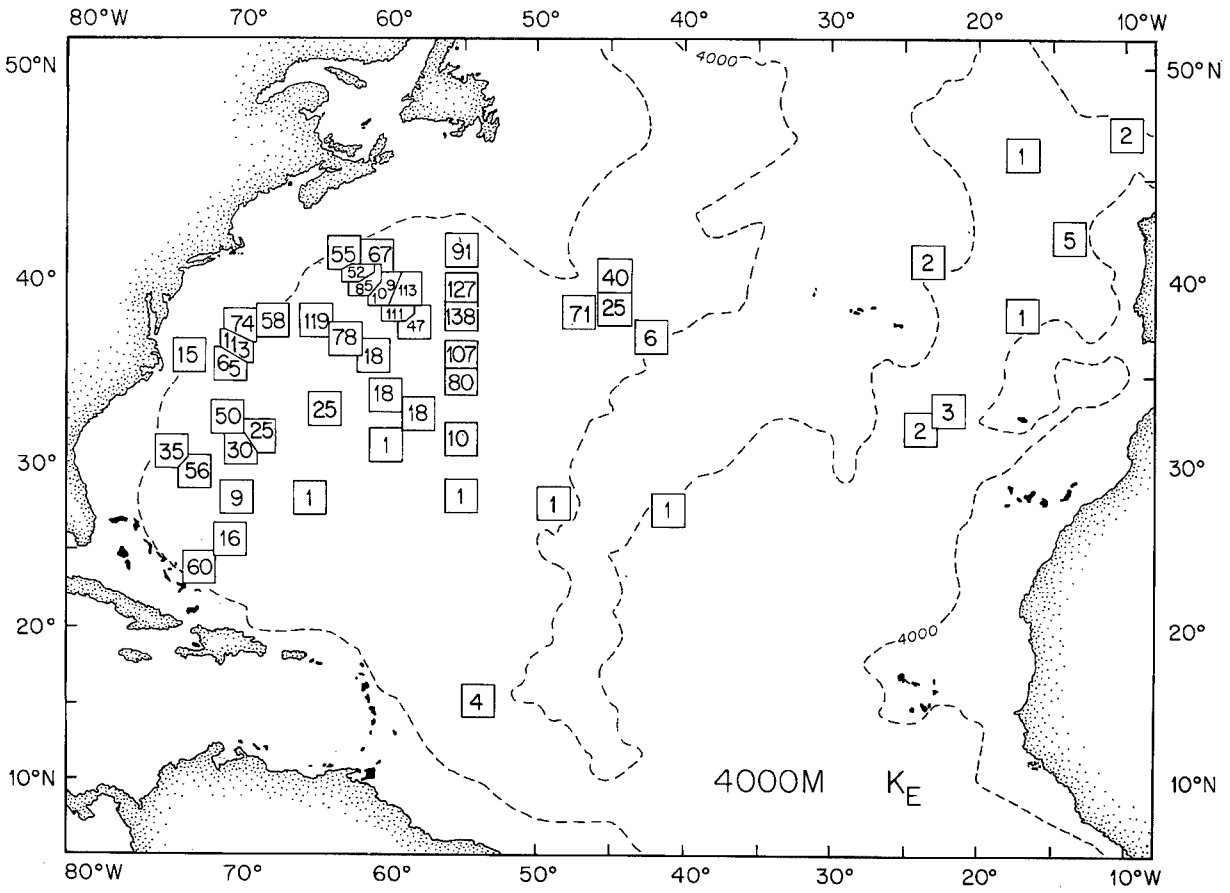

Figure I-99: Abyssal (~ 4000 m depth) eddy kinetic energy ($cm^2\ s^{-2}$) for the North Atlantic, according to Schmitz (1984).

most energetic eddies occur primarily in the vicinity of strong currents. This is clearly related to the dominant energy source for mesoscale eddies — instabilities in strong currents (or fronts), in partial analogy to the situation for atmospheric synoptic scale eddies and fronts. Surface K_E distributions are contained in Figures I-13 and I-17, and another is shown in Figure I-98. The corresponding pattern for K_M was shown in Figure I-16. K_E for 4000 m is shown in Figure I-99, P_E in Figure I-100. A section of K_E in the vicinity of the DWBC off Abaco is shown in Figure I-101. K_E at 700 m was shown in Figure I-30, and a section of K_E across the Gulf Stream in Figure I-33. Riser and Rossby (1983) have published nice maps of quasi-Lagrangian kinetic energy in the western-most Atlantic, at depths of 700 and 2000 m.

Eddy time scales are in some sense less spatially inhomogeneous than K_E. Spectral shapes are found to be roughly grouped into two major categories in subtropical gyres (Schmitz and Luyten, 1991), dominated by the mesoscale time scale (20–200 days, say) near and in strong currents and dominated by the secular time scale (200 days and longer) in the gyre interior (Schmitz, 1989; Schmitz *et al.*, 1988). Near the surface, atmospheric (-forcing) time scales are noticeable. Near or in the presence of strong bottom slopes, topographic wave time scales (order a few days) become prominent. Various spectra of eddies near strong currents are shown in Figure I-102a. A global spectral summary is contained in Figure 102b. Vertical structures in the vicinity of some strong currents are contained in Figure I-103a. A comparison of these strong current K_E (z) distributions with similar observations from the Agulhas retroflection is

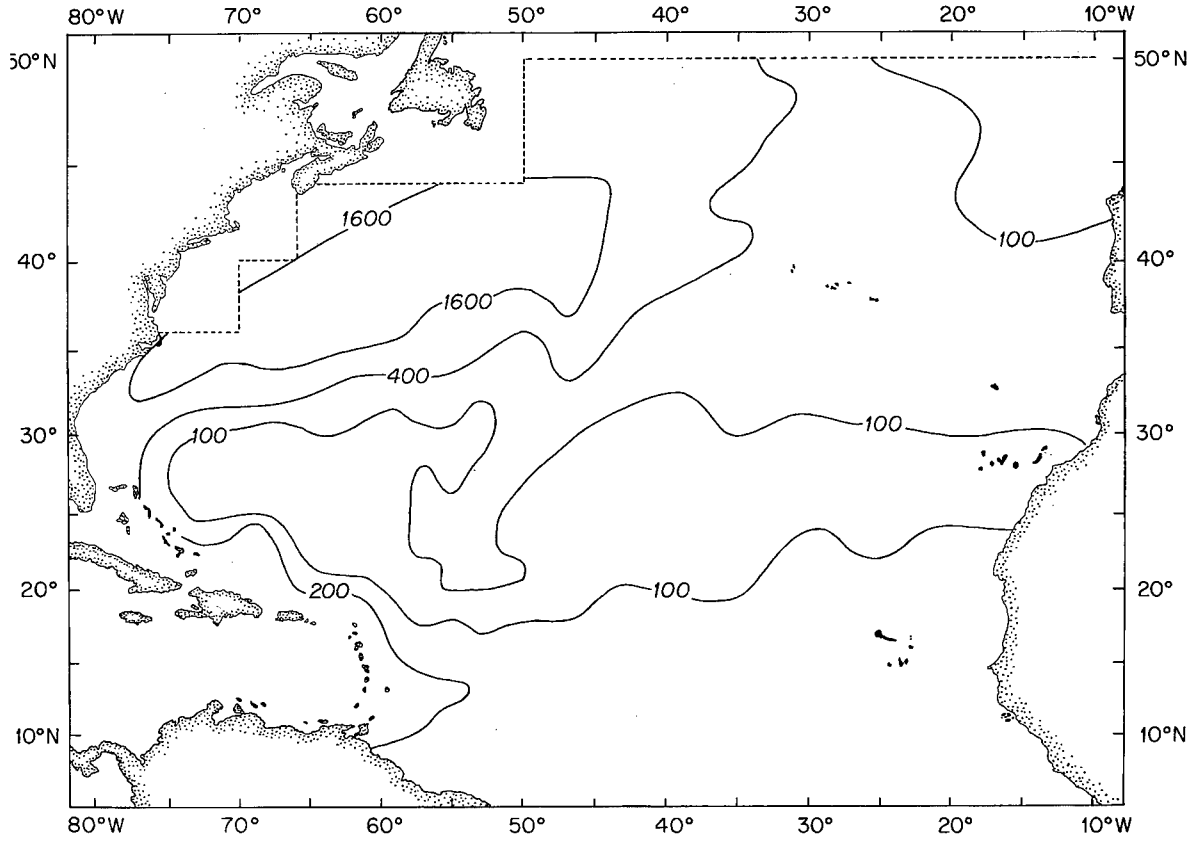

Figure I-100: Eddy potential energy ($cm^2\ s^{-2}$) in the North Atlantic, according to Dantzler (1977).

shown in Figure I-103b. A similar intercomparison but including K_E (z) from the North Brazil Current System (taken from Johns *et al.*, 1990) is contained in Figure 103c.

The first-ever detailed intercomparison of eddy-resolving numerical models with observation was by Schmitz and Holland (1982), where the basic weakness of the model runs (see also Holland, 1978, 1979) was found to be a short zonal penetration scale for the Gulf Stream System and its associated eddy field (Holland and Schmitz, 1985). Later model–data intercomparisons based on eight-layer numerical experiments yielded amplitudes and space and time scales similar to those observed near the mid-latitude jets for both the North Pacific and the North Atlantic (Schmitz and Holland, 1986). As realistic coastlines and bottom topography were added to these and other models, other problems have developed, notably with boundary current separation (see also Spall, 1996a, b), boundary conditions (*e.g.*, Chassignet and Gent, 1991), both vertical and horizontal resolution issues (*e.g.*, Barnier *et al.*, 1991; Beckmann *et al.*, 1994; and Böning and Budich, 1992), and various parameter choices. The effect of horizontal resolution on penetration scale and on the relationship between the general circulation and the eddy field (Hurlburt *et al.*, 1996; Schmitz and Thompson, 1993; Thompson and Schmitz, 1989; Thompson *et al.*, 1992) can be decisive. Some numerical model-related results for the eddy field are shown in Figures I-104 through I-107. In Figure I-104, the observed vertical distribution of eddy kinetic energy at a site near the Gulf Stream (mooring 780 plus drifter data) was

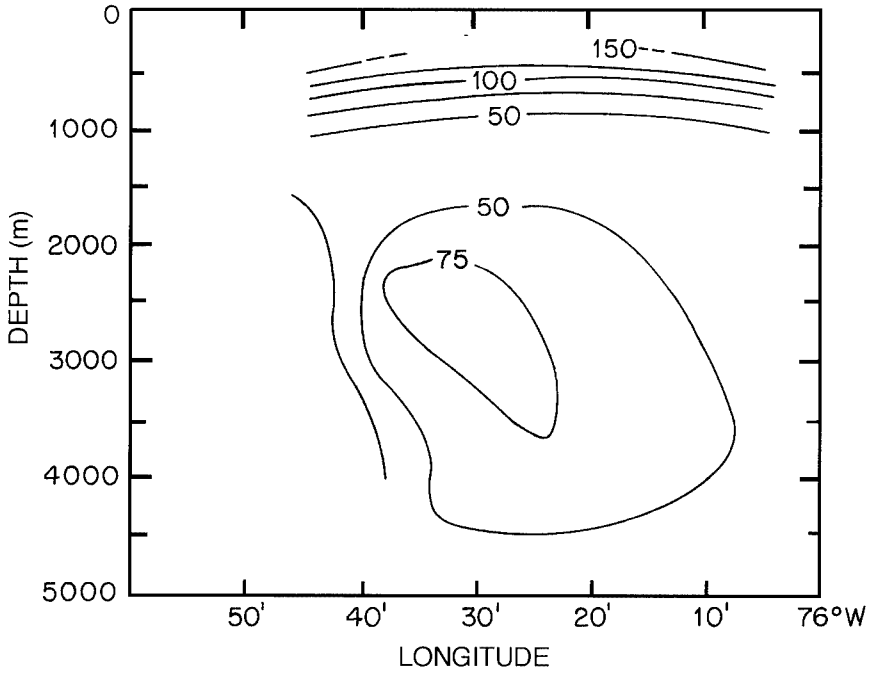

Figure I-101: Eddy kinetic energy ($cm^2\ s^{-2}$) in the vicinity of the DWBC along 26.5°N, according to Lee *et al.* (1990).

a

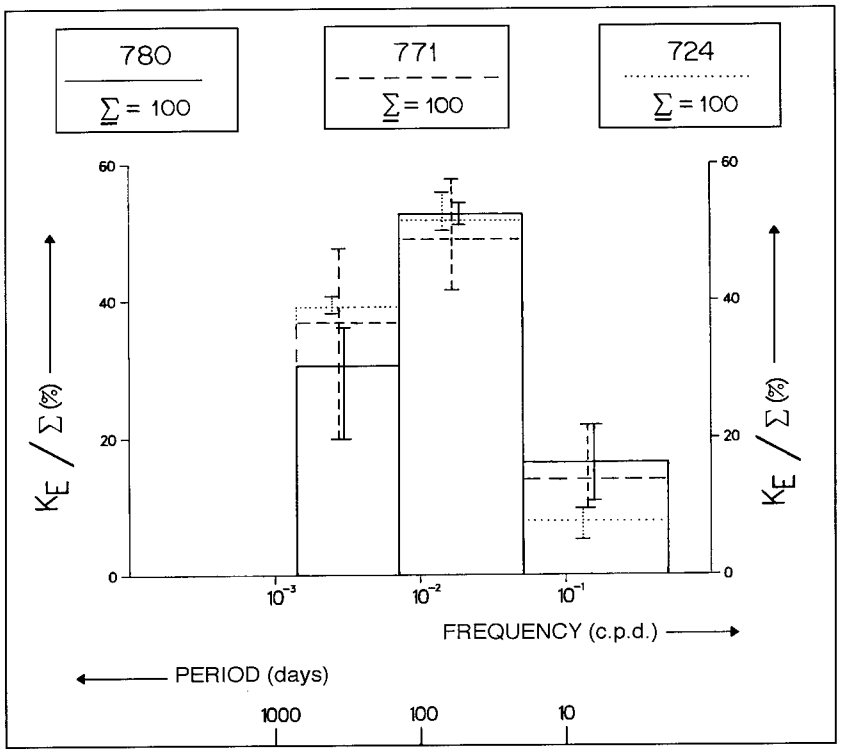

Figure I-102: Spectral intercomparisons (in percent contribution to total K_E): (a) across the Gulf Stream (moorings 771 and 780) and the Kuroshio (mooring 724), adapted from Schmitz and Holland (1986); (b) averaged across many sites in strong current regimes by Schmitz and Luyten (1991), including also the Agulhas Current System.

b

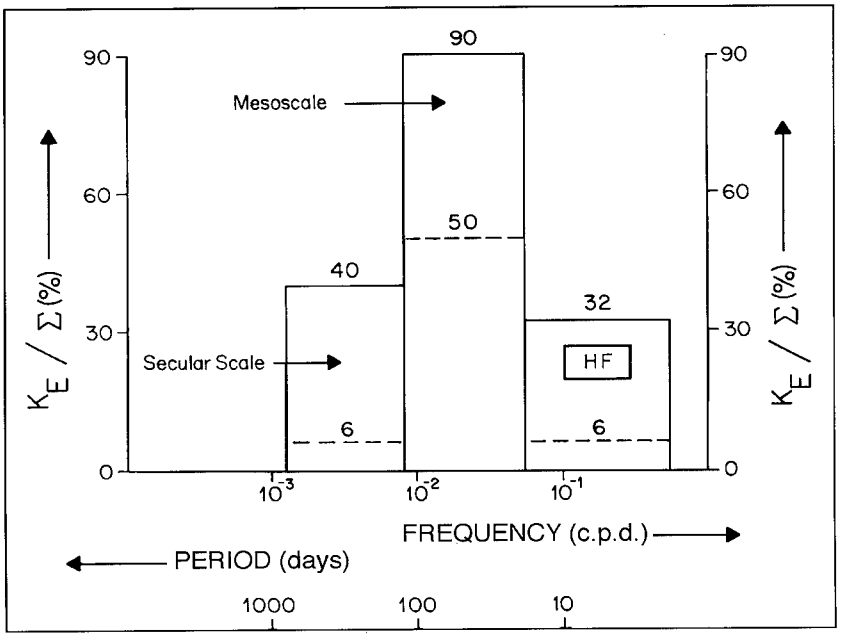

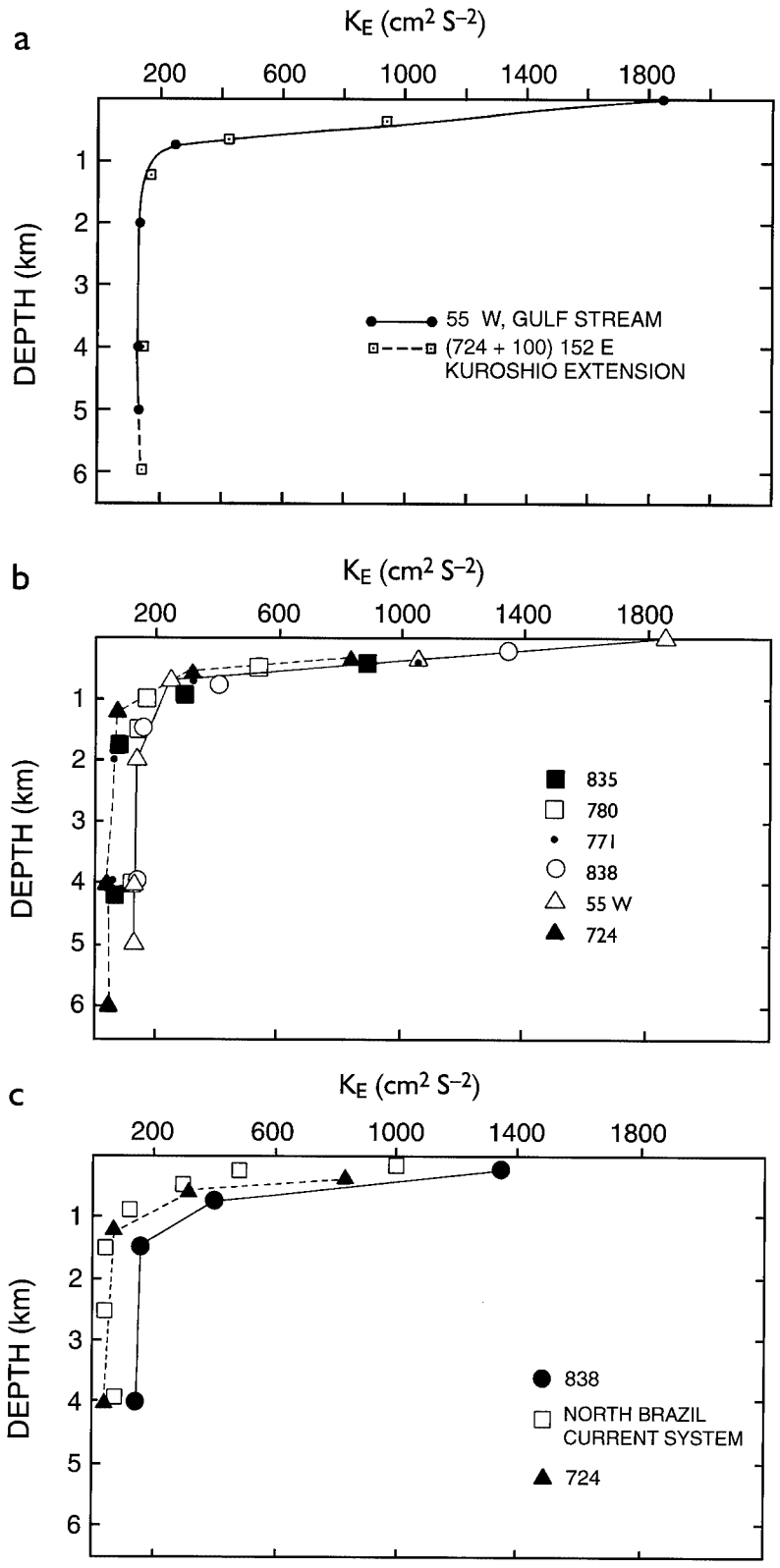

Figure 103: (a) The vertical distribution of K_E at key sites in the Gulf Stream (along 55°W) and in the Kuroshio (mooring 724), (b) at sites in the Gulf Stream (moorings 771 and 780 and near 55°W), Kuroshio, and Agulhas Retroflection (moorings 835 and 838, and (c) including a site near the North Brazil Current.

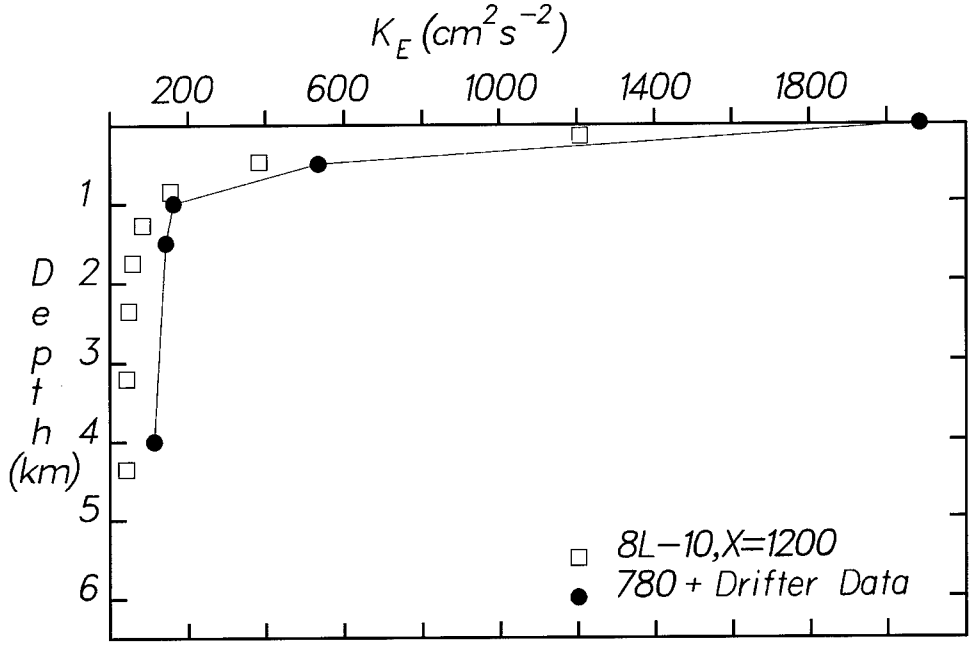

Figure I-104: The vertical structure in the Gulf Stream (mooring 780 + drifter data), compared with results from a particular numerical experiment, 8L-10; see Schmitz and Holland (1986).

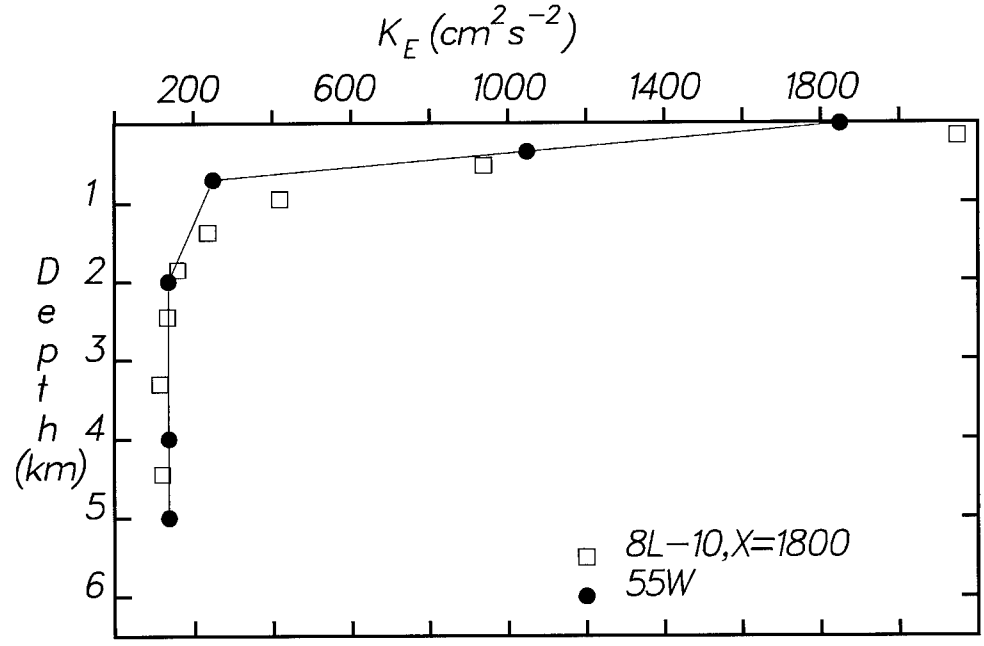

Figure I-105: Another intercomparison of model and observed vertical structure in the GSS by Schmitz and Holland (1986); now the site is "55°W."

favorably intercompared with a particular (labeled 8L-10) numerical experiment (Schmitz and Holland, 1986), ditto in Figure I-105 (the site is 55°W). Spectral intercomparisons are shown in Figure I-106. Figure 107 contains energy budget (conversion) diagrams for two-layer numerical experiments by Schmitz and Thompson (1993). For the case shown in Figure I-107: (a) as the horizontal resolution was increased from 20 km (Run 9.3) to 10 km (Run 9.4), the total EKE (eddy kinetic energy increased by a factor of about 2) and the nature of the energy transfer terms changed qualitatively; and (b) moving from 10 km (run 9.4) to 5 km horizontal resolution (Run 2.0) changes in overall energy or nature of energy budget were small. For the highest resolution runs, the dominant eddy-related energy transfers were (i) from mean kinetic energy (MKE1) to eddy kinetic energy (EKE1) in the upper layer and (ii) from mean potential energy (MPE) to eddy potential energy (EPE) to eddy kinetic energy (EKE2) in the lower layer, with some secondary transfer from upper layer eddy kinetic energy to

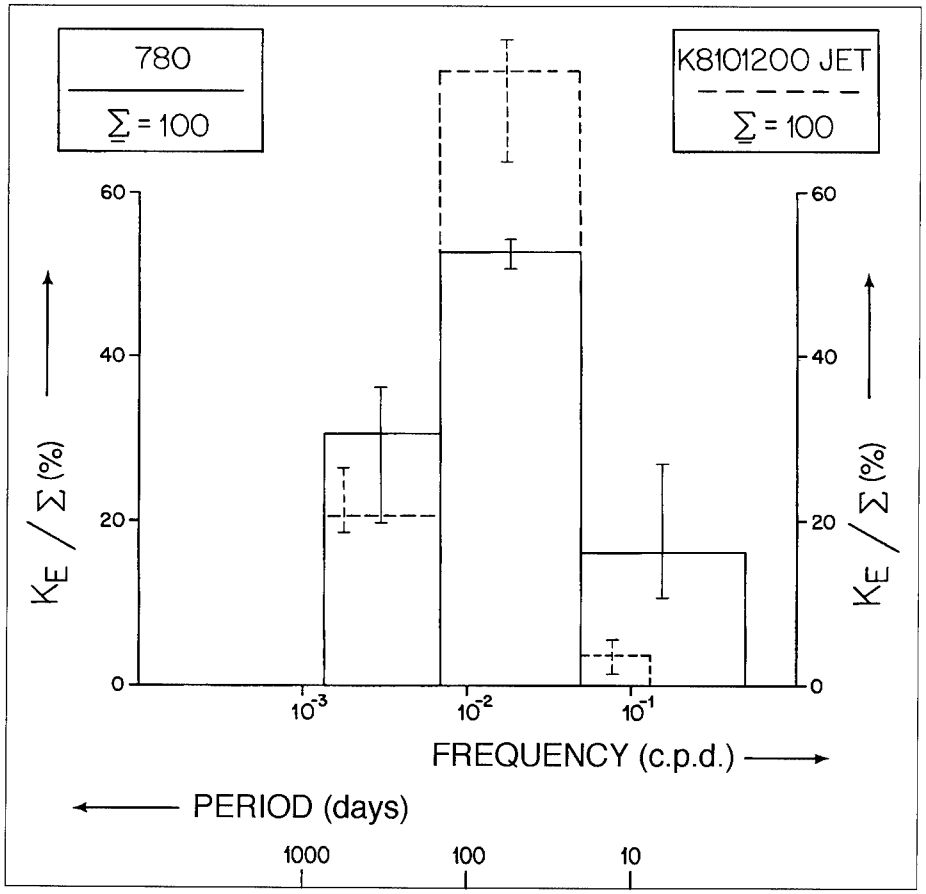

Figure I-106: Comparison of spectral distributions for the results in Figure I-104.

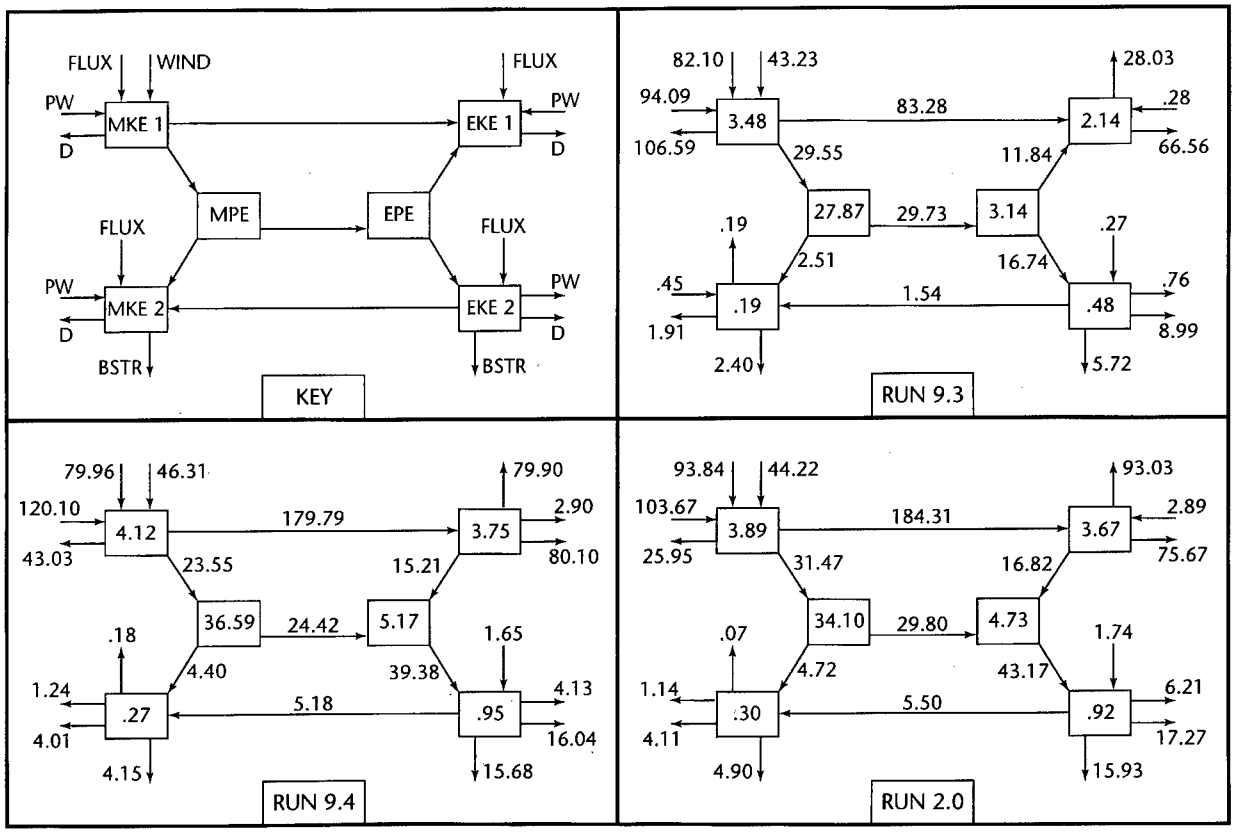

Figure I-107: An energy budget diagram from the results of Schmitz and Thompson (1993), where the variety of symbols used, which are standard, are defined; also please see text.

eddy potential energy to lower layer eddy kinetic energy. In the lower layer, eddy kinetic energy was also converted to mean kinetic energy (MKE2).

Some of the biggest problems with numerical eddy-resolving experiments have continued to be their ability to simulate separation (or path location) and zonal penetration for the Gulf Stream (and to some extent the Kuroshio) realistically (Schmitz and Holland, 1982; Holland and Schmitz, 1985; Schmitz and Thompson, 1993; Hurlburt *et al.*, 1996). The influence of the DWBC on a model-derived path of the Gulf Stream and associated eddy field has been discussed by several authors (Ezer and Mellor, 1992; Holland and Bryan, 1994; Mellor *et al.*, 1982; Thompson and Schmitz, 1989; Spall, 1996a, b). The eddy field on global scale will be discussed in some detail in Volume III, as will the role of the thermohaline circulation.

10. Brief Summary

In this volume (I) of my final report to ONR I have discussed the low-frequency large-scale circulation of the North Atlantic Ocean, and to some extent the global ocean, from an observational point of view. This includes the general circulation and the mesoscale eddy field. Emphasis is on those circulation features I am personally most familiar with, from having worked on them during my career.

The eddy field in the North Atlantic (see previous sections) and to some extent in the global ocean (Schmitz, 1996) is comparatively well documented at this time. Mesoscale eddies are formed by instability processes in strong currents and can be trapped to these strong currents or can propagate into other oceanic areas; this leads to order of magnitude variability in K_E and P_E moving away from strong currents. Spectral shape is comparatively homogeneous within and near these strong currents. In the early days of the modern observational description and dynamical investigation of the eddy field, it was thought that eddies might strongly influence the general circulation in the interior of subtropical gyres. But this perspective has been set aside; rather, the primary role of eddies in the general circulation (that have been identified) takes place in the vicinity of strong currents. Eddies act as an energy sink for the mean circulation in strong currents as a result of their formation [Spall (1996a, b, c) has suggested that energy exchange with eddies can be the primary "dissipative mechanism" for strong frontal currents, with transfer down spatial scales and bottom friction being important in the eddies themselves]. Secondly, eddies may be rectified to at least partially drive recirculations [Schmitz *et al.*, 1983; Spall (1992) has identified a thermodynamic mechanism as well]. In the GSS, there are both northern and southern recirculations. My guess is that the northern recirculation is primarily eddy-rectification-driven, whereas in the south wind and thermohaline forcing and inertial effects also play a significant role in this recirculation. A "new" idea put forth in this report volume is that the Subpolar Gyre System may also be thought of as a strong current (the North Atlantic Current) with a southern (the Newfoundland Basin Eddy, see *e.g.*, Mann, 1967) and a northern recirculation, the Subpolar Gyre proper. There is also the possibility (that needs to be explored much further) that eddies also act as "mixing agents" near deep strong currents and near the bottom. All in all, the mesoscale eddy field is adequately (± 25%, say, on average) described and understood in general terms at first order in the World's Oceans. However, there are still unresolved issues, and

numerical models are lagging [relative to what I would have thought based on Schmitz and Holland (1986), oops, wrong again!] in their ability to agree with observational detail as these models become more complex. Computer time/grid resolution issues may be the limiting factor now for eddy-resolving model runs; "mixing" parameterizations might be the ultimate choke points for general circulation models.

The general circulation of the North Atlantic has proven more difficult to get a good first order ($\sim \pm$ 25%) description of than is the case for the mesoscale eddy field. On the other hand there have been several successes in the recent past (see for example, Hogg and Johns, 1995, and McCartney, 1994), and "new" large field programs are providing a much better observational base for the large scale circulation in the North Atlantic, and in other oceans as well. In Volume I, I have provided several new (or updated) summary pictures for the North Atlantic Circulation (I-21, 22, 51, 86, 89), along with historical and global contexts. Figures I-1, I-12 and I-91 are new global summaries. This will all be discussed further in Volume III.

Acknowledgements

This report and 35 years of oceanographic research were supported primarily by the Office of Naval Research, for which I am deeply grateful. Portions of the author's time on this report were covered by the Clark Foundation. Barbara Gaffron, Elizabeth Suwijn, Jack Cook and Jeannine Pires made high-quality and important contributions in producing this report. This volume is dedicated in memory of Hank Stommel, Val Worthington and Bill Richardson. I would also like to acknowledge the education I have received from Mike McCartney and Joe Reid.

References

Arhan, M., On the large scale dynamics of the Mediterranean outflow, *Deep-Sea Res., 34*, 1187–1208, 1987.

Atkinson, L. P., Distribution of Antarctic Intermediate Water over the Blake Plateau, *J. Geophys. Res., 88,* 4699–4704, 1983.

Bane, J. M., Jr., The Gulf Stream System: An observational perspective. Chapter 6 in: *The Oceans: Physical-Chemical Dynamics and Human Impact*, S. K. Majumdar, E. W. Miller, G. S. Forbes, R. F. Schmalz and A. A. Panah, eds., The Pennsylvania Academy of Science, pp. 99–107, 1994.

Barnier, B., B. L. Hua, and C. Le Provost, On the catalytic role of high baroclinic modes in eddy–driven large–scale circulations, *J. Phys. Oceanogr., 21,* 976–997, 1991.

Beckmann, A., C. W. Böning, C. Köberle, and J. Willebrand, Effects of increased horizontal resolution in a simulation of the North Atlantic Ocean, *J. Phys. Oceanogr., 24*, 326–344, 1994.

Böning, C. W., and R. G. Budich, Eddy dynamics in a primitive equation model: Sensitivity to horizontal resolution and friction, *J. Phys. Oceanogr., 22*, 361–381, 1992.

Böning, C. W., R. Döscher, and H.–J. Isemer, Monthly mean wind stress and Sverdrup transports in the North Atlantic: A comparison of the Hellerman–Rosenstein and Isemer–Hasse climatologies, *J. Phys. Oceanogr., 21*, 221–235, 1991a.

Böning, C. W., R. Döscher, and R. G. Budich, Seasonal transport variation in the western subtropical North Atlantic: Experiments with an eddy-resolving model, *J. Phys. Oceanogr., 21*, 1271–1289, 1991b.

Broecker, W. S., The biggest chill, *Nat. Hist. Mag., 97*, 74–82, 1987.

Broecker, W. S., The great ocean conveyor, *Oceanography, 4*, 79–89, 1991.

Brown, W. S., W. E. Johns, K. D. Leaman, J. P. McCreary, R. L. Molinari, P. L. Richardson, and C. Rooth, A Western Tropical Atlantic Experiment (WESTRAX), *Oceanography, 5,* 73–77, 1992.

Bruce, J. G., J. L. Kerling, and W. H. Beatty, III, On the North Brazilian Eddy field, *Prog. Oceanog., 14*, 57–63, 1985.

Bryden, H. L., and M. M. Hall, Heat transport by currents across 25°N latitude in the Atlantic Ocean. *Science, 207*, 884–886, 1980.

Bryden, H. L., and T. H. Kinder, Steady two-layer exchange through the Strait of Gibraltar, *Deep-Sea Res., 38,* Suppl. 1, S445–S463, 1991.

Chassignet, E. P., and P. R. Gent, The influence of boundary conditions on midlatitude jet separation in ocean numerical models, *J. Phys. Oceanogr., 21*, 1290–1299, 1991.

Clarke, R. A., Transport through the Cape Farewell–Flemish Cap section, *Rapp. P.-v. Réun. Cons. int. Explor. Mer, 185,* 120–130, 1984.

Clarke, R. A., and J.-C. Gascard, The formation of Labrador Sea Water, Part I: Large-scale processes, *J. Phys. Oceanogr., 13*, 1764–1778, 1983.

Clarke, R. A., H. W. Hill, R. F. Reiniger, and B. A. Warren, Current system south and east of the Grand Banks of Newfoundland, *J. Phys. Oceanogr., 10*, 25–65, 1980.

Cochrane, J. D., Low sea-surface salinity off northeastern South America in summer 1964, *J. Mar. Res., 27*, 327–334, 1969.

Cochrane, J. D., F. J. Kelly, Jr., and C. R. Olling, Subthermocline countercurrents in the western equatorial Atlantic Ocean, *J. Phys. Oceanogr., 9*, 724–738, 1979.

Cornillon, P., The effect of the New England Seamounts on Gulf Stream meandering as observed from satellite IR imagery, *J. Phys. Oceanogr., 16*, 386–389, 1986.

Dantzler, H. L., Potential energy maxima in the tropical and subtropical North Atlantic, *J. Phys. Oceanogr., 7*, 512–519, 1977.

da Silveira, I. C. A., L. B. de Miranda, and W. S. Brown, On the origins of the North Brazil Current, *J. Geophys. Res., 99*, 22,501–22,512, 1994.

Dickson, R. R., and J. Brown, The production of North Atlantic Deep Water: Sources, rates, and pathways, *J. Geophys. Res., 99*, 12,319–12,341, 1994.

Dickson, R. R., E. M. Gmitrowitz, and A. J. Watson, Deep-water renewal in the northern North Atlantic, *Nature, 344*, 848–850, 1990.

References

Dietrich, G., A new atlas of the northern North Atlantic Ocean, *Deep-Sea Res.*, Supplement to *16*, 31–34, 1969a.

Dietrich, G., Atlas of the hydrography of the northern North Atlantic Ocean based on the Polar Front Survey during the International Geophysical Year winter and summer 1958. *Conseil International pour l'Exploration de la Mer*, Service Hydrographique, Copenhagen, 140 pp., 1969b.

Dietrich, G., K. Kalle, W. Krauss, and G. Siedler, *General Oceanography, An Introduction*, 2nd ed., 626 pp., John Wiley, New York, 1980.

Duncan, C. P., and S. G. Schladow, World surface currents from ship's drift observations, *International Hydrographic Review, LVIII* (2), 101–112, 1981.

Ellett, D. J., The north-east Atlantic: A fan-assisted storage heater?, *Weather, 48,* 118–126, 1993.

Ezer, T., and G. L. Mellor, A numerical study of the variability and the separation of the Gulf Stream induced by surface atmospheric forcing and lateral boundary flows, *J. Phys. Oceanogr.*, *22*, 660–682, 1992.

Fine, R. A., Tracers, time scales, and the thermohaline circulation: The lower limb in the North Atlantic Ocean, *Rev. Geophys.*, Supplement, U.S. National Report to International Union of Geodesy and Geophysics 1991–1994, pp. 1353–1365, 1995.

Finlen, J. R., Transport investigations in the Northwest Providence Channel, Sc.M. thesis, University of Miami, Coral Gables, Florida, 110 pp., 1966.

Flagg, C. N., R. L. Gordon, and S. McDowell, Hydrographic and current observations on the continental slope and shelf of the western equatorial Atlantic, *J. Phys. Oceanogr.*, *16,* 1412–1429, 1986.

Fofonoff, N. P., The Gulf Stream system, in: *Evolution of Physical Oceanography, Scientific Surveys in Honor of Henry Stommel*, B. A. Warren and C. Wunsch, editors, The MIT Press, Cambridge, Massachusetts, pp. 112–139, 1981.

Fratantoni, D. M., W. E. Johns, and T. L. Townsend, Rings of the North Brazil Current: Their structure and behavior inferred from observations and a numerical simulation, *J. Geophys. Res.*, *100, 10*,633–10,654, 1995.

Friedrichs, M. A. M., M. S. McCartney, and M. M. Hall, Hemispheric asymmetry of deep water transport modes in the Atlantic, *J. Geophys. Res.*, *99*, 25,165–25,279, 1994.

Fuglister, F. C., Atlantic Ocean Atlas of Temperature and Salinity Profiles and Data from the International Geophysical Year of 1957–1958, *Woods Hole Oceanographic Institution Atlas Series, 1,* 209 pp., 1960.

Fuglister, F. C., Gulf Stream '60, *Prog. Oceanog., 1*, 265–373, 1963.

Fuglister, F. C., Cyclonic rings formed by the Gulf Stream 1965–66, in: *Studies in Physical Oceanography*, A. E. Gordon, editor, New York, Gordon and Breach, pp. 137–168, 1971.

Fuglister, F. C., and L. V. Worthington, Some results of a multiple ship survey of the Gulf Stream, *Tellus, 3*, 1–14, 1951.

Garrett, C., A stirring tale of mixing, *Nature*, *364*, 670–671, 1993.

Gordon, A. L., Interocean exchange of thermocline water, *J. Geophys. Res.*, *91*, 5037–5046, 1986.

Gould, W. J., The Northeast Atlantic Ocean, Chapter 7 in: *Eddies in Marine Science,* A. R. Robinson, editor, Springer-Verlag, Berlin, pp. 145–157, 1983.

Gould, W. J., Physical oceanography of the Azores front, *Prog. Oceanog., 14*, 167–190, 1985.

Gouriou, Y., and G. Reverdin, Isopycnal and diapycnal circulation of the upper equatorial Atlantic Ocean in 1983–1984, *J. Geophys. Res.*, *97*, 3543–3572, 1992.

Greatbatch, R. J., Y. Lu, and B. deYoung, The variation of transport through the Straits of Florida: A barotropic model study, *J. Phys. Oceanogr.*, *25*, 2726–2740, 1995.

Halkin, D., and H. T. Rossby, The structure and transport of the Gulf Stream at 73°W, *J. Phys. Oceanogr.*, *15*, 1439–1452, 1985.

Hall, M. M., Horizontal and vertical structure of the Gulf Stream velocity field at 68°W, *J. Phys. Oceanogr.*, *16*, 1814–1828, 1986.

Hall, M. M., and H. L. Bryden, Direct estimates and mechanisms of ocean heat transport, *Deep-Sea Res.*, *29*, 339–359, 1982.

References

Hall, M. M., and H. L. Bryden, Profiling the Gulf Stream with a current meter mooring, *Geophys. Res. Lett., 12,* 203–206, 1985.

Hall, M. M., and N. P. Fofonoff, Downstream development of the Gulf Stream from 68° to 55°W, *J. Phys. Oceanogr., 23,* 225–249, 1993.

Hautala, S. L., D. H. Roemmich, and W. J. Schmitz, Jr., Is the North Pacific in Sverdrup balance along 24°N?, *J. Geophys. Res., 99,* 16,041–16,052, 1994.

Heywood, K. J., E. L. McDonagh, and M. A. White, Eddy kinetic energy of the North Atlantic subpolar gyre from satellite altimetry, *J. Geophys. Res., 99,* 22,525–22,539, 1994.

Hogg, N. G., A note on the deep circulation of the western North Atlantic: Its nature and causes, *Deep-Sea Res., 30,* 945–961, 1983.

Hogg, N. G., On the transport of the Gulf Stream between Cape Hatteras and the Grand Banks, *Deep-Sea Res., 39,* 1231–1246, 1992.

Hogg, N. G., Observations of Gulf Stream meander–induced disturbances, *J. Phys. Oceanogr., 24,* 2534–2545, 1994.

Hogg, N. G., and W. E. Johns, Western boundary currents, *U.S. National Report to International Union of Geodesy and Geophysics 1991–1994,* Supplement to *Rev. Geophys.*, pp. 1311–1334, 1995.

Hogg, N. G., and H. Stommel, On the relation between the deep circulation and the Gulf Stream, *Deep-Sea Res., 32,* 1181–1193, 1985.

Hogg, N. G., R. S. Pickart, R. M. Hendry, and W. J. Smethie, Jr., The northern recirculation gyre of the Gulf Stream, *Deep-Sea Res., 33,* 1139–1165, 1986.

Holland, W. R., The role of mesoscale eddies in the general circulation of the ocean—Numerical experiments using a wind-driven quasi-geostrophic model, *J. Phys. Oceanogr., 8,* 363–392, 1978.

Holland, W. R., The general circulation of the ocean and its modelling, *Dyn. Atmos. Oceans, 3,* 111–142, 1979.

Holland, W. R., and F. O. Bryan, Modeling the wind and thermohaline circulation in the North Atlantic Ocean, in *Ocean Processes in Climate Dynamics: Global and Mediterranean Examples*, P. Malanotte-Rizzoli and A. R. Robinson, editors, *NATO ASI Series C, Vol. 419*, Kluwer Academic Publishers, Norwell, Massachusetts, pp. 111–134, 1994.

Holland, W. R., and W. J. Schmitz, Zonal penetration scale of model mid-latitude jets, *J. Phys. Oceanogr., 15*, 1859–1875, 1985.

Hurlburt, H. E., A. J. Wallcraft, W. J. Schmitz, Jr., P. J. Hogan, and E. J. Metzger, Dynamics of the Kuroshio/Oyashio current system using eddy-resolving models of the North Pacific Ocean, *J. Geophys. Res.*, *101*, 941–976, 1996.

Iselin, C. O'D., A study of the circulation of the western North Atlantic, *Pap. Phys. Oceanogr. Meteorol., 4* (4), 1–101, 1936.

Iselin, C. O'D., The influence of vertical and lateral turbulence on the characteristics of the waters at mid–depths, Trans., *Amer. Geophys. Union, 20*, 414–417, 1939.

Iselin, C. O'D., Preliminary report on long-period variations in the transport of the Gulf Stream System, *Pap. Phys. Oceanogr. Meteorol., 1,* 1–40, 1940.

Johns, W. E., and F. Schott, Meandering and transport variations of the Florida Current, *J. Phys. Oceanogr.*, 17, 1128–1147, 1987.

Johns, W. E., and D. R. Watts, Time scales and structure of topographic Rossby waves and meanders in the deep Gulf Stream, *J. Mar. Res.*, *44*, 267–290, 1986.

Johns, W. E., D. M. Fratantoni, and R. J. Zantopp, Deep western boundary current variability off northeastern Brazil, *Deep-Sea Res. I, 40*, 293-310, 1993.

Johns, W. E., T. N. Lee, F. A. Schott, R. J. Zantopp, and R. H. Evans, The North Brazil Current retroflection: Seasonal structure and eddy variability, *J. Geophys. Res.*, *95,* 22,103–22,120, 1990.

Johns, W. E., T. J. Shay, J. M. Bane, and D. R. Watts, Gulf Stream structure, transport, and recirculation near 68°W, *J. Geophys. Res.*, *100,* 817–838, 1995.

Käse, R. H., and G. Siedler, Meandering of the subtropical front south-east of the Azores, *Nature, 300*, 245–246, 1982.

References

Käse, R. H., and W. Zenk, Reconstructed Mediterranean salt lens trajectories, *J. Phys. Oceanogr.*, *17*, 158–163, 1987.

Käse, R. H., W. Zenk, T. B. Sanford, and W. Hiller, Currents, fronts and eddy fluxes in the Canary Basin, *Prog. Oceanog.*, *14*, 231–257, 1985.

Kelly, K. A., The meandering Gulf Stream as seen by the Geosat altimeter: Surface transport, position and velocity variance from 73° to 46°W, *J. Geophys. Res.*, *96,* 16,721–16,738, 1991.

Kelly, K. A., and S. T. Gille, Gulf Stream surface transport and statistics at 69°W from the Geosat altimeter, *J. Geophys. Res.*, *95,* 3149–3161, 1990.

Klein, B., and G. Siedler, On the origin of the Azores Current, *J. Geophys. Res.*, *94,* 6159–6168, 1989.

Knauss, J. A., A note on the transport of the Gulf Stream, *Deep-Sea Res.*, Suppl. to *16*, 117–123, 1969.

Krauss, W., The North Atlantic Current, *J. Geophys. Res.*, *91*, 5061–5074, 1986.

Krauss, W., Currents and mixing in the Irminger Sea and in the Iceland Basin, *J. Geophys. Res.*, *100*, 10,851–10,871, 1995.

Krauss, W., and J. Meincke, Drifting buoy trajectories in the North Atlantic Current, *Nature, 296* (5859), 737–740, 1982.

Krauss, W., R. H. Käse, and H.-H. Hinrichsen, The branching of the Gulf Stream southeast of the Grand Banks, *J. Geophys. Res.*, *95*, 13,089–13,103, 1990.

Larsen, J. C., Transport and heat flux of the Florida Current at 27°N derived from cross-stream voltages and profiling data: theory and observations, *Phil. Trans. R. Soc. London A, 338*, 169–236, 1992.

Lazier, J. R. N., Renewal of Labrador Sea Water, *Deep-Sea Res.*, *20*, 341–353, 1973.

Lazier, J. R. N., Seasonal variability of temperature and salinity in the Labrador Current, *J. Mar. Res., 40,* Suppl., 341–356, 1982.

Lazier, J. R. N., Observations in the Northwest Corner of the North Atlantic Current, *J. Phys. Oceanogr.*, *24*, 1449–1463, 1994.

Lazier, J. R. N., and D. G. Wright, Annual velocity variations in the Labrador Current, *J. Phys. Oceanogr.*, *23*, 659–678, 1993.

Leaman, K. D., Physical oceanographic measurement techniques at sea, in: *The Sea: Ocean Engineering Science, Volume 9*, John Wiley & Sons, Inc., New York, pp. 1163–1191, 1990.

Leaman, K. D., R. L. Molinari, and P. S. Vertes, Structure and variability of the Florida Current at 27°N: April 1982–July 1984, *J. Phys. Oceanogr.*, *17,* 565–583, 1987.

Leaman, K. D., E. Johns, and T. Rossby, The average distribution of volume transport and potential vorticity with temperature at three sections across the Gulf Stream, *J. Phys. Oceanogr.*, *19*, 36–51, 1989.

Leaman, K. D., P. S. Vertes, L. P. Atkinson, T. N. Lee, P. Hamilton, and E. Waddell, Transport, potential vorticity, and current/temperature structure across Northwest Providence and Santaren Channels and the Florida Current off Cay Sal Bank, *J. Geophys. Res.*, *100*, 8561–8569, 1995.

Lee, A. J., Oceanic circulation of the North Atlantic region, in: *Sea Fisheries Research,* F. R. H. Jones, editor, pp. 1–30, Elek Science, London, 1974.

Lee, T. N., and E. Williams, Wind-forced transport fluctuations of the Florida Current, *J. Phys. Oceanogr.*, *18*, 937–946, 1988.

Lee, T. N., F. A. Schott, and R. Zantopp, Florida Current: Low-frequency variability as observed with moored current meters during April 1982 to June 1983, *Science, 227*, 298–302, 1985.

Lee, T. N., W. Johns, F. Schott, and R. Zantopp, Western boundary current structure and variability east of Abaco, Bahamas at 26.5°N, *J. Phys. Oceanogr.*, *20*, 446–466, 1990.

Lee, T. N., K. Leaman, E. Williams, T. Berger, and L. Atkinson, Florida Current meanders and gyre formation in the southern Straits of Florida, *J. Geophys. Res.*, *100*, 8607–8620, 1995.

Lee, T. N., W. E. Johns, R. J. Zantopp, and E. R. Fillenbaum, Moored observations of Western Boundary Current variability and thermohaline circulation at 26.5°N in the subtropical North Atlantic, *J. Phys. Oceanogr.*, in press, 1996.

References

Leetmaa, A., P. Niiler, and H. Stommel, Does the Sverdrup relation account for the mid-Atlantic circulation? *J. Mar. Res.*, *35*, 1–10, 1977.

Leetmaa, A., J. P. McCreary, Jr., and D. W. Moore, Equatorial currents: Observations and theory, in: *Evolution of Physical Oceanography, Scientific Surveys in Honor of Henry Stommel*, B. A. Warren and C. Wunsch, editors, The MIT Press, Cambridge, Massachusetts; pp. 184–196, 1981.

Levitus, Climatological Atlas of the World Ocean, *NOAA Professional Paper 13*, U.S. Government Printing Office, Washington, D.C., 173 pp., 1982.

Lozier, M. S., M. S. McCartney, and W. B. Owens, Anomalous anomalies in averaged hydrographic data, *J. Phys. Oceanogr.*, *24*, 2624–2638, 1994.

Lozier, M. S., W. B. Owens, and R. G. Curry, The climatology of the North Atlantic, *Prog. Oceanog.*, *36*, 1–44, 1995.

Luyten, J., Scales of motion in the deep Gulf Stream and across the continental rise, *J. Mar. Res.*, *35*, 49–74, 1977.

Lynn, R. J., and J. L. Reid, Characteristics and circulation of deep and abyssal waters, *Deep-Sea Res.*, *15*, 577–598, 1968.

Mann, C. R., The termination of the Gulf Stream and the beginning of the North Atlantic current, *Deep-Sea Res.*, *14*, 337–359, 1967.

Mantyla, A. W., and J. L. Reid, Abyssal characteristics of the World Ocean waters, *Deep-Sea Res.*, *30*, 805–833, 1983.

Mantyla, A. W., and J. L. Reid, Origins of deep and bottom waters of the Indian Ocean, *J. Geophys. Res.*, *100*, 2417–2439, 1995.

Mauritzen, C., A study of the large scale circulation and water mass formation in the nordic seas and Arctic Ocean, Ph.D. Dissertation, Massachusetts Institute of Technology and Woods Hole Oceanographic Institution, 212 pp., 1993.

Mazeika, P. A., Circulation and water masses east of the Lesser Antilles, *Dtsch. Hydrogr. Z.*, Jahrgang *26*, Heft 2, 49–73, 1973.

Mazeika, P. A., D. A. Burns, and T. H. Kinder, Mesoscale circulation east of the southern Lesser Antilles, *J. Geophys. Res.*, *85*, 2743–2758, 1980.

McCartney, M. S., Recirculating components to the deep boundary current of the northern North Atlantic, *Prog. Oceanog., 29*, 283–383, 1992.

McCartney, M. S., Crossing of the equator by the Deep Western Boundary Current in the western Atlantic Ocean, *J. Phys. Oceanogr., 23*, 1953–1974, 1993.

McCartney, M. S., Towards a model of Atlantic Ocean circulation: The plumbing of the climate's radiator, *Oceanus, 37* (1), 5–8, 1994.

McCartney, M. S., On the origin of the warm inflow to the nordic seas, in preparation, 1996.

McCartney, M. S., and R. A. Curry, Trans-equatorial flow of Antarctic Bottom Water in the western Atlantic Ocean: Abyssal geostrophy at the equator, *J. Phys. Oceanogr., 23*, 1264–1276, 1993.

McCartney, M. S., and L. D. Talley, Warm-to-cold water conversion in the northern North Atlantic Ocean, *J. Phys. Oceanogr., 14*, 922–935, 1984.

McCartney, M. S., S. L. Bennett, and M. E. Woodgate-Jones, Eastward flow through the Mid-Atlantic Ridge at 11°N and its influence on the abyss of the eastern basin, *J. Phys. Oceanogr., 21*, 1089–1121, 1991.

Mellor, G. L., C. Mechoso, and E. Keto, A diagnostic calculation of the general circulation of the Atlantic Ocean, *Deep-Sea Res., 29*, 1171–1192, 1982.

Metcalf, W., Shallow currents along the northeastern coast of South America, *J. Mar. Res., 26*, 232–243, 1968.

Metcalf, W. G., Caribbean-Atlantic Water exchange through the Anegada–Jungfern Passage, *J. Geophys. Res., 81*, 6401–6409, 1976.

Metcalf, W., and M. Stalcup, Origin of the Atlantic Equatorial Undercurrent, *J. Geophys. Res., 72*, 4959–4975, 1967.

MODE Group, The, The Mid-Ocean Dynamics Experiment, *Deep-Sea Res., 25*, 859–910, 1978.

Model, V. F., Pillsburys Stommessungen und der Wasserhaushalt des Amerikanischen Mettelmeeres, *Dtsch. Hydrogr. Z., 3*, 57–61, 1950.

References

Molinari, R. L., W. D. Wilson, and K. D. Leaman, Volume and heat transports of the Florida Current: April 1982 through August 1983, *Science, 227*, 295–297, 1985.

Montgomery, R. B., Circulation in upper layers of southern North Atlantic deduced with use of isentropic analysis, *Pap. Phys. Oceanogr. Meteorol., 6* (2), 55 pp., 1938.

Montgomery, R. B., Transport of the Florida Current off Habana, *J. Mar. Res., 4*, 198–220, 1941.

Montgomery, R. B., and M. J. Pollak, Sigma-t surfaces in the Atlantic Ocean, *J. Mar. Res., 5*, 20–27, 1942.

Morrison, J. M., and W. D. Nowlin, Jr., General distribution of water masses within the eastern Caribbean Sea during the winter of 1972 and fall of 1973, *J. Geophys. Res., 87*, 4207–4229, 1982.

Müller, T. J., and G. Siedler, Multi-year current time series in the eastern North Atlantic Ocean, *J. Mar. Res., 50*, 63–98, 1992.

Müller, T. J., F. A. Schott and G. Siedler, Observations of overflow on the Iceland Faeroe Ridge, *"Meteor" Forsch.-Ergebnisse,* Reihe A, No. 15, 49–55, 1974.

Niiler, P. P., and W. S. Richardson, Seasonal variability of the Florida Current, *J. Mar. Res., 31,* 144–167, 1973.

Niiler, P. P., R. E. Davis, and H. J. White, Water-following characteristics of a mixed layer drifter, *Deep-Sea Res., 34,* 1867–1881, 1987.

Niiler, P., D. Hansen, D. Olson, P. Richardson, G. Reverdin, and G. Cresswell, "The Pan-Pacific Surface Current Study," Lagrangian drifter measurements: 1988–1994, *Prog. Oceanog.,* in press, 1996.

Olson, D. B., F. A. Schott, R. J. Zantopp, and K. D. Leaman, The mean circulation east of the Bahamas as determined from a recent measurement program and historical XBT data, *J. Phys. Oceanogr., 14*, 1470–1487, 1984.

Owens, W. B., A synoptic and statistical description of the Gulf Stream and subtropical gyre using SOFAR floats, *J. Phys. Oceanogr., 14,* 104–113, 1984.

Owens, W. B., A statistical description of the vertical and horizontal structure of eddy variability on the edge of the Gulf Stream recirculation, *J. Phys. Oceanogr.*, *15*, 195–205, 1985.

Owens, W. B., A statistical description of the mean circulation and eddy variability in the northwestern Atlantic using SOFAR floats, *Prog. Oceanog.*, *28*, 257–303, 1991.

Owens, W. B., J. R. Luyten, and H. L. Bryden, Moored velocity measurements on the edge of the Gulf-Stream recirculation, *J. Mar. Res.*, Suppl. to *40*, 509–524, 1982.

Owens, W. B., P. L. Richardson, W. J. Schmitz, Jr., H. T. Rossby, and D. C. Webb, Nine-year trajectory of a SOFAR float in the southwestern North Atlantic, *Deep-Sea Res.*, *35*, 1851–1857, 1988.

Parr, A. E., Report on hydrographic observations at a series of anchor stations across the Strait of Florida, *Bull. Bingham Oceanogr. Collect.*, *6* (3), 62 pp., 1937.

Philander, S. G. H., Equatorial undercurrent: Measurements and theories, Rev. *Geophys. Space Phys.*, *11*, 513–570, 1973.

Philander, S. G. H., and R. C. Pacanowski, A model of the seasonal cycle in the tropical Atlantic Ocean, *J. Geophys. Res.*, *91*, 14,192–14,206, 1986a.

Philander, S. G. H., and R. C. Pacanowski, The mass and heat budget in a model of the tropical Atlantic Ocean, *J. Geophys. Res.*, *91*, 14,212–14,220, 1986b.

Pickart, R. S., Water mass components of the North Atlantic deep western boundary current, *Deep-Sea Res.*, *39*, 1553–1572, 1992.

Pickart, R. S., Interaction of the Gulf Stream and Deep Western Boundary Current where they cross, *J. Geophys. Res.*, *99*, 25,155–25,164, 1994a.

Pickart, R. S., Where currents cross: Intersection of the Gulf Stream and the Deep Western Boundary Current, *Oceanus*, *37* (1), 16–18, 1994b.

Pickart, R. S., and N. G. Hogg, A tracer study of the deep Gulf Stream cyclonic recirculation, *Deep-Sea Res.*, *36*, 935–956, 1989.

Pickart, R. S., and W. M. Smethie, Jr., How does the deep western boundary current cross the Gulf Stream?, *J. Phys. Oceanogr.*, *23*, 2602–2616, 1993.

References

Pickart, R. S., and D. R. Watts, Deep Western Boundary Current variability at Cape Hatteras, *J. Mar. Res., 48*, 765–791, 1990.

Pillsbury, J. E., The Gulf Stream—A description of the methods employed in the investigation, and the results of the research, *Rept. Supt., U.S. Coast Geod. Surv., Appendix 10*, 461–620, 1890.

Pollard, R. T., and S. Pu, Structure and circulation of the upper Atlantic Ocean northeast of the Azores, *Prog. Oceanog.*, 14, 443–462, 1985.

Poulain, P.-M., A. Warn-Varnas, and P. P. Niiler, Near surface circulation of the nordic seas as measured by Lagrangian drifters, *J. Geophys. Res.*, accepted, 1996.

Price, J. F., and M. O'N. Baringer, Outflows and deep water production by marginal seas, *Prog. Oceanog., 33*, 161–200, 1994.

Reid, J. L., On the mid-depth circulation and salinity field in the North Atlantic Ocean, *J. Geophys. Res., 83*, 5063–5067, 1978.

Reid, J. L., On the mid-depth circulation of the World Ocean, in *Evolution of Physical Oceanography, Scientific Surveys in Honor of Henry Stommel*, B. A. Warren and C. Wunsch, editors, The MIT Press, Cambridge, Massachusetts; pp. 70–111, 1981.

Reid, J. L., On the total geostrophic circulation of the North Atlantic Ocean: Flow patterns, tracers, and transports, *Prog. Oceanog., 33*, 1–92, 1994.

Reid, J. L., and R. J. Lynn, On the influence of the Norwegian-Greenland and Weddell seas upon the bottom waters of the Indian and Pacific Oceans, *Deep-Sea Res., 18*, 1063–1088, 1971.

Richardson, P. L., Gulf Stream rings, *Oceanus, 19* (3), 65–68, 1976.

Richardson, P. L., On the crossover between the Gulf Stream and the Western Boundary Undercurrent, *Deep-Sea Res., 24*, 139–159, 1977.

Richardson, P. L., Gulf Stream trajectories measured with free-drifting buoys, *J. Phys. Oceanogr., 11*, 999–1010, 1981.

Richardson, P. L., A vertical section of eddy kinetic energy through the Gulf Stream system, *J. Geophys. Res., 88,* 2705–2709, 1983.

Richardson, P. L., Average velocity and transport of the Gulf Stream near 55°W, *J. Mar. Res., 43*, 83–111, 1985.

Richardson, P. L., Worldwide ship drift distributions identify missing data, *J. Geophys. Res., 94,* 6169–6176, 1989.

Richardson, P. L., A census of eddies observed in North Atlantic SOFAR float data, *Prog. Oceanog., 31*, 1–50, 1993.

Richardson, P. L., Giant eddies of South Atlantic water invade the north, *Oceanus, 37* (1), 19–21, 1994.

Richardson, P. L., and J. A. Knauss, Gulf Stream and western boundary undercurrent observations at Cape Hatteras, *Deep-Sea Res., 18*, 1089–1109, 1971.

Richardson, P. L., and T. K. McKee, Average seasonal variation of the Atlantic equatorial currents from historical ship drifts, *J. Phys. Oceanogr., 14,* 1226–1238, 1984.

Richardson, P. L., and S. G. H. Philander, The seasonal variations of surface currents in the tropical Atlantic Ocean: a comparison of ship drift data with results from a general circulation model, *J. Geophys. Res., 92*, 715–724, 1987.

Richardson, P. L., and G. Reverdin, Seasonal cycle of velocity in the Atlantic North Equatorial Countercurrent as measured by surface drifters, current meters, and ship drifts, *J. Geophys. Res., 92,* 3691–3708, 1987.

Richardson, P. L., and W. J. Schmitz, Jr., Deep cross-equatorial flow in the Atlantic measured with SOFAR floats, *J. Geophys. Res., 98,* 8371–8387, 1993.

Richardson, P. L., and D. Walsh, Mapping climatological seasonal variations of surface currents in the tropical Atlantic using ship drifts, *J. Geophys. Res., 91,* 10,537–10,550, 1986.

Richardson, P. L., A. E. Strong, and J. A. Knauss, Gulf Stream eddies: Recent observations in the western Sargasso Sea, *J. Phys. Oceanogr., 3*, 297–301, 1973.

Richardson, P. L., R. E. Cheney, and L. V. Worthington, A census of Gulf Stream rings, spring 1975, *J. Geophys. Res., 83,* 6136–6144, 1978.

Richardson, P. L., G. Hufford, R. Limeburner, and W. S. Brown, North Brazil Current retroflection eddies, *J. Geophys. Res., 99,* 5081–5093, 1994.

References

Richardson, W. S., and J. R. Finlen, The transport of Northwest Providence Channel, *Deep-Sea Res.*, *14,* 361–367, 1967.

Richardson, W. S., W. J. Schmitz, Jr., and P. P. Niiler, The velocity structure of the Florida Current from the Straits of Florida to Cape Fear, *Deep-Sea Res.*, Suppl. to *16*, 225–231, 1969.

Rintoul, S. R., and C. Wunsch, Mass, heat, oxygen and nutrient fluxes and budgets in the North Atlantic Ocean, *Deep-Sea Res.*, *38*, suppl. 1, S355–S377, 1991.

Riser, S. C., and H. T. Rossby, Quasi-Lagrangian structure and variability of the subtropical western North Atlantic circulation, *J. Mar. Res., 41*, 127–162, 1983.

Roemmich, D., Circulation of the Caribbean Sea: A well-resolved inverse problem, *J. Geophys. Res.*, *86*, 7993–8005, 1981.

Roemmich, D., and C. Wunsch, Two transatlantic sections: Meridional circulation and heat flux in the subtropical North Atlantic Ocean, *Deep-Sea Res.*, *32*, 619–664, 1985.

Rosenfeld, L. K., R. L. Molinari, and K. D. Leaman, Observed and modeled annual cycle of transport in the Straits of Florida and east of Abaco Island, the Bahamas (26.5°N), *J. Geophys. Res.*, *94,* 4867–4878, 1989.

Saunders, P. M., Circulation in the eastern North Atlantic, *J. Mar. Res., 40,* Suppl., 641–657, 1982.

Schmitz, W. J., Eddy kinetic energy in the deep western North Atlantic, *J. Geophys. Res., 81*, 4981–4982, 1976.

Schmitz, W. J., Jr., On the deep general circulation in the western North Atlantic, *J. Mar. Res., 35*, 21–28, 1977.

Schmitz, W. J., Jr., Observations of the vertical distribution of low frequency kinetic energy in the western North Atlantic, *J. Mar. Res., 36*, 295–310, 1978.

Schmitz, W. J., Jr., Weakly depth-dependent segments of the North Atlantic circulation, *J. Mar. Res., 38*, 111–133, 1980.

Schmitz, W. J., Jr., Abyssal eddy kinetic energy in the North Atlantic, *J. Mar. Res., 42*, 509–536, 1984.

Schmitz, W. J., Jr., SOFAR float trajectories associated with the Newfoundland Basin, *J. Mar. Res., 43*, 761–778, 1985.

Schmitz, W. J., Jr., The MODE Site revisited, *J. Mar. Res., 47,* 131–151, 1989.

Schmitz, W. J., Jr., On the interbasin-scale thermohaline circulation, *Rev. Geophys., 33,* 151–173, 1995.

Schmitz, W. J., Jr., On the eddy field in the Agulhas retroflection, with some global considerations, *J. Geophys. Res.*, in press, 1996.

Schmitz, W. J., Jr., and W. R. Holland, A preliminary comparison of selected numerical eddy-resolving general circulation experiments with observations, *J. Mar. Res., 40*, 75–117, 1982.

Schmitz, W. J., Jr., and W. R. Holland, Observed and modeled mesoscale variability near the Gulf Stream and Kuroshio Extension. *J. Geophys. Res.*, *91*, 9624–9638, 1986.

Schmitz, W. J., Jr., and J. R. Luyten, Spectral time scales for mid-latitude eddies, *J. Mar. Res., 49,* 75–107, 1991.

Schmitz, W. J., Jr., and M. S. McCartney, On the North Atlantic circulation, *Rev. Geophys., 31*, 29–49, 1993.

Schmitz, W. J., Jr., and P. L. Richardson, On the sources of the Florida Current, *Deep-Sea Res.*, *38*, Suppl. 1, S389–S409, 1991.

Schmitz, W. J., Jr., and W. S. Richardson, On the transport of the Florida Current, *Deep–Sea Res., 15*, 679–693, 1968.

Schmitz, W. J., Jr., and J. D. Thompson, On the effects of horizontal resolution in a limited–area model of the Gulf Stream system, *J. Phys. Oceanogr.*, *23,* 1001–1007, 1993.

Schmitz, William J., Jr., A. R. Robinson, and F. C. Fuglister, Bottom velocity observations directly under the Gulf Stream, *Science, 170*, 1192–1194, 1970.

Schmitz, W. J., Jr., W. R. Holland, and J. F. Price, Mid-latitude mesoscale variability, *Rev. Geophys. Space Physics, 21,* 1109–1119, 1983.

References

Schmitz, W. J., Jr., J. F. Price, and P. L. Richardson, Recent moored current meter and SOFAR float observations in the eastern Atlantic near 32°N, *J. Mar. Res., 46,* 301–319, 1988.

Schmitz, W. J., Jr., J. D. Thompson, and J. R. Luyten, The Sverdrup circulation for the Atlantic along 24°N, *J. Geophys. Res., 97,* 7251–7256, 1992.

Schmitz, W. J., Jr., J. R. Luyten, and R. W. Schmitt, On the Florida Current *T/S* envelope, *Bull. Mar. Sci., 53,* 1048–1065, 1993.

Schott, F. A., T. N. Lee, and R. Zantopp, Variability of structure and transport of the Florida Current in the period range of days to seasonal, *J. Phys. Oceanogr., 18,* 1209–1230, 1988.

Schott, F. A., L. Stramma, and J. Fischer, The warm water inflow into the western tropical Atlantic boundary regime, spring 1994, *J. Geophys. Res., 100,* 24,745–24,760, 1995.

Shay, T. J., J. M. Bane, D. R. Watts, and K. L. Tracey, Gulf Stream flow field and events near 68°W, *J. Geophys. Res., 100,* 22,565–22,589, 1995.

Siedler, G., N. Zangenberg, R. Onken, and A. Morlière, Seasonal changes in the tropical Atlantic circulation: Observation and simulation of the Guinea Dome, *J. Geophys. Res., 97,* 703–715, 1992.

Siedler, G., W. Zenk, and W. J. Emery, Strong current events related to a subtropical front in the northeast Atlantic, *J. Phys. Oceanogr., 15,* 885–897, 1985.

Spall, M. A., Cooling spirals and recirculation in the subtropical gyre, *J. Phys. Oceanogr., 22,* 564–571, 1992.

Spall, M. A., Dynamics of the Gulf Stream / Deep Western Boundary Current Crossover, Part I: Entrainment and recirculation, *J. Phys. Oceanogr.*, in press, 1996a.

Spall, M. A., Dynamics of the Gulf Stream / Deep Western Boundary Current Crossover, Part II: Low frequency internal oscillations, *J. Phys. Oceanogr.*, in press, 1996b.

Spall, M. A., Baroclinic jets in confluent flow, *J. Phys. Oceanogr.*, submitted, 1996c.

Speer, K. G., and M. S. McCartney, Tracing Lower North Atlantic Deep Water across the equator, *J. Geophys. Res., 96,* 20,443–20,448, 1991.

Stalcup, M. C., and W. G. Metcalf, Current measurements in the passages of the Lesser Antilles, *J. Geophys. Res., 77,* 1032–1049, 1972.

Stommel, H., The westward intensification of wind-driven ocean currents, *Trans. Amer. Geophys. Union, 29*, 202–206, 1948.

Stommel, H., A survey of ocean current theory, *Deep-Sea Res., 4*, 149–184, 1957.

Stommel, Henry, *The Gulf Stream: a Physical and Dynamical Description*, University of California Press, Berkeley, and Cambridge University Press, London, 202 + xiii pp, 1958.

Stommel, H., *The Gulf Stream, A Physical and Dynamical Description,* University of California Press, Berkeley, second edition, 248 pp., 1965.

Stommel, H., and F. Schott, The beta spiral and the determination of the absolute velocity field from hydrographic station data, *Deep-Sea Res., 24*, 325–329, 1977.

Stommel, H., P. Niiler, and D. Anati, Dynamic topography and recirculation of the North Atlantic, *J. Mar. Res., 36*, 449–468, 1978.

Stramma, L., Geostrophic transport in the Warm Water Sphere of the eastern subtropical North Atlantic, *J. Mar. Res., 42*, 537–558, 1984.

Stramma, L., Geostrophic transport of the South Equatorial Current in the Atlantic, *J. Mar. Res., 49*, 281–294, 1991.

Stramma, L., Y. Ikeda, and R. G. Peterson, Geostrophic transport in the Brazil Current region north of 20°S, *Deep-Sea Res., 37*, 1875–1886, 1990.

Stramma, L., J. Fischer, and J. Reppin, The North Brazil Undercurrent, *Deep-Sea Res. I, 42*, 773–795, 1995.

Sverdrup, H. U., M. W. Johnson, and R. H. Fleming, *The Oceans: Their Physics, Chemistry, and General Biology*, Prentice-Hall, Englewood Cliffs, N.J., 1087 pp., 1942.

Swallow, J. C., and L. V. Worthington, Measurements of deep currents in the western North Atlantic. *Nature, Lond., 179*, 1183–1184, 1957.

Swallow, J. C., and L. V. Worthington, An observation of a deep countercurrent in the western North Atlantic, *Deep-Sea Res., 8*, 1–19, 1961.

References

Sy, A., Investigation of large-scale circulation patterns in the central North Atlantic: The North Atlantic Current, the Azores Current, and the Mediterranean Water plume in the area of the Mid-Atlantic Ridge, *Deep-Sea Res.*, *35*, 383–413, 1988.

Sy, A., U. Schauer, and J. Meincke, The North Atlantic Current and its associated hydrographic structure above and eastwards of the Mid-Atlantic Ridge, *Deep-Sea Res.*, *39,* 825–853, 1992.

Talley, L. D., and M. S. McCartney, Distribution and circulation of Labrador Sea Water, *J. Phys. Oceanogr.*, *12*, 1189–1205, 1982.

Thompson, J. D., and W. J. Schmitz, Jr., A limited-area model of the Gulf Stream: Design, initial experiments, and model / data intercomparison, *J. Phys. Oceanogr., 19,* 791–814, 1989.

Thompson, J. D., T. L. Townsend, A. Wallcraft, and W. J. Schmitz, Jr., Ocean prediction and the Atlantic basin: Scientific issues and technical challenges, *Oceanography,* 5, 36–41, 1992.

Toole, J. M., K. L. Polzin, and R. W. Schmitt, Estimates of diapycnal mixing in the abyssal ocean, *Science, 264*, 1120–1123, 1994.

Tsuchiya, M., Circulation of the Antarctic Intermediate Water in the North Atlantic Ocean, *J. Mar. Res., 47*, 747–755, 1989.

U.S. Naval Oceanographic Office, *Oceanographic Atlas of the North Atlantic Ocean, Section I, Tides and Currents, Publ. 700*, 77 pp., Defense Mapping Agency Hydrographic Center, Washington, D.C., 1965.

Webster, F., Vertical profiles of horizontal ocean currents, *Deep-Sea Res.*, *16*, 85–98, 1969.

Wegner, G., Geostrophische Oberflächenströmung im nördlichen Nordatlantischen Ozean im Internationalen Geophysikalishchen Jahr 1957–58, *Ber. Dt. Wiss. Komm. Meeresforsch., 22,* 411–426, 1973.

Weller, R. A., Overview of the Frontal Air–Sea Interaction Experiment (FASINEX): A study of air–sea interaction in a region of strong oceanic gradients, *J. Geophys. Res.*, *96*, 8501–8516, 1991.

Wennekens, M. P., Water mass properties of the Straits of Florida and related waters, *Bull. Mar. Sci. Gulf Caribb., 9,* 1–52, 1959.

Wertheim, G. K., Studies of the electrical potential between Key West, Florida and Havana, Cuba, *Trans. Am. Geophys. Union, 35*, 872–882, 1954.

Wilson, W. D., and W. E. Johns, Velocity structure and transport in the Windward Islands passages, *Deep-Sea Res.*, in press, 1996.

Wilson, W. D., E. Johns, and R. L. Molinari, Upper layer circulation in the western tropical North Atlantic Ocean during August 1989, *J. Geophys. Res.*, *99,* 22,513–22,523, 1994.

Worthington, L. V., The 18° Water in the Sargasso Sea, *Deep-Sea Res.*, *5*, 297–305, 1959.

Worthington, L. V., On the North Atlantic circulation, *The Johns Hopkins Oceanographic Studies, 6*, The Johns Hopkins University Press, 110 pp., 1976.

Worthington, L. V., and W. R. Wright, North Atlantic Ocean Atlas of Potential Temperature and Salinity in the Deep Water, Including Temperature, Salinity, and Oxygen Profiles from the *Erika Dan* Cruise of 1962, *Woods Hole Oceanographic Institution Atlas Series 2*, 58 plates, 1970.

Wright, W. R., and L. V. Worthington, The Water Masses of the North Atlantic Ocean; a Volumetric Census of Temperature and Salinity, *Ser. Atlas Mar. Envir., 19,* 8 pages, 7 plates, 1970.

Wüst, G., Schichtung und Zirkulation des Atlantischen Ozeans, Die Stratosphäre, *Wiss. Ergebn. Dtsch. Atlanti. Exped. Meteor 1925–1927, 6,* 1st Part, 2, 180 pp., 1935. (Also published as *The Stratosphere of the Atlantic Ocean*, edited by W. J. Emery, 112 pp., Amerind, New Delhi, 1978.)

Wyrtki, K., L. Magaard, and J. Hager, Eddy energy in the oceans, *J. Geophys. Res.*, *81,* 2641–2646, 1976.

Zenk, W., and T. J. Müller, Seven-year current meter record in the eastern North Atlantic, *Deep–Sea Res.*, *35*, 1259–1268, 1988.

Zenk, W., B. Klein, and M. Schröder, Cape Verde Frontal Zone, *Deep-Sea Res.*, *38*, Suppl. 1, S505–S530, 1991.

Appendix

William Joseph Schmitz, Jr.
Physical Oceanographer
Senior Scientist
W. Van Alan Clark Chair
Woods Hole Oceanographic Institution

Birth: December 20, 1937

Sc.B., University of Miami, 1961
Ph.D., Physical Oceanography, University of Miami, 1966

Research Aide, 1959–1961; NDEA Fellow, 1961–64; Instructor, 1964–66, Institute of Marine Science, University of Miami

Postdoctoral Fellow, 1966–67, Nova University

Assistant Scientist, 1967–71; Associate Scientist, 1971–79, awarded tenure, 1974; Senior Scientist, 1979–; W. Van Alan Clark Chair for Excellence in Oceanography, 1992–, Woods Hole Oceanographic Institution

Senior Queen's Fellow, Commonwealth of Australia, 1984

Interim Director, Institute for Naval Oceanography, 1986

Fellow, American Geophysical Union, 1987–

Member, Naval Research Advisory Committee, 1990–1996

Meritorious Public Service Award, Department of the Navy, March 1991

Visiting Investigator, Institut für Meereskunde, Universität Kiel, September, 1993

Visiting Investigator, Scripps Institution of Oceanography, University of California, San Diego, February–March, 1995

Research Interests: Low frequency, large scale ocean circulation

Author or co-author of 60 referenced scientific publications

DOCUMENT LIBRARY

Distribution List for Technical Report Exchange – February 1996

University of California, San Diego
SIO Library 0175C
9500 Gilman Drive
La Jolla, CA 92093-0175

Hancock Library of Biology & Oceanography
Alan Hancock Laboratory
University of Southern California
University Park
Los Angeles, CA 90089-0371

Gifts & Exchanges
Library
Bedford Institute of Oceanography
P.O. Box 1006
Dartmouth, NS, B2Y 4A2, CANADA

Commander
International Ice Patrol
1082 Shennecossett Road
Groton, CT 06340-6095

NOAA/EDIS Miami Library Center
4301 Rickenbacker Causeway
Miami, FL 33149

Research Library
U.S. Army Corps of Engineers
Waterways Experiment Station
3909 Halls Ferry Road
Vicksburg, MS 39180-6199

Institute of Geophysics
University of Hawaii
Library Room 252
2525 Correa Road
Honolulu, HI 96822

Marine Resources Information Center
Building E38-320
MIT
Cambridge, MA 02139

Library
Lamont-Doherty Earth Observatory
Columbia University
Palisades, NY 10964

Library
Serials Department
Oregon State University
Corvallis, OR 97331

Pell Marine Science Library
University of Rhode Island
Narragansett Bay Campus
Narragansett, RI 02882

Working Collection
Texas A&M University
Dept. of Oceanography
College Station, TX 77843

Fisheries-Oceanography Library
151 Oceanography Teaching Bldg.
University of Washington
Seattle, WA 98195

Library
R.S.M.A.S.
University of Miami
4600 Rickenbacker Causeway
Miami, FL 33149

Maury Oceanographic Library
Naval Oceanographic Office
Building 1003 South
1002 Balch Blvd.
Stennis Space Center, MS, 39522-5001

Library
Institute of Ocean Sciences
P.O. Box 6000
Sidney, B.C. V8L 4B2 CANADA

National Oceanographic Library
Southampton Oceanography Centre
European Way
Southampton SO14 3ZH UNITED KINGDOM

The Librarian
CSIRO Marine Laboratories
G.P.O. Box 1538
Hobart, Tasmania AUSTRALIA 7001

Library
Proudman Oceanographic Laboratory
Bidston Observatory
Birkenhead
Merseyside L43 7 RA UNITED KINGDOM

IFREMER
Centre de Brest
Service Documentation - Publications
BP 70 29280 Plouzane FRANCE

50272-101

REPORT DOCUMENTATION PAGE	1. REPORT NO. WHOI-96-03	2.	3. Recipient's Accession No.

4. Title and Subtitle
On the World Ocean Circulation: Volume I, Some Global Features / North Atlantic Circulation

5. Report Date
June 1996

6.

7. Author(s)
William J. Schmitz, Jr.

8. Performing Organization Rept. No.
WHOI-96-03

9. Performing Organization Name and Address
Woods Hole Oceanographic Institution
Woods Hole, Massachusetts 02543

10. Project/Task/Work Unit No.

11. Contract(C) or Grant(G) No.
(C)
(G) N00014-89-J-1039
N00014-95-1-0356

12. Sponsoring Organization Name and Address
Office of Naval Research and the Clark Foundation

13. Type of Report & Period Covered
Technical Report

14.

15. Supplementary Notes
This report should be cited as: Woods Hole Oceanog. Inst. Tech. Rept., WHOI-96-03.

16. Abstract (Limit: 200 words)

This is the first volume of a "final report" that summarizes, often in a speculative vein, what I have learned over the past 35 years or so about large-scale, low-frequency ocean currents, primarily with support from the Office of Naval Research (ONR). I was also fortunate to have been partially supported by the National Science Foundation and, during the preparation of this report, by the Clark Foundation.

This report is meant to be an informal, occasionally anecdotal, state-of-the-art summary account of the World Ocean Circulation (WOC). Seemingly simple questions about how ocean currents behave, such as where various brands of sea water are coming from and going to, have been exciting and difficult research topics for many years. This report is not remotely about "all" of the WOC, it is simply a set of comments about what I have looked into. I believe that the results in this report, although presented in a personal way, are consistent with community wisdom. The report is intended to be readable by non-specialists who have a basic scientific/technical background, especially in other oceanographic areas or meteorology or physics or the geophysical disciplines, not just by specialists in physical oceanography. Anyone wishing to get spun up on the observational basis for the WOC could use this report and associated reference lists as a starting point.

Volume I concentrates on the North Atlantic Ocean although there is preliminary discussion of global features. Highlights of this global summary are a new type of composite schematic picture of the World Ocean Circulation in its "upper layers" (Figure I-1) and new summaries (Figures I-12, 21, 91) of the global "thermohaline" circulation.

17. Document Analysis a. Descriptors

global ocean circulation
North Atlantic circulation
ocean currents

b. Identifiers/Open-Ended Terms

c. COSATI Field/Group

18. Availability Statement	19. Security Class (This Report)	21. No. of Pages
Approved for public release; distribution unlimited.	UNCLASSIFIED	150
	20. Security Class (This Page)	22. Price

(See ANSI-Z39.18) *See Instructions on Reverse*

OPTIONAL FORM 272 (4-77)
(Formerly NTIS-35)
Department of Commerce

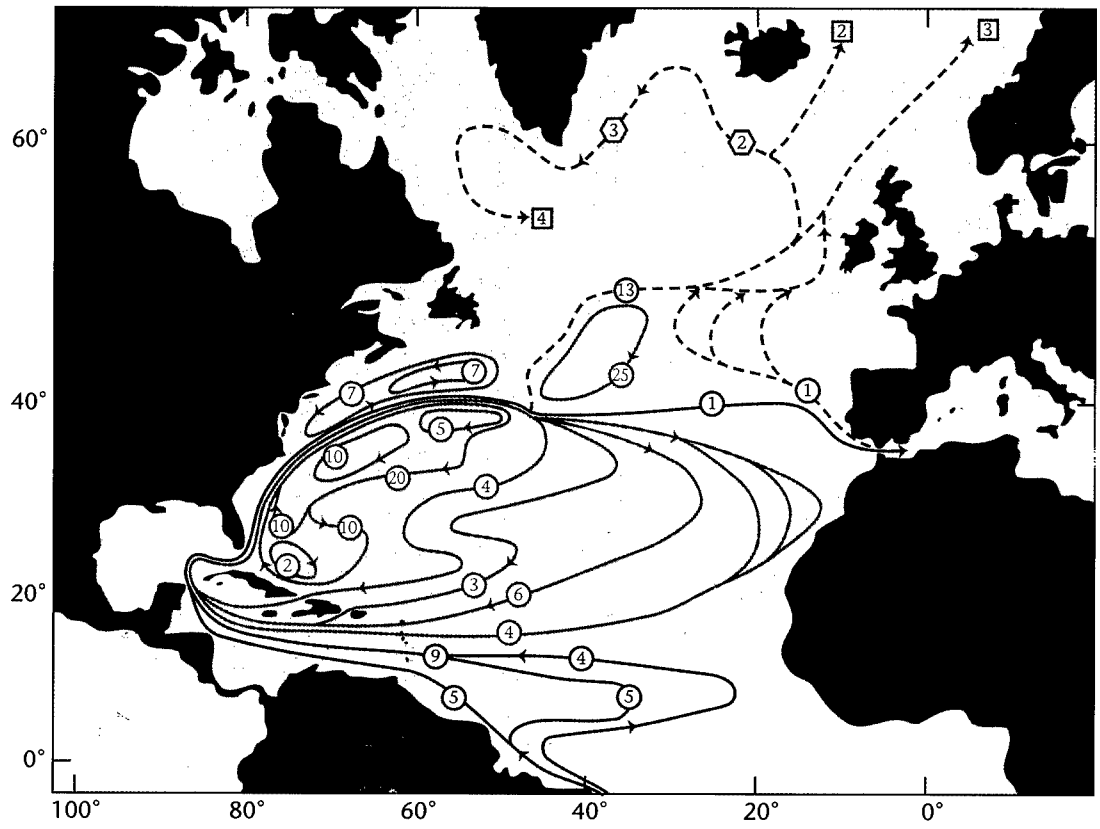

Upper layer transports for the North Atlantic circulation in circles (in Sverdrups). Transports in squares denote sinking and a hexagon denotes entrainment. Red lines denote the replacement flow for the meridional cell involving NADW, the latter formation being shown in blue boxes attached to dashed red lines, which indicate that significant cooling may take place. Solid green lines characterize the subtropical gyre and recirculations as well as the Newfoundland Basin Eddy. Dashed blue lines denote the addition of Mediterranean Water to the system.

WOODS HOLE OCEANOGRAPHIC INSTITUTION
1930